Biochemical and Structural Characterization of Ovine Alpha-1-Antitrypsin

A Thesis Submitted to the

Department of Biochemistry

University of Mysore, Mysore

In fulfillment of the requirements for the degree of

Doctor of Philosophy

by

Vivek Kumar Gupta

Under the supervision of

Dr. Lalitha R. Gowda

Department of Protein Chemistry and Technology

Central Food Technological Research Institute
Mysore –570 020, India

April, 2008

DECLARATION

I hereby declare that this thesis entitled "**Biochemical and structural characterization of ovine alpha-1-antitrypsin",** submitted herewith, for the degree of Doctor of Philosophy in Biochemistry of the University of Mysore, Mysore, is the result of work done by me in the Department of Protein Chemistry and Technology, Central Food Technological Research Institute (CFTRI), Mysore, India, under the guidance and supervision of Dr. Lalitha R. Gowda, during the period of February, 2003 - April, 2008.

I further declare that the results of this work have not been previously submitted for any other degree or fellowship.

Mysore
April, 2008. **Vivek Kumar Gupta**

Guide

Head of the Department

Dr. Lalitha R. Gowda
Department of Protein Chemistry and Technology

CERTIFICATE

I hereby certify that this thesis entitled **"Biochemical and structural characterization of ovine alpha-1-antitrypsin,"** submitted by **Mr. Vivek Kumar Gupta** to the University of Mysore, Mysore, for the degree of **Doctor of Philosophy in Biochemistry** is the result of research work carried out by him in the Department of Protein Chemistry and Technology, Central Food Technological Research Institute (CFTRI), Mysore, under my guidance and supervision. This work has not been submitted either partially or fully for any other degree or fellowship.

Mysore
Date:

Abstract

α-1-Proteinase inhibitor (α-1-PI), the archetypal serpin causes rapid, irreversible stoichiometric inhibition of renegade serine protease activity and is associated with the maintenance of protease-inhibitor equilibrium in vascular and peri-vascular spaces and regulation of inflammatory response. It is the major physiological serine protease inhibitor in humans. Abnormalities in the normal synthesis or secretion of α-1-PI lead to the development of fatal progressive emphysema and hepatic cirrhosis. Ovine α-1-PI, was purified to apparent homogeneity by subjecting ovine serum to $(NH_4)_2SO_4$ precipitation, blue sepharose, size-exclusion and concanavalin-A chromatography. The purified protein of mass 58310 Da is an acidic glycoprotein. The association rate constants (K_{ass}) for elastase, trypsin and chymotrypsin were observed to be in the range of 10^6 to 10^7 M^{-1} s^{-1}.

Human α-1-PI was more thermolabile in comparison with ovine α-1-PI. The higher thermolability is mainly attributed to poorer glycosylation. Enzymatic deglycosylation of human and ovine α-1-PI resulted in diminished thermostability with a sharp decline in the thermal transition temperature yet retaining their original inhibitory potency. The glycan portion does not appear to have any influence on the inhibitory potential of α-1-PI although it plays an important role in the stability of the molecule.

Extensive insights into the trypsin, chymotrypsin and elastase interaction with ovine α-1-PI, by reactive center loop (RCL) peptide mapping point towards the involvement of Phe^{350}-Leu^{351} besides the largely conserved Met^{356}–Ser^{357} in serine protease recognition and consequent inhibition. Chemical modification of Arg, Lys and Met residues individually proves the presence of diffused sub-sites in the vicinity of Met^{356}. The molecular models of ovine α-1-PI-RCL docked against elastase, trypsin and chymotrypsin active site confirm the experimental observations that trypsin recognition site stands distinct when compared to elastase and chymotrypsin recognition sites.

Catalytic amounts of anti-coagulant heparin bind to α-1-PI and enhance its protease inhibitory activity phenomenally. The activation is allosteric and is characterized by a dual mode of interaction, a weak followed by a strong binding as depicted by

fluorescence spectroscopy. The K_{ass} for ovine and human α-1-PI inhibition of elastase was increased ~45 and 38 fold respectively. Using a combinatorial approach of multiple sequence alignment, surface topology, chemical modification of Arg and Lys residues and tryptic peptide mapping both in the presence and in the absence of heparin to identify the sequence of the heparin binding region; it was demonstrated that heparin binds to the lysyl rich region of the F-helix of α-1-PI, which differs from that of heparin-antithrombin and other heparin-serpin interactions. Molecular docking prediction approximates the three positively charged lysines (K^{154}, K^{155}, K^{174}) of human α-1-PI in this interaction. This heparin α-1-PI interaction was exploited to develop an affinity purification method, which can be used universally to obtain homogenous preparations of mammalian α-1-PIs useful for augmentation therapy. Collectively, all these findings imply that α-1-PI has a major role in regulating extracellular protease activity and the physiological activator is heparin.

Dynamic light scattering and size exclusion chromatography revealed that ovine α-1-PI undergoes a decrease in the Stokes' radius upon heparin binding. The binding constant (K_α) was $1.98\pm0.2 \times 10^{-6}$ M using fluorescence spectroscopy and $2.1\pm0.2 \times 10^{-6}$ M by equilibrium dialysis. The stoichiometry of heparin binding to ovine α-1-PI was evident to be 1.0±0.2 both by fluorescence and equilibrium dialysis. CD and FT-IR spectroscopy projected the systematic structural reorientations that α-1-PI undergoes upon heparin binding with a decrease in both α-helical and β-sheet content and a concomitant increase in β-turn and random coil elements. It is likely that these conformational changes result in the movement of the α-1-PI RCL into an extended structure that is better poised to combat the cognate protease and accelerate the inhibition.

.....Dedicated to my beloved father

Acknowledgements

*All gratitude and praise to **The lord**, for the ocean of blessings, He has showered on me.*

*I wish to express my sincere gratitude to my research supervisor **Dr. Lalitha R. Gowda,** for suggesting the problem, able guidance, valuable insight, constant encouragement and support throughout the investigation.*

*My sincere thanks to **Dr. V. Prakash,** Director, CFTRI, Mysore, for providing the necessary facilities to work in the institute and permitting me to submit the results in the form of the thesis.*

*I am grateful to **Dr. A. G. Appu Rao,** Head, Protein Chemistry and Technology, for his constant help and encouragement. My grateful acknowledgements to **Dr. Ramakrishna Gowda** for extending his openhanded advice during the course of investigation. I am also indebted to him for his support and encouragement.*

*I thank **Dr. M. R. N. Murthy** Chairman, MBU, IISc, Bangalore, for useful discussions and allowing me to use the Dynamic Light Scattering Instrument. I am grateful to **Dr. Asha Martin,** FSAQCL, for useful discussions. I thank **Ms. Asha,** CISF for all her help in FTIR experimentation and analysis. I thank my well wishers Deepa, Devaraj, Devavratha, Jimsheena, Lingaraju, Mallikarjuna, Pradeep, Rajashekar, Rohini, Santosh, Sujith, Thippeswamy, Vijay and Vinod and for their company, friendship and cooperation.*

*I am indebted to all **scientists**, **staff members** in the department, both past and present, for creating an inspiring working atmosphere to complete my research work. The help rendered by Ms. Anupama, Gopal, Basavanna and Chikkaswamy is profoundly acknowledged.*

*It is my profound duty to thank **CSIR,** New Delhi for the financial support in the form of fellowship. I acknowledge the timely help and cooperation of the staff of FOSTIS-Library and Central Instrument Facility and Services.*

*Very special thanks to my sister, **Veer Bala** and brother-in-law, **Ravi,** who stood as a tower of strength during moments of frustration & motivated me towards the achievement of my goal.*

*No words suffice my gratefulness and how indebted I am to my brothers, **Jagveer** & **Vishal** without whose moral support and encouragement, I would have never been able to reach this stage of life.*

*Special thanks to my little nephew, **Shivam,** whose mere presence in my life inspired me to move ahead successfully.*

*I have saved the best compliments for my Father, **Sh. Jagmohan Gupta,** who I feel God sent to make me strong and took him away to make me stronger.*

*To the one person whom I try to convey my thanks, words fail me as she stood by me through the thick and thin in all my endeavors. At this juncture, "Dear **Mama,** All I can say is Thank You."*

Knowledge is piling up facts, and wisdom is simplifying it. Thanks to the creators of google, entire web sources, journals, magazines, newspapers, for helping me in acquisition of thoughts and translation of scientific knowledge.

Vivek Kumar Gupta

CONTENTS

LIST OF ABBREVIATIONS

λ	Wavelength
α-1-PI	α-1-proteinase inhibitor
°C	Degree centigrade
µg	Microgram
[E]	Enzyme concentration
[I]	Inhibitor concentration
[S]	Substrate concentration
µL	Microliter
3D	Three dimensional
Å	Angstrom unit
A.U.	Absorbance unit
A1AT	Alpha-1-antitrypsin
AM1	Austin model 1
APNE	N-acetyl-DL-phenylalanine-β-napthyl ester
APS	Ammonium persulfate
AT	Antithrombin
BAPNA	α-N-Benzoyl-DL-arginine-*p*-nitroanilide
BCIP	5-Bromo-4-chloro-3-indolylphosphate
BSA	Bovine serum albumin
BTPNA	N-Benzoyl-L-tyrosine-*p*-nitroanilide
CAPS	3-[Cyclohexylamino]-1-propanesulfonic acid
CBB	Coomassie brilliant blue
CD	Circular dichroism
cDNA	Complementary DNA
CIU	Chymotrypsin inhibitory units
cm	Centimeter
Con-A	Concanavalin-A

CU	Chymotrypsin unit
Da	Daltons
DEAE	Diethylaminoethyl
DLS	Dynamic light scattering
DMSO	Dimethylsulfoxide
E_a	Activation energy
EDTA	Ethylene diamine tetra acetic acid
EIU	Elastase inhibitory units
FTIR	Fourier transform infra-red
g	Grams
GAG	Glycosaminoglycan
GlcNAc	N-acetyl glucosamine
h	Hour
HC II	Heparin co-factor II
HPLC	High performance liquid chromatography
HRP	Horse raddish peroxidase
IU	Inhibitory units
K_α	Binding constant
K_{ass}	Association rate constant
K_B	Boltzmann constant
kcal	Kilo-calorie
K_D	Dissociation constant
K_i	Inhibitory constant
kJ	Kilo-joule
K_r	Inactivation rate constant
K_{sv}	Stern-Volmer constant
L	Liter
LMWH	Low molecular weight heparin
M	Molar concentration
MALDI-TOF	Matrix Assisted Laser Desorption Ionization-Time of flight
min	Minute

mL	Milliliter
mM	Millimolar
MNDO	Modified neglect of diatomic differential overlap
M_r	Molecular weight
N. D.	Not determined
NaPi	Sodium phosphate
nm	Nanometer
NMR	Nuclear magnetic resonance
NSAPNA	N-Succinyl-Ala-Ala-Ala-*p*-nitroanilide.
PAGE	Polyacrylamide gel electrophoresis
PAI-1	Plasminogen activator inhibitor-1
PBS	Phosphate buffered saline
PDB	Protein data bank
PEDF	Pigment epithelium derived factor
pI	Isoelectric point
PITC	Phenylisothiocyanate
PNGase-F	Peptide: N-glucosidase-F
PPE	Porcine pancreatic elastase
PVDF	Polyvinilidine diflouride membrane
R. M. S. D.	Root mean square deviation
RCL	Reactive center loop
RP	Reverse phase
R_s	Stokes' radius
R_T	Retention time
S	Second
SDS	Sodium dodecyl sulfate
SPAAT	Short C-terminal peptide from alpha-1-antitrypsin
TEA	Triethylamine
TEMED	N,N,N'N'-Tetramethyl 1, 2-diaminoethane
TFA	Trifluoroacetic acid
TIU	Trypsin inhibitory unit

TLCK	Tosyl-lysine chloromethylketone
T_m	Melting temperature
TNBS	2, 4, 6-Trinitrobenzenesulfonic acid
TPCK	Tosyl-phenyalanine chloromethylketone
Tris	Tris (hydroxymethyl) amino methane
TU	Trypsin unit
UFF	Universal force field
UV-VIS	Ultraviolet-visible
v/v	Volume by volume
V_e	Elution volume
VMD	Visual molecular dynamics
vs	Versus
w/v	Weight by volume
ε	Molar extinction coefficient

LIST OF ILLUSTRATIONS

LIST OF TABLES

1. INTRODUCTION

Protein protease inhibitors are ubiquitous and vital for maintaining protease-protease inhibitor equilibrium in the living systems. Protease or peptidase is any enzyme that conducts proteolysis, that is, begins protein catabolism by hydrolysis of the peptide bonds that link amino acids together in the polypeptide chain. A tremendous amount of research has been carried out to study protease inhibitor structure and function ever since Fermi and Pernossi (1894) reported the protease inhibitory activity in human serum. This is essential considering that proteases constitute 1-5 % of the gene content in all organisms and are involved in a multitude of physiological reactions from simple digestion of food proteins to highly regulated cascades (e.g., the blood clotting, inflammation, the complement system, apoptosis pathways, signalling pathways and the invertebrate prophenoloxidase activating cascade in both prokaryotes and eukaryotes). Proteases determine the lifetime of other proteins like hormones, antibodies, or other enzymes, constituting one of the fastest switching-on and off regulatory mechanisms of an organism. By complex co-operative action the proteases proceed as a cascade of reactions which result in amplification of the organism response to the physiological signal. Spatio-temporal control of protease activity by inhibitors is crucial for maintenance of several physiological functions. These inhibitors may be serine, threonine, cysteine, aspartic acid, metallo- or glutamic acid protease inhibitors. The serine protease inhibitors are highly diverse and important both structurally and functionally. A particular class of serine protease inhibitors (serpins) is a highly interesting and unique class of suicide inhibitors, which encounters serine proteases and inhibits them. These are 40,000-60,000 Da glycoproteins which react with serine proteases irreversibly. These have been studied extensively as model systems for elucidation of the mechanism of inhibition of proteases and protein polymerization. Ligand protein interactions and the resultant conformational changes is another distinctive feature of serpins. The involvement of serpins in prevention of tumorogenesis, inflammation and fluid phase biological events has gained considerable momentum. A variety of serpins have been identified and characterized from a wide range of species both intra-cellular and extra-cellular. Serpins have been reviewed extensively (Silverman et al., 2001, Gettins, 2002; Parfrey et al., 2003; van Gent et al., 2003; Wood and

Stockley, 2007). In the past 10 years, the general structural and mechanistic features of the serpins have been significantly resolved. Although several mechanistic questions persist, the field has matured to the point that most of the remaining issues relate to the biological functions of individual serpins, and although new serpins are being identified almost daily, it is still not known what many of the old ones do. A comprehensive review of the literature on physiological serine proteases, serpins and their mechanism of action is presented in this section. The effect of glycosaminoglycan (GAG) heparin on the serpin activity is also reviewed. The essential role of protein-GAG interactions in the regulation of various physiological processes has been recognized for several decades but it is only recently that the molecular basis underlying such interactions has emerged.

Serine Proteases

Serine proteases are a class of peptidases that are characterised by the presence of a Ser residue at the active site of the enzyme. The serine-dependent mechanism of peptide bond hydrolysis is most widely studied as the serine proteases (EC 3.4.21) are the most abundant group, and are extremely widespread and diverse. Serine proteases are grouped according to sequence and structural homology.

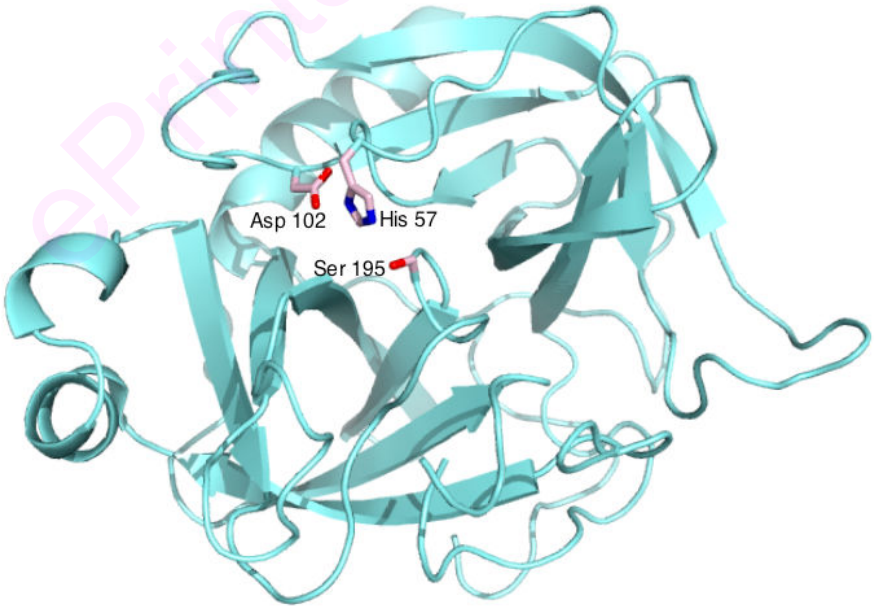

Figure 1. 1. An archetype serine protease chymotrypsin (PDB ID 4CHA). The three catalytic residues (His^{57}, Asp^{102} and Ser^{195}) are labeled.

The major clans found in humans include the chymotrypsin, the subtilisin-like, alpha/beta hydrolase, and signal peptidase (James, 1976). Some of the most important physiological functions are attributed to the chymotrypsin family members. Figure 1. 1. represents the general structure of a chymotrypsin family member.

Chymotrypsin-family of serine proteases

The three serine proteases of the chymotrypsin-like clan that have been studied in greatest detail are elastase, trypsin and chymotrypsin. All three enzymes are synthesized by the pancreatic acinar cells and secreted into the small intestine. These enzymes are present in abundance elsewhere in the physiological system and exhibit considerable similarity in their three dimensional structure. They are differentiated by the highly specific scissile peptide bond which is being cleaved. Each of the digestive serine proteases target different regions of a polypeptide, based upon the side chains of the amino acid residues surrounding the site of cleavage:

- Chymotrypsin is responsible for the preferred cleavage of peptide bonds following a bulky hydrophobic amino acid residue including Phe, Trp and Tyr which fit into its snug hydrophobic pocket.
- Trypsin is responsible for cleaving peptide bonds following a positively-charged amino acid residue. There exists an aspartic acid residue at the base of the pocket. This can interact with positively-charged residues such as Arg and Lys on the peptide to be cleaved.
- Elastase is responsible for cleaving peptide bonds following a small neutral amino acid residue, such as Ala, Gly and Val. The pocket that is there in "chymotrypsin" is now partially filled with Val and Thr, rendering it a mere depression, which can accommodate these smaller amino acid residues.

The combination of these three enzymes renders an incredibly effective digestive team, primarily responsible for the digestion of proteins. It is evident from the superimposed structures of these three proteases that they exhibit close overall homology (Figure 1. 2)

Figure 1. 2. Superimposition of the three dimensional structures of trypsin (yellow) elastase (violet) and chymotrypsin (green). The active site residues are indicated in red (http://chemistry.umeche.maine.edu/).

Catalytic mechanism of serine proteases

The main player in the catalytic mechanism in the chymotrypsin family of enzymes is the catalytic triad which is located in the active site of the enzyme, where catalysis takes place, and is conserved in all serine proteases. The triad is a co-ordinated structure consisting of three essential amino acids: histidine (His^{57}), serine (Ser^{195}) and aspartic acid (Asp^{102}) located in proximity to each other (Figure 1. 2).

During catalysis, an ordered mechanism occurs in which several intermediates are generated. The catalysis of the peptide cleavage can be seen as a ping-pong catalysis, in which a substrate binds (the polypeptide being cleaved), a product is released (the N-

A)

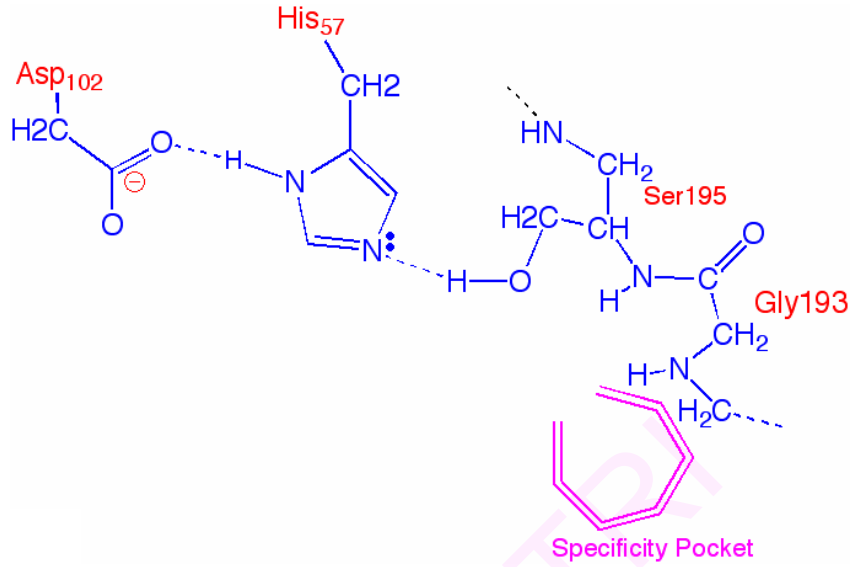

B)

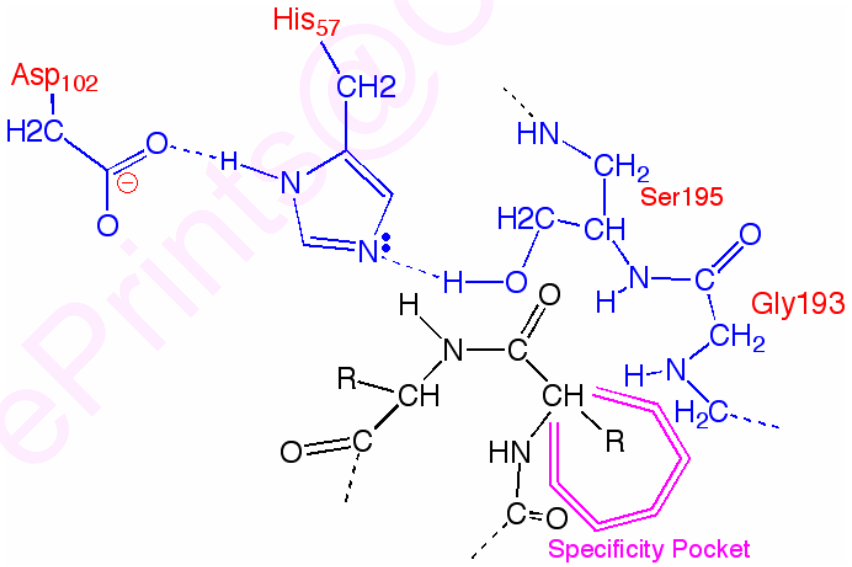

Figure 1. 3. Role of the catalytic triad in the serine proteases. A) enzyme alone B) the substrate side chain is recognised by a specific pocket on the enzyme and a proton is transferred from Ser^{195} to His^{57}. The positively charged imidazole ring is stabilized by electrostatic interaction with negatively charged Asp^{102}

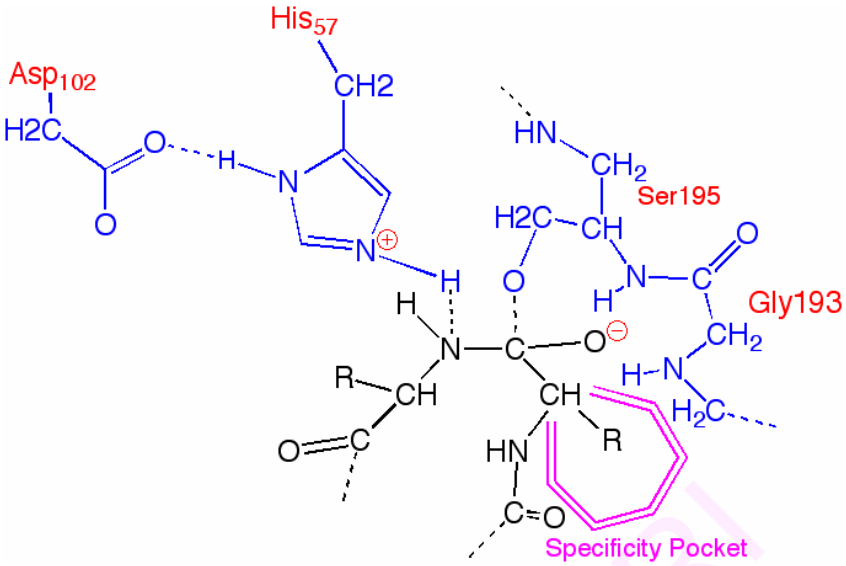

Figure 1. 3. (contd) (c) the nucleophillic attack of the active site Ser on the carbonyl carbon atom of the scissile peptide bond to form the tetrahedral intermediate which decomposes to the acyl-enzyme intermediate through general acid catalysis by the polarised His. This is followed by loss of the amine product and its replacement by the H_2O molecule. The acyl enzyme intermediate is further hydrolysed by H_2O and active enzyme liberated.

terminal half of the peptide), another substrate binds (water), and another product is released (the C-terminal half of the peptide). The process can be condensed into three steps: a) substrate binding b) progress to transition state and c) collapse from transition state as summarized in Figure 1. 3.

A conserved Ser^{195} of chymotrypsin has an -OH group that acts as a nucleophile, attacking the carbonyl carbon of the scissile peptide bond of the substrate.

- The polypeptide substrate binds to the surface of the enzyme in such a way that scissile bond is inserted into the active site of the enzyme.
- The Ser-OH attacks the carbonyl carbon, and the nitrogen of His accepts a proton from the -OH and a pair of electrons from the double bond of the carbonyl oxygen moves to the oxygen of –OH to form a tetrahedral intermediate (Figure 1. 3 B).

- The bond between C-N of the peptide bond is now broken. The covalent electrons creating this bond move to attack the hydrogen of the His, breaking the connection. The electrons that previously moved from the carbonyl oxygen double bond move back from the negative oxygen to recreate the bond, generating an acyl-enzyme intermediate.
- Water comes in to the reaction and replaces the NH_2-terminus of the cleaved peptide, and attacks the carbonyl carbon. Once again, the electrons from the double bond move to the oxygen making it negative, as the bond between the oxygen of the water and the carbon is formed. This is co-ordinated by the nitrogen of the His which accepts a proton from the water. Overall, this generates another tetrahedral intermediate.
- In a final reaction, the bond formed in the first step between the Ser and the carbonyl carbon moves to attack the hydrogen that His just acquired. Now electron-deficient carbonyl carbon re-forms the double bond with the oxygen. As a result, the C-terminus of the peptide is now ejected.

Protein-protease inhibitors

Protease inhibitors by definition are molecules that inhibit the function of proteases. Most of the naturally-occurring protease inhibitors happen to be proteins. Normal human plasma contains at least seven protease inhibitors, which account for more than 10 % of the total protein and control a variety of critical events associated with connective tissue turnover, coagulation, fibrinolysis, complement activation and inflammatory reactions (Haupt et al., 1970). After albumin and immunoglobulins these constitute by weight the third largest group of functional proteins in human plasma. Protein-protease inhibitors are classified either by the type of protease they inhibit, or by their mechanism of action. These belong to cysteine, serine, threonine, aspartic acid or metalloprotease class of inhibitors. Based on their mechanism of inhibition they are either active site, transition state or suicide inhibitors. In medicine, the term protease inhibitor is often used interchangeably with alpha 1-antitrypsin (A1AT or α-1-PI). which is involved in a pathological state, namely alpha 1-antitrypsin deficiency.

Suicide or mechanism based inhibition

Suicide inhibition, also known as mechanism-based inhibition, is an irreversible enzyme inhibition that occurs when an enzyme binds a substrate analogue and forms a complex during the "normal" catalytic reaction. Mechanism-based protease inhibitors are substrates that undergo a molecular re-arrangement to a reactive species after cleavage by the cognate enzyme. The product then binds covalently to the enzyme and inactivates it. The enzyme does not do the deed willingly, but is the victim of deceit (Miesowicz and Bloch, 1979). The catalysis generates one of three reactive groups on the substrate analogue: an α- or β-haloketone, a βγ unsaturated carbon, or a βγ acetylenic carbon. Suicide inhibitors are most useful in rational drug designing. The main goal of this approach is to create substrates that are recognised by the enzyme as highly specific until within active site, but once the reaction initiates they entrap the enzyme in such a way that it can function no more in its normal capacity. Molecules based on this approach have the advantage of offering very few side effects.

In the case of those inhibitors obeying this mechanism, hydrolysis of the reactive site peptide bond does not proceed to completion (Laskowski and Kato, 1980) between the modified form of inhibitor either with peptide bond intact or with peptide bond cleaved. The following simplified kinetic scheme summarizes the reaction:

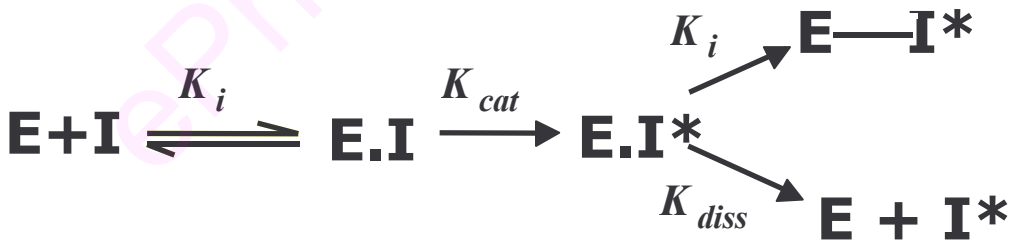

$K_i >> K_{diss}$

where E is the protease, I and I* are virgin and modified inhibitor respectively, and E-I* is the stable complex.

The serpins constitute the best studied example of suicidal protein inhibitors: they form 1:1 complexes with their target protease. Subsequently the complexes are removed from circulation and catabolised (Carrell and Travis, 1985). In general terms, the serpins

are thought to function by presenting the reactive site as an ideal substrate to the target protease: a lock into which the key fits so precisely that it fails to leave it.

Serpins

Serpins are a group of proteins with similar structure that were first identified as a set of proteins able to inhibit proteases. These comprise of a single polypeptide chain and variable number of oligosaccharide side chains: four in antithrombin, three in alpha-1-protease inhibitor (α-1-PI) and one in ovalbumin. The greatest variation occurs at the NH_2-terminus, where extension of the structure provides for special functions.

The acronym 'Serpin' was coined in 1985 (Carrell and Travis, 1985) to describe a family of serine protease inhibitors that shared a precise structural architecture and a modest sequence identity (Hunt and Dayhoff, 1980). As the only protease inhibitor family found in all branches of life (bacteria, archaea, eukarya and viruses), it is not an exaggeration to say that serpins are everywhere. Every new genome that is sequenced reveals serpins in the most unexpected places. These form the main protein component of chicken eggs, the third most abundant protein family in the blood, part of the host defense mechanism of insects, and present in hyper-thermophilic bacteria, nematodes and even plants (Silverman et al., 2001; Gettins, 2002; Van Gent et al., 2003; Irving et al., 2003). The first members of the serpin superfamily to be extensively studied were the human plasma proteins antithrombin and α-1-PI, which play key roles in controlling blood coagulation and in the maintainence of physiological protease-inhibitor equilibrium, respectively. Hunt and Dayhoff (1980) made the surprising discovery that both these molecules share significant amino acid sequence similarity to ovalbumin, and they proposed a new serpin protein superfamily. Serpins are thus the largest and most diverse family of protease inhibitors (Rawlings et al., 2004). While most serpins control proteolytic cascades, certain serpins do not inhibit enzymes, but instead perform diverse functions such as storage (ovalbumin), hormone carrying proteins (thyroxine-binding globulin, cortisol binding globulin) and tumor suppressor proteins (maspin) (Silverman et al., 2001). As serpins control processes such as coagulation and inflammation, these proteins are at the centre stage of medical research.

The average protein size of a serpin family member is 350-400 amino acids, but gene structure varies in terms of number and size of exons and introns (Patson, 2000). The majority of serpins act to control proteolytic activity in a myriad of contexts, including coagulation, fibrinolysis and complement activation. Additionally, they can also be found in the intra-cellular (even intra-nuclear) compartment and perform biological functions that do not necessarily require their protease inhibitory function (Medcalf, 2005). Serpins use an extraordinary mechanism of protease inhibition that depends on a rapid and marked conformational change and causes destruction of the covalently linked protease. Serpins thus provide stoichiometric, irreversible inhibition, and their dependence on a conformational change is exploited for signaling and clearance (Huntington, 2006). This mechanistic complexity however renders serpins highly susceptible to disease causing mutations. Recent crystal structures reveal the intricate conformational rearrangements involved in protease inhibition, activity modulation and the unique molecular pathology of the remarkable shape shifting serpins.

The serpin activity and conformational stability is greatly influenced and regulated by certain ligands e.g., heparin binding to antithrombin, HC-II and PCI increases their rate of protease inhibition manifold (Pike et al., 2005). Similarly, citrate ion increases the conformational stability of α-1-PI (Bottomley and Tew, 2000).

Serpin classification

The serpin nomenclature was established in 2001 (Silverman et al., 2001). The naming system is based upon a phylogenetic analysis of ~ 500 serpins. Serpins are divided into groups based on their composition (Irving et al., 2000). The human serpins are classified in nine groups A to I. The largest groups are the α-1-PI–like and ovalbumin-like serpins which are designated as Serpin A (10 members) and Serpin B (14 members) respectively. The groups serpin C and serpin D consist of antithrombin and heparin cofactor II. Serpin I is comprised of nine serpins. The serpin family continues to grow and to date over 1000 serpins have been identified (Irving et al., 2002).

Extracellular and intracellular localization of serpins

Serpins regulate the proteolytic cascades central to blood clotting (antithrombin), the inflammatory response (α-1-PI, antichymotrypsin and C1 inhibitor) and tissue remodelling (Plasminogen activator inhibitor-1 or PAI-1). Approximately two thirds of mammalian serpins perform extracellular roles, which is not necessarily inhibitory in function. For example, thyroxine-binding globulin and cortisol binding globulin transport the sterol hormones thyroxine and cortisol respectively (Barrett and Rawlings, 2001; Klieber et al., 2007).

Several intracellular members of the serpin superfamily have been identified (Campbell, 2003; Zhou et al., 2006). All the nine serpins in *Caenorhabditis elegans* lack signal sequences and are intracellular (Remold-O'Donnell, 1992). It seems likely that the serpin ancestral to human α-1-PI was an intracellular molecule. The primary target proteases of intracellular inhibitory serpins are difficult to identify. These molecules appear to perform overlapping roles and also there is lack of precise functional equivalents of human serpins in laboratory animals. An important function of intracellular serpins is to probably protect against the inappropriate activity of proteases inside the cell (Coughlin, 1993). For example, one of the best characterized human intracellular serpins is SERPINB9, which inhibits protease granzyme B. Thus, SERPINB9 has a role in protection against inadvertent release of granzyme B and unwanted activation of apoptotic pathways (Pak et al., 2004).

Intracellular serpins also perform roles distinct from protease inhibition. For example, maspin, a non-inhibitory serpin, is important for preventing metastasis in breast and prostate cancers (Bird et al., 1998; Bird, 1999). Non-inhibitory heat shock serpin HSP47, is an exception, which is a chaperone essential for collagen folding and shuttles between the golgi bodies and the endoplasmic reticulum (Luo et al., 2007). Avian nuclear cysteine protease inhibitor MENT acts as a chromatin remodelling molecule in avian blood cells (Zou et al., 1994; Schick et al., 1998). Phylogenetic studies reveal that most of the intracellular serpins belong to a single clade.

The serpin metastability

The native form of most proteins is thermodynamically the most stable (Anfinsen, 1973). However, the native form of serpins is not their most stable but a metastable state (Wiley and Skehel, 1987; Huber and Carrell, 1989). The native metastability of serpins is crucial to their physiological functions, such as plasma protease inhibition (Huber and carrel, 1989; Stein and Carrell, 1995), hormone delivery (Pemberton et al., 1988), Alzheimer filament assembly (Abraham et al., 1988; Ma et al., 1994; Carrell and Lomas, 1997) and extracellular matrix remodeling (Stefansson and Lawrence, 1996). The final stable state of serpins is only reached when the function (complex formation with a protease) is executed. Other metastable proteins include influenza hemagglutinin (Bullough et al., 1994) and α-lytic protease (Baker et al., 1992). All these proteins use their metastability as a source of stored potential energy that is expended to perform their biological function. For serpins, the metastable native state possesses an intrinsic structural flexibility, which permits a rapid conformational change that is required for protease inhibition. The energetic basis of this inhibitory mechanism is the incorporation of the reactive center loop (RCL) as a strand into the β-sheet A that is thermodynamically favorable (Bruch et al., 1988). However, mutated serpins can also adapt another thermodynamically favorable state by inserting their RCL into an adjacent serpin molecule rendering them vulnerable to protein misfolding and the formation of inactive long chain polymers (serpinopathies) (Lomas et al., 1992; Carrell and Lomas, 1997). Pathologically, this is manifested into a range of loss-of-function diseases such as emphysema, liver cirrhosis, thrombosis and dementia (Lomas and Carrell, 2002). An understanding of the determinants of metastability in serpins thus has relevance to important human pathologies. Thus, serpins are of particular interest to the structural biologists and protein chemists, because of the unique and dramatic conformational change these undergo when they inhibit target proteases (Huntington et al., 2000). This is unlike most classical protease inhibitors which function as simple "lock and key" molecules that bind to and block access to the protease active site (bovine pancreatic trypsin inhibitor).

Alpha 1-proteinase inhibitor (α-1-PI)

α-1-PI has been studied and characterized extensively over the past two decades from a wide array of organisms especially mammals including human (*Homo sapiens*) (Bao et al., 1988), rabbit (*Oryctolagus cuniculus*) (Saito and Sinohara, 1990), rat (*Rattus norvegicus*) (Misumi et al., 1990), horse (*Equus caballus*) (Patterson et al., 1991), sheep (*Ovis aries*) (Mistry et al., 1991), guinea Pig (*Cavia porcellus*) (Suzuki et al., 1991), pig (*Sus scrofa*) (Archibald et al., 1996), cow (*Bos taurus*) (Harhay et al., 2005) and mouse (*Mus musculus*) (Bernhard et al., 2007).

The first function ascribed to α-1-PI was the inhibition of trypsin; hence it is also termed α-1-antitrypsin (Schultze et al., 1962). Its deficiency state was first described by Laurell and Eriksson (1963). Human α-1-PI has been shown to inactivate virtually all mammalian serine proteases tested to date, including pancreatic and neutrophil elastase (Schwick et al., 1966; Janoff, 1972; Baugh and Travis, 1976), pancreatic trypsin and chymotrypsin (Schwick et al., 1966), neutrophil cathepsin G (Beatty et al., 1980), thrombin (Matheson and Travis, 1976), plasmin (Rimon et al., 1966; Hercz, 1974), acrosin (Fritz et al., 1972), tissue kallikrein (Fritz et al., 1969), Factor Xa (Ellis et al., 1982), Factor XIa (Scott et al., 1982), skin and synovial collagenases (Tokoro et al., 1972; Harris et al., 1969) and urokinase (Clemmensen and Christensen, 1976).

The mechanism by which α-1-PI inhibits a host of different serine proteases has been well documented. α-1-PI protects tissues from enzymes of inflammatory cells, primarily elastase, and is present in human blood at 1.5 - 3.5 g/L. The translated protein sequence of the ovine α-1-PI shows a homology of 97 % with the amino acid sequence of the human α-1-PI (Brown et al., 1989). The concentration of α-1-PI in sheep plasma is 1.69±0.21 g/L and is comparable to α-1-PI concentration in human plasma (Tetley et al., 1989). The liver synthesizes and secretes approximately 2 g of α-1-PI per day into circulation. In the absence of α-1-PI, elastase is free to break down elastin which contributes to the contractility of the lungs resulting in respiratory complications such as emphysema and chronic obstructive pulmonary disease (COPD). α-1-PI has also been thought to protect plasma proteins against the deleterious effects of trypsin which is massively liberated into the blood stream in the course of acute pancreatitis. It is capable

of inhibiting a wide variety of serine protease, including proteases involved in blood coagulation, fibrinolysis and kinin generation (Heimburger and Trobisch, 1971; Janoff, 1972; Kueppers, 1973; Ohlsson and Olsson 1973). Even though α-1-PI is a plasma protein of hepatic origin; its primary site of physiological action is the lung. α-1-PI appears to be transported by passive diffusion into the alveolar structure of the lung, protecting this organ from destruction by polymorphonuclear leucocyte elastase (Laurell, 1963; Briscoe et al., 1966; Sharp et al., 1969; Olsen et al., 1975; Tuttle, 1975).

Purification and molecular properties of α-1-PI

α-1-PI has a M_r close to antichymotrypsin, and albumin, which is the major serum protein. This renders α-1-PI preparations susceptible to contamination by other proteins. Several purification procedures have been reported using size-exclusion, DEAE-ion exchange chromatography, concanavalin-A sepharose affinity chromatography, thiol exchange matrices, α-1-PI-antibody affinity chromatography and sepharose-4B bound anhydro-chymotrypsin (Melgarejo et al., 1996; Mistry et al., 1991; Liener et al., 1973; Drechsel et al., 1984). Recently, high yielding homogenous preparation protocols have been reported (Gupta et al., 2008; Gupta and Gowda, 2008).

The inhibition capacity of α-1-PI towards elastase, cathepsin G and trypsin is determined with Suc-Ala-Ala-Ala-NH-Np, Suc-Ala-Ala-Ala-Pro-Phe-NH-Np and Bz-Arg-NH-Np as substrates (Nakajima et al., 1979; Erlanger et al., 1961). Human α-1-PI inhibits trypsin, chymotrypsin and elastase on a 1: 1 molar basis. This is unlike ovine α-1-PI which although is a potent inhibitor of trypsin (1: 1 molar ratio) but is a poor inhibitor of human leucocyte and porcine pancreatic elastase (elastase/α-1-PI molar ratios 0.07: 1 and 0.13: 1 respectively) (Mistry et al., 1991).

Trypsin and chymotrypsin compete for inhibitory sites on α-1-PI suggesting that the inhibitor has the same or overlapping inhibitory sites on α-1-PI. It inhibits subtilisin, a proteolytic enzyme that contains Ser, His and Asp residues at its active site in common with mammalian serine proteases. It fails to inactivate acetyl-cholinesterase, a non-proteolytic enzyme whose active site contains a reactive serine residue, suggesting that this residue alone is not sufficient for inhibition by α-1-PI.

Human α-1-PI contains a Met residue at 358 position in the reactive site and thus is highly susceptible to oxidative inactivation. The protease inhibitory activity can be partly restored on providing a reducing environment (Griffiths et al., 2002). Treatment of α-1-PI with phenylglyoxal blocks its action on trypsin but not on chymotrypsin. The change in activity is presumptive evidence that Arg residues are responsible for trypsin specific inhibition and that trypsin inhibitory site contains an Arg residue (Cohen et al., 1973). Antitryptic activity can be regenerated with removal of the blocking groups.

Structure and function of α-1-PI

The 12.2 kb α-1-PI gene is composed of seven exons and six introns and is located on the long arm of the fourteenth chromosome (14q32.1). Translation of the gene results in a 418-amino-acid protein that includes a signal peptide. The α-1-PI protein is post-translationally modified in the endoplasmic reticulum to produce a 53,000 Da glycosylated protein. It is comprised of 394 amino acids and three N-linked carbohydrate chains. The α-1-PI molecule is fairly asymmetric, having overall dimensions of 67 × 32 × 32 Å (Kalsheker, 1989). The crystal structure of α-1-PI is shown in Figure 1. 4 and its various secondary structural elements labelled. The structure of α-1-PI reveals a chracteristic serpin fold (Loebermann et al., 1984; Stein et al., 1990). It has the typical three β-sheets (termed A, B and C) and eight or nine α-helices. Almost all of the polypeptide chain is involved in secondary structure. Sheet A contains six strands running parallel to the long axis of the molecule and extending about two-thirds of its length. The reactive site Met^{358} is at the end of one of the central strands of sheet A. Sheet B overlaps with sheet A at the opposite end from Met^{358}, and has six strands that are perpendicular to the strands of A. Four strand of sheet B, together with the three strands that comprise sheet C, form a β-barrel. Ser^{359} is located at the end of one of the outer strands of sheet C. A cluster of eight helices packs against sheets A and B, and one helix runs parallel to the opposite side of sheet A. Serpins also possess a protruded region termed the RCL which in inhibitory molecules determines the specificity for protease inhibition and comprise the initial interaction with the target protease. In α-1-PI, the RCL is held at the top of the molecule and is not pre-inserted into the A β-sheet. This

conformation commonly exists in dynamic equilibrium with a partially inserted native conformation (Whisstock and Bottomley, 2006).

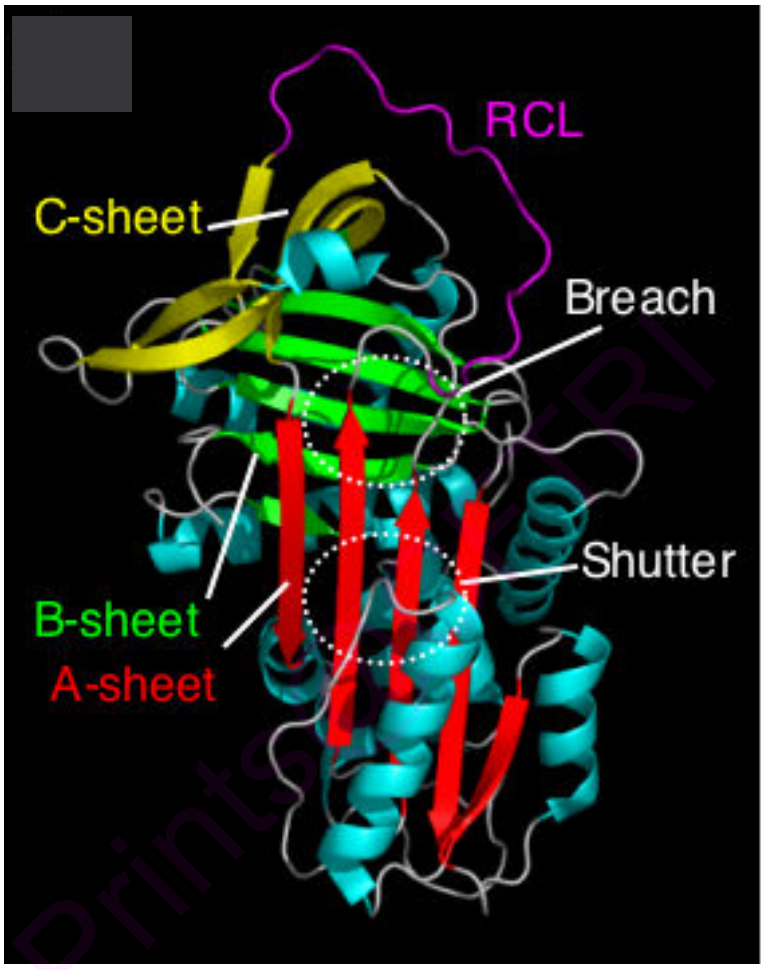

Figure 1. 4. The crystal structure of native human α-1-PI (PDB ID 1QLP). The five stranded A-sheet is in red, the six stranded B-sheet in green and the four stranded C-sheet in yellow. Alpha-helices are shown in cyan. The RCL is at the top of the molecule in magenta. Two functionally important regions of the serpin, the breach and the shutter, are labelled.

Most serpins inactivate enzymes by covalent binding, necessitating very high levels to perform their optimal function. In acute phase conditions, a still higher elevation is required to limit the damage caused by activated neutrophil granulocytes and the enzyme elastase. Like all serine protease inhibitors, α-1-PI has a characteristic secondary structure of beta sheets and alpha helices. Mutations in these areas can lead to

polymerisation and accumulation in the liver causing hepatic cirrhosis and pulmonary emphysema (DeMeo and Silverman, 2004; Perlmutter, 2005). α-1-PI covalently binds and irreversibly inactivates the proteases *in vitro*. Pulmonary symptoms of α-1-PI deficiency include dyspnea, cough, wheeze, sputum production, and lower respiratory tract infections. Within a few decades, the progressive destruction results in chronic obstructive bronchitis and lung emphysema (Needham and Stockley, 2004).

α-1-PI deficiency is often described as a storage disease of the hepatocellular endoplasmic reticulum. However, when one takes into account the better-known lysosomal storage diseases, α-1-PI deficiency may be better described as a conformational disease, similar to amyloidosis, because the reason for the storage is a change in peptide conformation rather than a functional deficit of cellular organelles (Perlmutter, 2002).

In addition to its antiproteinase activity, α-1-PI seems to have an important role in the regulation of inflammatory processes in the lung. The molecule as a whole has anti-inflammatory effects. It may inhibit immune responses; stimulate tissue repair and matrix production and exhibit antibacterial activities (Hadzic et al., 2006).

On the face of it, α-1-PI may appear to represent an unnecessarily complicated solution to the problem of protease inhibition. However, the serpin scaffold provides several important evolutionary advantages over more standard 'lock and key' like protease inhibitors, including the ability to function as highly controllable sensors and inhibitors of proteolysis. Conversely, complexity renders the α-1-PI scaffold vulnerable to non-productive outcomes, most notably the formation of domain-swapped loop-sheet polymers (Lomas et al., 1992). The reactive site of α-1-PI possesses Met which is not unusual since it has a polarizable side chain, which permits it to assume a positive charge in accommodating the active site of trypsin-like enzymes or to fit equally well into the hydrophobic centers of both chymotrypsin and elastase. Figure 1. 5 diagrammatically represents the protease-α-1-PI encounter. The serpin's RCL is recognized by the protease active site. The two interact with each other and α-1-PI is cleaved at the RCL. This brings about a massive conformational change in α-1-PI. The protease gets entrapped in this change and an inactive complex is formed.

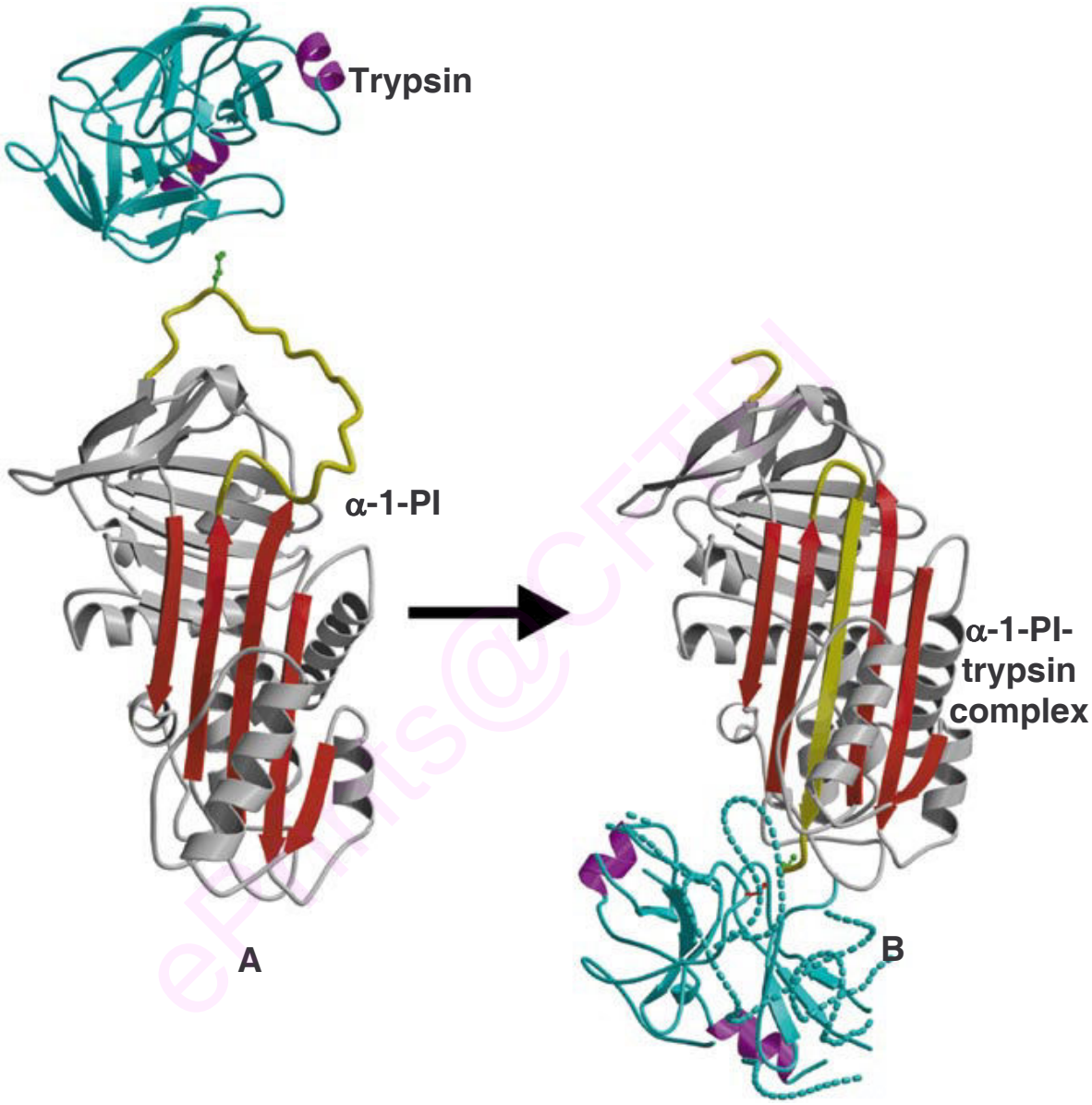

Figure 1. 5. Representation of α-1-PI interaction with trypsin before and after the reaction. A) Non-covalent interface between α-1-PI (PDB ID 1QLP) and rat trypsin (PDB ID 1K9O) prior to complex formation B) Final complex between α-1-PI and inactive trypsin (PDB ID 1EZX).

Nature of complex formation

The protein contains a single reactive site, centered around a Met-Ser sequence of 36 amino acid residues from the C-terminus. Proteases are inhibited by a 1:1 complex formation, which apparently involves cleavage of the reactive site peptide bond of the inhibitor. Such complexes are very stable and cannot be dissociated by either acidification or treatment with strong denaturing reagents. The modified inhibitor consists of two peptides of M_r 47,000 and 4000, which remain associated in 6 M guanidine and 1 % acetic acid, but can be separated by SDS-polyacrylamide gel electrophoresis (Johnson and Travis, 1978; Boswell et al., 1983).

α-1-PIs form complexes with their target enzymes that resist dissociation by denaturing agents such as SDS or urea. This implies that a covalent interaction must exist between the protease and inhibitor (Bieth et al., 1974; Moroi and Yamasaki, 1974; Owen, 1975; Harpel and Cooper, 1975; Moroi and Aoki, 1977). If a bond is formed it must exist between the O^{γ} of the catalytic serine of the enzyme and the carbonyl carbon of the reactive site peptide bond of the inhibitor; in other words inhibition is presumed to result from the establishment of a stable acyl enzyme derivative. Whether the native complex contains a fully formed covalent bond between enzyme and inhibitor or whether this bond is formed as a consequence of the denaturing conditions required for its detection has not yet been resolved; however, the establishment of a covalent link has been claimed as evidence for a functionally irreversible complex (Moroi and Yamasaki, 1974; Owen, 1975). The mechanism of protease inhibition by α-1-PI is explained in Figure 1. 6. The RCL of α-1-PI acts as a substrate and is recognized by the catalytic triad. The scissile bond of the RCL is cleaved but Ser^{195} forms a covalent bond and before the hydrolysis takes place the protease gets entrapped in the resultant conformational change of the serpin and gets distorted structurally during complex formation.

Human leucocyte elastase is the primary target of α-1-PI

α-1-PI is considered the most prominent serpin in medicine. The genetic deficiency of α-1-PI can be correlated with the development of pulmonary emphysema, a disease that can be artificially induced in animals by administration of proteases that can degrade elastin. There have been no other disorders reported for α-1-PI deficient

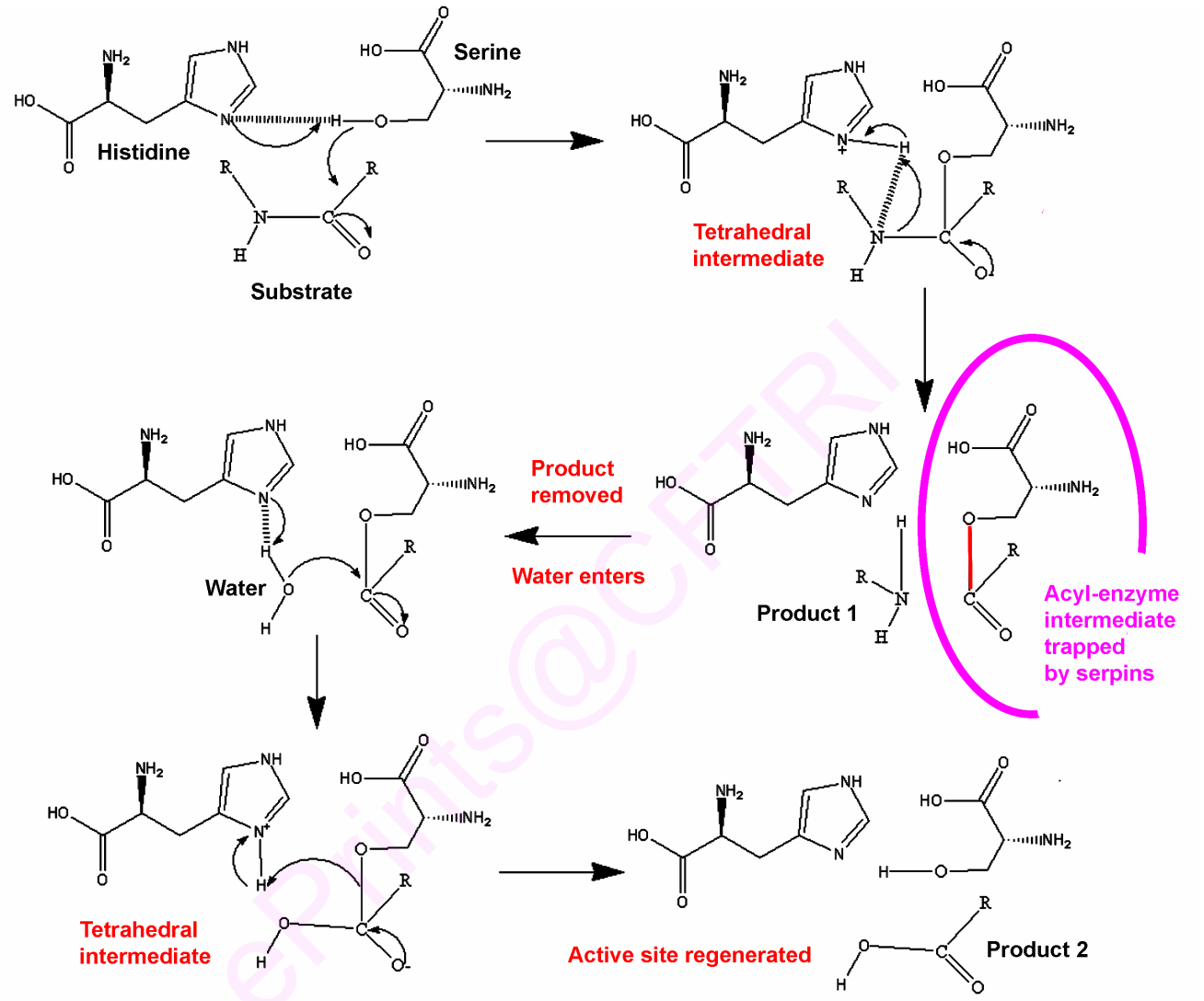

Figure 1. 6. Catalytic mechanism of serine protease inhibition by serpins. Magenta enclosure represents the stage in the cycle that is trapped by serpins. The ester bond in the acyl enzyme intermediate is highlighted in red (http://en.wikipedia.org/wiki/serpin).

individuals, indicating that other serine proteases which are encountered by α-1-PI are in fact, regulated by other inhibitors. The association rates for an array of serine proteases with α-1-PI indicate that human neutrophil elastase is inhibited far more rapidly than any other protease ($K_{ass} = 10^{-7}$ s^{-1}) (Beatty et al., 1980).

Neutrophil elastase is a predominantly neutral protease of polymorphonuclear neutrophil leucocyte origin with very broad substrate specificity. A broad range of proteins are readily hydrolyzed by this enzyme, including those from plasma, connective tissue, cells or foreign sources, although its primary substrate is elastin. Neutrophil elastase not only acts intracellularly on phagocytosed proteins, but also is important extracellularly in mediating tissue turnover. This implicates the need for an appropriate inhibitor to regulate enzymatic activity that restricts the protease to the intended site of action and not to damage healthy tissue (Baugh and Travis, 1976).

Molecular pathology of S and Z variants of α-1-PI

Any complex machinery is vulnerable to breakdown and α-1-PI is no exception. It is the archetypal serpin designed to ensnare proteases, a process that involves significant conformational changes within the molecule. Mutations in the α-1-PI gene lead to misfolding of the protein and accumulation within the endoplasmic reticulum of hepatocytes resulting in two different pathologic processes. First, the accumulation of mutant α-1-PI protein has a direct toxic effect on the liver, resulting in hepatitis and cirrhosis. Second, the resultant decrease in circulating α-1-PI results in protease-antiproteinase imbalance at the lung surface and emphysema ensues. α-1-PI deficiency therefore can be seen as two distinct disease processes: a conformational disease of the liver and a protease-antiproteinase imbalance of the lung. Serpins are particularly susceptible to destabilizing mutations that result in misfolding and the formation of pathogenic conformers. The S and Z variants of α-1-PI both result from single amino acid substitutions. In the S variant there is a substitution of a Val residue for Glu at position 264. This amino acid forms a stabilizing salt bridge within the molecule and the mutation results in misfolding and increased turnover of the molecule resulting in lower plasma levels (Curiel et al., 1989; Elliott et al., 1996). The Z abnormality differs from the S in that it is a problem of secretion rather than synthesis. The gene is normally translated

but 85 % of the protein produced is retained within the endoplasmic reticulum with only 15 % entering the circulation. The Z mutation results from the substitution of a positively charged Lys for a negatively charged Glu at position 342 located at the base of the reactive center loop. This mutation distorts the relationship between the loop and the β-pleated (A) sheet that forms the major feature of α-1-PI. The consequent perturbation in structure allows the loop of one molecule to interlock with the A sheet of another to form fibril-like polymers (Lomas et al., 1992) (Figure 1. 7). These chains of polymers become interwoven to form the insoluble inclusions that are the pathologic hallmarks of α-1-PI liver disease. The formation of polymers is a sequential event; once dimers are formed they initiate and propagate the inhibitor polymerization by having one exposed loop with an optimal conformation as a β-strand donor and a readily opened β-sheet as an acceptor (Zhou and Carrell, 2008). Experiments have indicated the possibility of polymer formation outside the hepatocytes (Elliott et al., 1998; Janciauskiene et al., 2002). Radial immunodiffusion and nephelometry are the commonly used quantitative techniques to study α-1-PI levels in blood. Isoelectrofocussing is another qualitative method which is widely used to study α-1-PI pathological conditions (Ferrarotti et al., 2007). The mechanism of polymerization is shown in Figure 1. 7.

Local production of α-1-PI in the lung

The potential cellular source of α-1-PI production in the lung includes epithelial cells, macrophages, and possibly neutrophils. *In vitro* data indicate that lung-derived epithelial cells are not only capable of α-1-PI production but also that this local production is increased in response to specific inflammatory mediators, including oncostatin M, interleukin-1 and dexamethasone (Cichy et al., 1997; Boutten et al., 1998; Kalsheker et al., 2002).

α-1-PI deficiency

The sequence of events leading to sudden respiratory failure in the adult respiratory distress syndrome suggests a breakdown in the anti-protease system (Fowler et al., 1982; Cochrane et al., 1983; Merritt et al., 1983; McCarthy et al., 1984). Presumably, neutrophils recruited to the lung are responsible for the break down of antiproteinase system, which leads to the appearance of free proteolytic activity.

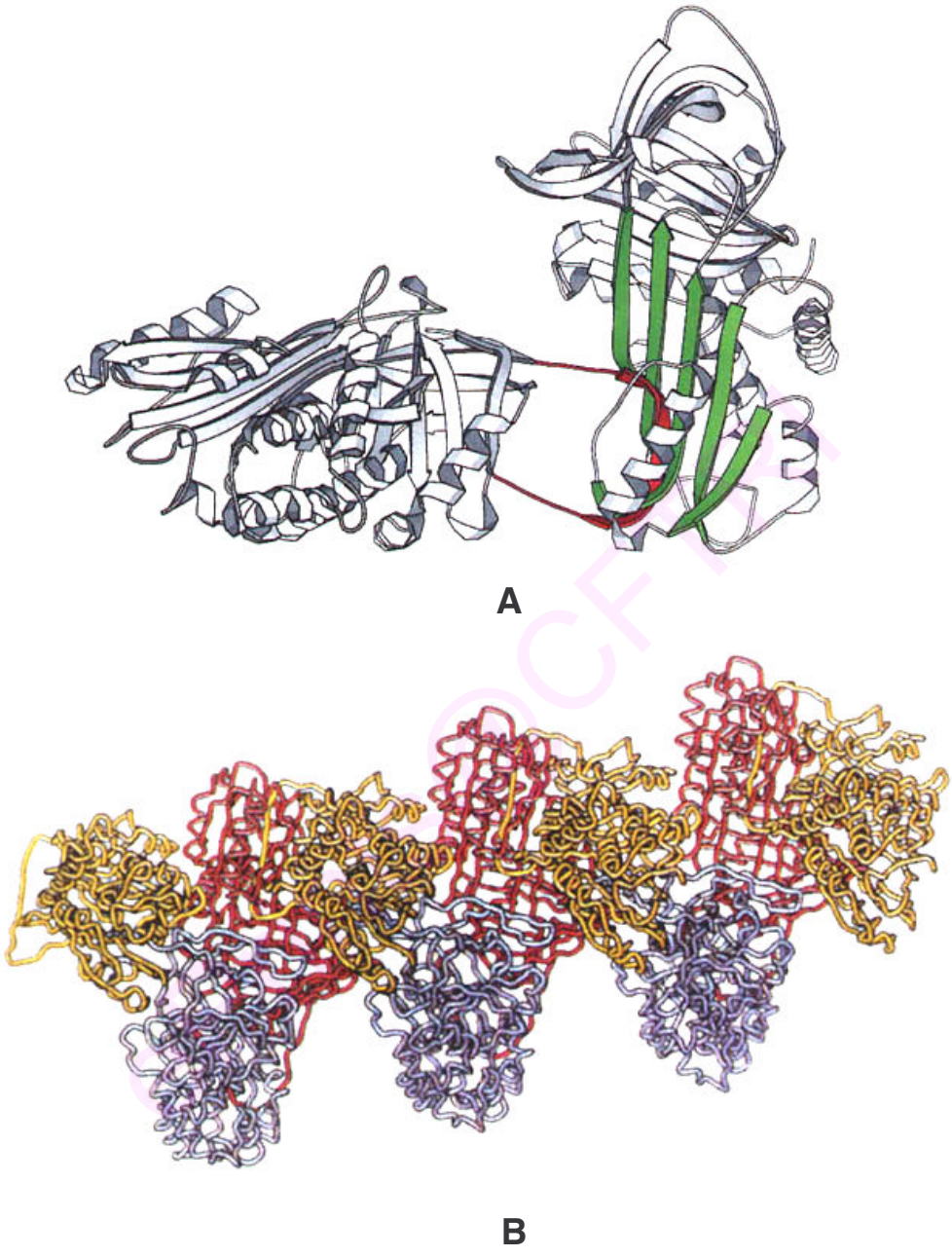

Figure 1. 7. Mechanism of serpin loop-sheet polymerization. A) The RCL is in red and the A β-sheet is in green. B) The RCL of one α-1-PI molecule is inserted into the bottom of the A-sheet of another (http://biochemsoctrans.org).

Severe pulmonary impairment, manifesting as COPD and pan-acinar lung emphysema result when α-1-PI serum concentration is below 35 % of the normal values. Pulmonary symptoms such as cough, sputum expectoration and exertional dyspnea and bronchial hyper-reactivity develop. The course of the disease is progressive and may lead to severe respiratory insufficiency (Kohnlein and Welte, 2008). α-1-PI deficiency results in development of liver disease less frequently than pulmonary manifestations. This is the most frequent reason for liver cirrhosis after viral hepatitis and alcohol abuse. Hepatic symptoms manifest initially as hepatitis followed by fibrosis. The underlying cause is the intra-hepatic accumulation of polymerized α-1-PI molecules (Hussain et al., 1991).

However, involvement of α-1-PI deficiency in a variety of other areas of clinical research is emerging. α-1-PI deficiency is also occasionally associated with Wegener's granulomatosis (Elzouki et al., 1994), Panniculitis and aneurysms of the aorta and brain arteries (Ortiz et al., 2005). Synovial fluid of patients with rheumatoid arthritis contains oxidatively inactivated α-1-PI with the reactive site Met oxidized (Wong and Travis, 1980).

α-1-PI production and function has been observed in tumours, including histiocytic lymphomas (Szporn et al., 1984; Thomas et al., 1984); Hodgkin's disease (Mir and Kahn, 1983); islet cell tumour (Ordonez et al., 1983) and breast tumour (Vasishta et al., 1984). α-1-PI increases in maternal serum with advancing gestation, and even higher values can be found in hypertensive pregnancies (Legge et al., 1984). The larvae of *Schistosoma mansoni* penetrate the skin of humans by proteolysis that has been reported to be inhibited by α-1-PI (McKerrow et al., 1983). This fact might be of great relevance in case of bilharziasis. The World Health Organization has recommended neonatal screening for α-1-PI deficiency given the prevalence of the disease and also the massive impact that smoking has on α-1-PI deficient individuals (Sveger and Thelin, 2000). Screening programs and subsequent advice may prevent adolescents identified with the condition from beginning to smoke (Wall et al., 1990; Sveger et al., 1997; Carpenter et al., 2007).

Polymorphism and micro-heterogeniety of α-1-PI

The term alpha-1 refers to the enzyme's behavior on protein electrophoresis. On electrophoresis, the protein component of the blood is separated by electric current giving rise to several clusters of bands, the first being albumin, the second alpha-globulins, third beta-globulins and the fourth gamma globulins. The alpha region can be further divided into two sub-regions, termed "1" and "2". α-1-PI is the main protein of the alpha-globulin 1 region.

The allelic variants of α-1-PI leading to disease was first investigated by Axelsson and Laurell (1965). Over 80 different versions of α-1-PI have been described. The maximum frequency of carrying a mutant form of α-1-PI is observed in North-Western European populations. As protein electrophoresis is imprecise, α-1-PI is analyzed by isoelectrofocusing analysis. Normal α-1-PI is termed "M", as it is neutral and does not run very far. Other variants are less functional, and are termed A-L and N-Z, dependent on whether they are proximal or distal to the M band. The presence of deviant bands on electrofocusing can signify the presence of α-1-PI deficiency.

Each individual has two copies of the α-1-PI gene so a heterozygote with two different copies of the gene may show two different bands upon electrofocusing. The electrofocusing results are notated as in P_iMM, where P_i stands for protease inhibitor and "MM" is the banding pattern of that individual genotype. The mutant forms fail to fold properly and have a tendency to polymerise and retain themselves in the endoplasmic reticulum. Some common genotypes and their serum levels are: P_iMM (normal): 100 %, P_iMS: 80 % , P_iSS: 60 %, P_iMZ: 60 %, P_iSZ: 40 %, P_iZZ (severe α-1-PI deficiency): 10-15 % PiZ is caused by a Glu^{342} to Lys mutation while P_iS is caused by a Glu^{264} to Val mutation. In all, there are about 80 such variants including certain rarer forms. The α-1-PI gene is expressed in cells of several lineages, with expression being highest in hepatocytes (Rogers et al., 1983). Serum α-1-PI is also actively transcribed and secreted by neutrophils, mononuclear phagocytes and enterocytes (Carlson et al., 1988; Molmenti et al., 1993). This micro-heterogeniety can in part be explained by differences in carbohydrate side chain moieties. In α-1-PI three carbohydrate side chains are attached, all at Asn residues. Two different forms of side chains are known to exist, bi-antennaries

and tri-antennaries (Hodges et al., 1979; Mega et al., 1980). The major isoforms of P_iM have been separated and found to contain different combinations of the two possible chains (Vaughan et al., 1982) with different amounts of the terminal sialic acid residues. The reason for the heterogeneity in the minor bands may be partial proteolysis at the NH_2-terminus of the native protein (Hercz, 1985). Several diseases have been suggested to be related to particular P_i types e.g., acute anterior uveitis, bronchial asthma, wheezing, chronic active hepatitis, hepatic cirrhosis, fibrosing alveolitis, juvenile chronic arthritis, and psoriasis (Brewerton, 1984; Eden et al., 2006). It is not clear whether; there are functional connections, or whether the P_i markers happen to be genetically linked to other important genes. A remarkable form of P_i, termed P_i Pittsburgh, functions as an antithrombin due to Met^{358}-Arg mutation.

Homology of reactive centers

The serpins share a homologous C-terminal reactive centre typified by that of α-1-PI.

P2-	P1-	P1`-	P2`-	P3`-	P4`
P-	M-	S-	I-	P-	P-

where the P2-P1 residues (Pro-Met) determine specificity, the P`1 site is almost invariably Ser or Thr, and P`2 site is usually a hydrophobic residue (Schechter and Berger, 1967). The reactive centre of α-1-PI is closely similar to the well-conserved reactive centres of the unrelated Bowman-Birk inhibitors, which is surprising (Johnson and Travis, 1978; Carrell et al., 1980). It leaves open the question as to why both α-1-PI and the Bowman-Birk inhibitors have selected a –Pro-Pro- sequence at the P`3-P`4 positions. Does this provide an optimal configuration of the reactive centre? A likely alternative is that this sequence, because of its resistance to proteolytic cleavage, provides some protection to an area which is exposed and where cleavage results in inactivation.

Structurally α-1-PI resembles other serpins so that it can be said that if you have seen one serpin you have seen them all. Amongst different mammalian species, α-1-PI exhibits a high degree of sequence, structural, mechanistic and epitopal homology and

this aspect is vital as it keeps the prospect of using non-human mammals as potential sources of α-1-PI production, alive.

α-1-PI is impaired by oxidation

The Met residues in proteins can be readily oxidized to give Met sulfoxide derivatives (Brot et al., 1984), and this frequently leads to modification or impairment of activity (Brot and Weissbach, 1982). α-1-PI contains eight Met residues, two of which are readily oxidized by mild agents such as chloramine-T (Johnson and Travis, 1979; Cohen, 1979), myeloperoxidase (Matheson et al., 1979; Clark et al., 1981) or activated polymorphonuclear leucocytes (Tsan et al., 1980). One of the readily oxidized Met residues is Met^{358} in the reactive site. It is observed that porcine pancreatic elastase is not inhibited by oxidized α-1-PI but degrades it (Matheson et al., 1981), whereas trypsin is inhibited normally by the oxidized protein indicating that trypsin may bind at a different site (Beatty et al., 1982; Gupta et al., 2008).

An oxidation theory of emphysema has evolved showing that the inhibitory capacity of α-1-PI can be switched-off by oxidation of the reactive site Met. The patho-physiological significance of this was demonstrated experimentally where dogs were treated with chloramine-T over an extended period. When the animals were examined after several months, all showed signs of pulmonary emphysema (Abrams et al., 1981).

As it is evident that the oxidative inactivation of α-1-PI may be a major factor in lowering lung defenses against degradation of elastins there have been several attempts to prepare mutant forms of α-1-PI wherein Met^{358} has been replaced by a non-oxidisable residue with retention of inhibitory activity.

Protease inhibitor and cigarette smoke in the pathogenesis of emphysema

Smoking is a risk factor in emphysema; therefore considerable effort has been focused on the mechanisms involved, especially as related to α-1-PI inactivation. Cigarette smoke oxidizes the reactive site of the inhibitor in the lungs, thus tipping the elastase-anti-elastase balance in favor of uncontrolled proteolysis. Carp and Janoff (1979) found *in vitro* suppression of serum elastase inhibitory capacity by cigarette smoke, which is prevented by oxidants. Cigarette smoke inhalation by rats caused a decrease in

the elastase inhibitory capacity of lung fluid that could be recovered by treatment with reducing agents (Janoff et al., 1979). Human serum samples, obtained immediately after smoking, also showed decreased elastase inhibitory activity, which could be restored with sodium metabisulfite as reductant (Gadek et al., 1979). Met sulfoxide has been found in α-1-PI obtained from smokers' lungs and associated with its decreased activity (Carp et al., 1982).

α-1-antichymotrypsin

Alpha-1-antichymotrypsin is another plasma protease inhibitor that is synthesized in the liver. This glycoprotein has an apparent affinity toward chymotrypsin-like enzymes (Travis, 1978) including neutrophil Cathepsin G and mast cell chymase, which are capable of converting angiotensin I to the biologically active vaso-constrictor angiotensin II *in vitro* (Wintroub, 1981; Reilly et al., 1982; Tonnensen, 1989). The similarities in structure between α-1-PI and α-1-antichymotrypsin suggest that α-1-chymotrypsin could also be involved in the maintenance of the overall protease-protease inhibitor balance in the lung. In fact, α-1-antichymotrypsin was found to be selectively concentrated in the bronchial lumen of patients with chronic infections (Reilly et al., 1982).

Interaction with non-serine proteases

A modified α-1-PI can also be formed by direct turnover of the reactive site peptide bond by non-serine proteases using the inhibitor strictly as a substrate such as papain (Johnson and Travis, 1977), mouse macrophage elastase (Banda et al., 1980), *Pseudomonas aeroginosa* elastase (Morihara et al., 1979) and *Serratia marcescens* metalloprotease (Virca et al., 1982), cysteine protease, rattlesnake venom protease II (Kress et al., 1979) and several metalloproteases. Papain cleaves the reactive site bond, Met^{358}-Ser^{359}, whereas the metalloproteases cleave the bond Pro^{357}-Met^{358}. In each case, the reaction causes a critical conformational change without disrupting the molecule as a whole. α-1-PI therefore plays a significant role in inactivating bacterial proteases that may prove detrimental in destroying tissues directly.

α-1-PI as a therapeutic agent

Replacement therapy in α-1-PI deficient patients with α-1-PI purified from human plasma shows promise in slowing the progression of lung disease and conferring anti-elastase activity. Treatment of P_iZ individuals with 4 g of α-1-PI weekly increases the levels of inhibitor by 70 %, a value which normally gives effective anti-elastase activity within the alveolar structures (Gadek et al., 1981).

Plasma derived supply is variable in purity and activity (Cowden et al., 2005), and is insufficient to meet demand, despite novel methods of α-1-PI extraction from plasma (Kumpalume et al., 2007). Unfortunately, the large amounts of α-1-PI needed for therapy are difficult to obtain. The gene for human α-1-PI has been expressed in a variety of hosts (Chandra et al., 1981; Courtney et al., 1984; Rosenberg et al., 1984) and it is possible to produce enough α-1-PI by biotechnology to treat all α-1-PI deficient individuals. Expression in *E. coli* has been most widely studied. The recombinant α-1-PI is not glycosylated, which affects the folding of the protein, leading to rapid aggregation. It has reduced activity and a shorter half-life in the blood after infusion. Yeast expression has an advantage over *E. coli* expression of therapeutic proteins, as they do not produce endotoxins and can provide some glycosylation (Karnaukhova et al., 2006). However, the glycosylation process in yeasts differs from that of humans, resulting in structures with high mannose content-a process known as hypermannosylation (Fukada, 2000). Active α-1-PI has been produced in insect cells hosting baculovirus expression vector systems (Sandoval et al., 2002) to utilize the benefits of post-translational modification but concerns regarding non-human glycans still persist (Karnaukhova et al., 2006). Sources of recombinant α-1-PI from transgenic organisms like rice (Terashima et al., 2000), mice (Zbikowska et al., 2002), rabbit (Massoud et al., 1991), sheep (Spencer et al., 2005) and goat (Ziomek, 1998) might overcome these problems, however antigenicity still remains a major issue.

Further, precise inhibition of polymerization of Z-form of α-1-PI can be achieved by annealing peptides to the RCL of β-sheet A. Peptides with 11-13 residues have been used for such studies effectively (Lomas et al., 1992). Chemical chaperones are another

alternative, which has been used to provide stability and increased secretion of α-1-PI (Burrows et al., 2000).

Replacement of defective or absent genes within a cell such that the treated cell functions properly, is the most direct method for the treatment of this genetic disorder and has been done using retroviral (Kay et al., 1992), adenoviral (Morral et al., 1998) and liposomal (Alino et al., 1994) vectors to transfect cells. Research using stem cells has also shown some potential for treatment of α-1-PI disorders. Stem cells can differentiate into liver cells capable of expressing α-1-PI (Moriya et al., 2007).

Effect of pH on α-1-PI

α-1-PI undergoes loop-sheet polymerisation at acidic pH. The inhibitory activity is rapidly lost at pH 3.0 but slowly recovers at pH 7.4 with variable first order rates. It undergoes a variation in intrinsic fluorescence intensity upon acidification. The acid treated α-1-PI is proteolysed at neutral pH by the proteases. Its acidification has mild effect on its secondary structure, strongly changes the tertiary structure and also the environment around Cys^{232} residue (Devlin et al., 2002; Boudier et al., 2007).

α-1-PI serpin C-terminal peptides are highly active biologically

Cleavage of α-1-PI occurs on α-1-PI reaction with target proteases. The C-terminal fragments of serpins that are released by such reactions are biologically highly active and have been implicated in numerous physiological processes. The hydrophobic C-terminal peptides liberated during cleavage of α-1-PI have been isolated from the phospholipid fraction of bile secretion (Johansson et al., 1992; Stark et al., 1999). The cleaved peptides have been detected in urine samples obtained from IgA nephropathy patients (Machii et al., 2005).

The α-1-PI C-36 peptide exhibits notable pro-inflammatory activity by the stimulation of cytokine and chemokine release by monocytes and protease release and chemotaxis in neutrophils. Macrophages and neutrophil derived proteases and oxidants promote the down-regulation of α-1-PI inhibitory activity by promoting protein degradation (Taggart et al., 2000) and the generation of peptide fragments. Immuno-histochemical studies indicate that cleaved fragments of α-1-PI, including a 44-residue

C-terminal peptide, arising from non-targeted proteolytic cleavage, is present in a variety of human tissues (Heath et al., 1994). Monoclonal antibody reaction against 36-residue C-terminal peptide of α-1-PI (C-36) indicates that lung tissues with and without histological characteristics of COPD, can be intensely affirmative for the C-36. Certain lung areas are known to be positive for the C-36 peptide, which shows amyloid-like deposits (Subramaniyam et al., 2008). Cleaved fragments of α-1-PI also act as potent chemo-attractants for neutrophils and stimulate cytokine and chemokine release from monocytes *in vitro* (Janciaskiene et al., 2001; Janciauskiene et al., 2004; Zelvyte et al., 2004).

Short C-terminal peptide from α-1-PI as protease inhibitor

SPAAT (short C-terminal peptide from α-1-PI) is the 44-residue C-terminal fragment of α-1-PI which inhibits serine proteases chymotrypsin, human neutrophil elastase and pancreatic elastase. Both natural and chemically synthesized SPAAT unlike full length α-1-PI are competitive inhibitors of chymotrypsin. Thus SPAAT may play an important role in the protection of extra-cellular proteins from inappropriate attack by serine proteases. Thus, two types of interactions between serpins and proteases are possible. A serpin can inhibit protease like elastase or cathepsin G by the formation of stable serpin-protease complex. Alternatively, the serpin can get cleaved by the protease like papain, stromelysin, collagenase or gelatinase to generate various fragments of the serpin. The cleavage of α-1-PI by stromelysin-3 generates SPAAT which inhibits certain serine proteases competitively (Niemann et al., 1997).

Glycosaminoglycans

Glycosaminoglycans (GAGs) are long unbranched polysaccharides consisting of a repeating disaccharide unit, consisting of an N-acetyl-hexosamine and a hexose or hexuronic acid, either or both of which may be sulfated. These are synthesized in either the endoplasmic reticulum or golgi apparatus. The combination of the sulfate group and the carboxylate groups of the uronic acid residues gives them a very high density of negative charge. GAGs form an important component of connective tissues. GAG chains may be covalently linked to a protein to form proteoglycans. Evolution has adapted some serpins to require cofactors like heparin or other GAGs to optimally inhibit target

proteases. GAGs can bind to some proteins and modulate signaling molecule activities in the cellular environment (Raman et al., 2005). About 60 crystal structures of complexes between protein and GAGs are available in the Protein Data Bank (Imberty et al., 2007). Recent crystallographic elucidations have provided structural information about the binding of some low molecular weight oligosaccharides from GAGs in interaction with proteins. Most of these GAG binding proteins establish salt bonds between basic groups of amino acid side chains and sulfated or acidic groups of the ligand (Imberty et al., 2007).

Members of the glycosaminoglycan family vary in the type of hexosamine, hexose or hexuronic acid unit they contain (e.g. glucuronic acid, iduronic acid, galactose, galactosamine, glucosamine) as well as in the geometry of the glycosidic linkage (Table 1. 1).

Table 1. 1. Various GAGs , their constituents and the type of linkage.

Name	Sugar 1	Sugar 2	Linkage
Chondroitin sulphate	N-Acetylgalactosamine	Glucuronic acid	beta (1,3)
Dermatan sulphate	Iduronic acid	N-Acetylgalactosamine	beta (1,3)
Keratan sulphate	Galactose	(varies)	beta (1,4)
Heparin	Glucuronic acid	Glucosamine	alpha (1,4)
Hyaluronic acid	Glucuronic acid	N-Acetylglucosamine	beta (1,3)

Heparin

Heparin is one of the oldest drugs still widespread in clinical use. Heparin discovery can be attributed to the research activities of Jay McLean and William Henry

Howell in 1916. Heparin, (*hepar* in Greek for "liver") as used therapeutically, is a hydrolysate of complex GAGs prepared from animal extracts, and is not normally present in this form in the blood. Its nearest equivalent in the circulation is the heparan side chains of the endothelial glycoproteins that line the capillaries and sinusoids of the circulation. These forms contain pentasaccharide sequences that specifically bind to antithrombin and localise it to micro-vasculature, the most thrombosis vulnerable part of the circulation (Choay et al., 1983; Lindhal et al., 1984; Marcum et al., 1984).

Heparin, a highly sulfated GAG is widely used as an anticoagulant and has the highest negative charge density of any known biological molecule (Cox and Nelson, 2004). High purity heparin is obtained from mucosal tissues of slaughtered animals such as porcine intestine or bovine lung (Linhardt and Gunay, 1999). One unit of heparin is the quantity of heparin required to keep 1 mL blood fluid for 24 hrs at 0°C and is equivalent to 0.002 mg of pure heparin.

Heparin structure

Heparin is a polymer with M_r ranging from 500 to 40,000 Da, of variably sulfated repeating disaccharide unit. The most common disaccharide unit is composed of a 2-O-sulfated iduronic acid and 6-O-sulfated, N-sulfated glucosamine, IdoA(2S)-GlcNS(6S). This makes up 85 % of heparin from lung and about 75 % of that from porcine intestinal mucosa. There are certain rare disaccharides containing a 3-O-sulfated glucosamine (GlcNS(3S,6S) or a free amine group ($GlcNH_3^+$).

Under physiological conditions the ester and amide sulfate groups are deprotonated and attract positively charged counter-ions to form a heparin salt. It is in this form that heparin is usually most effective as an anticoagulant. The solution structure of a heparin dodecasacchride composed solely of six GlcNS(6S)-IdoA(2S) repeat units has been determined using NMR and molecular modelling techniques (Mulloy et al., 1993). In these models heparin adopts a helical conformation, the rotation of which places clusters of sulfate groups at regular intervals of about 17 Å (1.7 nm) on either side of the helical axis (Figure 1. 8). Lys, Arg or Gln are frequently involved in contacts with the GAG sulfate and carboxyl groups and their spacing, sometimes determined by secondary structure, may control the binding specificity (Tumova et al., 2000). Due to its

polyelectrolyte nature, heparin binds to many plasma proteins in addition to serpins including fibrinogen (Longas et al., 1980), fibronectin (Hayashi and Yamada, 1982; Griffin et al., 1986), histidine rich glycoprotein (Lijnen et al., 1983), platelet factor IV (Kaplan et al., 1979; Bock et al., 1980) and thrombin (Rosenberg et al., 1980; Smith and Sundboom, 1981; Heuck et al., 1985).

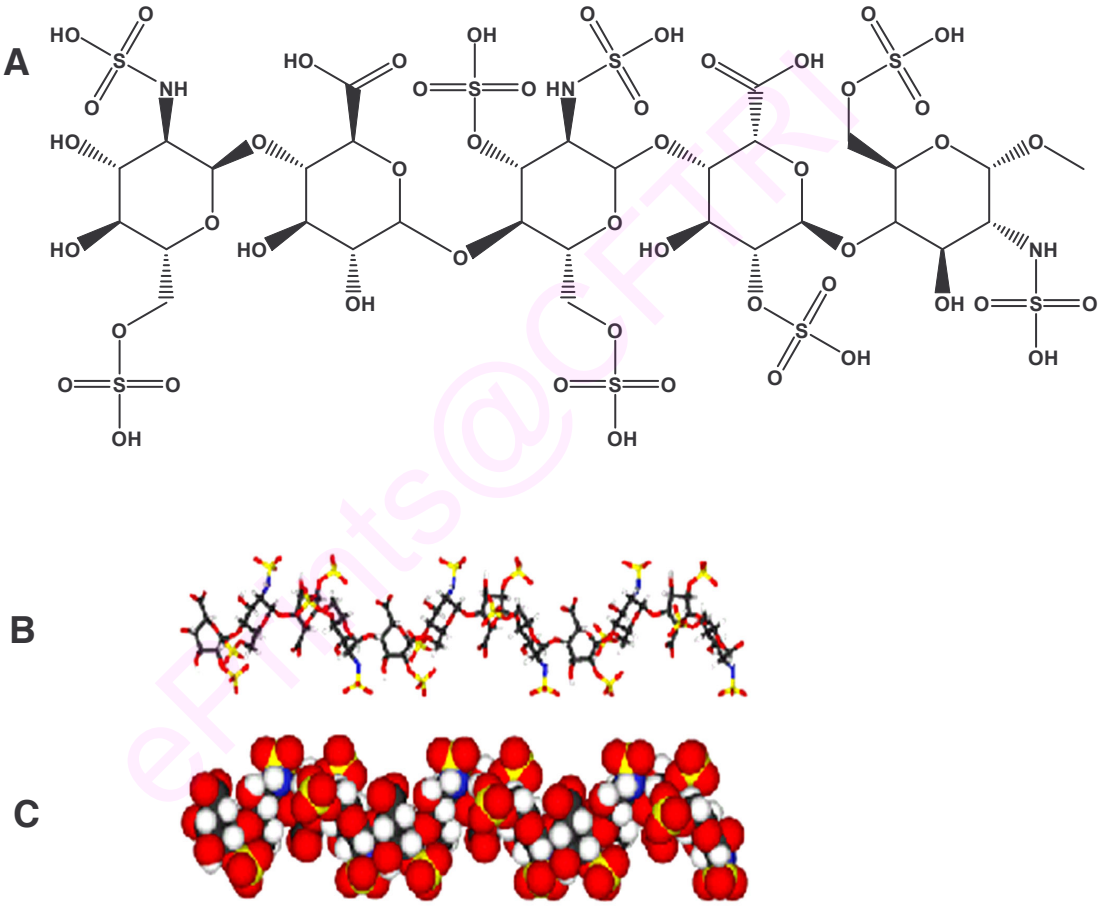

Figure 1. 8. Structure of the natural heparin. A. Penta-saccharide, generated using ChemDraw Ultra 7.0. B and C. Three dimensional structures of the heparin oligomer (PDB ID 1HPN).

Medical applications

Heparin acts as an anticoagulant and prevents the extension of existing clots within the blood unlike tissue plasminogen activator which breaks down the clots that have already formed. Heparin is used as an anticoagulant for myocardial infarction, atrial fibrillation, deep-vein thrombosis and pulmonary embolism. The use of low molecular weight heparin (LMWH) has allowed periodic dosing, thus not requiring a continuous infusion of the drug. Several low molecular weight heparins (LMWHs) and more recently Fondaparinux as pharmaceutical anticoagulant have been developed. Fondaparinux is a synthetic pentasaccharide whose chemical structure is almost identical to the structure to AT-III binding pentasaccharide sequence that can be found within polymeric heparin and heparan sulfate. With LMWH and Fondaparinux, there is a reduced risk of osteoporosis, heparin-induced thrombocytopenia and an improved partial thromboplastin time. Alternatively, Danaparoid, a mixture of heparan sulfate, dermatan sulfate and chondroitin sulfate can also be used as an anticoagulant. Because Danaparoid does not contain heparin or heparin fragments, cross-reactivity of Danaparoid with heparin-induced antibodies is absent. Heparin's exact physiological role is still unclear, because blood anti-coagulation is mostly achieved by endothelial cell-derived heparan sulfate proteoglycans (Kojima et al., 1992). Heparin is stored within the secretory granules of mast cells and only released into the vasculature at sites of tissue injury. Mast cells play a role during allergic reactions and are also active during other chronic and acute inflammatory conditions. Upon stimulation, the mast cells are activated and the granular components are released (Galli, 2000).

Evolutionary conservation of heparin

In addition to the bovine and porcine tissue from which pharmaceutical grade heparin is commonly extracted, heparin has also been extracted and characterized from turkey (Warda et al., 2003), whale (Ototani et al., 1981), dromedary camel (Warda et al., 2003), mouse (Bland et al., 1982), humans (Linhardt et al., 1992), lobster (Hovingh and Linker, 1982), fresh water mussel (Hovingh and Linker., 1993), clam (Pejler et al., 1987), shrimp (Dietrich et al., 1999), mangrove crab (Medeiros et al., 2000) and sand dollar

(Medeiros et al., 2000). This demonstrates that heparin is highly conserved evolutionarily with similar molecules being present in a diverse range of organisms.

Mechanism of serpin activation by heparin

Most of the mammalian serpins are activated and their rate of protease inhibition increases several fold upon binding to negatively charged heparin. Prominent ones are antithrombin, heparin cofactor II, PAI-1, protein C inhibitor and protease nexin 1. The rate of protease inhibition may be of an order of 10^2-10^3. Heparin oligosaccharides may induce activation either by a bridging mechanism, where the heparin simultaneously binds to both the serpin and the protease and brings them into close proximity in proper orientation for optimal inhibition of the protease or binding to serpin alone and bringing about a conformational change in the serpin in such a way that the RCL becomes more exposed and readily available to the cognate protease for rapid inhibition. Antithrombin and heparin cofactor II adapt both the bridging and conformation based approaches while other serpins are known to be activated primarily by the bridging mechanisms.

i) Activation by proximity effect

A pre-requisite for the bridging is the presence of heparin binding domains on both the serpin and cognate protease at appropriate locations. Except Protein-C inhibitor, all other serpins discussed above have a heparin binding site on helix-D. Antithrombin in addition has heparin binding residues at the N-terminus and at the P-helix, which probably are responsible for its higher heparin binding affinity and consequent activation (Jin et al., 1997). In case of protein C-inhibitor, the heparin binding site is present at helices A and H (Kuhn et al., 1990). An illustration of the way in which such bridging results in bringing together serpin and protease components is given by a model ternary complex of heparin-antithrombin and thrombin (Figure 1. 9). Such a type of bridging requires a minimum length of the oligosaccharide essential to bind both the protease and inhibitor. The minimum chain-length in case of thrombin-antithrombin interaction is 18 saccharide units (Olson et al., 1992), 14 units in case of PAI-1-thrombin reactions (Patston and Schapira, 1994) and 24 units for HC-II-thrombin reactions (Tollefsen, 1990).

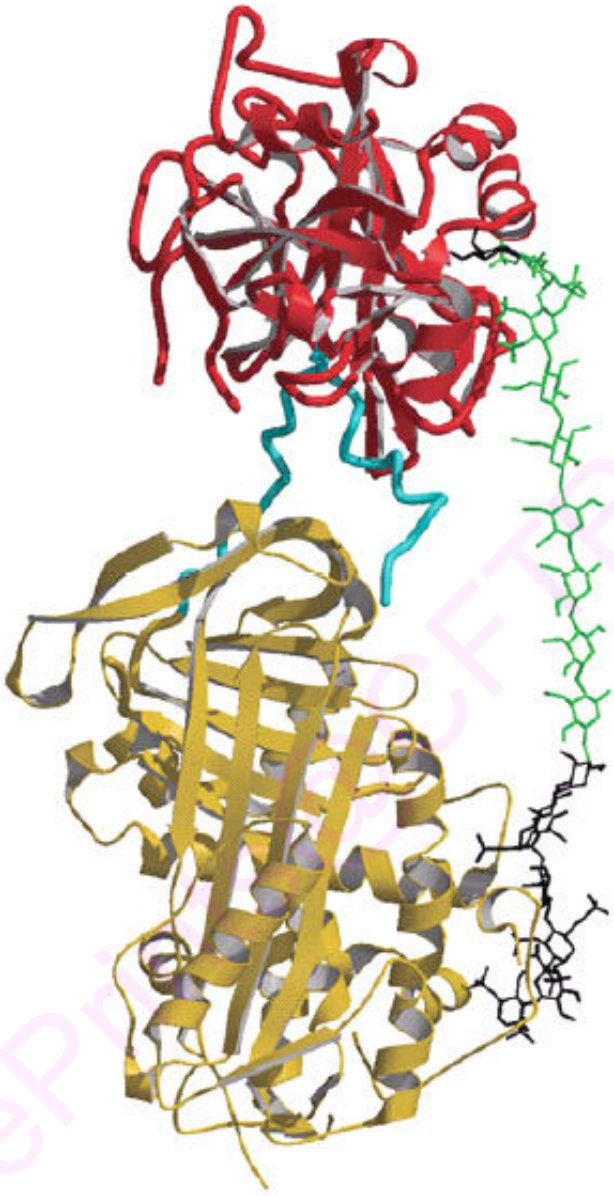

Figure 1. 9. Ribbon drawing of the ternary complex of antithrombin thrombin and heparin octasaccharide. Serpin antithrombin is in gold, with the exception of the reactive center loop (cyan). Protease thrombin is red and the heparin oligomer is in stick form (Reproduced with kind permission from J. A. Huntington) (Li et al., 2004).

ii) Heparin induced expulsion-activation mechanism and conformational changes

Heparin binding induces conformational changes within the serpin molecules. These changes are very prominent in case of antithrombin and HC-II and responsible for the activation with respect to protease inhibition. Crystal structures of heparin bound antithrombin molecules have shown that specific heparin pentasaccharide binds to basic residues of helix-D (residues 112-119) of antithrombin and causes its extension. This helix-D is connected to β-sheet A, in such a way that helix extension causes its contraction, which in turn is connected to the RCL (Van Boeckel et al., 1994). These changes within the heparin binding site are somehow propagated to the RCL region and are accompanied by expulsion of the hinge residues P14 and P15. This binding is two step: an initial low affinity binding followed by a conformational change leading to high affinity binding. Mutagenesis and biophysical studies have established the role of different positively charged residues in heparin binding to the serpin. Mutations in helix-H in antithrombin have also been reported recently to decrease the stimulation of protease inhibition (Olson and Shore, 1981; Carrell et al., 1994; Jin et al., 1997; Meagher et al., 1998; Desai et al., 2000; Li et al., 2004; Pike et al., 2005; Gonzales et al., 2007).

The crystal structure of HC-II complex with thrombin provides insights into structural dynamics of HC-II (Baglin et al., 2002). The heparin binding site in HC-II is at similar location as antithrombin but the P1 residue of HC-II is Leu rather than Arg (Ragg, 1986; Whinna et al., 1991). However, even in the case of heparin activation of serpins with a bridging contribution, the role of allosteric activation is dominant, as shown by mutagenesis studies. α-1-PI production in the liver, its activation by heparin, interaction with various proteases and the production of cleaved C-terminal fragments has been explained diagrammatically (Figure 1. 10).

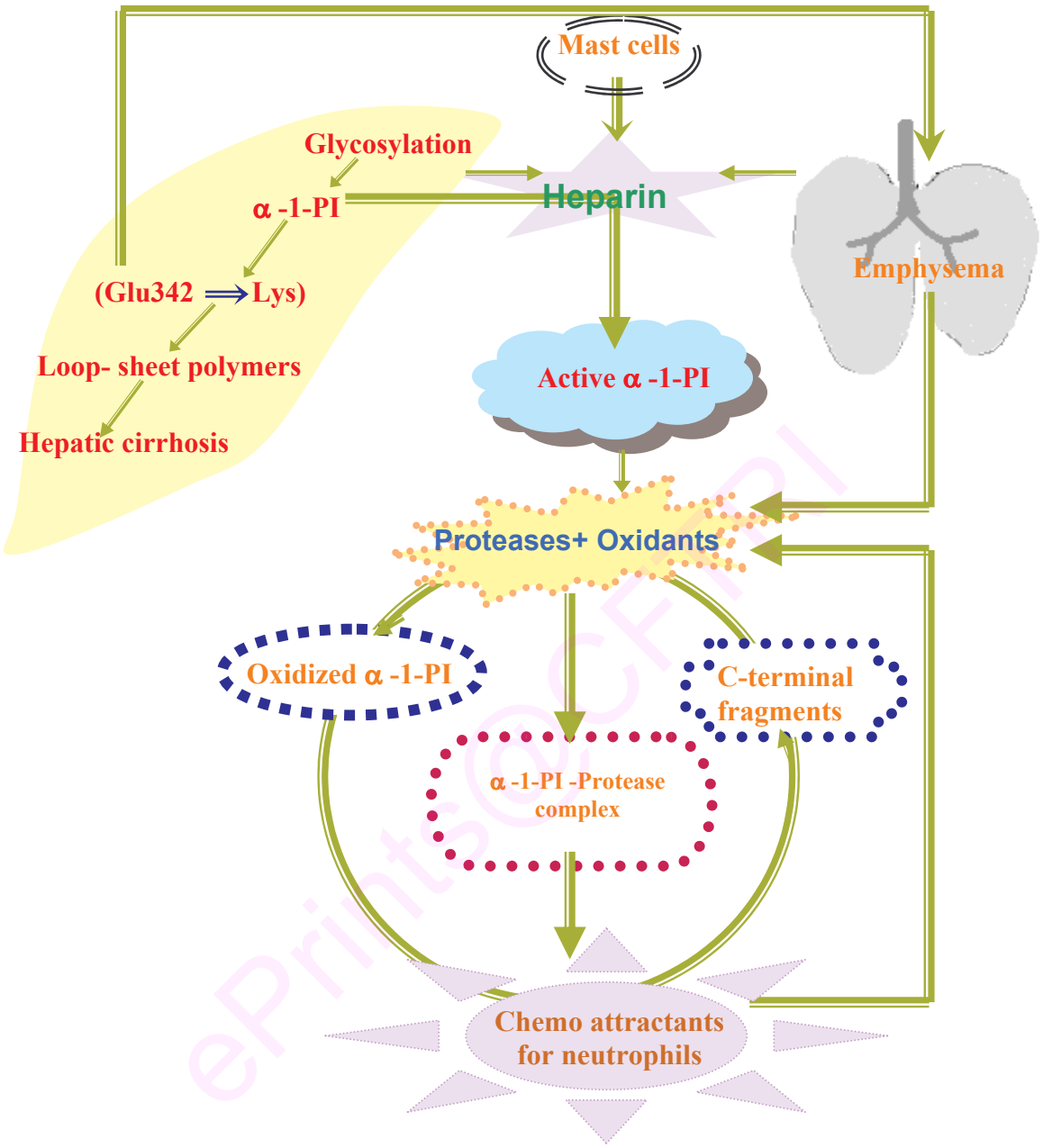

Figure 1. 10. Schematic representation of α-1-PI production and its activation by heparin. Active α-1-PI interacts with serine proteases resulting in complex formation and generation of cleaved fragments which in turn act as chemoattractants for neutrophils. Mutations in α-1-PI lead to its polymerization and pathological manifestations in the form of emphysema and liver cirrhosis.

Aim and scope of the present investigation

Serpins comprise of a large family of proteins that are involved in the regulation of many fundamental physiological processes by maintaining the protease inhibitor-protease balance. Mammalian serpins irrespective of their high sequence, structural and mechanistic homology display noticeable differences in stability, specificity and protease inhibitory activity. Serpins comprise 2 % of total human plasma protein, 70 % of which is the archetype of the family, α-1-PI. Its major physiological role is to protect pulmonary elastin fibres from excessive degradation by neutrophil elastase. α-1-PI has been implicated in regulating vital fluid phase biological events viz. blood coagulation, fibrinolysis, complement activation, apoptosis, matrix remodeling, reproduction, tumour progression and inflammatory response. Genetically induced α-1-PI deficiency due to the Z-mutation (Glu^{342}-Lys) and/or oxidative inactivation of the inhibitor active site leads to enzymatic degradation of lung connective tissue and ultimately pulmonary emphysema and hepatic cirrhosis. α-1-PI is the primary blood-borne serine protease inhibitor for a broad range of destructive neutrophil proteases including elastase, cathepsin G, protease-3, pancreatic elastase, trypsin and chymotrypsin and skin and synovial collagenases. α-1-PI is responsible for 80-90 % of plasma leucocyte elastase inhibitory activity in man. Alteration in the protease inhibitor-protease balance in the lungs leads to emphysema. This can be alleviated by therapeutic use of synthetic inhibitors or by α-1-PI supplementation therapy, which has been licenced for treatment of α-1-PI deficient individuals with pulmonary emphysema. Naturally occurring protein inhibitors of proteases especially α-1-PI has typically evolved to such a level of sophistication that it is highly flexible without any compromise on the aspect of strength of binding to target proteases. Thus it appears to be an ideal candidate for use as a model drug for the treatment of above disorders. Structural modifications in α-1-PI in order to increase the activity, stability, capability as well as flexibility of the protein to bind with target enzymes will be altogether a new chapter in the story of proteases, their inhibitors and the treatment of associated disorders. The lack of availability as well as stability and susceptibility to oxidative impairment of human α-1-PI reduces its potential effectiveness. Human α-1-PI has been characterized extensively but not much is known

about the comparative physical and biochemical properties of α-1-PI from related mammalian sources. Detailed investigations make it conceivable to obtain α-1-PI from unconventional sources such as ovine serum. The vast availability of ovine blood as well as the observed higher stability of ovine α-1-PI compels a thorough biochemical and structural characterisation of the molecule, to understand the differences between human and related α-1-PIs.

The study on ovine serum α-1-PI is envisaged to understand the biochemical and structural differences between human and other related α-1-PIs and the incorporation of advantageous features into a new more stable and potent molecule, which would be of high therapeutic importance. It can be easily purified, is structurally homologous to human α-1-PI and is more thermostable. In the present investigation, the main focus would be towards purification, biochemical and structural characterisation of ovine serum α-1-PI and its interaction with physiologically important serine proteases.

The main objectives of the present investigation are:

- Purification of α-1-PI from ovine serum
- A comparative study of the kinetic and molecular properties of α-1-PI inhibition of physiological serine proteases.
- Stoichiometric studies on the inhibition of physiological serine proteases.
- Molecular modeling to study protease-α-1-PI interaction.
- Effect of structural modifications on the biochemical and kinetic properties of α-1-PI.

Understanding the interactions of multiple serine proteases with α-1-PI, heparin induced activation and the resultant conformational changes would not only be important from a viewpoint of protein chemistry but also provide a platform for designing potent mechanism based inhibitors as effective anti-emphysema, anti-inflammatory and anti-tumour agents.

2. MATERIALS AND METHODS

2. MATERIALS AND METHODS

2.1. Materials

2.1.1. Chemicals

The chemicals used in the present investigation were procured from the following sources:

Porcine pancreatic elastase (2× crystallized, pancreopeptidase E, EC 3.4.21.36), porcine pancreatic trypsin (2× crystallized, type III, EC 3.4.21.4), bovine pancreatic ∝-chymotrypsin (3× crystallized, type II, EC 3.4.21.1), chloromethylketone (TPCK)-treated trypsin, chloromethylketone (TLCK)-treated chymotrypsin, low molecular weight heparin, chondroitin sulfate, hyaluronic acid, human α-1-PI antibodies, bovine serum albumin (BSA), carbonic anhydrase, lysozyme, hemoglobin, acrylamide, N-N'-methylene bis-acrylamide, tris (hydroxymethyl) amino methane (Trizma base), coomassie brilliant blue R-250, triethylamine (TEA), trifluoroacetic acid (TFA), α-N-benzoyl-DL-arginine-*p*-nitroanilide HCl (BAPNA), N-benzoyl-L-tyrosine-*p*-nitroanilide (BTPNA), N succinyl Ala-Ala-Ala-*p*-nitroanilide (NSAPNA), N-acetyl-DL-phenylalanine-β-napthyl ester (APNE), N-N, N'-N'-tetramethyl 1, 2-diaminoethane (TEMED), DL-dithiothreitol (DTT), 2, 4, 6-trinitrobenzenesulfonoic acid (TNBS), 3-[cyclohexylamino]-1-propanesulfonic acid (CAPS), phenylmethyl-sulfonyl fluoride (PMSF) and heparin were purchased from Sigma Chemical Co., St. Louis. MO, USA.

Peptide N-Glucosidase-F (PNGase-F) was obtained from New England Biolabs Inc. Beverly MA USA.

Coomassie brilliant blue G-250 was from Eastman Kodak Co., Rochester, NY, USA.

β-Mercaptoethanol was purchased from Fluka, Switzerland and ammonium persulfate (APS) was procured from ICN Biomedicals Inc., Aurora, Ohio.

Nitrocellulose (0.45 μm) membrane was from Schleicher and Schuell, Germany. Immobilon-P (polyvinyldiflouride membrane PVDF; 0.45 μm) was obtained from Millipore Corporation, USA.

Ammonium sulfate, sodium chloride, sodium dihydrogen orthophosphate, disodium hydrogen orthophosphate, sodium hydroxide, ethylene diamine tetra acetic acid (EDTA) and potassium acetate were from Qualigens Fine Chemicals, Mumbai, India. Glycine and sodium acetate were from E. Merck (India) Ltd., Mumbai, India.

Amino acid standards (Pierce H.), sodium dodecyl sulfate (SDS), phenylisothiocynate (PITC) and citraconic anhydride were from Pierce Chemical Company, Rockford, Illinois, USA.

Purification materials Sephadex G-200, concanavalin-A sepharose, cibacron blue Sepharose 3GA and heparin sepharose were from Pharmacia LKB, Uppsala, Sweden.

Pyrex™ brand hydrolysis and derivatization tubes were from Corning, NY, USA. The vacuum vials and reusable enclosures were from Waters Associate, Milford, MA, USA.

SDS-PAGE molecular weight markers, 5-bromo-4-chloro-3-indolylphosphate (BCIP)/nitroblue tetrazolium (NBT) and substrate for alkaline phosphatase were purchased from Bangalore Genie Pvt. Ltd., Bangalore, India.

High performance liquid chromatography (HPLC) grade solvents were obtained from Spectrochem Pvt. Ltd. India.

All other chemicals used were of analytical grade.

2.1.2. HPLC columns

BioSep-SEC-S 2000 (300 × 7.8 mm, 5 μm) and BioSep-SEC-S 3000 (300 × 7.8 mm, 5 μm) were from Phenomenex, Torrance, USA. Discovery ™ BIO Wide Pore C_{18} (21.2 mm × 25 cm, 10 μm) was from Supelco, Supelco Park, Bellefonte, PA, USA. Symmetry Shield RP_{18} (150 × 4.6 mm, 5 μm) and Pico-Tag amino acid analysis column (150 × 3.9 mm, 4 μm) were from Waters Associate, Milford, MA, USA.

2.2. Methods

2.2.1. Preparation of serum

Human blood was drawn from healthy voluntary donors. Porcine and ovine blood were obtained from the local abattoir. Rat blood was obtained from white albino rats

(*Rattus norvegicus*). The freshly drawn blood was placed in a centrifuge tube, incubated in a water bath at 37 °C for 30 min and then centrifuged at 2500 rpm for 10 min. The serum was gently aspirated as supernatant.

2.2.2. Ammonium sulfate fractionation

Mammalian serum was fractionated by controlled addition of finely powdered $(NH_4)_2SO_4$ to a final concentration of 40 %, allowed to stand overnight and centrifuged at 10500 × *g* for 30 min. Solid $(NH_4)_2SO_4$ was further added to the supernatant to obtain 70 % saturation and the solution allowed to equilibrate for 2 h at 4 °C. This was subjected to centrifugation at 14000 × *g* for 30 min. The precipitate obtained was resuspended in 0.05 M Tris-HCl buffer, pH 8.2 containing 0.05 M NaCl, and dialyzed extensively (2 L × 5) against the same buffer.

2.2.3. Assay methods

The elastase, trypsin and chymotrypsin activity and their inhibitory activity were spectrophotometrically measured by assaying amidolytic activity for elastase, trypsin and chymotrypsin in the absence and presence of a known quantity of α-1-PI using the chromogenic substrates NSAPNA, BAPNA and BTPNA respectively. All the spectrophotometric measurements were performed on a Shimadzu UV-Vis recording spectrophotometer (Model UV-1601).

2.2.3.1. Assay of elastase and elastase inhibitory activity

The reaction velocity was determined by measuring the absorbance of *p*-nitroanilide resulting from the hydrolysis of NSAPNA. The stock of NSAPNA (10 mM) was prepared by dissolving 10 mg in 2 mL of DMSO and then made up to 100 mL with 50 mM Tris-HCl buffer, pH 7.4 containing 20 % DMSO (v/v). Elastase solution (40-50 µg in 0.5 mL of 1 mM HCl) was added to 0.5 mL of distilled water and incubated with 1.25 mL of substrate at 37 °C for 10 min. The reaction was stopped by adding 0.25 mL of 30 % acetic acid and the liberated product, *p*-nitroanilide measured at 410 nm against an appropriate blank.

Assay of elastase inhibitory activity

The elastase solution was incubated with an aliquot of α-1-PI solution for 10 min at 37 °C and the reaction started by the addition of 1.25 mL NSAPNA diluted in buffer and incubated at 37 °C for 10 min. The reaction was arrested by addition of 30 % acetic acid and the residual elastase activity measured by recording the absorbance at 410 nm.

Elastase and elastase inhibitory unit

One elsatase activity unit (EU) is arbitrarily defined as an increase in absorbance by 0.01 at 410 nm under assay conditions. The elastase inhibitory unit (EIU) is defined as the number of elastase units inhibited by α-1-PI under the same conditions.

2.2.3.2. Assay of trypsin and trypsin inhibitory activity

Trypsin was assayed according to the modified photometric method of Kakade et al., (1969) using the substrate BAPNA. Forty mg of BAPNA was dissolved in 2 mL DMSO and then diluted (1:100) in 50 mM Tris-HCl buffer, pH 8.2 containing 20 mM $CaCl_2$, prior to enzyme assay. The assay reaction consisted of 0.5 mL of trypsin solution (40-50 μg of trypsin in 1 mM HCl), 0.5 mL of water and 1.25 mL of the substrate. The reaction was carried out at 37 °C for 10 min and the reaction arrested by adding 0.25 mL of 30 % acetic acid. The absorbance of *p*-nitroanilide liberated was measured at 410 nm against an appropriate blank in which the reaction was arrested by adding 30 % acetic acid prior to the addition of BAPNA.

Assay of trypsin inhibitory activity

The trypsin solution was incubated with an aliquot of inhibitor solution for 10 min at 37 °C and the reaction started by the addition of 1.25 mL BAPNA diluted in buffer and incubated at 37 °C for 10 min. The reaction was arrested by addition of 30 % acetic acid and the residual trypsin activity was measured colorimetrically at 410 nm.

Trypsin and trypsin inhibitory unit

One trypsin activity unit (TU) is arbitrarily defined as an increase in absorbance by 0.01 at 410 nm under the assay conditions. The trypsin inhibitory unit (TIU) is defined as the number of trypsin units inhibited under the same conditions (Kakade et al., 1969).

2.2.3.3. Assay of chymotrypsin and chymotrypsin inhibitory activity

The reaction velocity was determined by measuring the absorbance of *p*-nitroanilide at 410 nm resulting from the hydrolysis of BTPNA. The stock of BTPNA (20 mM) was prepared by dissolving 16.2 mg in 2 mL of DMSO and then made up to 100 mL with 50 mM Tris-HCl buffer, pH 7.8 containing 100 mM $CaCl_2$ and 20 % DMSO (v/v). Chymotrypsin solution (40-50 μg in 0.5 mL of 1 mM HCl) was added to 0.5 mL of distilled water and incubated with 1.25 mL of substrate at 37 °C for 10 min. The reaction was stopped by adding 0.25 mL of 30 % acetic acid and the liberated product, *p*-nitroanilide measured at 410 nm against an appropriate blank.

Assay of chymotrypsin inhibitory activity

Chymotrypsin inhibitory assay was performed similar to that of trypsin and elastase inhibitory assay and the residual activity of chymotrypsin was calculated by measuring the absorbance at 410 nm.

Chymotrypsin and chymotrypsin inhibitory unit

One chymotrypsin (CU) unit is arbitrarily defined as an increase in absorbance by 0.01 at 410 nm under assay conditions. The chymotrypsin inhibitory unit (CIU) is defined as the number of chymotrypsin units inhibited under the same conditions.

2.2.4. Preparation of purification matrices

2.2.4.1. Preparation of Cibacron blue sepharose 3GA column

Lyophilized Cibacron blue sepharose 3GA matrix (10 g) was rehydrated with at least 200 mL/g of 0.05 M Tris-HCl buffer, pH 8.2 containing 0.05 M NaCl. Rehydration was done overnight at 4 °C. The medium was packed in a glass column (1.5 × 30 cm) at a flow rate of 24 mL/h. The matrix was equilibrated with 5-10 column volumes of equilibration buffer. It is essential that the lactose used to stabilize the media during lyophilization and free dye be completely washed out with equilibration buffer prior to usage.

2.2.4.2. Preparation of Sephadex G-200

Fifteen grams of Sephadex G-200 dry powder was allowed to swell in 500 mL of 0.05 M Tris-HCl buffer, pH 7.4 containing 0.9 % NaCl (w/v) and 1mM Cys for 72 h. Sephadex G-200 has a dry bead size of 10-40 μm, which gives a bed volume of 20-25 mL per gram of dry gel. The fractionation range of Sephadex G-200 is 5000-250,000 Da for globular proteins. After swelling, the gel slurry was packed into a glass column (1.5 × 90 cm) at a flow rate of 18 mL/h. Size exclusion chromatography on Sephadex G-150 was used as an intermediate step in the purification of ovine α-1-PI based on M_r. The column was stored in buffer containing 0.05 % sodium azide.

2.2.4.3. Preparation of Concanavalin-A sepharose (Con-A) column

Concanavalin-A sepharose is concanavalin-A (tetrameric metalloprotein isolated from *Canavalia ensiformis*) coupled to Sepharose-4B using cynogen bromide. Con-A binds molecules containing α-D-mannopyranosyl, α-D-glucopyranosyl and sterically related residues. Con-A Sepharose is routinely used for separation and purification of glycoproteins, polysaccharides and glycolipids. Ten g Con-A sepharose with a density of 10-16 mg Con-A/mL and 20-45 mg thyroglobulin binding capacity/mL of media was prepared as a slurry and washed with 10 bed volumes of binding buffer (0.05 M sodium phosphate buffer, pH 6 .0 containing 0.25 M NaCl and 1mM Mg^{2+}, Ca^{2+} and Mn^{2+} ions) to remove the preservative. The medium was packed in a glass column (1.5 × 10 cm) at a flow rate of 18 mL/h.

2.2.4.4. Preparation of heparin-sepharose column

Heparin is a naturally occurring GAG which serves as an effective affinity binding and ion exchange ligand for a wide variety of biomolecules including coagulation factors, serpins, lipoproteins, protein synthesis factors, enzymes that act on nucleic acids and steroid receptors. The pre-swollen heparin Sepharose 6 Fast Flow (4 mg heparin/mL drained medium) was gently packed into a glass column (1.5 × 20 cm). The preservative solution in commercial matrix preparation was replaced with binding buffer (0.1 M Tris-HCl buffer, pH 8.2) before use and equilibrated with same buffer.

2.2.5. Polyacrylamide gel electrophoresis (PAGE)

Vertical slab gel electrophoresis was carried out on a Broviga mini slab gel electrophoresis unit, at 25±2 °C.

2.2.5.1. SDS-Polyacrylamide gel electrophoresis (SDS-PAGE)

SDS-PAGE at pH 8.3 was carried out according to the method of Laemmli (1970) in a discontinuous buffer system.

Reagents

A. 30 % Acrylamide: Acrylamide (29.2 g) and bisacrylamide (0.8 g) were dissolved in water (100 mL), filtered and stored in a dark brown bottle at 4 °C.

B. 4× Separating gel buffer (1.5 M, pH 8.8): Tris (18.15 g), was dissolved in water, the pH of the solution was adjusted to 8.8 with HCl (6 N), the volume made up to 100 mL and stored at 4 °C.

C. 4× Stacking gel buffer: (0.5 M, pH 6.8): Tris (6 g) was dissolved in water. The pH of the solution was adjusted to 6.8 with HCl (6 N), volume made up to 100 mL with water and stored at 4 °C.

D. 10 % Sodium dodecyl sulfate: SDS (10 g) was dissolved in 100 mL water.

E. 10 % Ammonium persulfate: was freshly prepared by dissolving 50 mg in 0.5 mL of distilled water.

F. 10× Tank buffer: (0.25 M Tris, 1.92 M Glycine): Tris (3.0 g), Gly (14.41 g) were dissolved in 100 mL of water.

G. Staining solution: Coomassie brilliant blue (CBB) R-250 (0.2 g) was dissolved in a mixture of methanol: acetic acid: water (25:15:60 v/v). The reagent was filtered and stored at 25±2 °C.

H. Destaining solution: Methanol: acetic acid: water (25: 15: 60, v/v).

I. 2× Sample buffer: It was prepared in solution C diluted 1:4, containing SDS (4 % w/v), β mercaptoethanol (10 % v/v), glycerol (20 % v/v) and bromophenol blue (0.1 % w/v).

Preparation of separating and stacking gel: The contents of separating gel (Table 2. 1) were mixed, degassed and poured between the assembled glass plates with edges sealed with agar (2 % w/v). The gel was layered with 0.5 mL of distilled water and allowed to polymerize at 25±2 °C for 30 min. The contents of stacking gel were mixed and poured above the polymerized separating gel. The gels thus prepared were of the size 10.5×9 cm and thickness 0.8 mm. Samples were prepared by dissolving protein (10-25 μg) in solution I diluted 1:1. The samples were heated in a boiling water bath for 5 min. Cooled samples were loaded into the wells immersed in 1× tank buffer (25 mM Tris, 192 mM glycine and 0.1 % SDS) and run at constant voltage (60 V) for 3-4 h or until the tracking dye, reached the anode tank buffer. Medium range protein M_r markers: phosphorylase b (97,400 Da), BSA (66,300 Da), ovalbumin (43,000 Da), carbonic anhydrase (29,000 Da), soybean trypsin inhibitor (20,100 Da) and lysozyme (14,300 Da) were used. The markers were obtained as a pre-mixed solution with each protein at a concentration of 2.5 mg/mL. The markers were diluted 1:1 with solution I and boiled prior to use.

Staining: The gels were stained for protein with reagent G for 6 h at 25±2 °C. and destained in reagent H.

2.2.5.2. Native PAGE (Non-denaturing)

Polyacrylamide gel electrophoresis under non-denaturing condition was carried out to evaluate the purity of α-1-PI. Separating gels (10 % T, 2.7 % C; 12.5 % T, 2.7 % C) were prepared as shown in Table 2. 1. except that solution D was omitted.

Tank buffer (solution F) and Sample buffer (solution I) was prepared as explained earlier except that SDS and β-mercaptoethanol were not added. About 5-20 μg of protein was mixed with an equal volume of sample buffer and loaded on to the gel. Following electrophoresis at constant voltage (100 V), proteins were visualized using CBB R-250.

2.2.5.3. Gelatin embedded PAGE for trypsin and chymotrypsin inhibitory activity staining

Gelatin–PAGE (Felicioli et al., 1997) was performed by adding gelatin (1 %, w/v final concentration) to the acrylamide gel as described in Section 2.2.5.1. and 2.2.5.2.

Following electrophoresis, the gel was washed with distilled water three times and then incubated at 37 °C in 0.1 M Tris-HCl buffer (pH 8.0 for trypsin and pH 7.8 for chymotrypsin) containing either trypsin or chymotrypsin (40 μg/mL) for 1 h. After gelatin hydrolysis, the gel was washed with distilled water and stained with CBB R-250 and destained. The presence of α-1-PI was detected as a dark blue band in a clear background due to the complex of the unhydrolyzed gelatin with the stain.

Table 2. 1. Preparation of separating gel and stacking gel.

Solution	Separating gel (mL)		Stacking gel (mL)
	(12.5% T, 2.7% C)	(10% T, 2.7% C)	(5% T, 2.7% C)
Solution A	3.33	2.66	0.83
Solution B	2.00	2.00	-
Solution C	-	-	1.25
Distilled water	2.55	3.22	3.03
Solution D	0.08	0.06	0.05
TEMED	0.01	0.01	0.01
Solution E	0.03	0.03	0.03
Total	8.00	8.00	5.00

2.2.5.4. Glycoprotein staining

This stain was used to identify the presence of glycoproteins. The periodic acid-Schiff's staining was carried out following the method of Robert et al., (1969) and Kapitany and Zebrowski (1973). After electrophoresis the gel was immersed in 12.5 % TCA (w/v) for 30 min, then rinsed lightly with distilled water for 15 sec, and incubated in 1 % periodic acid in 3 % acetic acid for 30 min. The gel was washed with distilled water (6 × 50 mL) 10 min each. The washed gel was immersed in Schiff's reagent and then allowed to develop color in the dark at 4 °C. The dark pink color appeared in about 50

min. Freshly prepared 0.5 % sodium metabisulfite (50 mL) was added to the gel and washed. Finally the gel was incubated in water overnight and stored in 3 % acetic acid. Glycoproteins appeared as pink color bands in the stained gel. Ovalbumin was used as the positive control.

2.2.6. Protein estimation

Protein concentration was determined by the dye binding method of Bradford (1976) and Zor and Selinger (1996). BSA was used as the standard. This method is based on the reaction between basic amino acids and CBB G-250 to form a colored complex. The intensity of this product is detected at 595 nm and related to protein concentration.

2. 2. 7. Carbohydrate estimation

Total neutral sugar was determined colorimetrically by the phenol-sulfuric acid method (DuBois et al., 1956) using glucose as standard. Heparin estimation was performed by the improved detection and quantitation method of Farndale et al. (1986). This method makes use of the binding behavior of metachromatic dye dimethylmethylene blue with heparin and the detection of the resultant purple colored complex at 525 nm.

2. 2. 8. Capillary electrophoresis

The purified α-1-PI was electrophoresed on a Prince Technologies capillary electrophoresis system equipped with a coated capillary (Prince Technologies B.V., Netherlands) (i.d. = 75 μm, length = 100 cm), at 28 °C by applying a voltage of 30 KV. Prior to analysis, the capillary was equilibrated with Tris-HCl buffer (0.05 M, pH 7.4). The protein sample (1 mg/mL in running buffer) was injected at 20-mBar pressure for 10 sec. The inhibitor was detected at 230 nm with an online lambda detector 1010 Bishoff set at 230 nm.

2. 2. 9. Isoelectrofocussing

Reagents

Anode solution: Orthophosphoric acid, 34.0 mL of (88-93 %) H_3PO_4 was diluted to 500 mL with distilled water.

Cathode solution: Sodium hydroxide solution; 4 g of NaOH was dissolved in 100 mL of distilled water.

Fixing solution: 10 % tricholroacetic acid (w/v).

Equilibration solution: Aqueous solution of 25 % methanol, 5 % acetic acid (v/v).

Staining solution: 0.1 % (w/v) CBB G-250 in an aqueous solution of 25 % methanol and 5 % acetic acid (v/v).F

Destaining solution: 25 % methanol, 5 % acetic acid (v/v).

Pre-cast ampholine PAG gel of dimensions 245 × 110 × 1mm, pH range 4.0-6.5, 5 % T, 3 % C, were used. The PAG gel was placed on a pre cooled (10 °C) Multiphor plate, avoiding trapping of air bubbles. With the help of gel loading strips, the samples (10-15 µg) and pI markers were loaded. The anode and cathode buffer strips were pre-equilibrated in anode and cathode solutions separately. The wet buffer strips were carefully placed at the anode and cathode ends of the gel. The electrodes were arranged to come in contact with the buffer strips. The proteins were allowed to focus for 90 min at 1500 V, for 1 h. At the end of the run the gel was fixed in fixing solution for 1 h. The gel was then immersed in staining solution, preheated to 60 °C for 30 min. The gel was destained using several change of destaining solution.

2. 2. 10. Electroblotting of proteins

Preparation of PVDF membrane: The PVDF membrane cut to the required size (slightly larger than the gel) was soaked in methanol for 5 min prior to transfer. (Matsudaira, 1987; Speicher, 1989).

Blotting: Following electrophoresis, the gel was immediately rinsed in transfer buffer (10 mM CAPS, pH 11.0 containing 10 % methanol (v/v) and 0.1 % SDS (w/v) for 15 min. Semi-dry electro-blotting was carried out using a semi-dry blotting apparatus (Towbin et al., 1979). The transfer was carried out for 2 h using a current of 0.8 mA/cm^2 of the blotting paper. The membranes were stained with CBB R-250 and destained for protein sequencing or probed with antibodies as described later (Section 2.2.11).

Destaining: The PVDF membrane was destained in 50 % methanol. For NH_2-terminal sequence the corresponding bands were excised, washed with 100 % methanol and dried.

2.2.11. Immunodetection of α-1-PI

Following immobilization or electro-transfer, the membrane was washed with immunoblot buffer (5 % skimmed milk powder in PBS, pH 7.0) four times (4 × 30 min). The membrane was incubated overnight at 4 °C in immunoblot buffer containing antibodies raised against α-1-PI (1:1000 dilution). After repeated washes (4 × 30 min) in the immunoblot buffer, the membrane was incubated with the secondary antibody, alkaline phosphatase conjugated goat anti-rabbit immunoglobulins, for 2 h at 25±2 °C. After four washes (4 × 10 min) in immunoblot buffer and a final wash with the reaction buffer (0.1 M Tris, 0.5 M NaCl, 5 mM $MgCl_2$, pH 9.5), alkaline phosphatase activity was detected with a mixture of BCIP and NBT in the reaction buffer. Alternatively when a HRP conjugate was used the HRP activity was detected using benzamidine.

For dot blot analysis About 100 μg of the purified α-1-PIs were immobilized on a nitrocellulose membrane by repeated application employing a current of hot dry air to accelerate the drying until the required protein was immobilized. Following immobilization the α-1-PIs were sequentially treated with primary and secondary antibodies and immunodetected using alkaline phosphatase activity or HRP activity as described above.

2.2.12. Molecular weight determination

2.2.12.1. Molecular weight determination by analytical gel filtration chromatography and SDS-PAGE

The apparent M_r of the purified α-1-PI was examined by analytical gel filtration using BioSep SEC-S 2000 (300 × 7.8 mm, 5 μm). α-1-PI was eluted in 0.1 M Tris-HCl buffer (pH 7.4) containing 0.9 % NaCl at a flow rate of 0.5 mL/min. The detector was set at 280 nm. The column was calibrated with alcohol dehydrogenase (150,000 Da), bovine serum albumin (66,000 Da), carbonic anhydrase (29,000 Da) and cytochrome C (14,400 Da).

The M_r of α-1-PI was also confirmed by SDS-PAGE (10 % T, 2.7 % C) where the purified α-1-PI was electrophoresed along with a series of commercial SDS-PAGE M_r markers. A calibration curve was constructed and the apparent M_r of the inhibitor approximated based on its mobility.

2.2.12.2. Molecular weight determination by Matrix Assisted Laser Desorption Ionization-Time of flight (MALDI-TOF)

The exact molecular mass of the purified human, rat and ovine α-1-PIs as well as heparin used for all experimental purposes were obtained from MALDI-MS analysis performed on a Bruker Daltonics Ultraflex MALDI TOF/TOF system (Bruker Daltonics, Bremen, Germany) in the reflective positive ion mode. The instrument was calibrated with masses ranging between 10,000-100,000 Da for inhibitors and 1000-10, 000 Da for heparin. The purified samples were desalted and concentrated using C_{18} reverse phase chromatography matrix. The samples were dialyzed extensively against water. The samples were then prepared by mixing with equal volumes of matrix. Matrix used was saturated α-cyano-4-hydroxycinnamic acid (Sigma Aldrich Chemie GmbH) prepared separately in CH_3CN/H_2O/TFA (80:20:0.1). The samples were then dried at 25 ºC under atmospheric pressure, loaded on to probe slide and the data collected.

2.2.13. Amino acid analysis

Amino acid analysis was performed according to the method of Bidlingmeyer et al., (1984) using a Waters Associate Pico-Tag amino acid analysis system.

The amino acid analysis was carried out using a three-step procedure. In the first step, protein samples were acid hydrolyzed to free amino acids. Amino acids were modified by PITC in the second step and the last step included the separation of the modified amino acids by RP-HPLC.

Hydrolysis of Protein: An aliquot of 50 µL of reverse phase purified samples were pipetted in to a tube (6 × 50 mm Pyrex ^{TM}) and placed in the special vacuum vial. The vial was attached to the Waters Associates Pico-Tag workstation manifold and the samples were dried under vacuum to 50-60 mtorr. Post-drying, the vacuum was released and 200 µL of constant boiling HCL (6 N) containing phenol 1 % (v/v) was pipetted in to

bottom of the vacuum vial. The vacuum vial was then reattached to the manifold, evacuated and sealed under vacuum. Samples were hydrolyzed in the workstation at 110 °C for 24 h. After hydrolysis the residual HCl inside the vacuum vial was removed under vacuum. Standard free amino acid mixture (Pierce H) containing up to 25 nmol of each amino acid was placed in the tubes (6 × 50 mm) and dried under vacuum. Standard free amino acid mixture and the hydrolyzed samples were dried down under vacuum after the addition of re-drying solution (20 μL) containing ethanol: water: triethylamine (TEA) in the ratio of 2:2:1. When a 50-60 mtorr vacuum was attained, the samples were ready for derivatization.

Derivatization of hydrolyzed amino acids: The derivatization reagent consisted of ethanol:triethylamine:water :PITC (7:1:1:1) and was made fresh each time. The PITC was stored at –20 °C under N_2 to avoid its degradation. To make 300 μL reagent, sufficient for 12 samples, 210 μL of ethanol was mixed thoroughly with 30 μL each of PITC, TEA and water. PTC amino acids were formed by adding 20 μL of the reagent to the dried samples and sealing them in the vacuum vials for 20 min

Table 2. 2. The gradient programme for amino acid analysis

Time (min)	Flow (mL)	% A	% B	Curve
00.01	1.0	100	0	
10.00	1.0	54	46	7
11.00	1.0	0	100	6
13.00	1.0	0	100	6
14.00	1.0	100	0	6
25.00	1.0	100	0	6

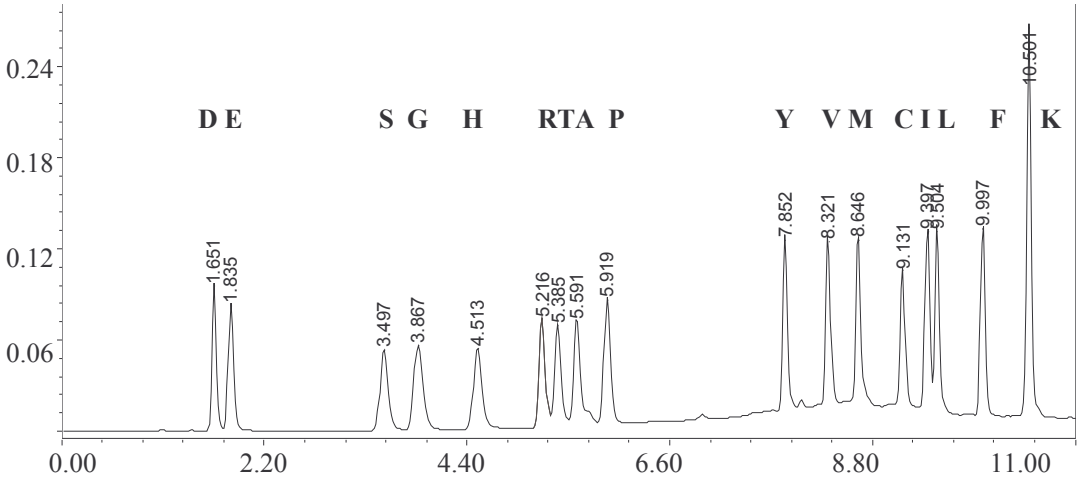

Figure 2. 1. Elution profile of PTC-amino acids using a Pico-Tag amino acid analysis system. The amino acids are represented by the single letter code. Column: Pico-Tag™ (150 × 3.9 mm, 4 μm); flow rate: 1.0 mL/min; wave length: 254 nm; temperature: 38 °C; injection volume: 5 μL (312.5 pmole of each amino acid); solvent A: 140 mM Na acetate, 3.6 mM triethylamine (TEA), pH 6.4/acetonitrile (94/6); solvent B: 60 % acetonitrile.

at 25 ± 2°C. The excess of reagents were then removed under vacuum using the workstation. When the vacuum reached 50-60 mtorr, the samples were ready for analysis by RP-HPLC.

Chromatography: The HPLC was carried out using a Waters Associate HPLC system consisting of binary gradient pumping system and photodiode array detector (Model 2996) with a Millennium data processor. The temperature was controlled at 38 ± 1 °C with a column heater. Samples were injected in volumes ranging from 5-50 μL. The column was an application specific Pico-Tag column (150 × 3.9 mm).

Solvent systems: Solvent system consisted of two eluents, (A) an aqueous buffer (0.14 M Sodium acetate containing 0.5 mL/L of TEA) titrated to pH 6.4 with glacial acetic acid: acetonitrile (94:6) and (B) 60 % acetonitrile in water. The gradient run for the separation consisted of 0 % B traversing to 46 % B in 10 min. After the run a washing step in 100 % B was included so that the residual sample components were eliminated.

The PTC amino acids were detected at 254 nm. The gradient elution programme is shown in Table 2.2 and the separation of a standard amino acid mixture is shown in the Figure 2.1.

2.2.14. Automated gas phase protein sequencing

The NH_2-terminal sequence of α-1-PI from various mammalian species and the digested α-1-PI peptides was determined by Edman degradation using an Applied Biosystems 491A automated gas phase protein sequencer (Procise 491A). This sequenator carries out Edman-degradation by supplying gaseous reagents for the coupling and cleavage reactions. The flow diagram for the sequence of events is shown in Figure 2. 2.

The protein was electroblotted on to a PVDF membrane and the band detected by CBB staining. The band was excised, destained thoroughly with methanol, and subjected to several alternate washes with water and methanol (Section 2.2.10).

The membrane was carefully loaded on to a quartz holder, dried over a stream of argon and directly used for the pulsed gas phase sequencing. Alternatively, the protein or peptide purified, collected over several runs of reverse phase HPLC and concentrated was used. It was spotted on a to glass fiber disc previously coated with polybrene and washed for three cycles. The coupling reaction is carried out with phenyl isothiocynate (R1) in the presence of gaseous methyl piperidine (R2).

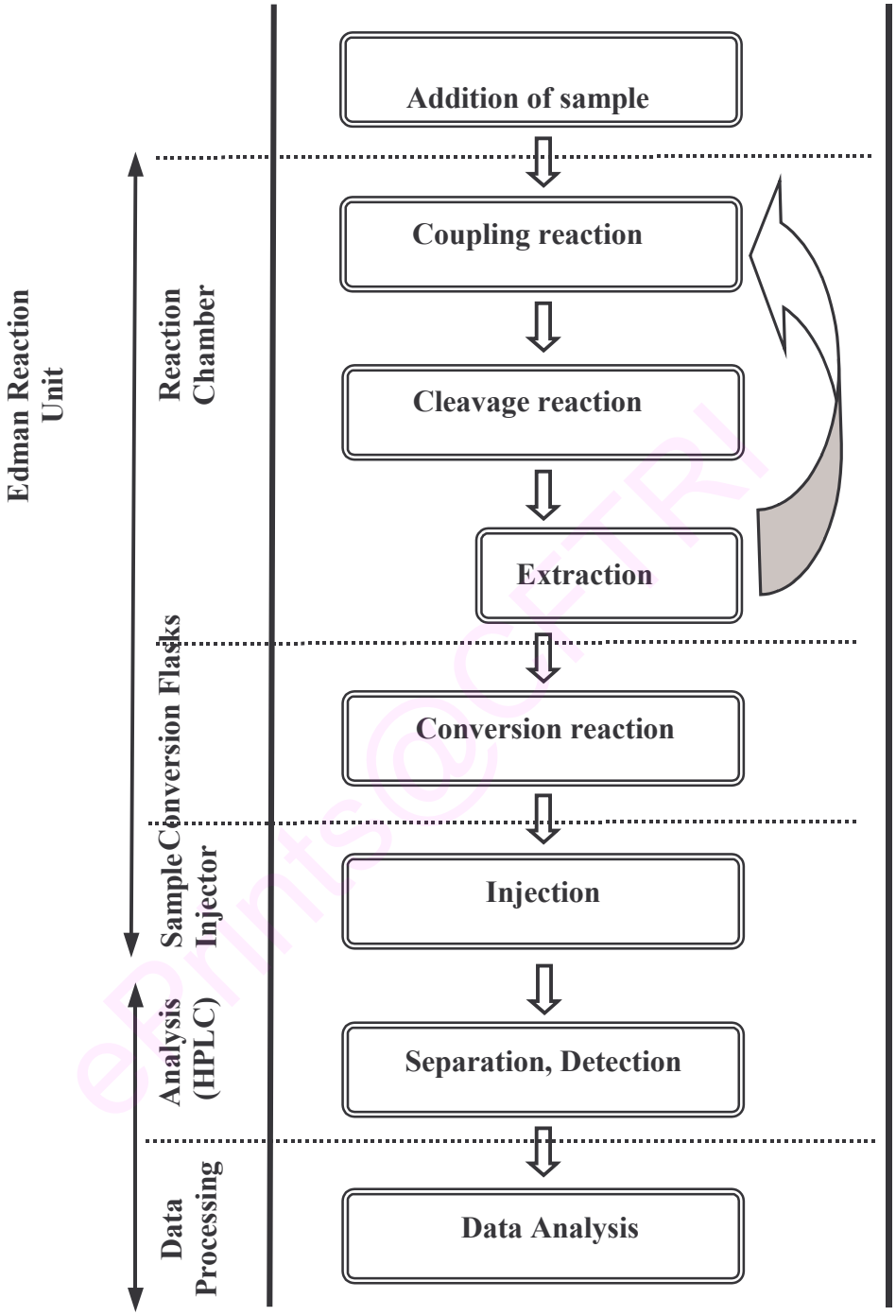

Figure 2. 2. Flow diagram of the reactions that occur during gas phase sequencing of protein or peptide on ABI-477A (Applied Biosystem) sequenator.

Excess of reagents and by products were washed with *n*-heptane (S1) and ethyl acetate (S2). The cleavage reaction is carried out with the gaseous TFA to form an aniline-thiazolinone (ATZ) derivative. Both the coupling and cleavage reactions are performed in a temperature controlled reaction chamber. The free ATZ-amino acid extracted from conversion flask by n-butyl chloride (S3) is converted to the more stable PTH-amino acid by reaction with 25 % TFA (R4). The PTH-amino acid dissolved in acetonitrile (S4) is automatically injected into the HPLC. The PTH-amino acids were separated by RP-HPLC and detected at 269 nm.

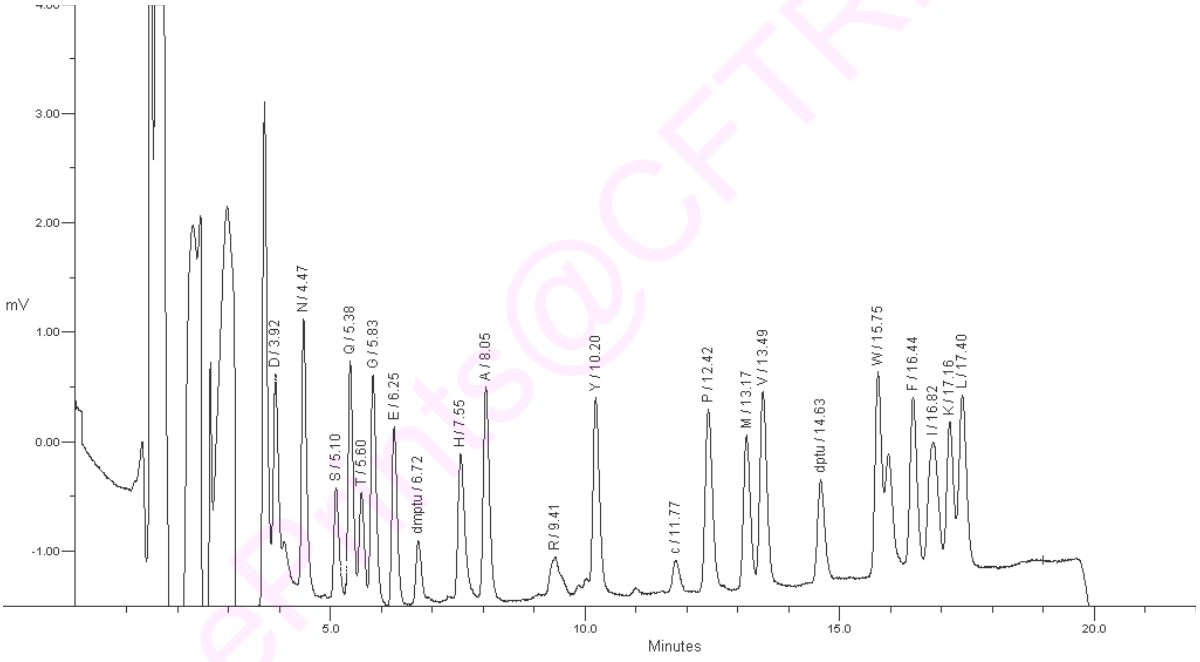

Figure 2. 3. RP-HPLC separation of PTH-amino acid standards on the automated protein sequenator.

The PTH-amino acid in each cycle was identified, quantified and recovery percentage calculated using the Seq. 2. 2 programme. The results were displayed and recorded. Figure 2. 2. represents the separation profile of the standard PTH-amino acid mixture. β-

Lactoglobulin was used as a standard protein for the performance check of the instrument.

2.2.15. Stoichiometry of protease-α-1-PI interaction

To evaluate the stoichiometry of protease binding to inhibitor, a fixed quantity of elastase/trypsin/chymotrypsin was incubated individually with increasing amount of α-1-PI in presence of the cognate substrate NSAPNA, BAPNA or BTPNA respectively under optimal conditions. The residual protease activity was measured as described earlier (Section 2.2.3.1. and 2.2.3.2). Extrapolation of the plot of [I]/[E] versus % residual activity indicated the stoichiometry of binding.

2.2.16. Heparin induced activation of α-1-PI

The heparin induced activation of human and ovine α-1-PI was evaluated by pre-incubating 1 μM of α-1-PI with varying concentrations of heparin (0-10 μM) in 0.15 M Tris-HCl, pH 7.4 at 37 °C followed by assessing the elastase and trypsin inhibitory activity as described earlier (Section 2.2.3.2).

2.2.17. Evaluation of association rate constants of α-1-PI

Second order association rate constants of the serine protease elastase with respect to both native and heparin activated human and ovine α-1-PIs were studied by estimating the liberated product, *p*-nitroanilide from the chromogenic substrate NSAPNA upon cleavage. The reactions were carried out under pseudo-first order conditions in 0.15 M Tris-HCl buffer pH 7.4 at 37 ºC as described earlier (Djie et al., 1996). Varying concentrations of α-1-PI were incubated with elastase (50 μg) at 37 °C for different periods of time. In case of heparin activated α-1-PIs, the inhibitors were pre-incubated with 0.5 μM of heparin for 15 min. Aliquots were removed at regular intervals and residual α-1-PI activity determined from the initial rate of the substrate cleavage. The reactions were stopped by addition of 30 % acetic acid. The absorbance of product, *p*-nitroanilide liberated was measured at 410 nm against appropriate blanks.

Similarly, inhibition of trypsin and chymotrypsin by both human and ovine α-1-PI was studied. The assays were repeated by pre-incubating α-1-PI with same

concentrations of heparin. The time dependence of enzyme inhibition loss was fit to a single exponential function. Second order association rate constants were determined from the slopes of linear regression fits. The results obtained are an average of three separate experiments.

2.2.18. pH stability of α-1-PI

Stability of the native human, rat, ovine and porcine α-1-PI as a function of pH was evaluated by pre-incubating the inhibitors individually in 0.05 M buffer with pH varying from 2.5 to 11.0 for 1 h at 37 ºC. The buffers used were Gly-HCl (pH 2.5), Citric acid-Na_2HPO_4 (pH 3.5, 4.5, 5.5 and 6.5), Tris-HCl (pH 7.4 and 8.2), Gly-NaOH (pH 9.0 and 10.0) and Na_2HPO_4-NaOH (pH 11.0). The residual trypsin inhibitory activity was assayed in 0.05 M Tris-HCl buffer, pH 8.2 as described earlier (Section 2.2.3.2).

2.2.19. Deglycosylation of α-1-PI

The deglycosylation of human and ovine α-1-PI was achieved using the enzyme Peptide N-Glucosidase-F. To study the structure and function of a glycoprotein it is often desirable to remove the glycans. This approach allows the assignment of specific biological functions to particular components of the glycoprotein. PNGase-F is the most widely used enzyme for the deglycosylation of glycoproteins both in gel and in solution. The enzyme releases Asn-linked oligosaccharides from glycoproteins. The shift in M_r on deglycosylation can be observed by SDS-PAGE analysis. Twenty μg of α-1-PI was incubated with 2500 units of PNGase-F for 1 h at 37 ^oC and analyzed by SDS-PAGE and gelatin embedded PAGE for differences in mobility and protease inhibitory activity.

2.2.20. Thermal inactivation studies

The loss of inhibitor activity as a function of temperature was studied for both human and ovine α-1-PI and their deglycosylated forms. Native α-1-PIs and their deglycosylated forms were incubated for 15 min in 0.1 M sodium phosphate buffer, pH 7.4 at different temperatures ranging from 27-90 ^oC .The residual inhibitory activity was measured at 37 ^oC. The midpoint of thermal inactivation, T_m, was calculated from the plot of % residual activity versus temperature. Kinetics of thermal inactivation of ovine α-1-PI was studied using a constant temperature bath at desired temperatures. Aliquots of

protein were removed at periodic intervals and cooled in an ice bath prior to assay. The residual inhibitory activity was measured and expressed as percentage of initial activity. From the semi- logarithmic plot of residual activity as a function of time, the inactivation rate constant (K_r) was calculated. The apparent half-life was estimated and energy of activation (E_a) calculated from the slopes of Arrhenius plot. Thermodynamic functions were calculated according to the following relationships:

$$\Delta H^* = E_a - RT$$

$$\Delta G^* = -RT\ln (Kr)\, h/k_B T$$

$$\Delta S^* = (\Delta H^* - \Delta G^*)/T$$

Where h is the Planck constant, K_B the Boltzmann constant, R the gas constant and K_r the rate constant.

2.2.21. Chemical modification of amino acids

2.2.21.1. Modification of amino group by 2,4,6–trinitrobenzene sulfonic acid (TNBS)

Free amino groups present in ovine α-1-PI were modified with TNBS using the procedure of Haynes *et al*., (1967). To different aliquots of inhibitor solution (0.5 mg/mL), 1 mL of 4 % sodium hydrogen carbonate, pH 8.5 and 1 mL of 0.1 % TNBS in water was added and incubated at 25 °C. Aliquots (0.2 mL) of the solution were removed from the reaction mixture at regular time intervals, diluted with ice-cold water to stop the reaction and assayed for the residual inhibitor activity. The extent of free $–NH_2$ group modification was followed spectrophotometrically at 344 nm (Habeeb, 1966) that corresponds to the maximal absorption of the final product N-trinitrophenylamines.

2.2.21.2. Modification of Lys residues by citraconic anhydride

The ε-amino groups of the Lys residues of ovine α-1-PI were modified at 25 ± 2 °C with specific blocking agent citraconic anhydride by the method of Dixon and Perham (1968), thereby shifting the net charge of the protein to a more negative value. The protein (1 mg/mL) was dissolved in water and the pH adjusted to 8.0. Citraconic anhydride (1 μL/ mg of protein) was added to the solution, while maintaining pH 8.0 by

the addition of 5 M NaOH. A corresponding blank was maintained. Once the pH of the reaction mixture was stable, protein was dialyzed extensively and analyzed for protease inhibitory activity (Section 2.2.3).

2.2.21.3. Modification of Arg residues with 1,2-cyclohexanedione

Arg residues were modified by the reviewed method of Smith (1977) using 1, 2-cyclohexanedione. The protein was dissolved in 0.2 M sodium borate buffer, pH 9.0 (0.1 mg/mL) and reacted with 0.15 M 1, 2-cyclohexanedione at 37 °C in dark. Aliquots were extracted at periodic intervals and dialyzed immediately in cold using dialysis cassettes. An equivalent sample of ovine α-1-PI was treated in the same manner except that 1, 2-cyclohexanedione was omitted. The reaction mixture was acidified with 30 % acetic acid and dialyzed against 10 mM acetic acid to remove excess reagents. The two samples were adjusted to the same volume for analysis of inhibition and to the same protein concentration. The inhibitory activity was assayed as described earlier (Section 2.2.3).

2.2.21.4. Modification of Met residues by chloramine-T

Met residues of ovine α-1-PI were modified with 20 mM chloramine–T in 0.2 M Tris-HCl buffer, pH 8.0 (Mistry et al., 1991). Aliquots were removed periodically, dialyzed extensively against 0.2 M Tris-HCl at 4 ^{o}C using dialysis cassettes, and residual inhibitory activity assayed as described (Section 2.2.3).

2.2.21.5. Modification of Met residues by hydrogen peroxide

Purified ovine α-1-PI (0.1 mg/mL) was incubated for 6 h at 37 °C in a reaction mixture containing 0.05 M potassium phosphate, 0.1 M potassium chloride, 1 mM magnesium chloride at pH 5.0 and 3 % H_2O_2. The concentration of H_2O_2 was measured at 240 nm (ε = 39.4 ± 0.2 M^{-1} cm^{-1}) (Nelson and Kiesow, 1972). At this pH Met is oxidized selectively to Met sulfoxide (Brot and Weissbach, 1983). At the end of the reaction a sample was taken to measure anti-protease activity. The modified inhibitor was evaluated for protease inhibitory activity against elastase, trypsin and chymotrypsin of known activity with respective substrates and compared with appropriate blanks at 410

nm. The protease inhibitory activity was also assessed by gelatin embedded PAGE (Section 2.2.5.3).

2.2.22. Peptide mapping of α-1-PI reactive center loop (RCL)

Ovine α-1-PI (0.1 mg/mL) in 0.1 M Tris-HCl, pH 7.4 was incubated with sequencing grade elastase, trypsin and chymotrypsin individually at 37 °C for 30 min. in stoichiometric proportions to bring about complete protease inhibition. The reaction was arrested by boiling with SDS sample buffer and analyzed by SDS-PAGE. The cleaved peptides were transferred to a PVDF membrane as described (2.2.10). The membrane was stained with CBB R-250, peptide bands excised, thoroughly washed with 100% methanol and subjected to NH_2-terminal sequence analysis in an automated, calibrated gas phase protein sequencer.

2.2.23. Mapping of the heparin binding site of α-1-PI

Native and heparin bound forms of ovine α-1-PI were incubated with TPCK-trypsin (7.5 %, w/w) in 0.04 M NH_4CO_3 buffer containing 20 mM $CaCl_2$, pH 8.2 for 24 h at 37 °C for proteolytic digestion. The temperature, buffer and protease concentration used for proteolytic digestion were optimized to achieve complete digestion in 24 h. The proteolysis was arrested by incubating the reaction mixture for 20 min in a boiling water bath. The digest was concentrated to dryness and re-dissolved in 0.5 mL of 0.1 % TFA (Matsudaira, 1989). The peptides were separated by RP-HPLC as described below. The tryptic digests were analyzed by RP-HPLC using a Waters Symmetry Shield C_{18} column (4.6 mm × 150 mm; 5 μm) on a Waters HPLC system equipped with a 1525 binary pump and Waters 2996 photodiode array detector set at 230 nm at a flow rate of 0.7 mL/min. Solvent A was 0.1 % TFA in water and solvent B was 70 % CH_3CN containing 0.05 % TFA (Mahoney and Hermodson, 1980 and Hermodson and Mahoney, 1983). The water used in the preparation of the above solvents was Milli Q water having a conductance of 18.2 mhos. The aqueous solvents were degassed for 15 min and 2 min respectively using an oil vacuum pump before addition of TFA. Solvent strength was increased linearly from 0 to 100 % solvent B in 90 min. The peptide profile of heparin bound α-1-PI was compared and analyzed for the distinctly different peaks from the peptide profile of native α-1-PI. The identified peptide was collected over several runs. The amino acid

sequence of this peptide was determined by automated Edman degradation in an Applied Biosystems 491A automated gas phase protein sequencer. α-lactoglobulin was used as the standard to validate the performance of the instrument (Section 2.2.14).

2.2.24. Homology modeling

The entire computational analysis was performed on a Pentium 4, 3.20 GHz processor operating on Windows XP professional. The deduced amino acid sequence of ovine α-1-PI was retrieved from EMBL [Accession no. X15555] (Brown et al., 1989). The finest accessible template structure to carry out homology modeling of ovine α-1-PI was sought by a phylogenetic analysis of mammalian α-1-PIs. Ovine α-1-PI sequence was optimally aligned with human α-1-PI using a preliminary conventional pair wise sequence alignment tool employing EBLOSUM 62 scoring matrix finishing with a review of residue hydrophobicities (Smith and Waterman, 1981). The resulting file was uploaded to the SWISS-MODEL automated homology model-building server for model computation. A few knotty side chain conformations were acknowledged and rectified. All tertiary structural analysis, including viewing of three dimensional structures, superimpositions, and residue distance determinations were performed using the Swiss-PDB viewer program (SPdbV version 3.7) of ExPASy (http:I/www.expasy.ch). The ensuing structure was energy minimized using Deep View and the process was repeated.

Structural representations of the generated molecular model and the optimization of the geometries were carried out using two open public domain molecular graphics packages Visual Molecular dynamics (VMD) (Humphrey et al., 1996) and ArgusLab 4.0.1 (Thompson, Planaria software). Structural parameters and prediction quality of the modeled structure were evaluated and optimal model selected using the programs WHAT IF (v 4.99) and PROCHECK (v 3.5) from the Biotech web server (biotech.ebi.ac.uk).

2.2.25. Molecular docking of RCL peptide with Ser proteases

The structures of porcine trypsin, porcine elastase and bovine chymotrypsin were retrieved from Protein Data Bank (www.rcsb.org). The interacting residues of RCL of α-1-PI were brought into close proximity with the highlighted catalytic triad Ser^{195}, His^{57}, and Asp^{102} thereby adopting a conformation, accessible to the active site. This was

followed by extensive energy minimization using Deep View to aid in the packing of side chain atoms while harmonically constraining the α- carbon backbone. The side chains of amino acids with problems were fixed using SPdbV followed by an intensive cycle of energy minimization, applied to a region about 10 Å around the altered residue.

The Hamiltonian energy for the RCL from Thr^{349} to Pro^{360} in its stretched conformation was calculated by employing the Hartree-Fock operator as computed by Austin model 1(AM1) parameterization of the MNDO (Modified neglect of diatomic differential overlap) method (Dewar, 1985). The energy calculations were also performed using the Universal Force Field (UFF) method of molecular mechanics. All the energy calculations were performed at a net molecular charge of zero. Flexible docking was carried out using the genetic algorithm implemented in the program Argus lab (AScore scoring method). This dock engine was set to perform an exhaustive search for automated docking with complete ligand flexibility and partial protease flexibility in the neighborhood of the protease active site. A regular docking precision with standard augmented root node was applied and no inner augmented torsions were found. A medium dielectric constant of 15 and a non-bonded cut-off distance of 20 Å were used for all subsequent minimizations and molecular dynamics. Potentials, partial charges, and the cvff (consistent valence force field) were those supplied by the software manufacturer. Each run was optimized for 150 different poses. A high grid resolution of 0.35 Å was used in each case with average grid dimensions of 25 × 25 × 26 Å. The dimensions of the binding site box were extended to 25.59 × 26.99 × 26.65 Å. The optimal models were chosen based on bond angle stereochemistry using programs PROCHECK (Laskowski et al., 1993) and WHATIF (Vriend, 1990).

2.2.26. Sequence alignment, phylogenetic analysis and topology assessment

In order to reveal subtle conserved characteristics of serpin family and α-1-PI amongst different mammalian species a multiple sequence alignment was carried out. Aligned sequences were then analyzed using the PHYLIP program (Felsenstein, 1985). The sequences were analyzed by the maximum parsimony method using the PROTOPARS program. The unrooted phylogenetic tree was drawn.

The reported heparin binding sites of human antithrombin III (Carrell et al., 1994) were analyzed. The Po^le bioinformatique Lyonnais (http://pbil.univ-lyon1.fr/) and NCBI BLAST-Taxonomy (http://www.ncbi.nlm.nih.gov) databases were searched for α-1-PI sequences of various species related to the reported heparin binding sites of antithrombin. A multiple sequence alignment for these sequences with human antithrombin (Residue 120-149) was generated using CLUSTAL X (Higgins et al., 1996) with subsequent gap adjustments.

The Human α-1-PI (PDB ID 1HP7) was analyzed for surface positively charged domains using the public domain topology prediction programs (http://www.expasy.org/tools/#topology). The most positively charged surface domain sequence in α-1-PI (Residue 154-174) was aligned against α-1-PI from other mammalian species using CLUSTAL W multiple alignment algorithm (Higgins et al., 1994). The gap rich regions were removed using GENEDOC (Nicholas et al., 1997). CHROMA was used to format the multiple sequence alignment results (Goodstadt and Ponting, 2001).

2.2.27. Docking of heparin with α-1-PI

The model for α-1-PI used in studies here was derived from the co-ordinates of the structure labeled 1HP7 in the Brookhaven Protein Data Bank, which represents the uncleaved human α-1-PI at 2.1 Å resolution (Kim et al., 2001). The ligand octa-saccharide heparin was constructed in and submitted to the PRODRG site (Schuettelkopf and van Aalten, 2004). The initial geometry and topologies were retrieved. The ligand heparin was docked against human α-1-PI using MEDock algorithm (Chang et al., 2005) with a grid spacing of 0.4 Å. MEDock is available at http://medock.csie.ntu.edu.tw/ and http://bioinfo.mc.ntu.edu.tw/medock/. MEDock employs a global search strategy that exploits the maximum entropy property of the Gausian probability distribution, in the context of information theory (Hyvarinen et al., 2001). This algorithm is significantly superior when dealing with very rugged energy landscapes, which usually have insurmountable barriers. In the MEDock algorithm, 'n' Gaussian distributions are generated before the new population in the next generation is created. The main idea of the MEDock algorithm is to give a bias towards the low energy regions. The lower the energy, the more frequent the mining (Chang et al., 2005). The best ligand protein docked

model was evaluated and examined using the software PROCHECK and WHAT IF. Further calculations and graphical manipulations were performed using Arguslab (Thompson, Planaria software) and VMD (Humphrey et al., 1996).

2.2.28. Stokes' radius determination

The Stokes' radius (R_S), Stokes'-Einstein radius, or hydrodynamic radius R_H, named after George Gabriel Stokes indicates hydration and shape effects of the molecule. Since most molecules are not perfectly spherical, the Stokes' radius is generally smaller than the effective radius. Stokes' radius variations induced in ovine α-1-PI upon heparin binding were studied both by size-exclusion chromatography and dynamic light scattering measurements.

2.2.28.1. Size exclusion chromatography

Stokes' radii measurements were computed by size exclusion chromatography on a BioSep-SEC-S 3000 (300×7.8 mm, 5 μm) column, using a Shimadzu HPLC system, equipped with an SPD-M10A photodiode array detector. The column was equilibrated with 0.1 M sodium phosphate buffer, pH 7.4 containing 0.9 % NaCl at a flow rate of 0.5 mL/min. Ovine α-1-PI solution (5 μM) equilibrated in same buffer with varying heparin concentrations (0-10 μM) was injected in the column and eluted in the same buffer. The protein-ligand complex was detected at 230 and 280 nm. A set of proteins (thyroglobulin 660,000 Da, 79.9 Å; BSA 66,000 Da, 33.9 Å; carbonic anhydrase 29,000 Da, 23.6 Å; ribonuclease 13,700 Da, 19.3 Å) with known M_r and Stokes' radii were used to construct the calibration curve of log R_S versus migration rate. Blue dextran was used to determine the void volume.

2.2.28.2. Dynamic light scattering (DLS)

Stokes' radii measurements of α-1-PI (1 mg/mL in 0.1 M sodium phosphate buffer, pH 7.4 containing 0.9 % NaCl) in different concentrations of heparin (0-10 μM) were also performed by DLS on a Viscotek 802 DLS instrument with a thermostated cell holder. All solutions for the experiments were prepared using Milli-Q water. The experiments were performed at 90º scattering angle at 4±0.1 ºC. The samples were centrifuged at 12000 × g for 15 min to remove air bubbles from the samples and

subsequently into a quartz cuvette with a volume of 45 μL. Each spectrum obtained was an average of 10 scans. The results were analyzed by OmniSize 3.0 software. The Stokes' radius was obtained from the Stokes'-Einstein equation $R_S = kT/(6\pi\eta_0 D)$, where k is Boltzmann's constant, T the temperature (K), η_0 the solvent viscosity and D the translational diffusion coefficient.

2.2.29. Equilibrium dialysis of α-1-PI

Aliquots (1.5 mL) of protein solution (20 μM) in 0.05 M Tris-HCl buffer, pH 7.4 containing 0.9 % NaCl were dialyzed continuously for a period of 24 h at 4 ^{o}C against 30 mL buffer containing varying concentrations of heparin (0-100 μM). Corresponding 'blanks' containing only buffers were maintained. At the end of equilibration, the concentration of heparin in the outer solutions was estimated by the method of Farndale et al. (1986) (Section 2.2.7). Inner solutions could not be used since protein interfered with the estimation of heparin. From the observed difference in heparin concentration between 'blank' and experimental values, the number of heparin molecules bound per mole of protein was calculated. The experiment was carried out twice with different protein preparations and data analyzed by Scatchard plot.

2.2.30. Fluorescence studies

2.2.30.1. Intrinsic fluorescence

Fluorescence measurements were recorded on a Shimadzu RF 5000 spectrofluorimeter using a 3 mL, 10 mm path length quartz cell at 27±0.5 ^{o}C in 0.05 M Tris-HCl buffer, pH 7.4 equipped with a stir control. Excitation and emission slit widths were set at 5 nm each. Protein was excited at 280 and 295 nm and emission was recorded between 300 and 400 nm. Appropriate blanks were used for baseline correction of fluorescence intensity.

2.2.30.2. Fluorescence quenching by acrylamide

The quenching of α-1-PI fluorescence with the progressive additions of dynamic quencher acrylamide was measured for native and heparin activated forms. Trp perturbations both in the absence and in the presence of 0-5 μM heparin were followed at 295 nm and the emission spectra recorded at 335 nm. The fractional quenching (F_0/F)

was plotted against acrylamide concentration, where F_0 and F represent the fluorescence in the absence and presence of acrylamide respectively. Fluorescence intensities were corrected for dilution effects. The absorption of acrylamide at 295 nm was corrected using the equation.

$$F_{corr} = F_{abs}\, 10^{A/2}$$ (Lehrer and Leavis, 1978)

where A is the increase in the absorbance by the addition of acrylamide. Fluorescence quenching data were analyzed using the general form of Stern-Volmer equation

$$F_0/F = I + K_{sv}\,(Q)$$

where Q is quencher concentration and K_{sv} the dynamic quenching constant. To monitor conformational changes, fluorescence quenching data were also analyzed with modified Stern-Volmer equation (Lehrer, 1971)

$$F_0/\triangle F = 1/f_a\, K_{sv}\,(Q) + 1/f_a$$

where $\triangle F = F_0 - F$ and f_a is the maximum fractional accessible protein fluorescence.

2.2.30.3. Heparin binding studies

Binding of heparin to human and ovine α-1-PI was analyzed by fluorescence titrations in which the quenching of protein fluorescence accompanying heparin binding was used to monitor the interaction. Human and ovine α-1-PI (10 μM) in 0.15 M Tris-HCl buffer, pH 7.4 were independently titrated with aliquots of heparin solution (40 μM stock) with fluorescence detection at λ_{ex} 280 nm and λ_{em} 335 nm. Corrections for background fluorescence of the titrant were made by subtracting the signal observed in parallel titrations of heparin into buffer. The data was analyzed using Scatchard equation,

$$B/L.E_T = n/K_D - B/K_D.E_T$$

where L, B, E_T, n and K_D represent free heparin, bound heparin, α-1-PI concentration, number of binding sites and the dissociation constant for heparin-α-1-PI complex respectively. The bound heparin was calculated from the decrease in fluorescence induced by heparin binding

$$B = \Delta F/\Delta F_{max} \times E_T$$

The value of ΔF_{max} was deduced by extrapolating the double reciprocal plot of total heparin concentration versus fluorescence decrease (Hiratsuka, 1990). Titrations were analyzed by software origin 7.0 (Microcal Inc. Northampton, USA) based on iterative procedure to draw non-linear curve fits for the Scatchard plot to determine the average dissociation constant and stoichiometry of binding (Hiratsuka, 1990). All the data points plotted are an average of three experimental values.

The binding constant (K_α) is described by Lehrer and Fasman (1966) as:

$$K_\alpha = \beta/1\text{-}\beta \times 1/[L_f]$$

where $\beta = (Fl - Fl_P) / (Fl_{PL} - Fl_P)$ and $[L_f] = [L] - \beta[C]$; Fl_P, Fl_{PL} and Fl are the fluorescence intensities of unliganded α-1-PI, fully liganded α-1-PI and of the experimental mixture; $[L_f]$ and [L] are the concentrations of free heparin and total heparin present, and C is the concentration of binding sites in moles per liter. K_α was obtained from the slope of mass action plot between [Lf] and β/1-β.

2.2.31. Fourier transform infra red (FTIR) studies

Ovine α-1-PI (4 mg/mL) was incubated with heparin concentrations ranging from 0.1 μM to 10 μM in 20 mM sodium phosphate buffer pH 7.4. The protein-ligand complexes were lyophilized and FT-IR spectra for these samples were obtained to detect conformational changes in the ∝-1-PI structure, on a Nicolet 5700 FT-IR spectrometer, equipped with a DTGS detector. Samples were dried by blowing nitrogen, mixed with dry finely powdered KBr and the mixture was pressed into a disc. During measurements, the spectrometer was continuously purged with dry air to eliminate water vapor absorptions from the spectral regions of interest. Each spectrum was a result of signal averaging of 128 scans at a resolution of 2 cm^{-1} at 25±0.5 ºC. Second derivative spectra were obtained using Savitzky - Golay derivative function (Savitzky and Golay, 1964) software with a five data point window. Iterative curve-fitting method to achieve the best Gaussian shaped curves was used to calculate the relative areas of various components of the fitted band. The assignment of the composite bands of amide III region were achieved using Fourier self-deconvolution with an enhancement factor of $K = 1.8$ and a half width of 30.2 cm^{-1}. The free protein IR spectrum was obtained by subtracting the spectrum of

the heparin-buffer control. The percentage of each secondary element was calculated from the integrated areas of the component bands in amide III. BSA, lysozyme, α-chymotrypsin, Con-A and hemoglobin were used as standard and the experimental secondary structural content for these corresponded well with the reported values (Cai and Singh, 1999).

2.2.32. Circular dichroism (CD)

CD spectra were collected with a JASCO J-500A (Japan Spectroscopic Co. Tokyo, Japan) automatic recording spectropolarimeter equipped with 500N data processor, xenon lamp and a uniform temperature cell holder. Dry nitrogen was purged continuously before and during the experiment. The instrument was calibrated using ammonium (+)-10-camphorsulfonate. Conformational changes in the secondary structure of the protein (3.5 μM) in 50 mM Tris-HCl buffer, pH 7.4 at 27 °C were monitored in the far-UV region between 200 and 250 nm in the cuvette with a path length of 1 mm. After appropriate buffer and heparin blanks were run and subtracted, mean residue ellipticities were calculated using equation $[\theta] = \theta_{obs}MRW/cl$, where θ_{obs} is the observed ellipticity in degrees, MRW is the mean residue weight, c is the concentration of protein (mg/mL) and l is the path length in centimeters (Balasubramanian and Kumar, 1976). A mean residue molecular weight of 110 and sensitivity of 1 m°/cm (millidegree per centimeter) was used with a scan speed of 10 nm/min using a bandwidth of 1 nm. An average of three runs was recorded for each sample. The secondary structural changes were analyzed by the method of Yang et al. (1986).

RESULTS AND DISCUSSION

3. Ovine α-1-Proteinase Inhibitor: Purification and Characterization

The purification of ovine α-1-PI from serum to homogeneity has been encountered with serious problems including contamination with traces of albumin and other serpins family members, as well as low yields (Mistry et al., 1991; Sinha et al., 1988). The problems are further compounded by micro-heterogeneity observed in α-1-PI due to differing glycan sequences. This section describes the novel combinatorial approach of conventional chromatographic steps that were adapted to obtain a pure preparation of ovine α-1-PI. Ovine α-1-PI thus obtained was used for biochemical characterization with respect to its interactions with physiological serine proteases viz. elastase, trypsin and chymotrypsin, thermal stability studies and the effect of deglycosylation.

RESULTS

Ammonium sulfate fractionation

Ovine serum (50 mL) was subjected to 40 % $(NH_4)_2SO_4$ saturation (22.6 g/100 mL) by controlled addition of finely powdered $(NH_4)_2SO_4$ at 4 °C. The solution was allowed to stabilize for 2 h at 4 °C for complete precipitation. The precipitate obtained after centrifugation at 14000 × g for 30 min at 4 °C was discarded and supernatant was subjected to 70 % $(NH_4)_2SO_4$ (18.7 g/100 mL) precipitation. The solution was allowed to stabilize overnight for complete salting out of proteins. The precipitate collected by centrifugation at 14000 × g for 30 min at 4 °C was re-suspended in 0.05 M Tris-HCl buffer, pH 7.4 containing 0.9 % NaCl (w/v) and dialyzed against the same buffer (3×500 mL). The specific activity of ovine α-1-PI increased ~1.3 fold with a yield of 72 % (Table 3. 1). $(NH_4)_2SO_4$ precipitation helps in removal of fibrinogen, globulins and albumin.

Blue sepharose affinity chromatography

Blue sepharose has been shown to bind to several enzymes with known affinities to nucleotide cofactors. It has been shown to bind to dehydrogenases (Lamkin and King, 1976), kinases (Thompson et al., 1975), restriction endonuclease (Baksi et al., 1978), albumin (Travis et al., 1976) and interferons (Jankowski et al., 1976).

Affinity chromatography on blue-sepharose was effectively used to remove serum albumin, which binds strongly to cibacron blue dye. The dialyzed fraction from the previous step was loaded onto a cibacron blue sepharose 3GA column previously equilibrated with 0.05 M Tris-HCl buffer, pH 8.2 containing 0.05 M NaCl (w/v) at a flow rate of 24 mL/h. α-1-PI did not bind to blue sepharose at this pH and eluted as a single peak in the buffer wash (Figure 3. 1).

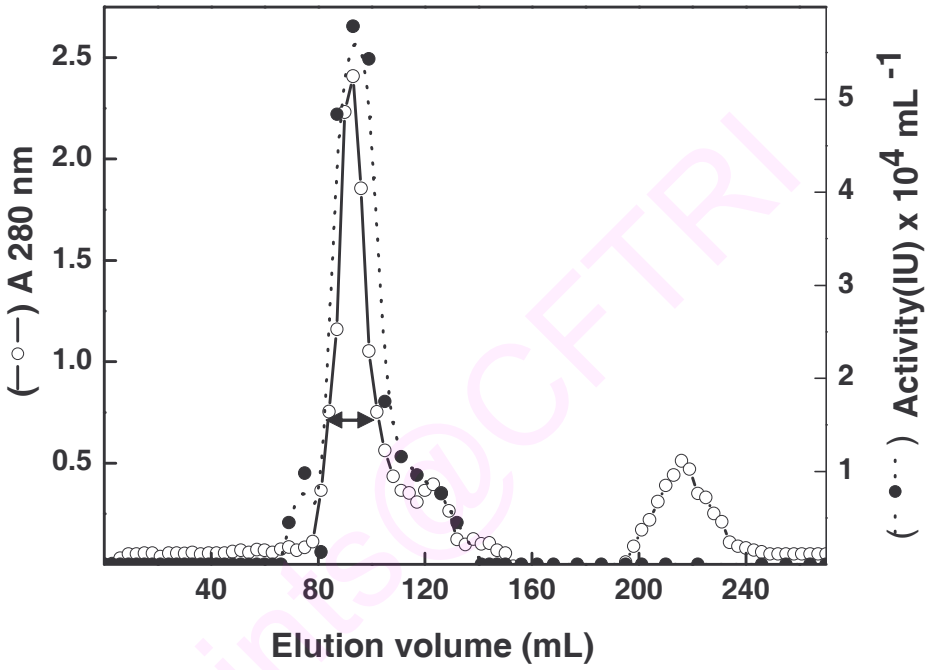

Figure 3. 1. Blue sepharose chromatography elution profile of ovine α-1-PI. The dialyzed $(NH_4)_2SO_4$ fraction was concentrated and loaded on to a blue sepharose column. The column was equilibrated with 0.05 M Tris-HCl buffer, pH 8.2 containing 0.05 M NaCl. The active fractions were pooled as shown.

The major contaminating protein, albumin bound to the matrix and was thus separated from α-1-PI. The fractions exhibiting α-1-PI activity were pooled as shown in the Figure 3. 1. The pooled fraction had a specific activity of 114.3 TIU/mg (Table 3. 1). A purification of 1.8 fold with a 51 % recovery of the original activity was achieved. The active fraction was concentrated by 80 % $(NH_4)_2SO_4$ saturation and the precipitate dissolved in minimal volumes of 0.05 M Tris-HCl buffer, pH 7.4.

Size exclusion chromatography

Size exclusion chromatography, which discriminates between molecules based on their size and is also valuable in desalting, was used as the next step. The soluble fraction of 80 % $(NH_4)_2SO_4$ precipitate post-centrifugation was loaded on to a Sephadex G-200 column (1.5 × 90 cm) equilibrated with 0.05 M Tris-HCl buffer, pH 7.4 containing 0.9 % NaCl (w/v) and 1mM Cys.

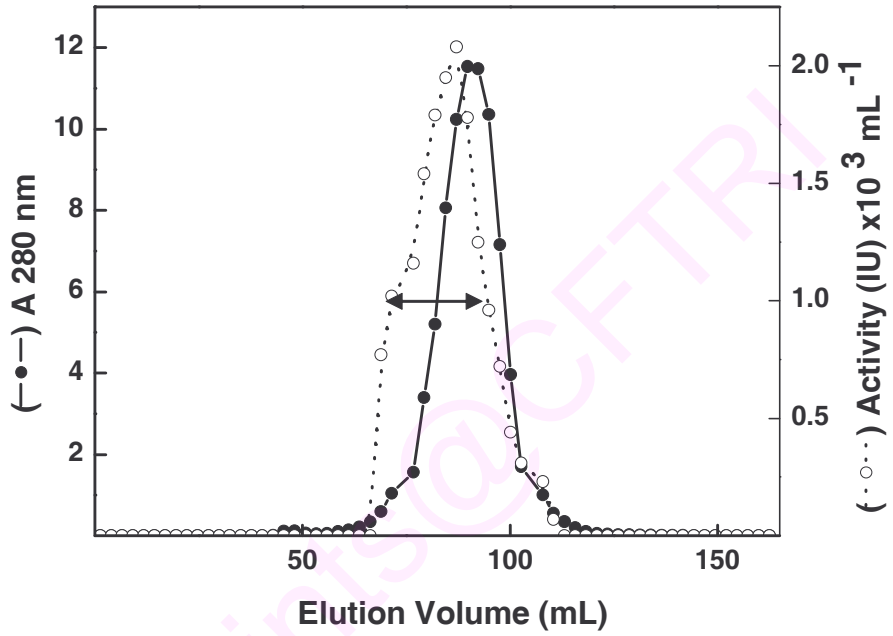

Figure 3. 2. Sephadex G-200 chromatography elution profile of ovine α-1-PI. The unbound active fractions of blue sepharose chromatography were concentrated and loaded on to Sephadex G-200 column. The column was pre-equilibrated with 0.05 M Tris-HCl buffer, pH 7.4 containing 0.9 % NaCl and 1mM Cys. Fractions of 2 mL were collected at a flow rate of 8 mL/h. The active fractions were pooled as shown.

Elution was carried out at a flow rate of 8 mL/h. α-1-PI eluted as a single peak on the ascending shoulder of the major protein peak (Figure 3. 2). The final recovery of α-1-PI was ~ 40 %, after a 3.6 fold purification, with a specific activity of 213 TIU/mg (Table 3. 1).

Concanavalin-A sepharose chromatography

Affinity chromatography employing Con-A sepharose was used to further purify α-1-PI. The pH of the pooled fractions obtained from the previous step was adjusted to 6.0. The column was pre-equilibrated in 0.05 M sodium phosphate buffer, pH 6.0 containing 0.25 M NaCl and 1mM Mg^{2+}, Ca^{2+}, Mn^{2+} ions. The inclusion of metal ions was essential for the carbohydrate binding behavior of lectin Con-A.

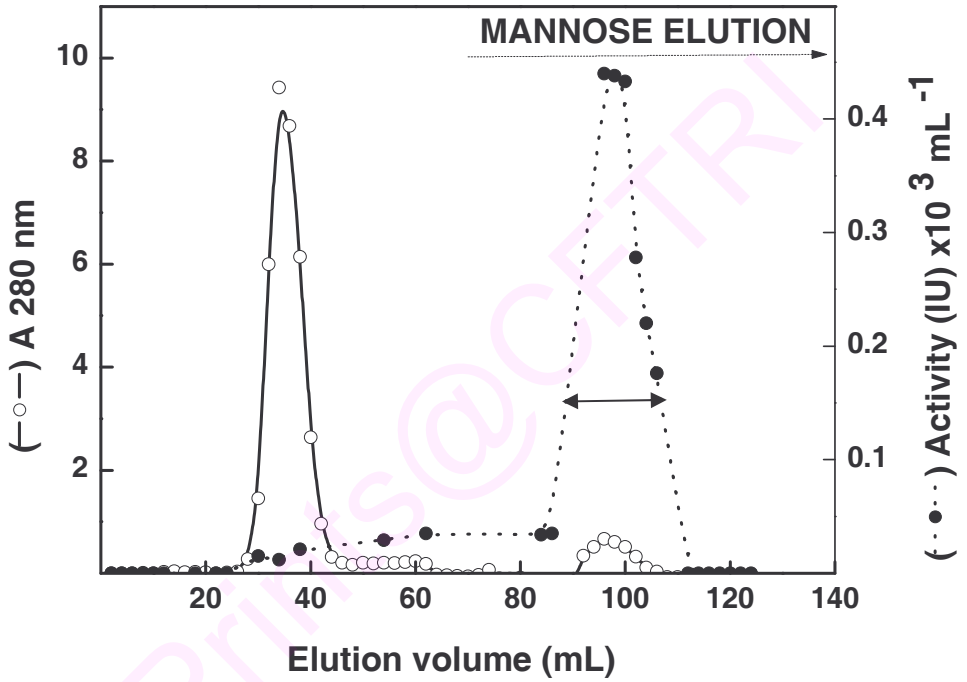

Figure 3. 3. Con-A sepharose chromatography elution profile of ovine α-1-PI. The active fractions of Sephadex G-200 chromatography were concentrated and loaded on to Con-A sepharose column pre-equilibrated in 0.05 M sodium phosphate buffer, pH 6.0. The elution of the bound α-1-PI was achieved using the same buffer containing 0.1 M mannose. The fractions exhibiting α-1-PI activity were appropriately combined, dialyzed against 0.05 M Tris-HCl buffer, pH 7.4 and concentrated.

In this step a major fraction of inactive protein eluted during wash with equilibration buffer. The elution of the bound α-1-PI was achieved using the same buffer containing 0.1 M mannose minus the metal ions. The elution profile of α-1-PI from Con-A sepharose is presented in Figure 3. 3. α-1-PI activity eluted as a single symmetric peak.

The fractions exhibiting α-1-PI activity were combined, dialyzed against 0.05 M Tris-HCl buffer, pH 7.4 and concentrated. This step resulted in an apparently homogenous form of α-1-PI. The fine recovery of α-1-PI was ~ 11.2 % after a 20 fold purification with a specific activity of 1175 U/mg protein for trypsin inhibition (Table 3. 1).

Table 3. 1. Summary of α-1-PI purification from ovine serum*

Sample	Activity (TIU/ml)	Protein (mg/ml)	Volume (ml)	Specific Activity (TIU/mg)	Fold Purification	Recovery (%)
Serum	4800	81	50	59.3	-	100
40-70 % $(NH_4)_2SO_4$	9560	125.8	18	76	1.3	71.7
Blue sepharose Chromatography	2710	25.7	45	114.3	1.8	50.8
80 % $(NH_4)_2SO_4$	16320	125	7	130	2.2	47.6
Sephadex G-200 Chromatography	2130	10	45	213	3.6	39.9
Con-A sepharose Chromatography	470	0.4	57.2	1175	19.8	11.2

* These are the results of a typical purification starting from 50 mL of ovine serum. These values were reproduced in three separate purifications.

Criteria of homogeneity

Native PAGE, capillary electrophoresis, RP-HPLC, NH_2-terminal sequencing and cross-reactivity with antibodies raised against human α-1-PI were used to assess the homogeneity of the protein. The purified inhibitor analyzed by native-PAGE (10 % T, 2.7 % C) in Tris–Gly buffer pH 8.3 revealed a single band by protein staining using CBB

R-250 (Figure 3. 4A), gelatin zymography (Figure 3. 4B) and specific inhibitor staining with APNE (Figure 3. 4C). α-1-PI resolved as a single peak by RP-HPLC on a Waters Symmetry Shield C_{18} column (Figure 3. 5A) using a gradient of H_2O and 70 % acetonitrile containing TFA and on capillary electrophoresis (Prince Technologies system) using 0.05 M Tris-HCl buffer, pH 7.4 and 20 mbar pressure (Figure 3. 5B). Ovine α-1-PI showed significant cross reactivity against human α-1-PI antibodies raised in rabbit, both by western blot (Figure 3. 6A) and dot blot analysis (Figure 3. 6B). Immuno-detection was carried out with human α-1-PI as positive and BSA as negative control.

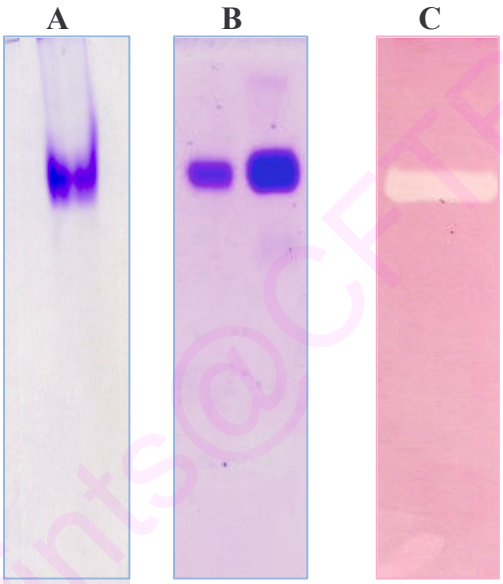

Figure 3. 4. Native PAGE (10 % T, 2.7 % C) of purified ovine α-1-PI. The gel was stained for Lane A: Protein; Lane B: Gelatin embedded zymography and Lane C: APNE protease inhibitor staining respectively.

SDS-denatured α-1-PI was transferred to PVDF membrane, the band excised and subjected to amino-terminal sequencing. The release of a single amino-terminal amino acid, Gly for both the native and denatured inhibitors further confirm that α-1-PI was homogenous. The sequence obtained after 22 cycles of automated Edman microsequencing was –NH_2-GVLQGHAVQETDDTAHQEAAAH---. This sequence is identical to the deduced sequence reported earlier by Mistry et al., (1991). All these studies reflect the homogeneity of the purified ovine α-1-PI.

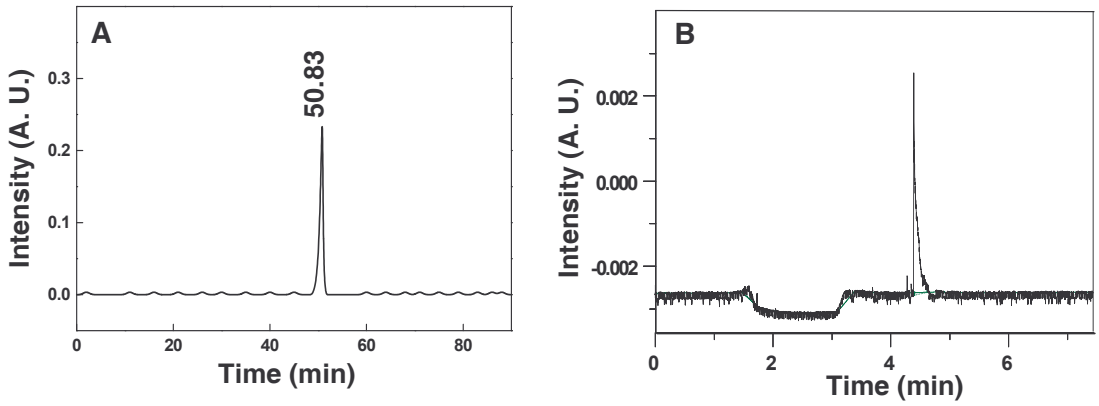

Figure 3. 5. Evaluation of homogeneity of ovine α-1-PI. A: RP-HPLC profile of ovine α-1-PI on a Symmetry Shield RP_{18} (150 × 4.6 mm, 5 μm) column detected at 280 nm B: Capillary electropherogram of purified ovine α-1-PI in 0.05 M Tris-HCl buffer, pH 7.4.

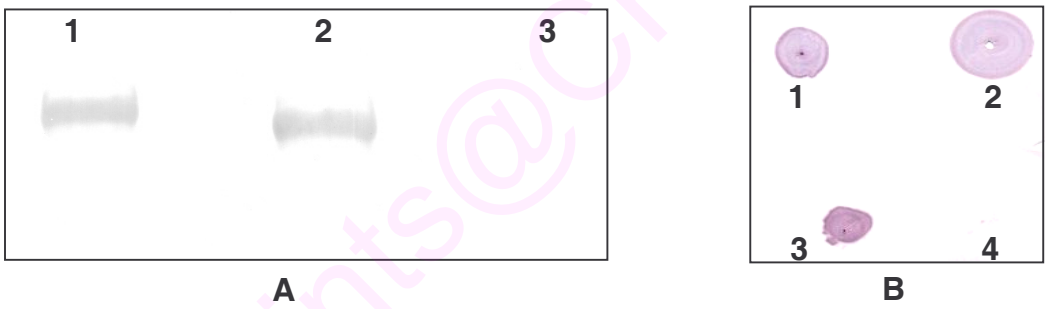

Figure 3. 6. Cross-reactivity studies of ovine and human α-1-PI. A. Protein (2 μg each) was transferred and probed with human α-1-PI antibodies; Lane 1: Ovine α-1-PI; Lane 2: Human α-1-PI and Lane 3: BSA. B. Dot blot analysis. 1 and 2. Human α-1-PI, 3. Ovine α-1-PI and 4. BSA.

Molecular weight

The apparent M_r of ovine α-1-PI was determined by analytical gel filtration on a BioSep-SEC-S 2000 (300 × 7.8 mm, 5 μm) HPLC column, SDS-PAGE (Laemmli, 1970) and by MALDI-TOF. The M_r of the purified inhibitor estimated by analytical HPLC was 60,000±3000 Da from a plot of log M_r versus V_e/V_o. The Mr markers used were BSA (66,000 Da), ovalbumin (43,000 Da) and ribonuclease (13,700 Da) (Figure 3. 7).

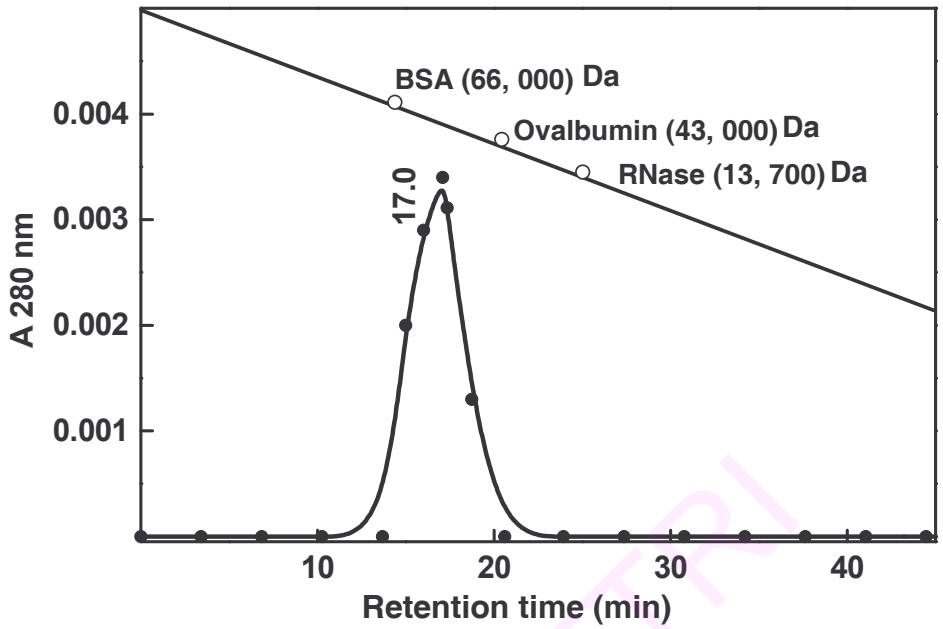

Figure 3. 7. HPLC size exclusion chromatography profile of ovine α-1-PI. Column used: BioSep-SEC-S 2000 (300 × 7.8 mm, 5 μm). Ovine α-1-PI was resolved in 0.1 M Tris-HCl buffer containing 0.9 % NaCl at a flow rate of 0.5 mL /min, the detector was set at 280 nm

SDS-PAGE (10 % T, 2.7 % C) of the purified α-1-PI was carried out in a discontinuous buffer system. The M_r markers used were phosphorylase b (97,400 Da), BSA (66,300 Da), ovalbumin (43,000 Da), carbonic anhydrase (29,000 Da) and soyabean trypsin inhibitor (20,000 Da). Protein staining using CBB R-250 showed a single subunit of 59,000±1500 Da (Figure 3. 8). The apparent subunit size is the same in the absence of β-mercaptoethanol (results not shown).

The exact M_r of ovine α-1-PI was determined by MALDI-TOF on a Bruker Daltonics Ultraflex system, Germany which uses a 337 nm nitrogen laser desorption and 1.7 nm linear flight path. The instrument was calibrated over the mass range of 10,000-100,000 Da. The results showed a single subunit of M_r 58,309.939 Da (Figure 3. 9).

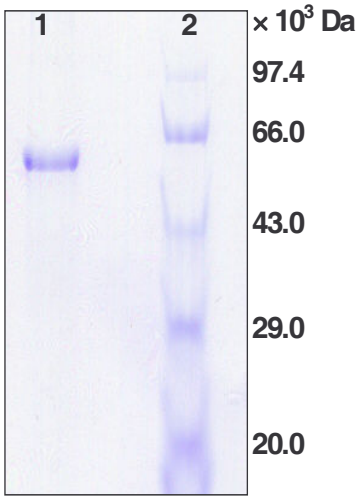

Figure 3. 8. SDS-PAGE (10 % T, 2.7 % C) profile of ovine α-1-PI. Lane 1: Purified ovine α-1-PI and Lane 2: M_r markers: phosphorylase b (97,400 Da), BSA (66,000 Da), ovalbumin (43,000 Da), carbonic anhydrase (29,000 Da) and soybean trypsin inhibitor (20,000 Da).

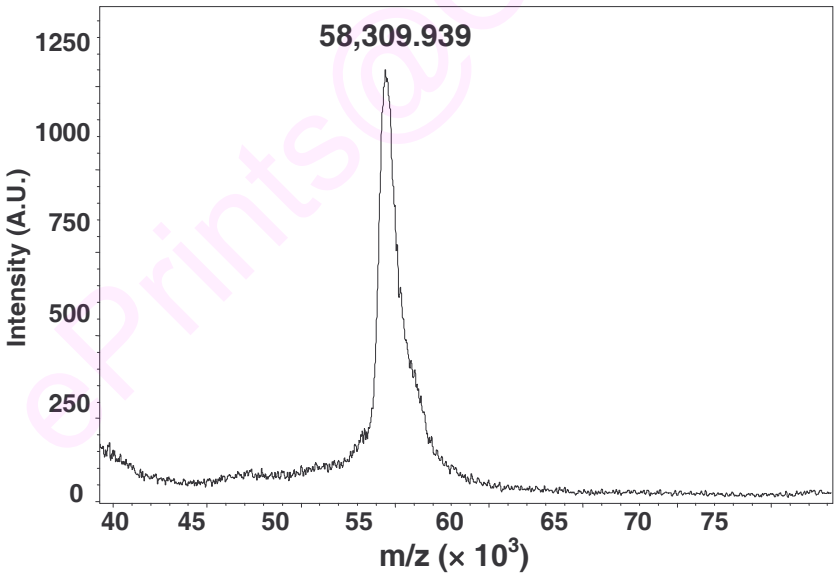

Figure 3. 9. MALDI-TOF profile of purified ovine α-1-PI.

Determination of isoelectric point (pI)

Isoelectic focussing of the purified ovine α-1-PI using pre-cast Ampholine PAG (pH 4.0-6.5) plates showed a single protein band at pI ~ 4.95, which is in close agreement to the pI ~4.5 reported for human α-1-PI. Ovine α-1-PI has apparently less acidic pI compared to human α-1-PI. Figure 3. 10 depicts the distance moved by proteins from cathode *vs* pI of marker proteins and α-1-PI.

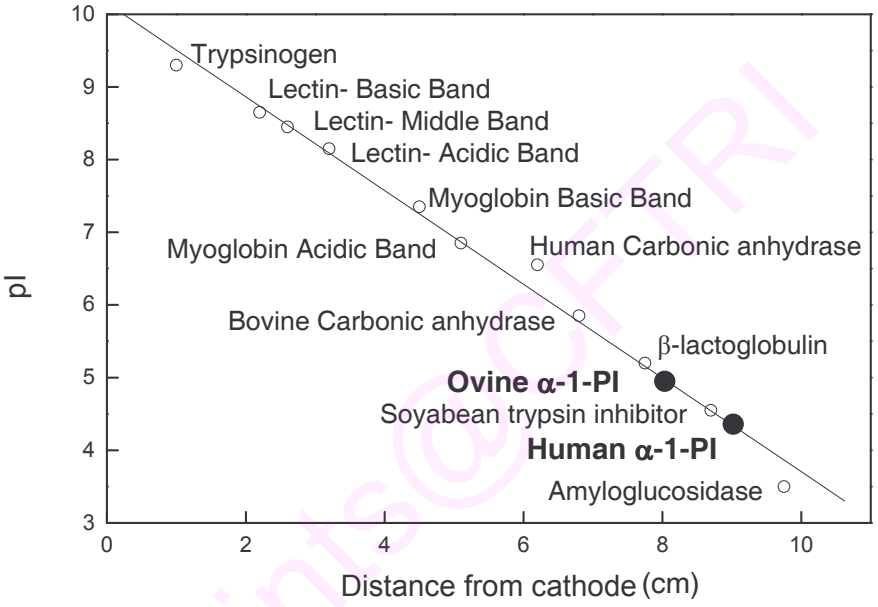

Figure 3. 10. Determination of isoelectric point of α-1-PI. The plot shows distance moved from cathode *vs* pI. Standard pI markers used are shown in the figure.

Amino acid composition

The relative amino acid compositions of the purified α-1-PI are shown in Table 3. 2. Glu and Gln are grouped as Glx and Asp and Asn as Asx. The high content of Glx and Leu are similar to that of human α-1-PI. However the content of Ser and Ala appear to be higher whereas Phe and Lys are low. The total amino acid composition is in good agreement with that determined for human α-1-PI and reported for other mammalian species.

Table 3. 2. Relative amino acid composition of ovine α-1-PI (mol %)*

Amino acid	Ovine α-1-PI	Human α-1-PI	Expected ovine α-1-PI #
B	9.7	9.9	11.5
Z	13.2	12.6	11.0
S	8.3	3.5	6.0
G	6.3	3.0	5.8
H	2.0	3.3	4.0
R	3.0	1.6	1.7
T	6.4	5.9	6.1
A	7.6	3.7	8.2
P	6.8	4.1	4.1
Y	2.3	1.9	2.0
W	N.D	1.0	0.9
V	6.3	4.8	6.1
M	0.4	2.0	1.2
C	0.2	0.4	0.8
I	4.7	4.0	4.6
L	12.1	10.0	12.7
F	4.9	7.9	5.7
K	5.2	8.3	7.5

*

Average of duplicates

Based on deduced amino acid sequence (Brown et al., 1989).

N.D- Not determined

Glycoprotein staining and carbohydrate estimation

α-1-PI is a glycoprotein as revealed by Periodic Acid Schiff's staining (Kapitany and Zebrowski, 1973) after SDS-PAGE (10 % T, 2.7 % C) (Figure 3. 11). The total neutral carbohydrate content of ovine α-1-PI was estimated to be ~14 % as determined

using the phenol-sulfuric acid method using glucose as standard (DuBois et al., 1956) and is in close agreement with 15 % reported by Mistry et al. (1991).

Figure 3. 11. Glycoprotein staining of purified ovine α-1-PI. Staining was performed after SDS-PAGE (10 % T, 2.7 % C), using Schiff's reagent. Lane 1: Ovalbumin and Lane 2: Ovine α-1-PI.

Inhibitory activity of ovine α-1-PI

The purified ovine α-1-PI was used for inhibition kinetic studies against porcine pancreatic elastase and trypsin and bovine pancreatic chymotrypsin. The effect of varying inhibitor concentrations on elastase, trypsin and chymotrypsin activity using their cognate substrates NSAPNA, BAPNA, and BTPNA respectively showed mixed inhibition type of curves at low concentrations of α-1-PI. The usual way of defining the specificity of a protein protease inhibitor is to determine its K_i for different proteases. However, literature is lacking information concerning K_i, presumably because reversibility of the inhibitor enzyme complex, a pre-requisite for determining K_i, has never been achieved. This is either due to a very low dissociation constant ($K_i \sim 10^{-10}$ M) or stabilization of the resultant complex by covalent bond or tetrahedral complex formation between enzyme and inhibitor (Beatty et al., 1980). Therefore, we decided to investigate the specificity of α-1-PI by measuring the association rate constants with different proteases. The

association rate constants for elastase, trypsin and chymotrypsin were observed to be in the range of 10^6 to 10^7 M^{-1} s^{-1} (Table 3. 3).

Table 3. 3. Rate constants of ovine α-1-PI for serine proteases.

Enzyme	Substrate	K_{ass} (M^{-1} s^{-1})
Trypsin	BAPNA	$4.65 \pm 0.4 \times 10^{7}$
Elastase	NSAPNA	$3.34 \pm 0.3 \times 10^{6}$
Chymotrypsin	BTPNA	$5.55 \pm 0.25 \times 10^{7}$

Stoichiometric titrations

The molar inhibitory capacity (mol. of enzyme inhibited/mol. of inhibitor) of ovine α-1-PI against porcine pancreatic elastase and trypsin and bovine pancreatic chymotrypsin is shown in the titration curves of Figure 3. 12. The results indicate that irreversible inhibition of trypsin occurs at 1: 1 molar ratio *in vitro*. However porcine pancreatic elastase and bovine pancreatic chymotrypsin inhibition required almost 10 fold molar excess of ovine α-1-PI. Albeit the complete inhibition of the proteases could not be achieved, and some amount of residual activity was still observed.

The molar ratio evaluated from a secondary plot of log of slopes (% log residual activity *vs.* time) *vs.* log of inhibitor concentrations re-confirmed the ratio for trypsin inhibition to be 1:1 whereas chymotrypsin and elastase are inhibited at a higher molar ratio (results not shown).

Effect of deglycosylation

The effect of deglycosylation on the thermal stability and activity of α-1-PI was evaluated. α-1-PI was deglycosylated using the enzyme Peptide: N-Glucosidase F from *Flavobacterium meningosepticum* (Plummer and Tarentino, 1991). It is an amidase which

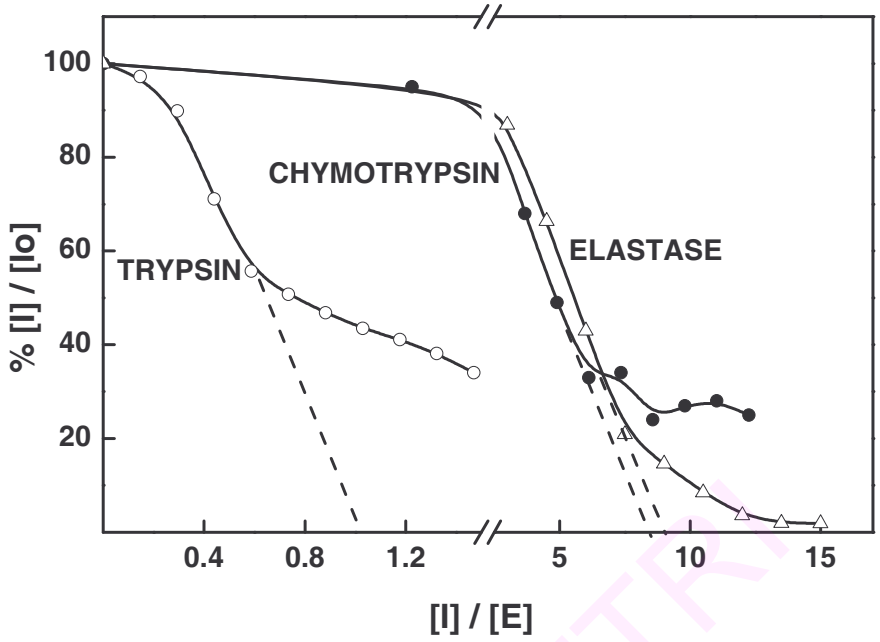

Figure 3. 12. Stoichiometric titrations of ovine α-1-PI with serine proteases. The x-intercept of the straight lines depicts the apparent binding proportions with respect to trypsin (-○-), chymotrypsin (-●-) and elastase (-△-).

between the innermost GlcNAc and Asn residues of high mannose, hybrid and complex oligosaccharides from N-linked glycoproteins (Maley et al., 1989).

Deglycosylation of ovine α-1-PI was confirmed by the mobility shift observed in SDS-PAGE due to altered M_r from 60,000 to 51,500 Da (Figure 3. 13A). However, both human and ovine deglycosylated forms depicted unaltered protease inhibitory activity as appraised from gelatin embedded PAGE zymography (Figure 3. 13B).

The trypsin and elastase inhibitory activity of deglycosylated human and ovine α-1-PI was 97 % of the virgin inhibitor. These results suggest that N-linked glycan portion plays no role in protease inhibitory prospective of α-1-PI. The T_m of native ovine, deglycosylated ovine, native human α-1-PI and its deglycosylated form were computed from the curves obtained by plotting % residual activity *vs* incubation temperature and these were observed to be 70.5, 60.5, 63, and 57 ^oC respectively (Figure 3. 14).

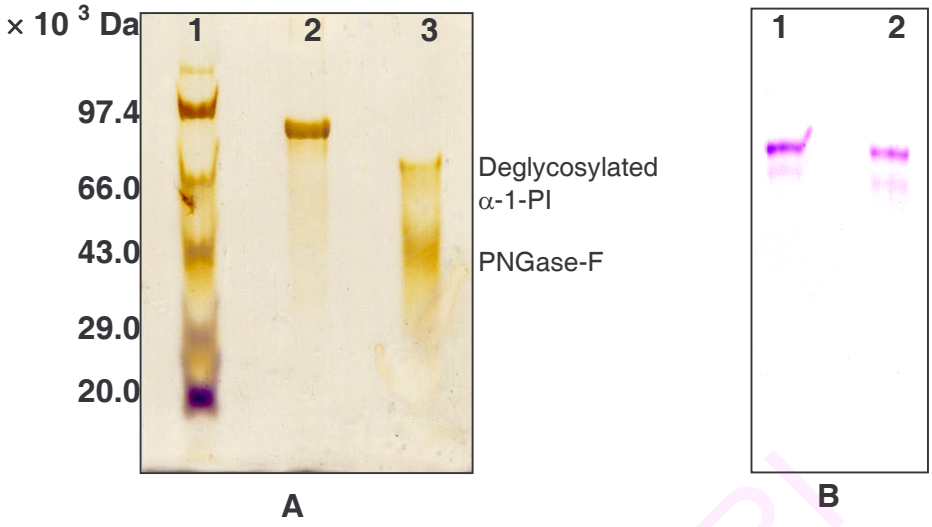

Figure 3. 13. Deglycosylation of ovine α-1-PI. A. SDS-PAGE (10 % T, 2.7 % C) Lane 1: M_r markers: phosphorylase b (97,400 Da), BSA (66,000 Da), ovalbumin (43,000 Da), carbonic anhydrase (29,000 Da) and soybean trypsin inhibitor (20,000 Da); Lane 2: Purified ovine α-1-PI; Lane 3: Deglycosylated ovine α-1-PI. B. Gelatin embedded PAGE (10 % T, 2.7 % C containing 0.5 % gelatin) Lane 1: Native ovine α-1-PI; Lane 2: Deglycosylated ovine α-1-PI.

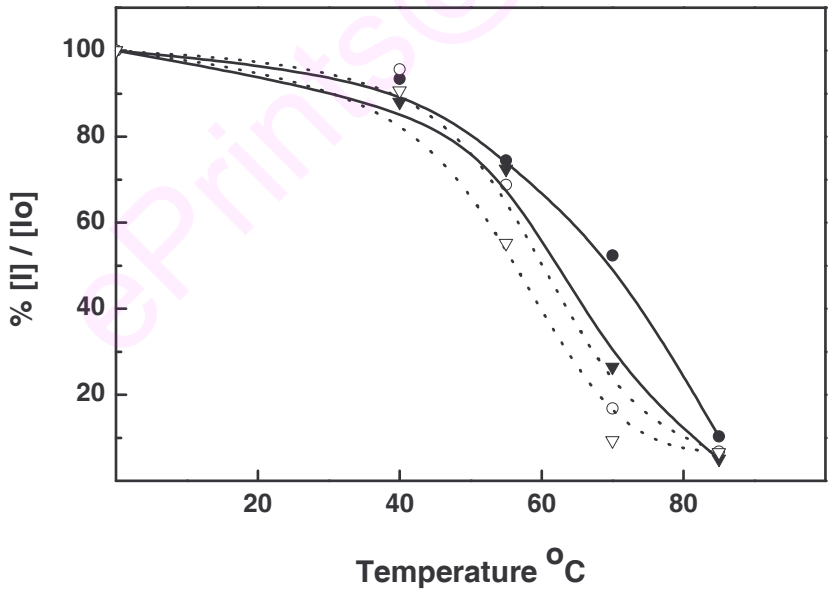

Figure 3. 14. Thermal transition profile of α-1-PI. Melting temperature curves of ovine α-1-PI (-●-), deglycosylated ovine α-1-PI (-○-), human α-1-PI (-▼-) and deglycosylated human α-1-PI (-▽-).

Thermal stability of ovine α-1-PI

The protease inhibitor activity of ovine α-1-PI towards the proteases evaluated remained constant between 20-70 ^{o}C, following which the inhibitor lost activity rapidly. In contrast the human α-1-PI was more thermolabile with loss in activity occurring at ~ 60 ^{o}C. The semi-logarithmic plots of residual α-1-PI activity *vs.* incubation time at different temperatures were characterized by single straight lines of $r > 0.98$. Therefore the denaturation process can be attributed to a single exponential decay, for both ovine and human α-1-PI. The semi-logarithmic plots also indicate that the thermal inactivation of ovine and human α-1-PI follow first order kinetics. The Arrhenius plots for irreversible denaturation, natural logarithmic of K_r *vs.* reciprocal of the absolute temperature were linear ($r > 0.99$) for both ovine and human α-1-PI in the temperature range evaluated.

The Arrhenius activation energy (E_a) was calculated to be 158.6 and 95.8 kJ mol^{-1} for ovine and human α-1-PI respectively. The half-life of ovine α-1-PI at 55 °C was 6 h whereas that of the human α-1-PI was 3 fold lower. Concurrently the activation energy of ovine α-1-PI is higher by 62.8 kJ mol^{-1}. The thermal inactivation parameters are summarized (Table 3. 4). The E_a for the deglycosylated ovine and human forms is lowered to 79.0 and 59.0 kJ mol^{-1} respectively. These observations suggest that deglycosylation of α-1-PI results in increased thermolability and hence glycosylation has a role to play in stabilization of the serpin molecule.

Discussion

α-1-PI is the major serine protease inhibitor in human plasma (Travis and Salvesen, 1983) reacting most rapidly with neutrophil elastase (Beatty et al., 1980). α-1-PI can compete with several mammalian serine proteases of varying specificities (Travis and Salvesen, 1983). In addition α-1-PI can itself be inactivated by bacterial proteases (Potempa et al., 1986). α-1-PI is responsible for tight control of neutrophil elastase activity, which if down regulated, may cause local excessive tissue degradation. Small changes in environment such as elevated temperature or pH or proteolytic action at the

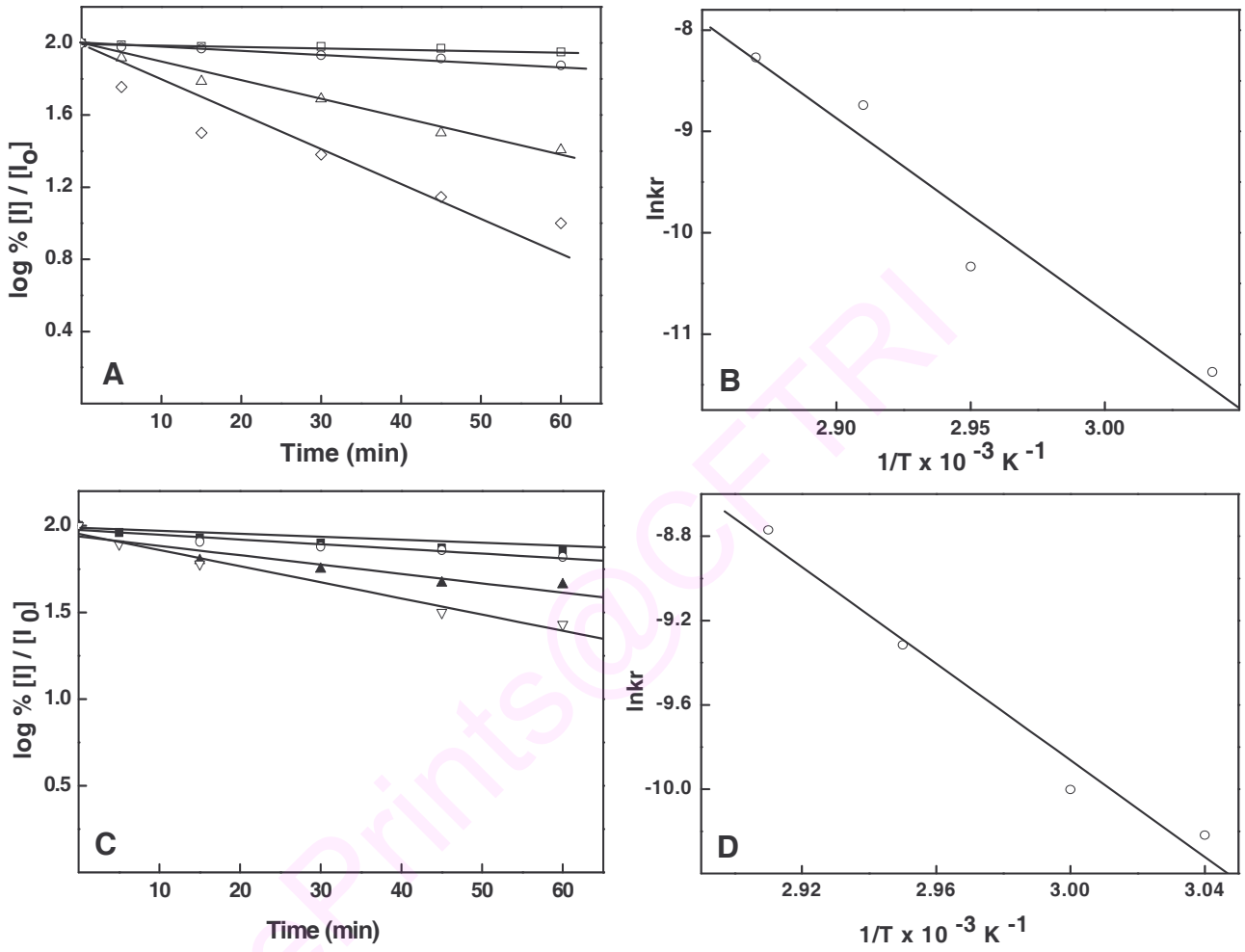

Figure 3. 15. Kinetics of thermal inactivation of native α-1-PI. A. Ovine α-1-PI incubated in 50 mM Tris-HCl, pH 7.4 containing 0.9 % NaCl , (—□—) 55 ºC, (—○—) 65 ºC, (—Δ—) 70 ºC, (—◊—) 75 ºC. B. Arrhenius plot of ovine α-1-PI inactivation. C. Human α-1-PI incubated in 50 mM Tris-HCl pH 7.4 containing 0.9 % NaCl, (—■—) 55 ºC, (—○—) 60 ºC, (—▲—) 65 ºC, (—▽—) 70 ºC. D. Arrhenius plot of human α-1-PI inactivation.

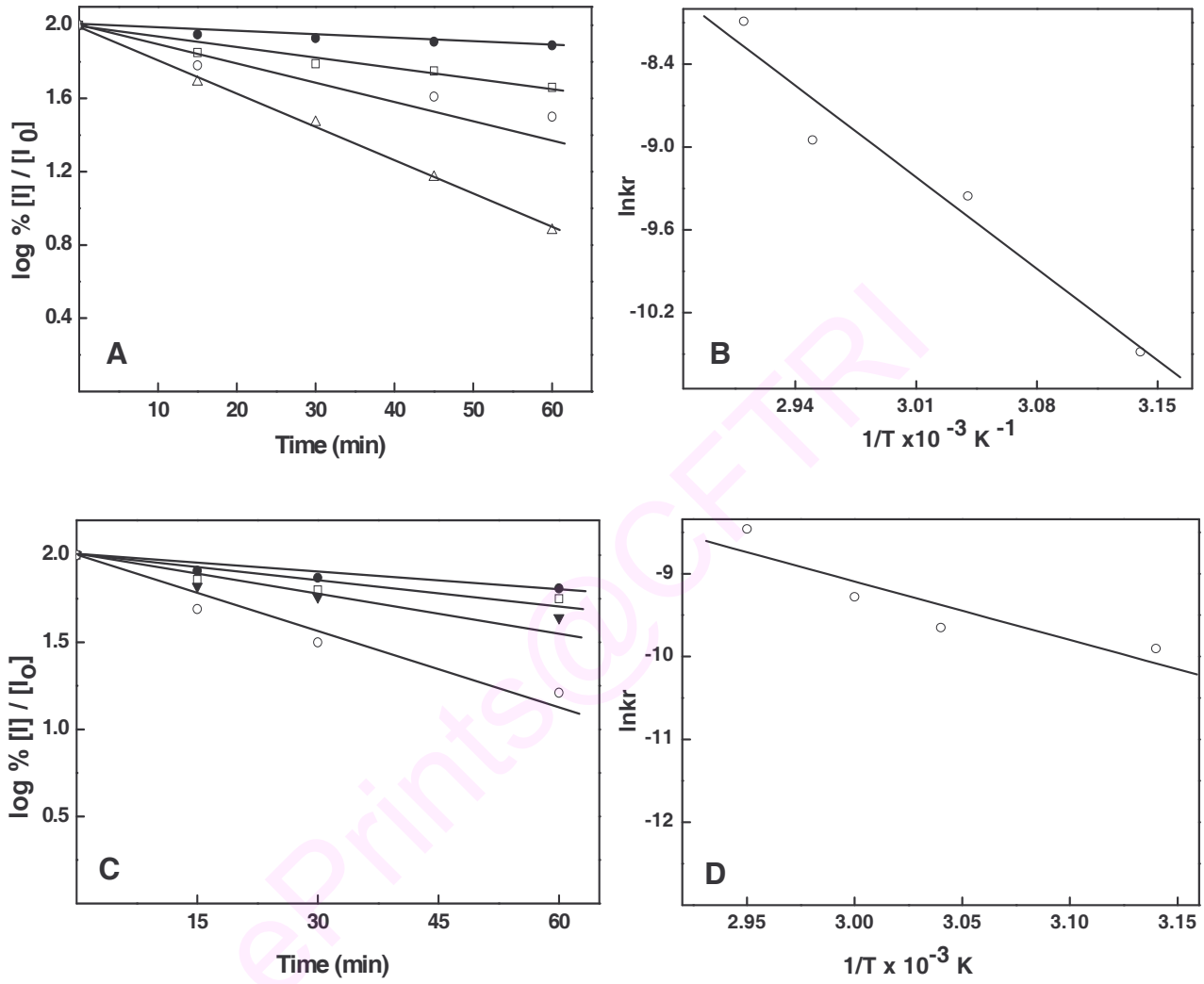

Figure 3. 16. Kinetics of thermal inactivation of deglycosylated α-1-PI. A. Ovine α-1-PI incubated in 50 mM Tris-HCl, pH 7.4 containing 0.9 % NaCl , (—● —) 45 ºC, (—□—) 55 ºC, (—○—) 65 ºC, (—Δ—) 70 ºC. B. Arrhenius plot of ovine α-1-PI inactivation. C. Human α-1-PI incubated in 50 mM Tris-HCl, pH 7.4 containing 0.9 % NaCl, (—●—) 45 ºC, (—□—) 55 ºC, (—▼—) 60 ºC, (—○—) 65 ºC. D. Arrhenius plot of human α-1-PI inactivation.

Table 3. 4. Thermal inactivation parameters of human and ovine α-1-PI

	Ea (kJ/ mol)	Incubation temp. (^oC)	Half life (min.)	T_m (^oC)	Inactivation rate constant (Kr x10^{-3} s^{-1})	ΔG* (kJ/ mol)	ΔH* (kJ/ mol)	ΔS* (J. K^{-1} .mol^{-1})
Ovine-α-1-PI	158.6	55	360	70.5	0.01	111.9	155.9	134.0
		65	165		0.03	111.8	155.8	130.0
		70	30		0.16	111.2	155.8	130.0
		75	17		0.26	110.5	155.7	130.0
Human-α-1-PI	95.8	55	120	63.0	0.03	108.7	92.3	50.0
		60	78		0.04	107.7	92.3	46.2
		65	40		0.09	107.5	92.2	45.4
		70	25		0.15	106.2	92.2	40.8
Deglycosylated ovine α-1-PI	79.0	45	135	60.5	0.02	105.2	75.4	93.7
		55	74		0.08	105.3	75.3	91.5
		65	29		0.13	103.6	75.2	84.0
		70	16		0.30	103.9	75.1	84.0
Deglycosylated human-α-1-PI	59.0	45	106	57.0	0.05	104.6	56.3	152.0
		55	72		0.07	107.2	56.2	155.7
		60	48		0.09	107.8	56.15	155.4
		65	24		0.21	107.0	56.1	150.8

RCL causes the native metastable state to rapidly convert to a stable inactive conformation indicating that the native state is only marginally stable (Chow et al., 2004; Benning et al., 2004; Delvin et al., 1995). The molecular tension imparted by the metastability of the native fold is the key to serpin biological function. The free energy release during this conformational change is instrumental in bringing about mechanical distortion and translocation of the protease from one end to another (Baumann et al., 1991).

Parenteral augmentation therapy for α-1-PI deficient individuals with pulmonary emphysema is through α-1-PI purified from pooled human plasma (Luisetti and Travis, 1996). However, the demand for a purified concentrate exceeds the amount of α-1-PI available. Hence it seemed reasonable to explore and purify α-1-PI from other suitable mammalian sources. Attempts are being made to either synthesize inhibitors for therapeutic use (McRae et al., 1980) or develop efficient techniques for isolation of the natural α-1-PI for supplementation (Glaser et al., 1982). In the present investigation α-1-PI was purified to homogeneity from ovine serum following a series of chromatographic procedures. The structural and functional characteristics of the purified ovine α-1-PI demonstrate that it is analogous to human α-1-PI. The experimentally evaluated N-terminal sequence is in concurrence with the deduced amino acid sequence reported by Brown et al. (1989).

Initial biochemical investigations of α-1-PI were carried out in early 1960s by Schultze et al. (1962). It is only over the past two decades that the multifaceted protein, α-1-PI has drawn the attention of a wide range of disciplines due to its importance in medicine. Protein biochemists used it as a model protein to explore protein-protein interactions and suicide inhibition mechanisms. More detailed knowledge of mammalian α-1-PIs will provide valuable information that would aid in elucidating the physiological functions attributed to it. α-1-PI is most widely distributed *bona fide* inhibitory serpin, identified in all major branches of life (Irving et al., 2000; Law et al., 2006). α-1-PI has been studied in several species prominent being Human (Kim et al., 2001; Gettins, 2002), Mouse (Barbour et al., 2002), Rat (Misumi et al., 1990), Cow (Harhay et al., 2005), Pig (Archibald et al., 1996), Rabbit (Saito and Sinohara 1991), Guinea pig (Suzuki et al.,

1991), Horse (Patterson et al., 1991), Silkworm (Takagi et al., 1990), Carp (Huang et al., 1995) Frog (Klein et al., 2002) and Squirrel (Takamatsu et al., 1997). The purification of human α-1-PI continues to be a problem compounded by the presence of albumin and other serpins. Ovine α-1-PI was purified and partially characterized by Mistry et al. (1991) and Sinha et al. (1988). We present here a purification protocol for ovine α-1-PI with higher specific activity and yield compared to previous reports, in order to make available a homogenous preparation for detailed biochemical characterization and structural investigations.

In this study, a combination of procedures, namely $(NH_4)_2SO_4$ fractionation, dye affinity chromatography, size exclusion chromatography and Con-A sepharose affinity chromatography have been used to purify ovine α-1-PI to homogeneity. Blue sepharose does not interact with α-1-PI at pH 8.2, which however binds to serum albumin, and was used effectively to eliminate it (Figure 3. 1). The size exclusion chromatography step on Sephadex G-200 (Figure 3. 2) restricted the contaminating proteins to a similar size range as the ovine α-1-PI and helped increase the specific activity to 213 U/mg (Table 3. 1). Con-A sepharose affinity chromatography provided a homogenous α-1-PI preparation with a significantly high specific activity of 1175 U/mg (Table 3. 1). A single protein species is observed in native PAGE both by inhibitor specific staining as well as protein staining (Figure 3. 4). The homogeneity was also revealed by the release of a single amino acid Gly during NH_2-terminal sequencing using Edman degradation and a single discrete peak in capillary electrophoresis and RP-HPLC (Figure 3. 5). All these results assured that the preparation was homogenous and could be used for structural and functional studies.

Molecular weight of α-1-PIs are in the range of 40,000 to 60,000 Da. However, it is reckoned that a certain degree of variability may be observed on account of micro-heterogeneity displayed by the serpin due to differences in glycan moities. The precise M_r of ovine α-1-PI is 58309.939 Da as revealed by mass spectrometry (Figure 3. 9), which correlates well with the M_r computed from analytical size exclusion chromatography (Figure 3. 7) and SDS-PAGE (Figure 3. 8). The size of ovine α-1-PI is higher to that reported for human α-1-PI (52,000 Da). Ovine α-1-PI akin to its counterparts from other

species is a single subunit protein. The amino-terminal sequence for the first thirty residues of ovine α-1-PI is identical with that reported by Mistry et al (1991). The pH optima of ovine α-1-PI for various serine proteases is in the range of 7.4-8.2. The optimum pH is influenced significantly by a number of experimental factors. Therefore it is often difficult to extrapolate data when substrates and enzymes vary. The pI of ~ 4.95 for ovine α-1-PI is similar to the pI for human α-1-PI ~ 4.5. This is against a theoretical pI of 5.75 for ovine α-1-PI calculated *in silico* sans the glycan moiety. This acidic pI explains the binding of α-1-PI to DEAE-sepharose at pH 8.2 as described by Liener et al., (1973). The relatively retarded mobility of α-1-PI during native PAGE (Figure. 3. 4) also is reckoned by this acidic pI. The NH_2-terminal sequence of a very closely migrating serpin having a M_r 56,000±500Da as revealed by SDS-PAGE, and often occurring as a major contaminant during purification from ovine serum, indicates it to be α-1-antichymotrypsin. The NH_2-terminal sequencing of this protein revealed the sequence to be--LQENVTPEGTHRGAAVDDHALLSSLD-- which showed a high level of homology with alpha-1-antichymotrypsin from other mammalian species. The isolation of both ovine α-1-antichymotrypsin (56,000 Da) and α-1-PI (58,310 Da) conclusively resolves any controversies in the M_r of α-1-PI reported by Mistry et al. (1991) as 56,000 Da and Sinha et al. (1988) as 62,000 Da. Amino acid composition analysis of the ovine α-1-PI post acid hydrolysis corresponded to the theoretical expected amino acid composition values derived from the deduced amino acid sequence (Brown et al., 1989) *in silico* using WinPep program, and to the human α-1-PI (Table 3. 2).

α-1-PI from human and ovine species were found to be immunologically similar as shown by the cross-reactivity (Figure 3. 6). The 11 % recovery of α-1-PI as compared to 0.22 % reported previously by Mistry et al. (1991) together with the close similarities in the biochemical characteristics indicate that this preparation is suitable for parenteral augmentation therapy. The ovine plasma α-1-PI purified by Mistry et al. (1991) was found to be immunologically distinct from that of human α-1-PI as is the case with α-1-PI isolated from plasma of other mammalian species.

Studies on the inhibition of porcine trypsin and bovine chymotrypsin by the purified α-1-PI indicate that both have essentially the similar association rate constants

(K_{ass}). The K_{ass} value with porcine elastase was an order lower. These results may be explained by the fact that the source was pancreas as compared to neutrophil elastase, the target protease of α-1-PI. Ovine α-1-PI is a 1:1 stoichiometric inhibitor of trypsin. It means, if equimolar amounts of α-1-PI and trypsin are allowed to complex, there will be no detectable change in absorbance at 410 nm upon addition of chromogenic substrate. The higher stoichiometry of inhibition observed experimentally for elastase and chymotrypsin could be due to non-specific cleavage of inhibitor by the elastase and chymotrypsin as the effective stoichiometry is determined only by the probability by which protease and inhibitor form a complex. The higher stoichiometry is also observed in cases where the rate of dissociation is considerably higher compared to the rate of protease distortion by the cleaved inhibitor ($K_i >> K_{diss}$) (Stratikos and Gettins, 1999).

Ovine α-1-PI exhibits a considerably higher thermostability compared to its human counterpart and requires higher activation energy for denaturation. The higher stability is evident from a difference of T_m of ~ 7.5 ^oC between ovine and human α-1-PI. Ovine α-1-PI analysis revealed a glycation to the extent of 14 %. Enzyme assisted deglycosylation was employed to determine whether the carbohydrate side chain of ovine α-1-PI had any effect on the inhibitory potential and thermal stability. The inhibitor-enzyme association and residual inhibitory activity were unaltered. In direct contrast deglycosylation was found to decrease the thermal stability relative to the native α-1-PI (Table 3. 4). Although, glycan portion does not appear to have any influence on the inhibitory potential of α-1-PI, it plays an important role in the stability of the molecule. Guzdek et al. (1990) demonstrated that incompletely glycosylated forms of human α-1-PI synthesized by human Hep G2 cells were heat sensitive relative to the native protein but essentially had similar inhibitory activity towards neutrophil elastase and pancreatic trypsin. Travis et al. (1985) indicate that the lack of carbohydrate in their yeast recombinant α-1-PI using glyceraldehyde-3-phosphate dehydrogenase promoter is probably responsible for its more sensitivity to heat inactivation than the plasma form. Presence of carbohydrate antennas stabilizes the molecule by decreasing the dynamic fluctuations of the molecule. Glycosylation, like mesenteries; reinforce the functional native structure and helps keep in position the relative secondary structure (Mer et al.,

1996). The non-glycosylated recombinant α-1-PI expressed in yeast and *E. coli* though depicting a comparable activity has a compromised stability (Guzdek et al., 1990; Courtney et al., 1984; Rosenberg et al., 1984). Several studies on viral glycoproteins have demonstrated that glycosylation contributes to enhanced antigenicity of the molecule (Dowling et al., 2007). Deglycosylation therefore may be suitably rewarded by the decreased antigenicity of the molecule and hence increased therapeutic role. The catalytic properties, immunological reactivity and secondary and quarternary structures of the native enzyme are not significantly altered on deglycosylation (Kalisz et al., 1991; Ahmad et al., 2006).

RESULTS AND DISCUSSION

4. α-1-Proteinase Inhibitor: Mechanism of Multiple Proteinase Inhibition

α-1-PI has an astounding ability to react and inhibit a diverse array of serine proteases despite the narrow specificities and different recognition sites of each protease. The inhibitor-protease reactions were followed in order to elucidate the mechanism of α-1-PI recognition by a multitude of proteases. This section describes the competitive binding studies along with the chemical modifications, reactive center loop (RCL) peptide mapping, molecular modeling and docking studies undertaken to understand the inhibition mechanism and differentiate the α-1-PI recognition sites for three widely distributed physiological proteases elastase, trypsin and chymotrypsin.

RESULTS

Competitive binding studies

The effect of varying inhibitor concentrations of ovine α-1-PI on elastase, trypsin and chymotrypsin using their cognate substrates NSAPNA, BAPNA and BTPNA respectively showed a mixed type of inhibition at low concentrations of α-1-PI. Competitive binding studies were performed with the purified ovine α-1-PI. To assess the existence of any competition of elastase with trypsin and chymotrypsin inhibition sites on α-1-PI RCL and *vice versa*, varied concentrations of elastase/ trypsin/chymotrypsin were added to a fixed concentration of the inhibitor and residual activity measured.

α-1-PI was pre-incubated with varying concentrations of porcine pancreatic trypsin for 10 min at 37 ^{o}C and bovine chymotrypsin and porcine pancreatic elastase inhibitory activity measured independently using BTPNA and NSAPNA as substrates respectively. Similarly α-1-PI was pre-incubated with varying concentrations of chymotrypsin/elastase and the effect on other two proteases measured using their cognate substrates. Six replicates were employed for each concentration of enzyme examined. The inhibition of trypsin by α-1-PI in the presence of elastase/ chymotrypsin was less than 5 %, indicating that pre-incubation with elastase/ chymotrypsin blocks the active site completely. Similar results were obtained for elastase and chymotrypsin. These results indicate α-1-PI has a single combat site for serine proteases unlike the bovine pancreatic trypsin inhibitor, which can simultaneously inhibit trypsin and chymotrypsin (Table 4. 1).

Table 4. 1. Simultaneous inhibition studies with a range of physiological serine proteases.

Enzyme inhibited	Pre-incubation		
	Trypsin	Chymotrypsin	Elastase
	Inhibition (%)		
Trypsin	-	16	20
Chymotrypsin	8	-	5
Elastase	14	5	-

Reactive site of ovine α-1-PI

Ovine α-1-PI (0.1 mg/mL) in 0.1 M Tris-HCl, pH 7.4 was incubated with porcine pancreatic elastase and trypsin and bovine pancreatic chymotrypsin individually at 37 °C for 30 min in stoichiometric proportions to bring about complete protease inhibition. Complete protease inhibition was ensured by protease inhibitory activity assays described in Section 2. 2. 3. such that a specific cleavage takes place at the α-1-PI-RCL at the C-terminus and no random proteolysis sets in. The reaction was stopped by boiling with SDS sample buffer and the cleaved peptides resolved by SDS-PAGE (Figure 4. 1). The released peptides were electro-blotted onto a PVDF membrane, detected by CBB R-250 staining, excised and subjected to NH_2-terminal sequence analysis by Edman degradation. The release of the peptide NH_2-SLPPDVEFN upon controlled proteolysis by elastase and chymotrypsin indicates that the reactive site peptide bond cleaved is Met^{356}-Ser^{357} (Figure 4. 1A, Lane 2 and 3). In contrast the sequence of peptide obtained upon controlled trypsin digestion was NH_2-LEAIPMSLP (Figure 4. 1, Lane 1) indicating the reactive site to be Phe^{350} -Leu^{351}. A comprehensive search was undertaken and sequences of α-1-PIs from various mammalian sources were retrieved from the NCBI protein sequence database and aligned using the CLUSTAL W multiple sequence alignment algorithm. A high degree of sequence homology was observed at the RCL containing the scissile peptide bonds (Figure 4. 1B).

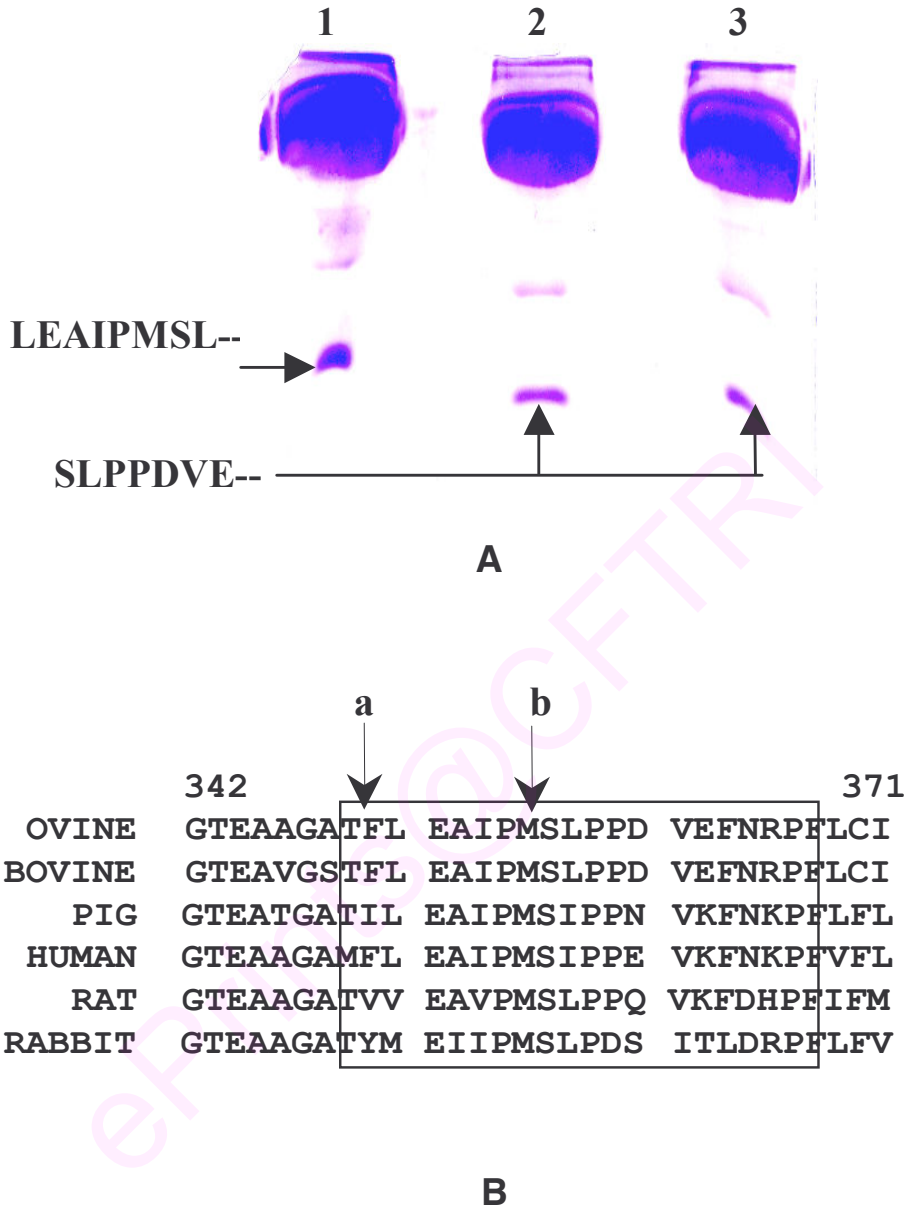

Figure 4. 1. Identification of the reactive site of ovine α-1-PI. A. SDS-PAGE of ovine α-1-PI treated with Lane 1: bovine trypsin, Lane 2: chymotrypsin and Lane 3: porcine pancreatic elastase. B. Multiple alignment of the mammalian α-1-PI sequences highlighting the signature sequence of the RCL. The numbering follows that of ovine α-1-PI. The peptide bond cleaved by porcine trypsin is indicated as **a** whereas **b** indicates the bond cleaved by bovine chymotrypsin and porcine elastase.

Rationale for chemical modification

Chemical modification was used as a preliminary tool to assess the role of different residues in specific protease inhibition. A closer evaluation of α-1-PI RCL reveals several potential protease recognition sites. Met^{356} (Met^{358} in human α-1-PI) with an easily recognizable side chain by all physiological serine proteases and feed back regulation due to oxidative inactivation susceptibility has been implicated at the reactive site of α-1-PI. Arg and Lys residues with basic side chains constitute the recognition sites for trypsin and trypsin-like proteases. The effects of chemically modifying Arg and Lys and Met residues of α-1-PI were studied.

Chemical modification of ovine α-1-PI

i) Arg modification

A closer evaluation of the reactive site peptide sequences (Figure 4. 1B) indicates the presence of conserved Arg residue at position 366, a potential site with trypsin specificity. In order to assess the role of Arg residues of ovine α-1-PI in relation to three proteases studied, the guanidinium group of Arg residues were modified using 1, 2 cyclohexanedione in a time dependent manner. Aliquots were removed and checked for protease inhibitory activity. A decrease in trypsin specific inhibition was observed while chymotrypsin and elastase inhibition remained almost unaltered as evident from a semi-logarithmic plot of % residual activity *versus* time (Figure 4. 2). These results indicate the involvement of an Arg residue in the interaction between α-1-PI and trypsin.

ii) Lys modification

The free ∈- amino groups of ovine α-1-PI were modified using 2, 4, 6-TNBS. TNBS reacts preferentially and quantitatively with free amino groups under mild conditions to give the corresponding tri-nitrophenol derivatives. No reaction occurs with the imidazole nitrogen of His, the guanidinium group of Arg or the hydroxyl group of Tyr or Thr (Haynes et al., 1967).

After incubation periods of 5, 10, 15, 20, 30, 45 and 60 min respectively, aliquots were taken and the modified amino groups determined. At each of the time intervals,

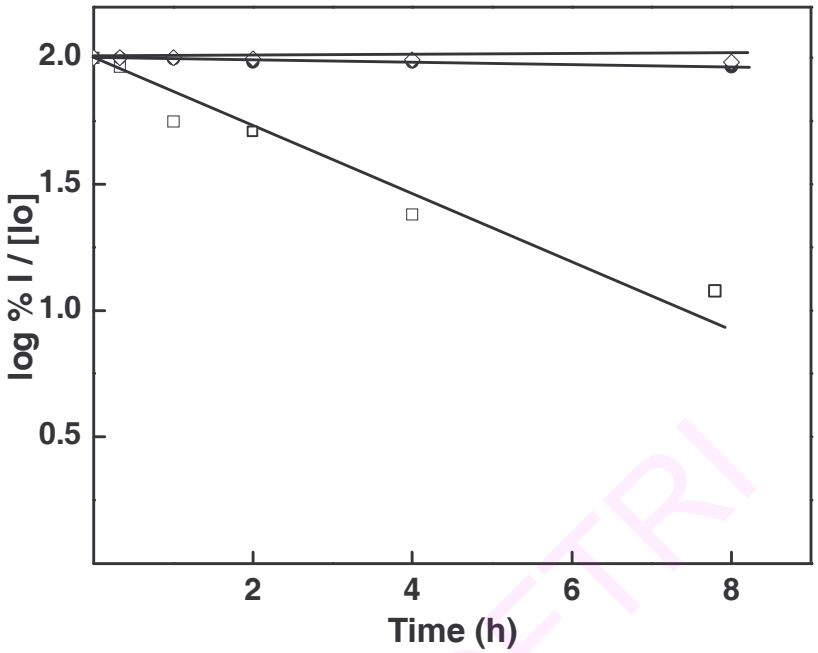

Figure 4. 2. Effect of Arg modification on α-1-PI activity. Time dependent inactivation curves of ovine α-1-PI activity for trypsin (-□-), chymotrypsin (-○-) and elastase (-△-).

0.5 mL of the solution was removed from the remaining solution, diluted with ice cold deionised water to stop the reaction and assayed for residual inhibitory activity. The loss in inhibitory activity was ~30 % for all the three proteases studied (Figure 4. 3). The close similarity in the decreased inhibitory capacity of all the three proteases advocates the involvement of a Lys residue in the α-1-PI and protease interaction.

The modification of Lys residues was simultaneously followed at 344 nm against a blank treated as above but containing water instead of protein solution and it indicated that all the Lys groups were modified. The tri-nitrophenyl derivative of amino groups can be quantified spectrophotometrically with much more accuracy than is possible with ninhydrin (Habeeb, 1966).

Although modification of the amino groups with TNBS caused a loss in inhibitory activity, the possibility still exists that this loss might have been due to modification of groups other than the amino groups or to steric, electrostatic or conformational effects.

Taking this into account the Lys residues of ovine α-1-PI were also chemically modified using citraconic anhydride. The modified ovine α-1-PI completely lost its inhibitory activity. The results of this modification are summarized in Table 4. 2.

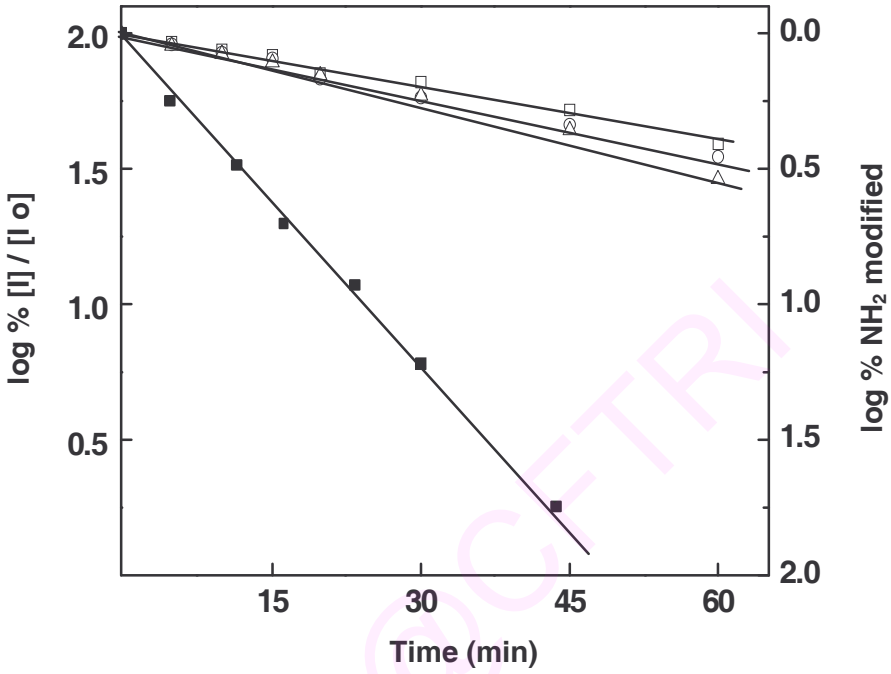

Figure 4. 3. Time course of free amino group modification and its effect on α-1-PI inhibitory activity. Effect of trinitrobenzenesulfonic acid on inhibitory activity of ovine α-1-PI. % free – NH_2 group modification (-■-) and its correlation with trypsin (-□-), chymotrypsin (-○-) and elastase (-△-).

Table 4. 2. Lys modification using Citraconic anhydride

iii) Met modification

Protease	% Inhibition	
	Control	Modified α-1-PI
Trypsin	100	0
Chymotrypsin	100	0
Elastase	100	0

Oxidation is one of the most prevalent forms of chemical modification, and the sulfur containing amino acid Met is susceptible to oxidation by a wide array of oxidants (Cleland et al., 1993). A mild oxidizing agent chloramine-T and a strong physiological oxidant H_2O_2 were used independently to oxidise Met to Met sulfoxide. Met residues were modified with chloramine–T at pH 8.0 (Mistry et al., 1991). Aliquots were aspirated, dialyzed extensively against 0.2 M Tris-HCl at 4 ^oC, and residual protease inhibitory activity assayed as described in section 2. 2. 3. Complete loss of elastase inhibition of α-1-PI was observed while trypsin and chymotrypsin inhibitory activities remained un-influenced (Figure 4. 4).

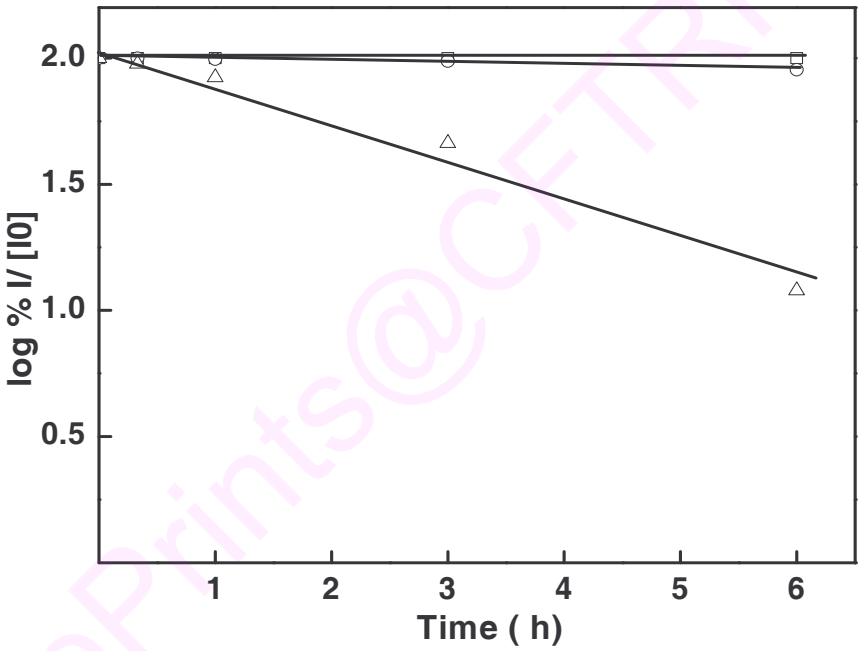

Figure 4. 4. Effect of Met modification on α-1-PI activity. Met modification using chloramine-T and time dependent inactivation curves of ovine α-1-PI activity for trypsin (-□-), chymotrypsin (-○-) and elastase (-△-).

H_2O_2 is a physiological oxidant associated with neutrophils and also a component of cigarette smoke known to be involved in inactivation of α-1-PI. Purified ovine α-1-PI (0.1 mg/mL) was incubated at 37 °C at pH 5.0 with 3 % H_2O_2. The concentration of H_2O_2 was measured at 240 nm ($\varepsilon = 39.4 \pm 0.2\ M^{-1}\ cm^{-1}$). At this pH Met is oxidized selectively

to Met sulfoxide (Brot and Weissbach, 1983). The modified inhibitor was evaluated by gelatin embedded PAGE zymography for protease inhibitory activity as described earlier.

Incubating α-1-PI with elastase prior to oxidation with either chloramine-T or H_2O_2 resulted in a meager loss of ~ 10 % in the inhibitory capacity. These results advocate that in the presence of the cognate protease, the reactive site Met is not amenable to oxidation. However, chymotrypsin and trypsin inhibition remained unaltered over a period of time (Figure 4. 5). These results suggest that Met is a determinant for elastase inhibition.

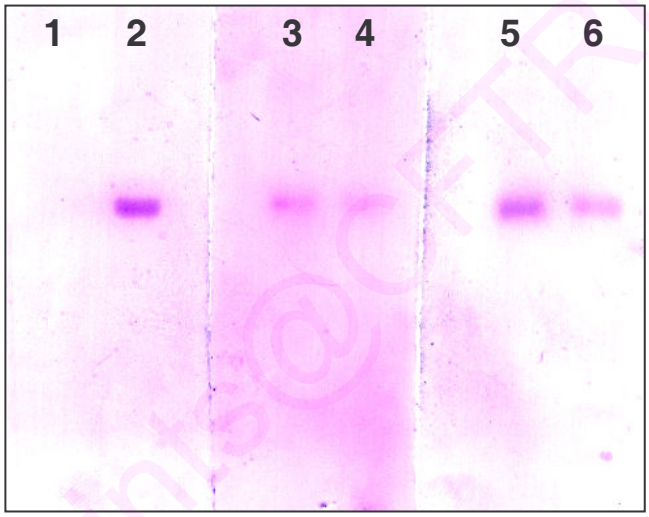

Figure 4. 5. Gelatin embedded PAGE zymography (10 % T, 2.7 % C) of ovine α-1-PI. Lanes 1, 3 and 5 represent elastase, chymotrypsin and trypsin inhibitory activities of α-1-PI treated with H_2O_2 and lanes 2, 4 and 6 without H_2O_2 treatment.

Homology modeling

Homology modeling is an apt and efficient method for determining the three dimensional structure of a protein. The construction of an appropriate theoretical protein model requires the selection of a suitable template with known sequence and structural motifs. The phylogenetic analysis revealed the close evolutionary relationships between different mammalian α-1-PIs (Figure 4. 6) indicating that the serpin α-1-PI exhibits considerably conserved primary structure. The results also show that evolutionary

conservation of RCL sequences is high within the antitrypsin family (Figure 4. 1) especially with reference to secondary and tertiary structural elements.

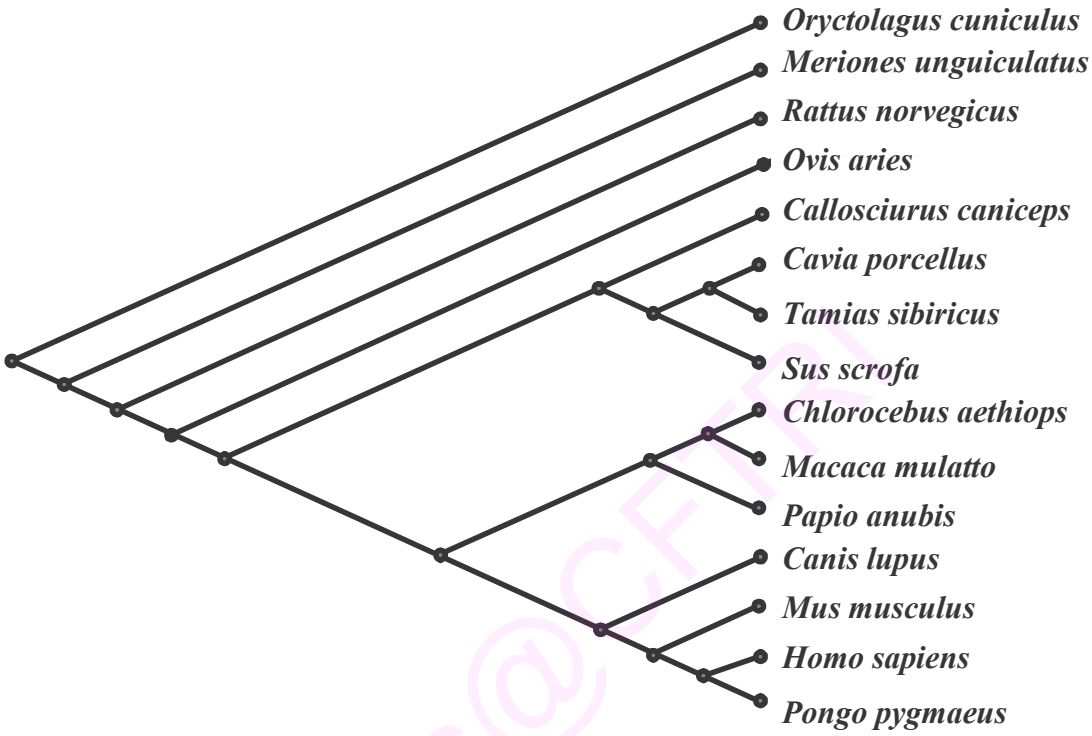

Figure 4. 6. Phylogenetic tree of mammalian α-1-PIs. Human, rat, ovine and porcine α-1-PIs are more closely related when compared to non-mammalian α-1-PIs.

The wealth of structural data available and the consistency within the serpin super family has resulted in the use of molecular modeling techniques to successfully predict the structures of serpins, for which no x-ray crystal structures are available, using the co-ordinates of other serpin family members (Katz and Christianson, 1993). A reliable model of ovine α-1-PI would steer future biochemical and genetic efforts in its evaluation as an emerging more stable therapeutic target. It is generally recognized that a template sequence identity above 25 % leads to reasonable homology models (Blundell et al., 1987). The cDNA sequence indicates that ovine α-1-PI is a polypeptide of 392 amino acids with a theoretical molecular mass of 43,586.67 sans post-translational

modifications. In the absence of a three dimensional structure, the molecular model of ovine α-1-PI based on the crystal structure co-ordinates of mature, uncleaved human α-1-PI (PDB ID 1HP7) was generated. Homology modeling was essential for any in depth bioinformatics approach to study ovine α-1-PI and its interactions with various physiological serine proteases.

The RCL sequence identity between the human and ovine α-1-PI was over 81.8 % and similarity 88.5 % (from residues P10 through P10`) using the P_n nomenclature of Schechter and Berger (1967). The sequence identity and structural similarity between human and ovine α-1-PI over the 392 residues was 70 and 76.5 % respectively. The modeled ovine α-1-PI is composed of three β-sheets labeled A, B and C and nine α-helices with each strand individually numbered as devised by the labeling system of Huber and Carrell (1989). The total energy of the molecule was found to be – 480.7 hartree (1 hartree = 627.51 kcal/mol) with a heat of formation of 97.54 hartree (AM1 method) and a net energy of 256.45 kcal/mol (UFF method). The structure of ovine α-1-PI (Figure 4. 7) was superimposed on human α-1-PI and the R. M. S. D. (Root Mean Square Deviation) was recorded to be 1.31 Å. Human α-1-PI has been well studied and displays close homology to the primary structure of ovine α-1-PI.

The R. M. S deviations of individual secondary structure elements between the template and the target are listed in Table 1. The Ramachandaran plot (data not shown) indicated that only eight residues (~ 2.2 %, excluding G and P) lie in the disallowed regions. As the R. M. S deviations are ≤ 2.0 Å, it is indicative of close superimposition.

Ovine α-1-PI reactive center loop docking against trypsin, chymotrypsin and elastase active sites

The modeled native stretched conformation of the ovine α-1-PI provided the initial peptide backbone for understanding the interactions at the interface of ovine α-1-PI RCL and the individual active sites of the three-serine proteases viz. elastase (PDB ID

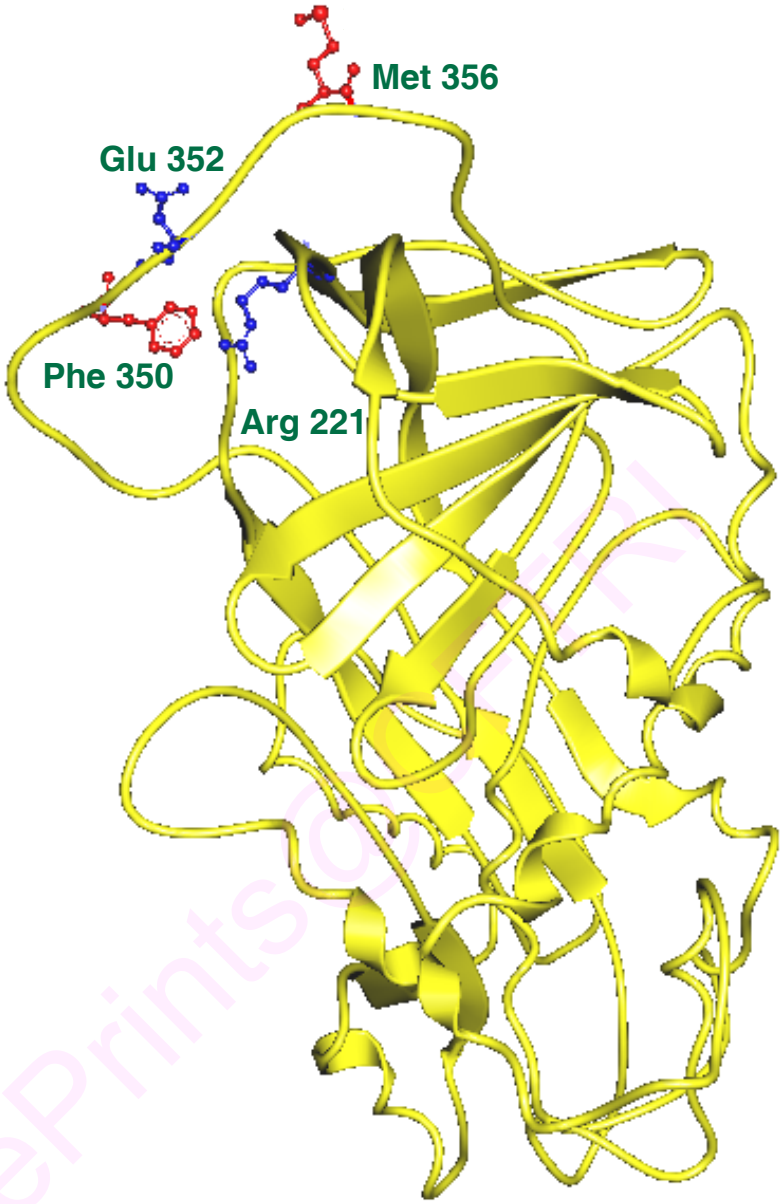

Figure 4. 7. Homology model of ovine α-1-PI. Human α-1-PI crystal structure (1HP7) was used as template to construct the ribbon model (yellow). Phe^{350} and Met^{356} in the RCL are highlighted in ball and stick mode (red). The model shows close contacts between Arg^{221}and Glu^{352}of the RCL with a distance of 4.3 Å (Blue, ball and stick).

Table 4. 3. R. M. S deviation of ovine α-1-PI with respect to human α-1-PI.

α-1-PI structural element		Residue range	R. M. S deviation (Å)
Helices		27-44	1.35
		54-65	0.45
		70-79	1.56
		89-103	1.47
		150-164	0.73
Sheet	A	215-232	1.27
		237-244	0.52
		248-255	1.5
		382-389	1.17
	B	112-121	0.0
		182-190	0.0
		331-340	1.21
	C	204-213	1.69
		282-289	1.8

1GVK, chain B), trypsin (PDB ID 1H9H, chain E) and chymotrypsin (PDB ID 1GL0, chain A) respectively.

Elastase depicts a global sequence identity of 40.2 % with trypsin and a local sequence identity ranging from 19.0 to 35.5 % with chymotrypsin. The elastase and chymotrypsin show a local sequence identity ranging from 33.3 to 50.0 %.

The best ligand pose energies for docking were calculated to be –14.58, –11.0, and –12.3 kJ mol^{-1} for RCL-elastase, RCL-trypsin and RCL-chymotrypsin interfaces respectively. As expected for well-minimized models, no bad contacts or clashes were observed and a small value (3.1 kJ/mol) was estimated for the standard deviation of the overall hydrogen bond energy.

Analysis for the distortion of the backbone, χ angles of side chains, atomic volume analysis and molecular packing yielded scoring factors corresponding to allowed conformations, and distributions of bond lengths and angles were within the accepted values for protein structures. The overall evaluation indicated that model of the ovine α-1-PI-RCL-protease complex intermediates ranked as acceptable structures.

Elastase, trypsin and chymotrypsin belong to the same chymotrypsin clan of serine proteases, and have a catalytic site comprised of a triad of His^{57}, Asp^{102} and Ser^{195}. From the graphical models (Figure 4. 8) it is evident that whereas Met^{356} side chain of ovine α-1-PI fits very well into this active site cervix of elastase and chymotrypsin which is their primary recognition site, same does not hold valid in case of trypsin. The active site of trypsin recognizes side-chain of Phe^{350} and it fits very well into its cavity. Therefore, the molecular modeling and docking data also agree well with the earlier experimental data that trypsin recognition site is different from elastase and chymotrypsin recognition site (Figure 4. 1).

DISCUSSION

The intriguing way of α-1-PI induced inhibition of multiple serine proteases motivated us to explore its mechanism of inhibition in detail. This was carried out by a multi-pronged approach employing competitive binding studies, α-1-PI-RCL peptide mapping and molecular docking of RCL peptide against elastase, trypsin and chymotrypsin reactive sites. The lack of a three-dimensional structure of ovine α-1-PI necessitated the construction of an effective practical protein model based on homology to other mammalian counterparts. BLAST search using www.ncbi.org indicates that ovine α-1-PI is a close relative of human and bovine α-1-PIs, and therefore, using human

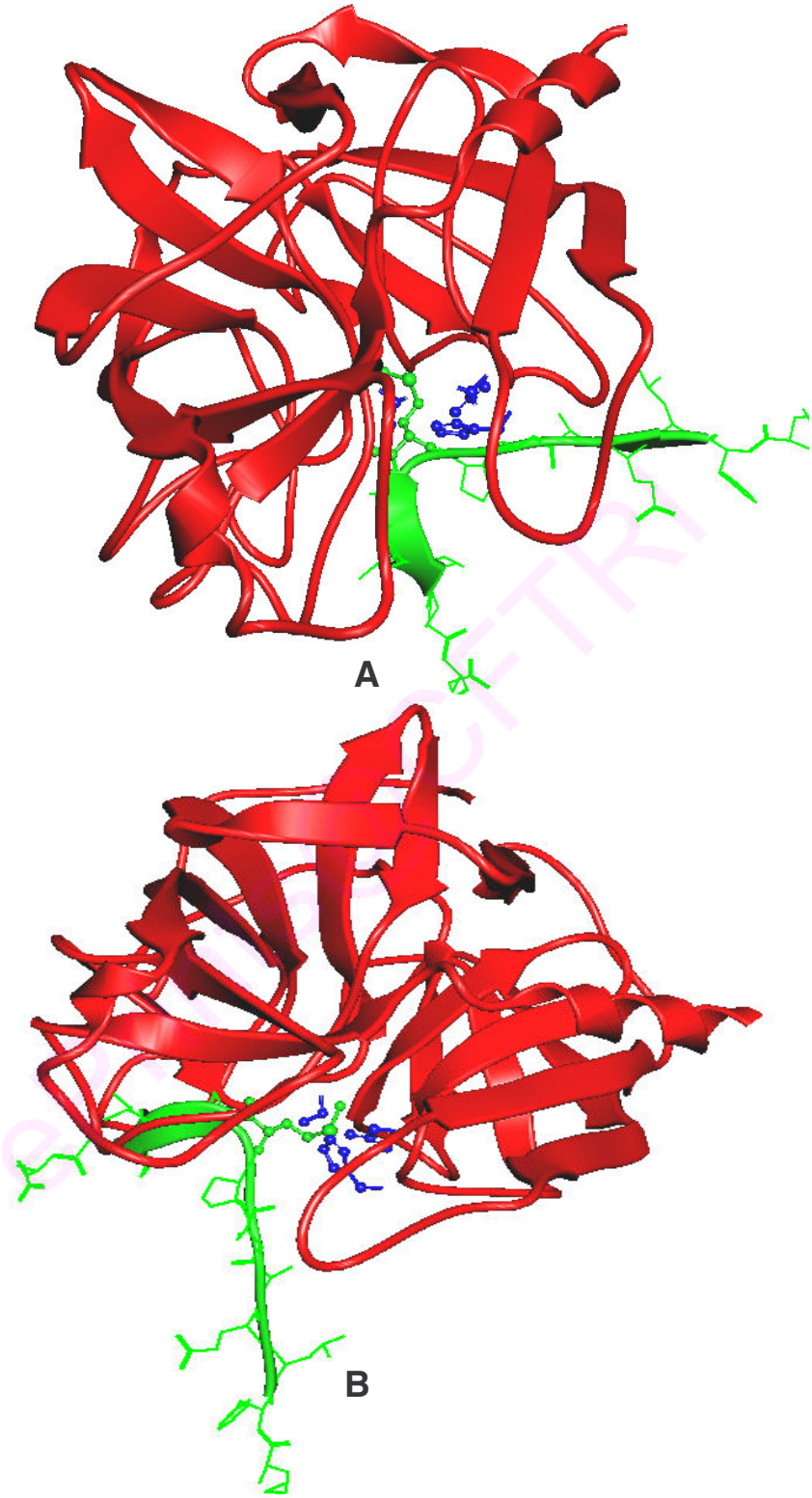

Figure 4. 8. Modeled structure of ovine α-1-PI protease interaction. RCL (Green) docked against A. Elastase (red) B. Chymotrypsin (red)

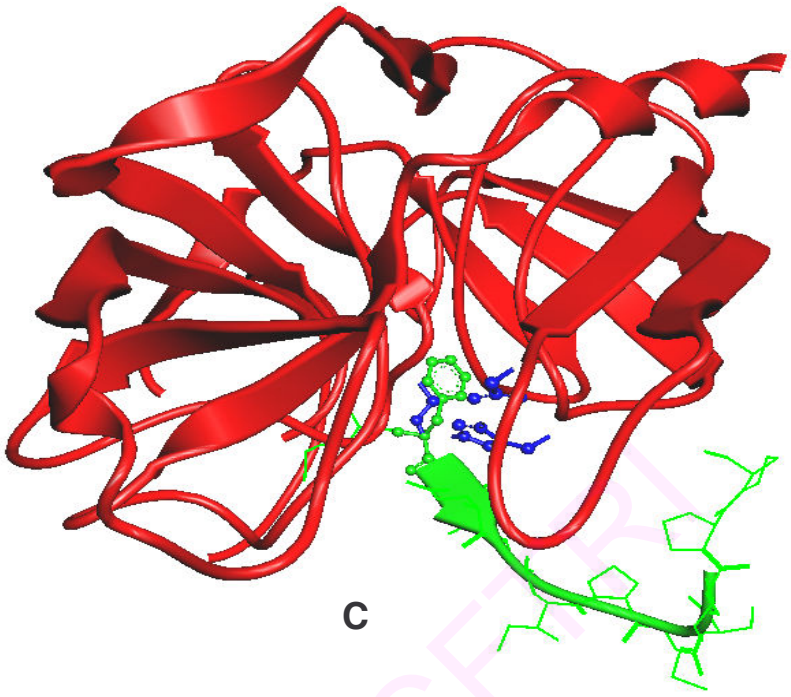

Figure 4. 8. (contd) C. Trypsin (red); protease active site residues His[57], Asp[102] and Ser[195] are shown in blue ball and stick mode. RCL Met[356] and Phe[350] are represented as green ball and stick structures.

α-1-PI as the template, a three-dimensional structure of ovine α-1-PI was generated, and used for all practical purposes.

It has been demonstrated for the first time that α-1-PI-RCL is a diffused reactive site that recognizes several proteases and interacts with them, using a combination of biochemical and molecular modeling approach. The pattern of inhibition unambiguously indicates that the exposed Pro anchored peptide stretch possessing a closely positioned Phe, Met and other hydrophobic amino acids is the key element in eliciting inhibition of serine proteases. The readily accessible natural substrate in the form of an exposed peptide stretch ensnares the protease into a lucrative encounter; the action inadvertently metamorphoses the molecule into a suicide inhibitor and warps the protease with its lethal conformational change.

Simultaneous inhibition studies with these three serine proteases point towards a single or an overlapping inhibitory site, which can combat only a single protease at a time. Ovine α-1-PI pre-incubated with one protease failed to inhibit the other proteases (Table 4. 1). Ovine α-1-PI reaction with elastase, trypsin and chymotrypsin in stoichiometric proportions as described in previous section resulted in the controlled proteolysis of ovine α-1-PI at the protease specific recognition site of the RCL. This resulted in the release of a C-terminal peptide. The NH_2-terminus of the C-terminal fragments generated by different serine proteases was found to differ by few amino acids. A multiple sequence alignment of the RCL stretch from different species with the peptides obtained showed that whereas trypsin cleaves at Phe^{350}, chymotrypsin and elastase cleave at Met^{356}. This indicates the presence of different recognition sites within the RCL. This RCL once cleaved undergoes conformational changes to trap the protease and as such is not available for any further protease inhibition reactions.

The above conclusions were further probed by individual amino acid chemical modifications. Arg, Lys and Met modifications were undertaken as these residues are present at the RCL and their side-chains constitute the potential serine protease recognition sites. Besides, Arg and Lys have occasionally been introduced at P1 position instead of Met by site directed mutagenesis and potent mutated molecules produced (Travis et al., 1985).

α-1-PIs are easily susceptible to oxidative inactivation and by cigarette smoke because of the presence of a Met residue at the P1 position of reactive site. Both chloramine-T and H_2O_2 treated α-1-PI showed a complete loss of inhibitory activity towards elastase (Figure 4. 4 and 4. 5) due to the oxidation of the reactive site Met residue. The fact that the inhibitory potency of α-1-PI was unaltered upon pre-incubation with elastase prior to oxidation further advocates the role of Met. In direct contrast the oxidation had no effect on the inhibition of trypsin (Figure 4. 4). This data suggests that Met^{356} of ovine α-1-PI (corresponding to Met^{358} of human α-1-PI) is not the primary cleavage site for bovine trypsin. This observation is supported by the fact that the bond cleaved by bovine trypsin is between Phe^{350} and Leu^{351} (Figure 4. 1B). The distance between Phe^{350} and Met^{356} of ovine α-1-PI is 17 Å in the homology model (Figure 4. 7).

Interaction of mouse macrophage elastase with native and oxidized human α-1-PI indicates that Met^{358} is the primary cleavage site whereas Phe^{352} is the secondary cleavage site (Banda et al., 1987). Alterations in the P1 residue of α-1-PI from Met to Val were shown by Travis et al. (1985) to increase the K_{ass} with pancreatic elastase but no longer inhibiting trypsin like serine proteases. Chymotrypsin recognizes the Met side-chain of α-1-PI as evident from RCL peptide mapping, yet remains unaffected upon Met oxidation. This can be explained by the fact that Met upon oxidation is converted to Met sulfoxide, which is more hydrophobic and bulky and therefore is rendered as a better recognition site for chymotrypsin.

Chemical modification of Arg with 1,2 cyclohexanedione results in a considerable loss of trypsin inhibitory activity of α-1-PI with no effect on elastase or chymotrypsin inhibition (Figure 4. 2). Cyclohexanedione was used as it reacts specifically with the guanidinium group of Arg residues at pH 8.0 to 9.0 in sodium borate buffer in the temperature range of 25-40 °C. The single product, N^7, N^8- (1,2-dihydroxycyclohex-1, 2-ylene)-L-arginine (DHCH-arginine) is stable in acidic solutions and in borate buffers (pH 8 to 9). A closer evaluation of the RCL of α-1-PI shows the presence of an Arg residue at the distal end. Whether this Arg has a role to play is yet to be investigated. Kang et al. (2004) showed that a non-covalent complex intermediate before the cleavage of P1-P1` scissile bond is the rate determining step. This step represents rearrangement of the RCL, which is regulated by a salt-bridge between the conserved Glu^{354} and Arg^{196} of human α-1-PI. The modeled ovine α-1-PI structure shows close contacts between Glu^{352} and $Arg^{221}$of the RCL with a distance of 4.3 Å. In addition, Arg^{221} is very close to the trypsin recognition site Phe^{350} at a distance of 2.2 Å.

The Lys residues of ovine α-1-PI were modified both with TNBS and citraconic anhydride. Lys modification irrespective of the chemical used resulted in a significant loss of protease inhibitory potential. TNBS is a bulky hydrophobic group that may introduce significant conformational changes in the molecule but has an advantage that it can be followed spectrophotometrically and the extent of free amino group modification estimated. In contrast, citraconic anhydride upon deblocking gives a homogenous protein that is identical with native protein both in its conformational and hydrodynamic

parameters (Singhal and Atassi, 1971). Citraconylation of the Lys residues of ovine α-1-PI resulted in a significant loss of elastase, trypsin and chymotrypsin inhibitory potential. These results advocate that a Lys residue of ovine α-1-PI is essential for inhibiting the three-serine proteases to the same extent. Huntington et al. (2000) in their crystallographic structure showed that two major contacts contribute to the typical serpin-protease complex formation. One of these is Lys^{328} of human α-1-PI, which forms a salt bridge with the conserved Asp^{194} of trypsin. Therefore it is not unreasonable to assume that modification of the corresponding Lys^{326} prevents the salt bridge between ovine α-1-PI and the protease reducing the inhibition. These interactions they showed are not specific to trypsin but common to any chymotrypsin family member where Asp^{194} is conserved. This explains why the loss in inhibitory activity towards the three enzymes was similar.

A cursory look at the phylogenetic tree reveals close evolutionary relationship between most of the mammalian α-1-PIs studied. Data available on human α-1-PI has allowed modeling of ovine α-1-PI to be undertaken at a relatively good confidence level. The measurements of the R. M. S. D demonstrate that the model of ovine α-1-PI superimposes on the X-ray crystal structure of human α-1-PI with little structural differences. The R. M. S deviations for the individual secondary structure elements between the two models (Table 4. 3) are < 2.0 Å, which is also indicative of close superimposition. Homology modeling is an appropriate and effective method for determining the three dimensional structure provided at least 25 % amino acid sequence identity for the template is available. Clearly ovine α-1-PI satisfied this criteria with ~70 % amino acid sequence identity with human α-1-PI. The close structural relationship between two inhibitors is indicative of same specificity and similar K_{ass} for the serine proteases. Indeed the measured constants (Table 3. 3 of earlier section) are very similar to that of human α-1-PI. Several molecular modeling studies have successfully predicted the structure of serpin proteins (Jarvis et al., 1992; Katz and Christianson, 1993).

In conclusion, until the three-dimensional structure of ovine α-1-PI is determined and refined at atomic resolution, the homology model of ovine α-1-PI serves as the next best structural reference for understanding structure/function relationships. This is the

first time that a tandem–modeling procedure (using molecular models of the RCL of an uncleaved serpin as a template for homology modeling) has been used to model the three-dimensional state of a serpin- serine protease interface.

The docking models of ovine α-1-PI RCL with elastase, trypsin and chymotrypsin (Figure 4. 8) provide a structural basis to account for the close similarities in the experimentally evaluated association constants (Table 3. 3 of earlier section). Besides, it confirms the experimental observations that trypsin recognition site stands distinct when compared to elastase and chymotrypsin recognition sites. Thus it is a synergistic approach adapted by RCL with responsibilities shifting between different amino acid residues, and a unique geometrical orientation that turns α-1-PI into an exclusive protease inhibitor that can interact with most of the serine and several non-serine proteases.

Evolutionary variations amongst mammalian species reflect sporadic differences within principally conserved interactive peptide stretches flanked by strategically positioned Pro residues. Differences between human and ovine α-1-PI are not prominent either with regard to kinetic parameters, primary structure, glycosylation, immunogenicity or three dimensional structures. Oxidation and proteolytic cleavage destroy the protease inhibitory activity of ovine α-1-PI. However, the easy availability, high sequence similarity and far higher stability with greater protease inhibition competence makes ovine α-1-PI a suitable serpin to be studied in detail and as an alternative to human α-1-PI for augmentation therapy.

RESULTS AND DISCUSSION

5. Heparin Induced Activation of α-1-Proteinase Inhibitor

Alpha-1-Proteinase inhibitor being the archetypal serpin displays significant structural and sequence homology towards other heparin binding serpins viz. antithrombin, heparin cofactor II (HC II) and plasminogen activator inhibitor-1 (PAI-1). α-1-PI binding to heparin and the resultant activation parameters are discussed in detail in this section. The heparin-binding domain was ascertained by peptide mapping of α-1-PI and molecular docking approaches. Chemical modifications of amino acids followed by affinity chromatography and protein topology studies were employed to identify the positively charged clusters of amino acids. A novel single step heparin-sepharose purification protocol for mammalian α-1-PIs was developed.

RESULTS

Activation of α-1-PI by heparin

The effect of increasing concentrations of an apparently homogenous heparin preparation (M_r 2530.191 Da) (Figure 5. 1) on the activity of purified human and ovine α-1-PI is represented in Figure 5. 2A.

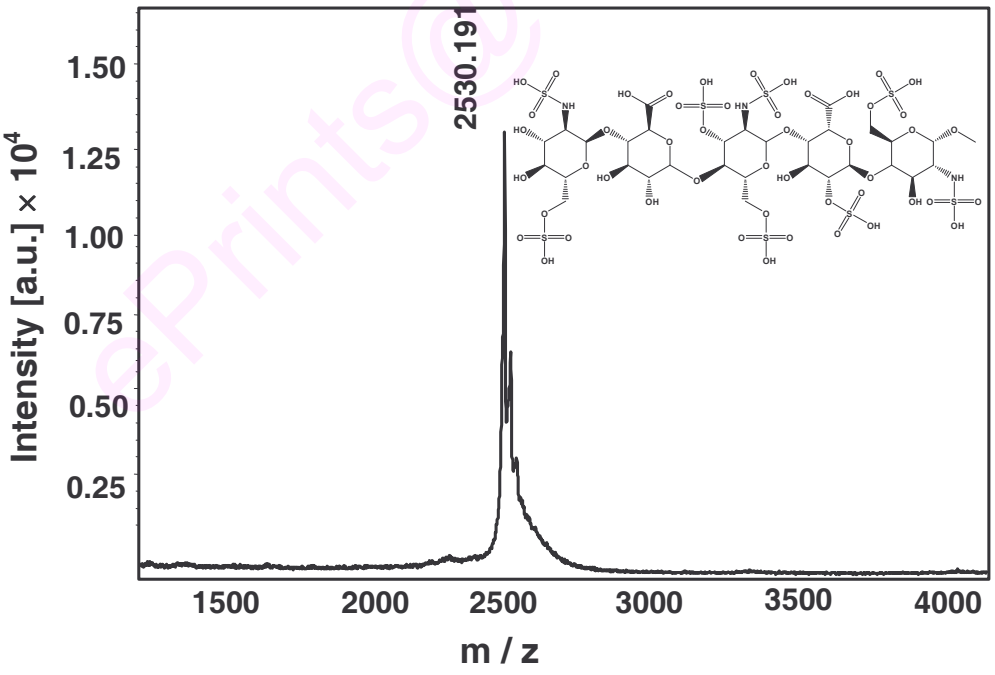

Figure 5. 1. Mass determination of heparin. MALDI-MS of the heparin used for all experimental purposes. Inset: Structure of the natural heparin penta-saccharide as generated using Chemdraw Ultra 7.0.

The sigmoidal shape of the curve is indicative of an allosteric activation. This sigmoidal behavior also signifies a two-step binding mechanism in which an initial weak activation of α-1-PI occurs at low heparin concentrations of 0-0.5 μM. A very sharp linear increase was observed between 1-6 μM with half the maximal activity observed at 2-3 μM. The most effective heparin concentration was 6±0.5 μM where the measured activity for human and ovine α-1-PI was 430 and 480±20 TIU/mg respectively. The maximum steady state was observed at 10 μM. A further increase in the heparin concentration had no effect on α-1-PI activity (Figure 5. 2A).

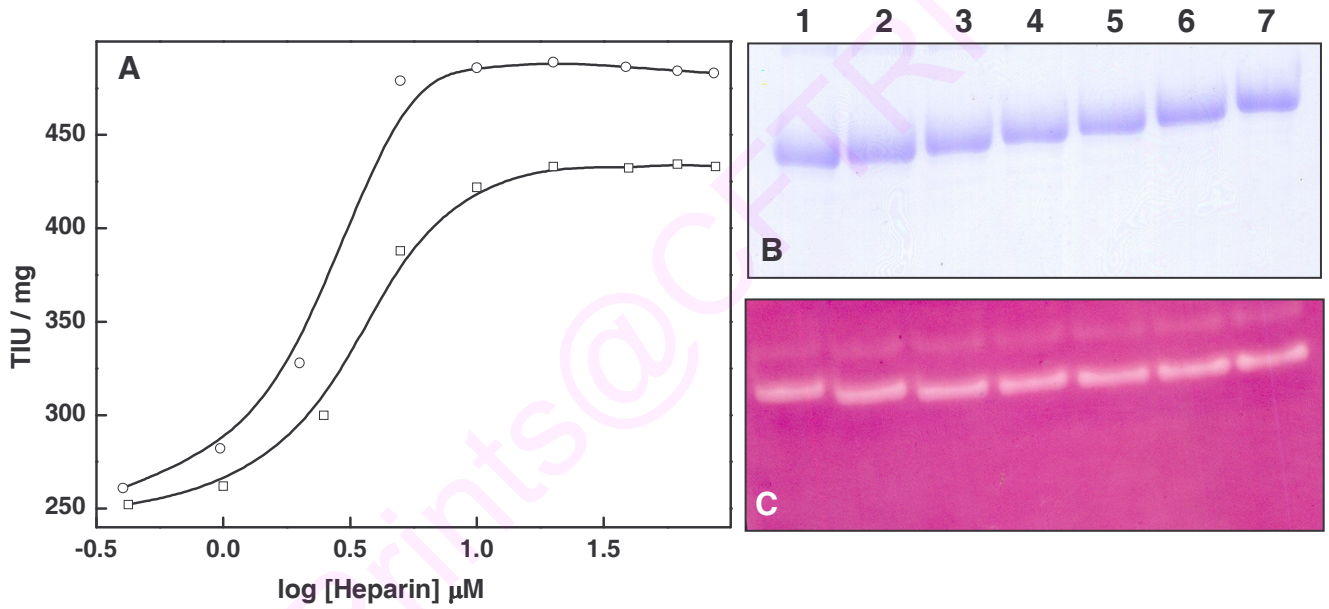

Figure 5. 2. Heparin induced activation of α-1-PI. A. Effect of varying concentrations of heparin as a function of inhibitory activity of human (-□-) and ovine (-○-) α-1-PI respectively. B. Mobility shift of ovine α-1-PI in PAGE (10 % T, 2.7 % C), stained with CBB R-250. C. APNE staining. Lanes 1-7 indicate 5 μg of ovine α-1-PI incubated with 0, 0.05, 0.1, 0.2, 0.3, 0.4 and 0.5 μg of heparin respectively.

The heparin activation of α-1-PI was also evaluated by native PAGE followed by protein and trypsin inhibitor staining. The results show that increasing heparin concentrations resulted in a decreased mobility of α-1-PI (Figure 5. 2B). The observed increase in the intensity of inhibitor specific stain (Figure 5. 2C) is concurrent with the

increased α-1-PI activity (Figure 5. 2A). The decrease in the electrophoretic mobility on native PAGE indicates an increase in both the molecular dimensions and surface charge neutralization of the α-1-PI upon binding to the linearly extended negatively charged polysaccharide.

Association rate constant (K_{ass}) determination

Proteases react with α-1-PI according to equation:

$$E + I \underset{K_{diss}}{\overset{K_{ass}}{\rightleftharpoons}} EI$$

where K_{diss} is negligible in case of suicide inhibitors. The high K_{ass} value and the irreversible character of the enzyme inhibitor binding render the inhibition process extremely efficient. The K_{ass} of both native as well as heparin activated α-1-PI was determined by the method of Djie et al. (1996) under pseudo-first order conditions by adding enzyme to inhibitor, substrate and heparin mixtures and recording the progress curves. Native ovine α-1-PI K_{ass} values for porcine elastase, trypsin and bovine chymotrypsin were determined earlier (Table 3. 3 of earlier section). The kinetic analysis of the both human and ovine α-1-PI rate constants with and without heparin binding revealed a significant shift in the K_{ass} values at physiological pH upon heparin activation. Active site titrations have shown that heparin treated human and ovine α-1-PI have higher K_{ass} values towards porcine elastase when compared to native state. Human α-1-PI was activated ~ 38±2 fold while ovine α-1-PI was activated ~ 45±2 fold (Table 5. 1). Pre-incubation of porcine pancreatic elastase with heparin did not have any effect on its rate of association with α-1-PI or its stability.

The semi-logarithmic plots of residual inhibitory activity at various inhibitor concentrations *versus* time were linear for both human and ovine α-1-PI, indicating that the activation followed pseudo-first order kinetics (Figure 5. 3A and 5. 4A). A plot of the first-order activation rate constants against various α-1-PI concentrations was also linear (Figure 5. 3B and 5. 4B).

Table 5. 1. Second order rates of association (K_{ass}) values for the reaction of serpins with proteases in the absence* and in the presence of heparin (values other than human and ovine α-1-PI are as cited by Pike et al. (2005).

Serpin	Protease	K_{ass} ($M^{-1}.s^{-1}$)
Human α-1-PI	PPE	1.7×10^5 *
		6.4×10^6
Ovine α-1-PI	PPE	3.3×10^6 *
		1.5×10^8
Antithrombin	Thrombin	1×10^4 *
		4×10^7
	Factor Xa	2×10^3 *
		4×10^7
HC II	Thrombin	7×10^2 *
		1×10^7
PCI	Activated Protein C	1×10^4 *
		2×10^4

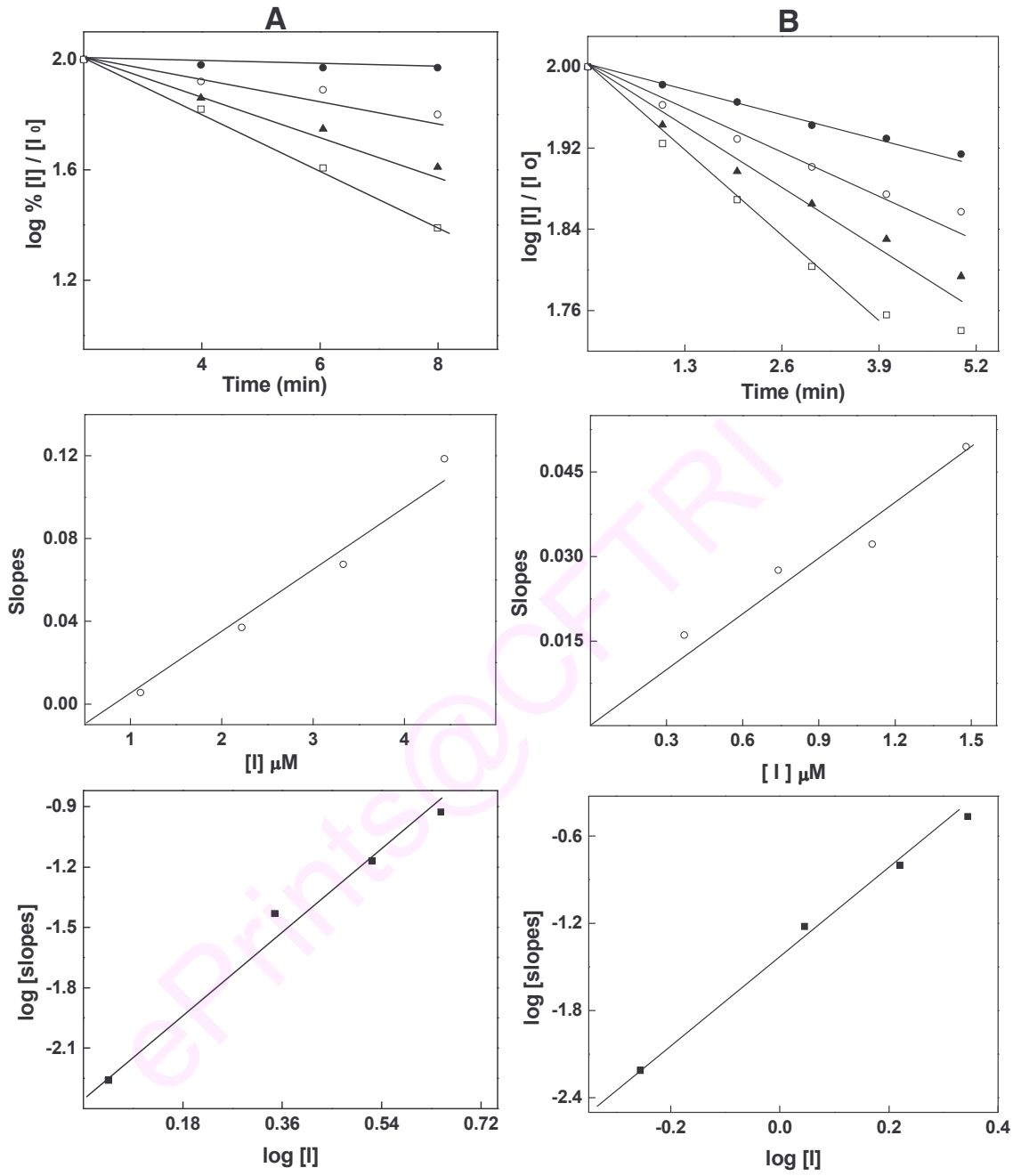

Figure 5. 3. Determination of human α-1-PI association rate constants with elastase. Panel (1) α-1-PI, Panel (2) heparin activated α-1-PI. Various concentrations of α-1-PI were titrated against a fixed concentration of elastase. A. (—●—) 0.5 μM, (—o—) 1 μM, (—▲—) 1.5 μM and (—□—) 2 μM in 0.15 M Tris-HCl, pH 7.4 at 37 °C. B. Plot of pseudo first order inhibition rate constant as a function of α-1-PI concentration. C. Double logarithmic plot of pseudo first order inhibition rate constant as a function of α-1-PI concentration.

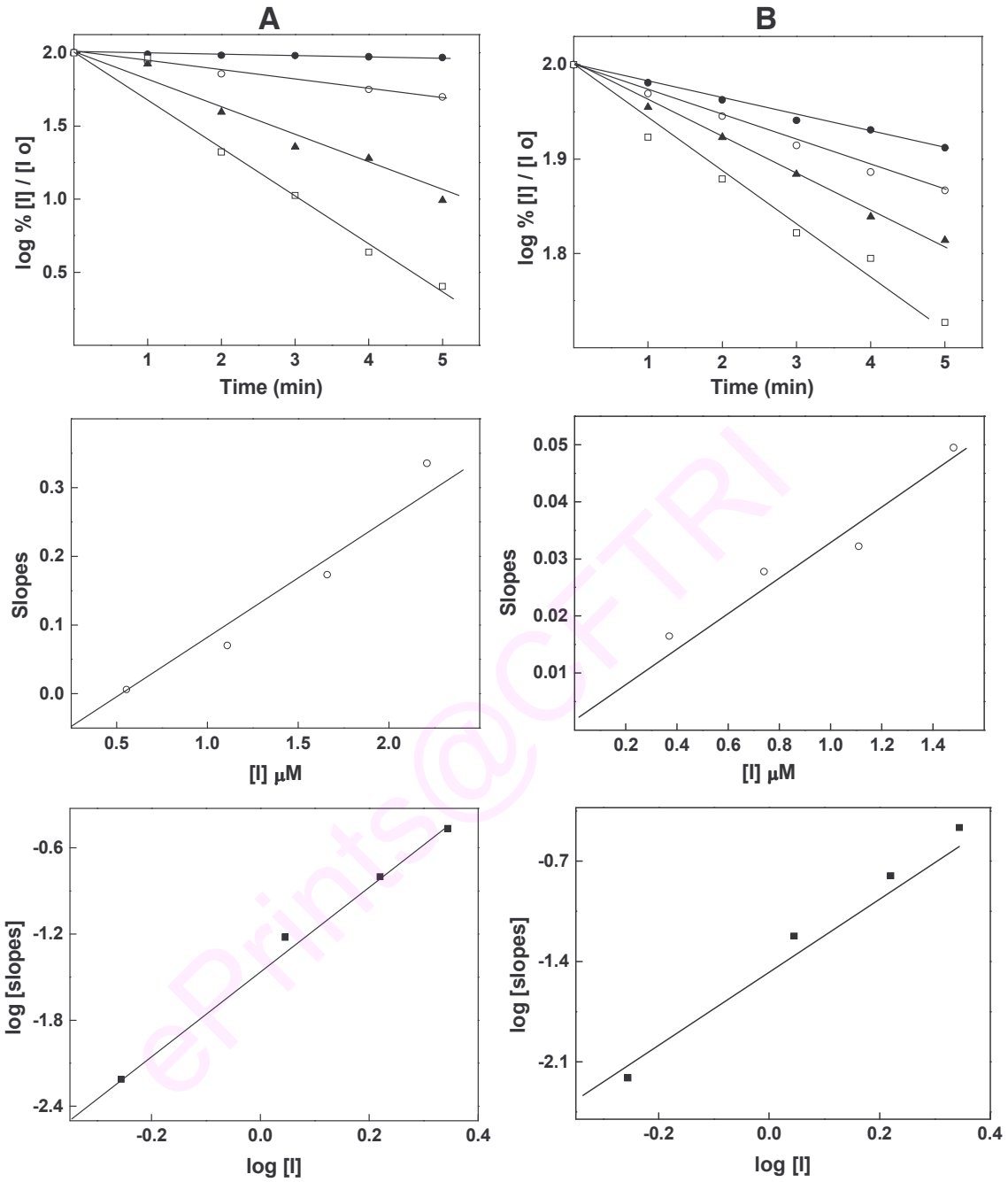

Figure 5. 4. Determination of ovine α-1-PI association rate constants with elastase. Panel (1) α-1-PI, Panel (2) heparin activated α-1-PI. Various concentrations of α-1-PI were titrated against a fixed concentration of elastase. A. (—●—) 0.5 µM, (—o—) 1 µM, (—▲—) 1.5 µM and (—□—) 2 µM in 0.15 M Tris HCl, pH 7.4 at 37 °C. B. Plot of pseudo first order inhibition rate constant as a function of α-1-PI concentration. C. Double logarithmic plot of pseudo first order inhibition rate constant as a function of α-1-PI concentration.

Binding of heparin to α-1-PI

To characterize the extent by which heparin alters the α-1-PI-protease reaction, binding of heparin to human α-1-PI was quantified by monitoring the protein fluorescence variations (Figure 5. 5A). The fluorescence spectra of native and heparin bound α-1-PI were measured in a Shimadzu (Model RF-5000) spectrofluorimeter.

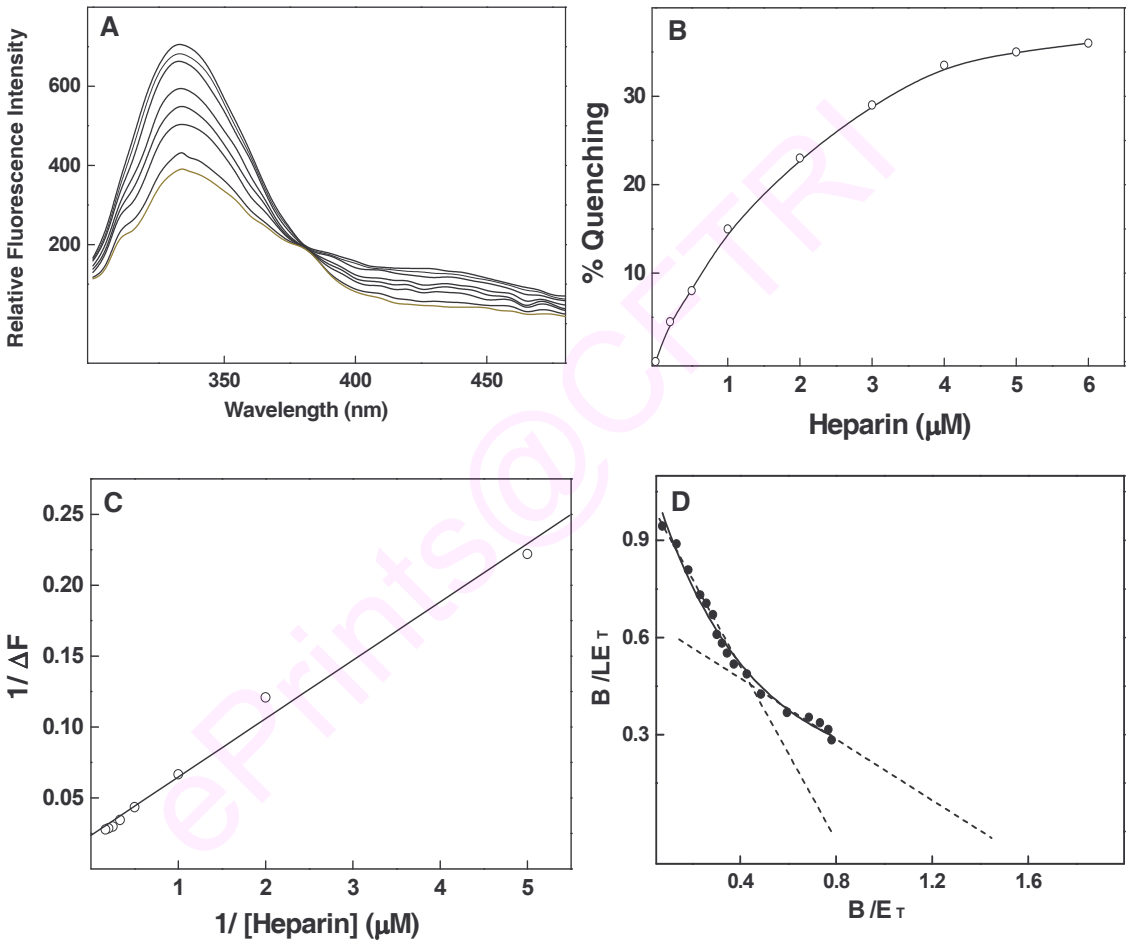

Figure 5. 5. Heparin binding studies of human α-1-PI with heparin using fluorescence spectroscopy. A. Emission spectra of α-1-PI in the presence of 0, 0.2, 0.5, 1, 2, 3, 4 and 5 μM heparin from top to bottom. B. A simplified plot quantifying the extent of heparin induced quenching. C. Double reciprocal plot of change in fluorescence as a function of heparin concentration. D. Scatchard plot of heparin binding to human α-1-PI at pH 7.4, determined by fluorescence titrations, as described under section 2.2.30.3.

Fluorescence was measured upon excitation at 282 nm. α-1-PI was incubated for 15 min in the presence of various concentrations of heparin. The emission spectra of native and heparin activated α-1-PI was measured between 300-500 nm (Figure 5. 5A). The change in the fluorescence intensity was measured without any shift in the emission maxima. The quenching increased with increasing heparin concentration. The fluorescence intensity decreased gradually upto ~ 4 μM heparin beyond which marginal or negligible decrease occurred. The shape of the titration curve was hyperbolic (Figure 5. 5B). Titrations of α-1-PI with heparin resulted in a saturable 37±2 % quenching in protein fluorescence observed at 6 μM of heparin, representing 70 % completion of the reaction as deduced from the double reciprocal plot (Figure 5. 5 C). A Scatchard plot of this data indicates two modes of binding- an initial high affinity-binding mode followed by a low affinity non-specific interaction (Figure 5. 5D) with a dissociation constant (K_D) of $7\pm2 \times 10^{-7}$ M and an average of one mole of heparin binding per mole of α-1-PI, at initial concentrations. At higher concentrations of heparin, however there is a weak low-affinity binding with a K_D of $2.09\pm2 \times 10^{-6}$ M. At lower concentrations of heparin the binding constant (K_α) with human α-1-PI was determined to be $2.5\pm0.2 \times 10^{-6}$ M by fluorescence quenching experiments with a stoichiometry of binding of 1±0.2: 1.

Sequence analysis and topology assessment of α-1-PI

The amino acid sequence of human antithrombin (AT) exhibits 30 % sequence and 26 % structural identity to human α-1-PI. Activation of AT by high affinity heparin pentasaccharide is proven to be due to heparin binding to basic residues in and around α-helix D (Gettins et al., 1993). A multiple sequence alignment (Residue 120-149) of AT depicts that among the basic side-chain residues, which have been implicated in heparin binding to AT, K^{125} and K^{133} are conserved in all mammalian α-1-PIs (Jin et al., 1997). Arg^{129} of AT critical for high affinity heparin binding is replaced by either Lys or Thr in the mammalian α-1-PIs (Figure 5. 6A). The space filling models of AT and α-1-PI reveal that the spatial orientations of these three residues (K^{125}, K^{133} and R^{129}) differ in the two molecules.

In AT these three residues are clustered in a single protruding domain whereas in human α-1-PI these residues are spatially separated (Figure 5. 6B) and therefore would

constitute a feeble site for co-operative interaction with heparin. Further domain topology analysis of α-1-PI revealed that the single largest positively charged domain of human α-1-PI contained three Lys residues K^{154}- K^{155} and K^{174}.

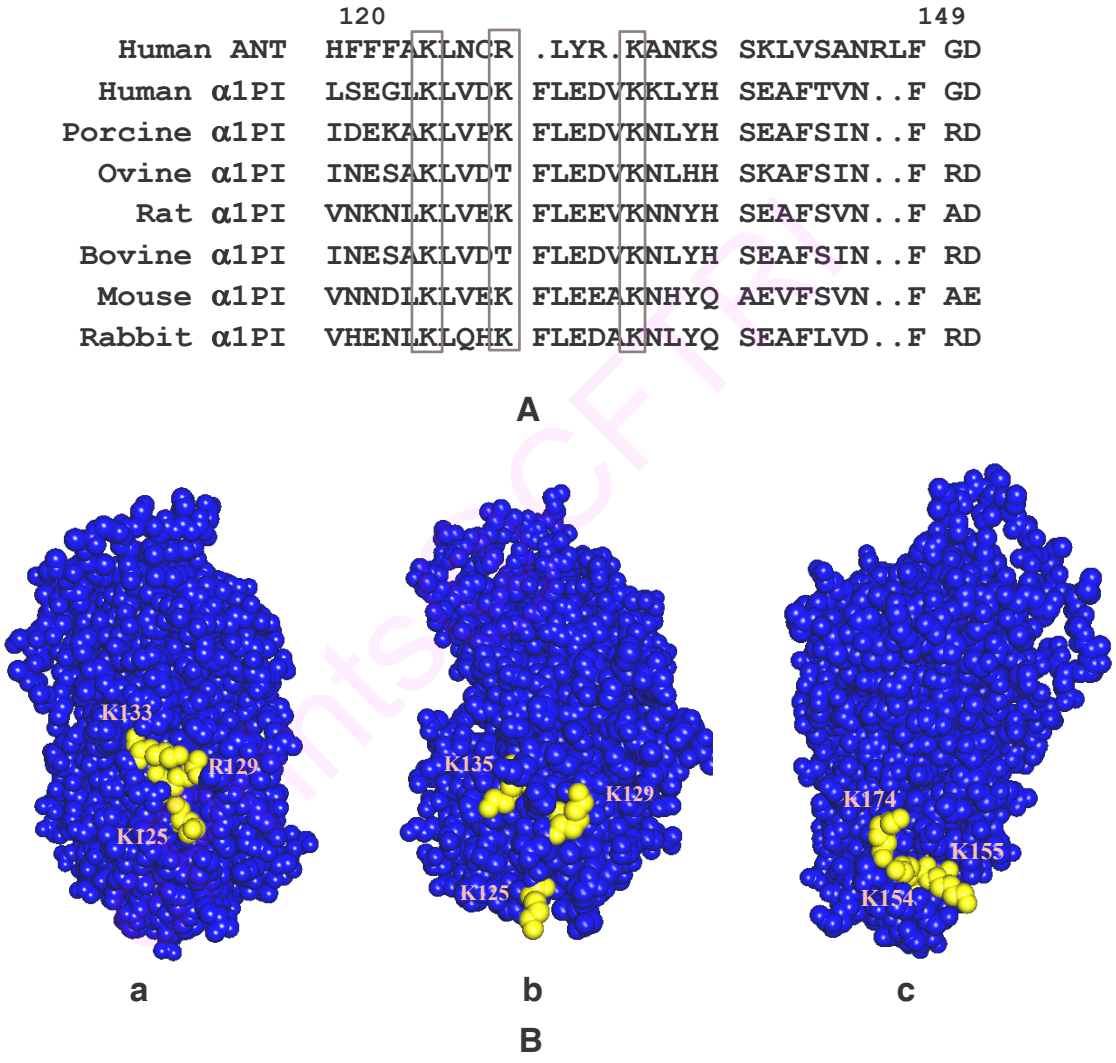

Figure 5. 6. Sequence alignment and topology assessment of the serpins. A. Multiple sequence alignment of heparin binding sequence of human antithrombin with mammalian α-1-PIs. B. Space filled models showing the positively charged clusters of a) human antithrombin, b) and c) α-1-PI. The residues involved in defining these clusters are shown in yellow.

The space filled model reveals that these residues are located on the α-helix F on the frontal side of α-1-PI and form a single cluster much like that observed for the heparin binding domain in AT (c of Figure 5. 6B). Multiple protein sequence alignment of this region (Residue 150-179) of mammalian α-1-PIs is shown in Figure 5. 7. The results show that K^{154} and K^{155} are highly conserved and almost invariant across the genus. In contrast K^{174} is invariant in all mammals except Pig (*Sus scrofa*) and rabbit (*Oryctolagus cuniculus*). This Lys rich domain could probably be the site of interaction with the negatively charged biological molecule like heparin and other GAGs. Ovine α-1-PI differs from other α-1-PIs in that it possesses three consecutive basic residues K^{152}-K^{153}-K^{154}, which could well be the reason for the observed higher activation compared to human α-1-PI (Figure 5. 2A).

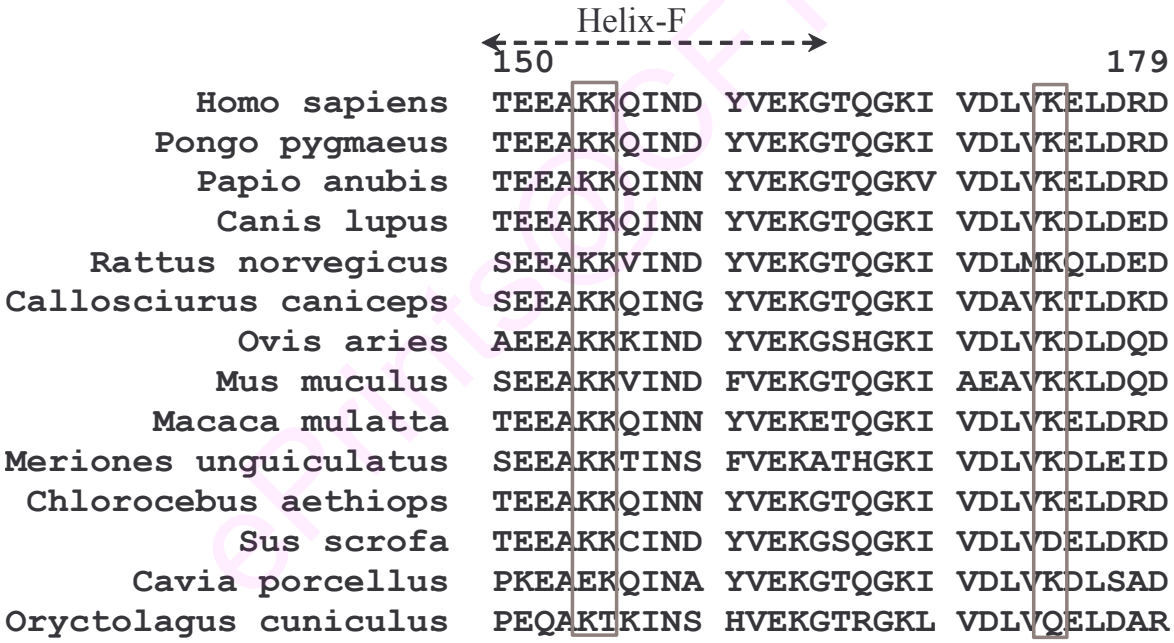

Figure 5. 7. Multiple sequence alignment of the α-helix F stretch of human α-1-PI (T^{150} to D^{179}) with other mammalian α-1-PIs. The highlighted residues Lys^{154}, Lys^{155} and Lys^{174} are largely conserved amongst the species studied *Pongo pygmaeus* (Orangutan), *Papio anubis* (Baboon), *Canis lupus* (Dog), *Rattus norvegicus* (Rat), *Calloscirus caniceps* (Squirrel), *Ovis aries* (Sheep), *Mus musculus* (Mouse), *Macaca mulatta* (Cynomolgus monkey), *Meriones unguiculatus* (Mongolian gerbil), *Chlorocebus aethiops* (Vervet monkey), *Sus scrofa* (Pig), *Cavia porcellus* (Guinea pig) and *Oryctolagus cuniculus* (Rabbit).

Chemical modification of α-1-PI and its effect on heparin interaction

The multiple alignment and surface topology comparison of α-1-PI with heparin binding site of AT implicate the involvement of either Lys and/or Arg residues. Both Arg and Lys have a positively charged side chain and have been shown to play a role in binding to poly-anionic heparin in several heparin binding serpins. To discern whether lysyl or arginyl residues are involved in heparin binding these residues of α-1-PI were chemically modified. Arg residues were selectively modified using 1, 2 cyclohexanedione.

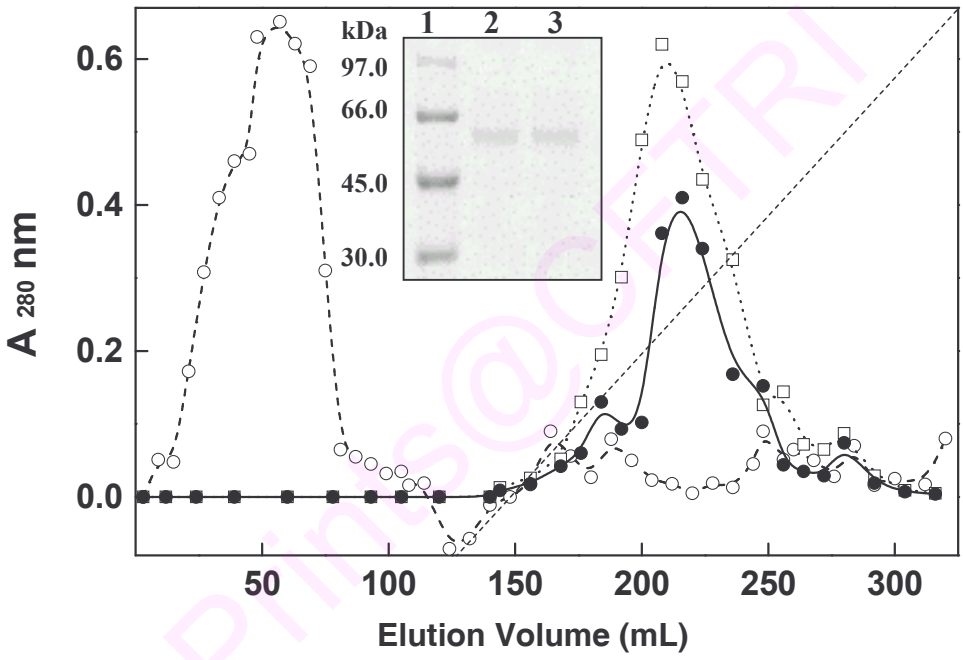

Figure 5. 8. Chemical modification and heparin affinity chromatography studies. Heparin sepharose chromatography profile of purified native (-●-), Lys modified (--○--) and Arg modified (..□..) human α-1-PI. Inset: SDS-PAGE (10 % T, 2.7 % C). Lane 1: M_r markers; Lane 2: Lys modified and Lane 3: Arg modified human α-1-PI.

A heterocyclic condensation product results upon 1, 2-cyclohexanedione treatment between the guanidinium group of Arg and the carbonyl of 1, 2 cyclohexanedione. The basic side-chains of Lys residues were chemically modified using citraconic anhydride. The heparin binding properties of these chemically modified α-1-PIs were compared with that of native α-1-PI and the changes assessed using a heparin

sepharose column. Native α-1-PI bound to the column and was eluted using a linear salt gradient (Figure 5. 8).

Citraconylated α-1-PI with the modified Lys residues did not bind to the column and appeared in the buffer wash. Citraconylation results in the acetylation of the free ∈-amino group of Lys. In contrast the heparin-sepharose binding property of the Arg modified α-1-PI remained unaffected as it bound to the column and eluted in the salt gradient. The elution of the protein was monitored at 280 nm and confirmed using SDS-PAGE (Figure 5. 8, Inset). From these results it is evident that lysyl residue (s) have a role to play in the heparin binding property of α-1-PI. Similar results were obtained for ovine α-1-PI (results not shown).

Identification of the heparin binding peptide of α-1-PI

Proteolysis followed by peptide mapping is regarded as the key step in analyzing protein primary structure (Lundell and Schreitmuller, 1999) and has a long history in the analysis of protein ligand interactions. In order to identify the heparin binding site of helix D or F, which are masked upon binding to heparin and therefore not accessible to trypsin digestion, ovine α-1-PI was reacted with TPCK-trypsin both in the presence and in the absence of catalytic amounts of heparin. Figure 5. 9A and B show the RP-HPLC profile of the tryptic digests of α-1-PI in the presence and absence of heparin.

Comparison of the peptide maps shows that there is a single peak (R_T = 27.3 min) in the tryptic map (shown by arrow), which is absent in the tryptic map of α-1-PI digested in the absence of heparin. This peak was collected and re-chromatographed to ensure purity and subjected to automated Edman degradation. This peptide had the sequence DAEEAKKKINDYVE and corresponded to the tryptic fragment spanning residues (149-162) of ovine α-1-PI. Heparin binding clearly shields this stretch of lysine residues in α-1-PI from proteolysis, which has allowed for the identification of the heparin binding site within the protein. These results explain why chemical modification of Lys results in the loss of heparin binding property (Figure 5. 8). These results further support the premise that heparin binds to the Lys rich stretch of the helix-F of ovine α-1-PI. A similar distinct peptide peak was detected upon proteolysis of heparin bound human α-1-PI (results not shown).

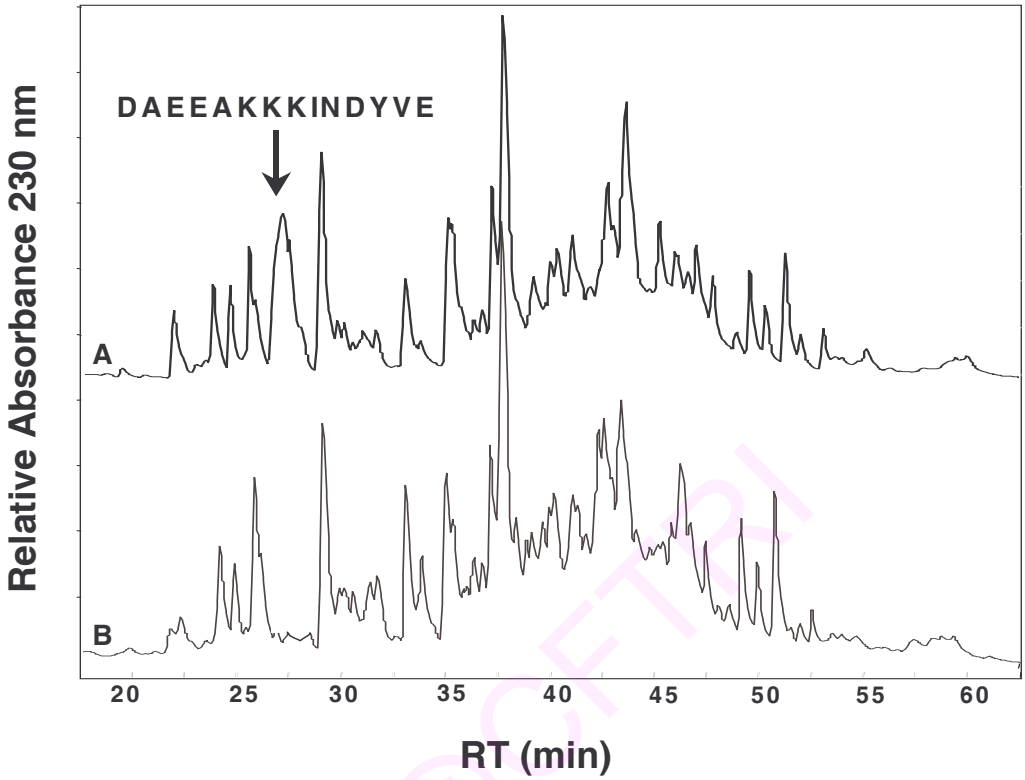

Figure 5. 9. RP-HPLC peptide maps of TPCK tryptic digest of α-1-PI. A. Ovine α-1-PI in the presence and B. in the absence of heparin. Total digests of α-1-PI digested with TPCK-trypsin in the presence of 1 μM of heparin and in the absence of heparin were chromatographed by RP-HPLC using a gradient of acetonitrile in 0.1 % TFA as described under section 2. 2. 23.

Molecular docking of heparin with α-1-PI

The prediction of ligand binding sites is an essential part of the protein ligand studies. The docking simulations aim to mimic the biochemical process of a ligand approaching the binding site of the receptor using computational methodologies. Computational modeling identified the binding site for heparin interaction with the F-helix of α-1-PI. The octasaccharide heparin was docked with human α-1-PI (PDB ID 1HP7). From the best ligand-binding pose of heparin to α-1-PI, the mean binding energy was calculated to be –2.40 kcal. mol $^{-1}$. As expected for well-minimized models, no bad contacts or clashes were observed.

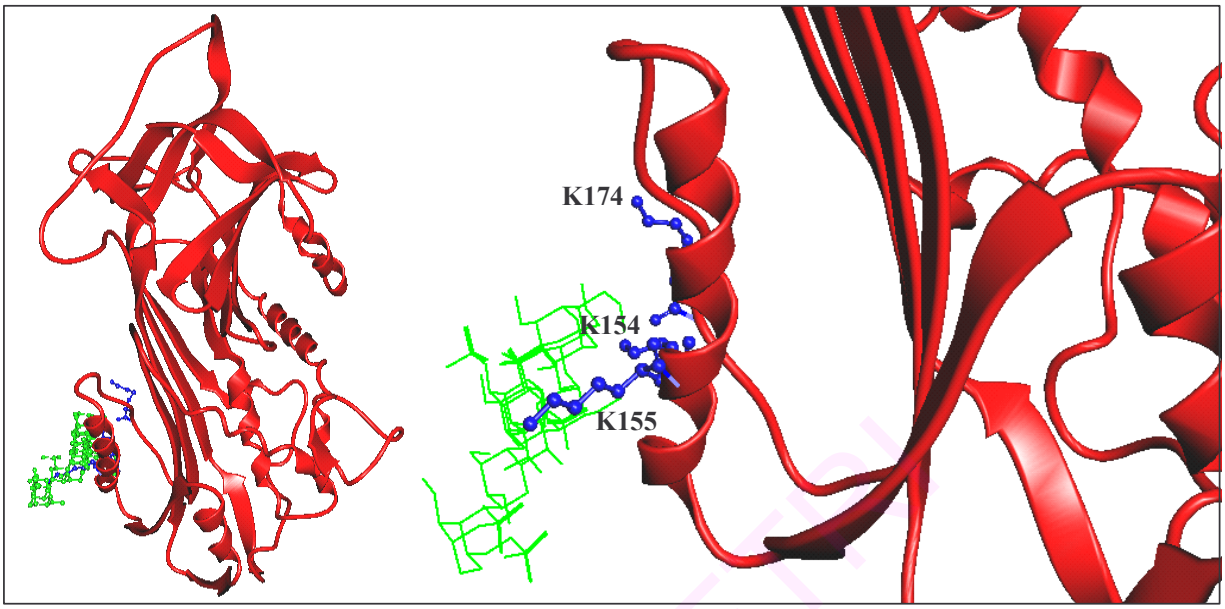

Figure 5. 10. Molecular docking of α-1-PI with heparin. Human α-1-PI (red ribbon) highlighting Lys^{154}, Lys^{155} at helix-F and adjoining Lys^{174} (blue ball and stick) with heparin octa-saccharide (green, wireframe). B. Enlarged view of human α-1-PI helix F-heparin interface.

An analysis of the heparin-α-1-PI complex reveals that heparin binds α-1-PI at the Lys rich domain located on the helix-F of the serpin. Heparin interacts with K^{154}-K^{155} segment (Figure 5. 10). A third Lys residue K^{174} of the positively charged domain also contributes to the electrostatic interaction between heparin and α-1-PI. The ε-amino side chain of K^{174} is present at a distance of 2.6 Å from the docked ligand heparin and interacts with it electrostatically. An enlarged view of the heparin interaction with the Lys residues present in the helix-F of α-1-PI and adjoining random coil are highlighted (Figure 5. 10). These results are commensurate with the identified heparin binding peptide sequence (Figure 5. 9).

Purification of mammalian α-1-PIs

The results on the involvement of the α-helix F in heparin binding to α-1-PI (Figure 5. 9 and 5. 10) and multiple sequence alignment data (Figure 5. 7) suggest that the binding of heparin should be similar in mammalian α-1-PIs.

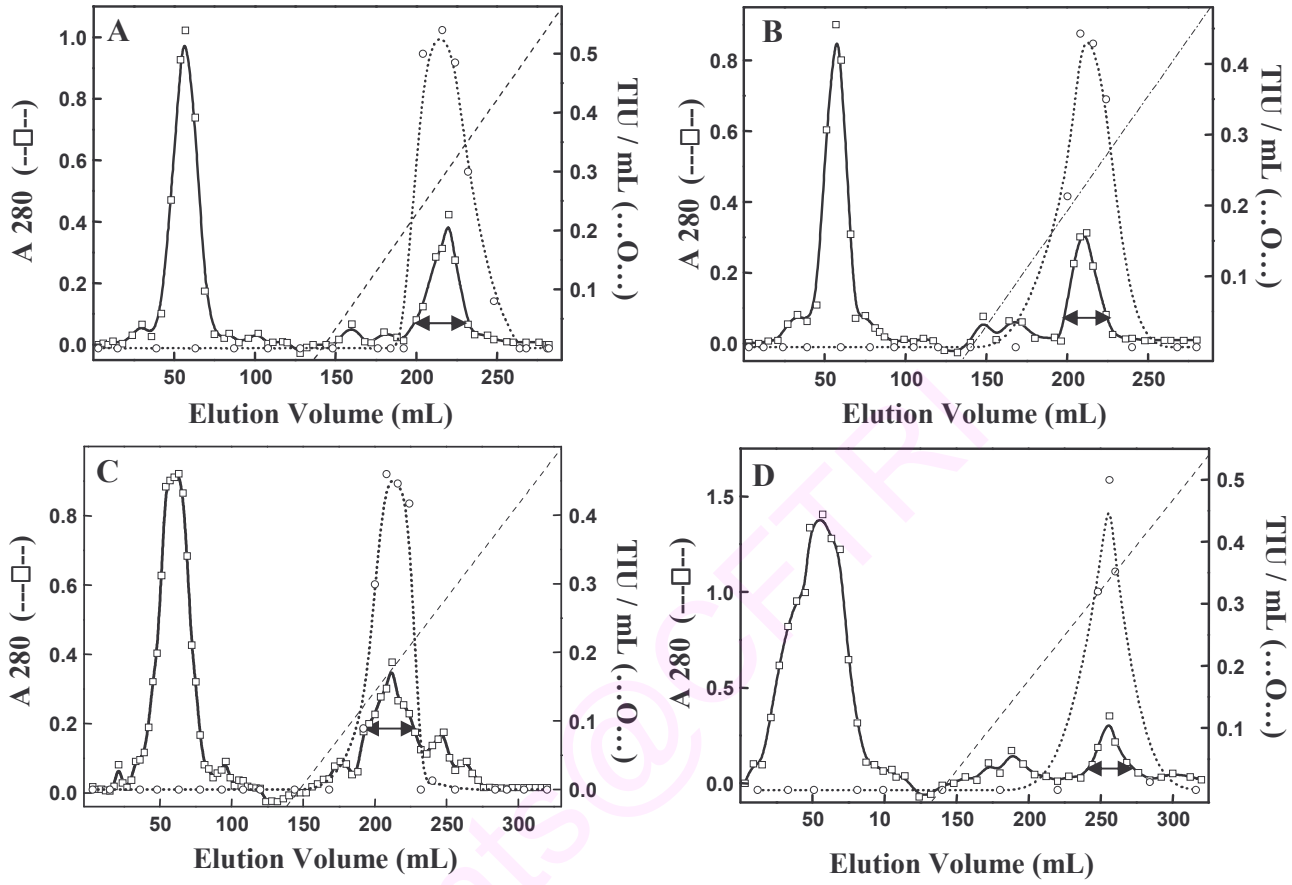

Figure 5. 11. Purification of α-1-PI using heparin-sepharose chromatography. A. Human. B. Rat C. Porcine and D. Ovine α-1-PI. The arrows represent the fractions pooled. Protein (—□—) and the protease inhibitory activity (--o--). pH gradient from 7.4 to 4.5 is represented by (---).

Therefore exploiting these observations, a universal affinity purification protocol for mammalian α-1-PIs using heparin sepharose chromatography was optimized. The purification of α-1-PI from human, rat, porcine and ovine serum was carried out using heparin sepharose affinity chromatographyThe results of the purification of the α-1-PIs are summarized in Table 5. 2. The precipitate obtained between 40-70 % $(NH_4)_2SO_4$ saturation of the human, rat, porcine and ovine serum exhibited maximum α-1-PI activity.

Table 5. 2. Summary of purification of α-1-PI from serum.

Step	Species	Activity (TIU/mL)	Protein (mg/ml)	Specific Activity (U/mg)	Fold Purification	Recovery (%)
Serum	Human	2805	55	51.0	-	100
	Rat	3640	65	56.0	-	100
	Ovine	4750	76	62.5	-	100
	Porcine	2335	68	34.3	-	100
40-70% $(NH_4)_2SO_4$	Human	7030.5	107.5	65.4	1.28	56.4
	Rat	8307.3	114.9	72.3	1.29	61.0
	Ovine	10160	129.6	78.3	1.25	64.1
	Porcine	8055.7	110.0	73.2	2.13	69.0
Heparin Sepharose Chromatography	Human	139.6	0.17	821.3	16.0	26.0
	Rat	127.0	0.15	845.5	15.0	17.5
	Ovine	278.0	0.30	926.6	14.8	19.6
	Porcine	157.6	0.25	630.4	18.3	13.5

*These values were reproduced in three separate purifications.

This fraction was applied to a heparin sepharose column equilibrated with 0.1 M Tris-HCl buffer, pH 8.2. As noted all the α-1-PIs bound to the heparin sepharose. The elution profile of the bound α-1-PIs are presented in Figure 5. 11. In this step a major unbound fraction of extraneous protein material eluted during the buffer wash, which exhibited no α-1-PI activity. The bound α-1-PIs in all the cases eluted as distinct symmetrical peaks on decreasing the pH of the elution buffer. The increase in specific activity of α-1-PI is almost similar in the sera of the different mammals studied. Specific activities of the α-1-PIs ranged from 600-925 U/mg. The fold purification achieved ranged from 15.0–18.0

with similar yields indicating that this purification protocol can be used for purification of all mammalian α-1-PIs. Human, rat and porcine α-1-PI eluted in the pH range 5.9 to 6.0 whereas desorption of ovine α-1-PI required a more acidic pH of 5.35 (Figure 5. 11). These results are indicative of a stronger affinity of ovine α-1-PI to heparin. This is not unexpected taking the precedence that the identified peptide of ovine α-1-PI contains three Lys residues (K^{154} to K^{156}) against two in human, rat and pig (K^{154} and K^{155}), resulting in a greater affinity to heparin-sepharose column (Figure 5. 7).

Criteria of homogeneity and molecular mass determination

The homogeneity of the purified α-1-PIs was assessed by native PAGE, RP-HPLC and amino-terminal sequencing. The purified inhibitors were analyzed by native-PAGE (10 % T, 2.7 % C) in Tris-glycine buffer pH 8.3 and located by inhibitor staining.

The purified inhibitor revealed a single band by specific inhibitor staining with APNE as well as protein staining (Figure 5. 12). The release of a single amino-terminal amino acid, for the native and denatured inhibitors indicates the inhibitors to be homogenous. All these studies advocate the homogeneity of the purified α-1-PIs. The apparent molecular masses of the purified human, rat, porcine and ovine α-1-PI by SDS-PAGE were 52,000, 54,000, 55,000 and 60,000±2000 Da respectively (Figure 5. 13). The purified α-1-PIs cross-reacted with the antibodies raised against human α-1-PI (Figure 5. 14) showing structural similarities. All these results suggest that this method could be used universally for the purification of mammalian α-1-PIs to homogeneity.

The exact molecular masses were also determined by MALDI-TOF and these were found to be 52766.509, 53699.884 and 58309.939±500 Da for human, rat and ovine α-1-PI respectively (Figure 5. 15). The molecular mass of porcine α-1-PI as determined by ESI-MS was 54865.03 Da. The amino terminal sequences of the purified α-1-PIs corresponded well with that reported for human (Long et al., 1984), rat (Chao et al., 1990), porcine (Archibald et al., 1996) and ovine (Gupta et al., 2008) α-1-PI respectively.

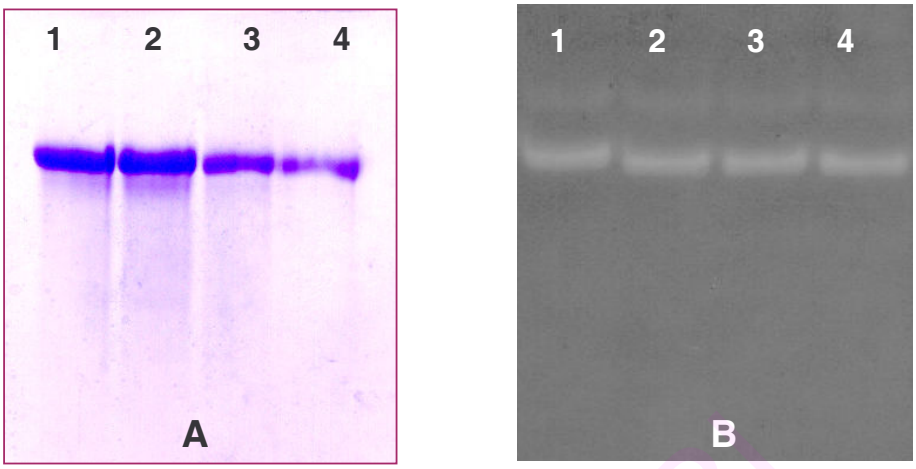

Figure 5. 12. Native PAGE (10 % T, 2.7 % C) of purified α-1-PIs. Lanes 1, 2, 3 and 4 represent ovine, porcine, rat and human α-1-PIs respectively. The gel was stained for A. Protein and B. APNE protease inhibitor staining.

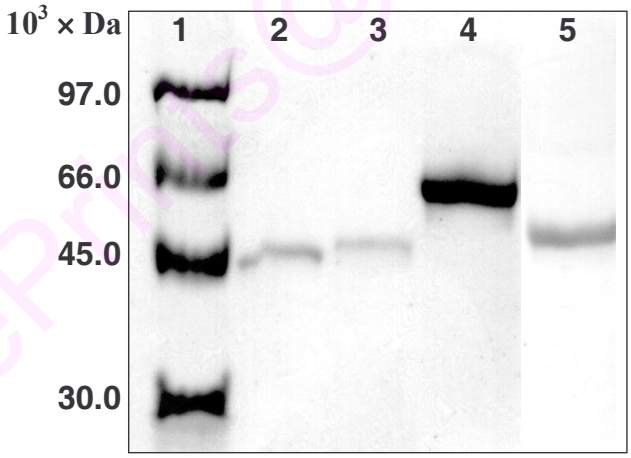

Figure 5. 13. A. Molecular weight determination of mammalian α-1-PIs. SDS-PAGE (10 % T, 2.7 % C). Lane 1: M_r markers, Lane 2: human, Lane 3: rat, Lane 4: ovine and Lane 5: porcine α-1-PI.

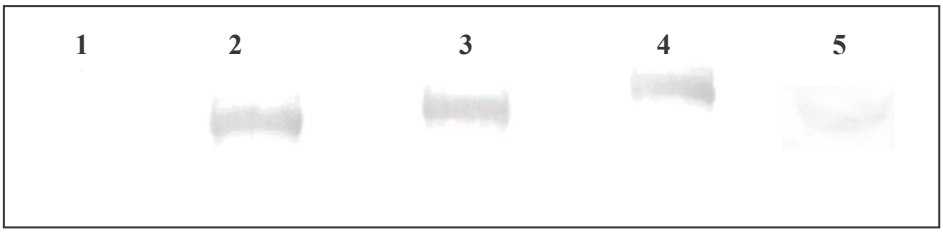

Figure 5. 14. Cross-reactivity of mammalian α-1-PIs against human α-1-PI antibodies raised in rabbit. Lane 1: bovine serum albumin, Lane 2: human, Lane 3: rat, Lane 4: ovine and Lane 5: porcine α-1-PI.

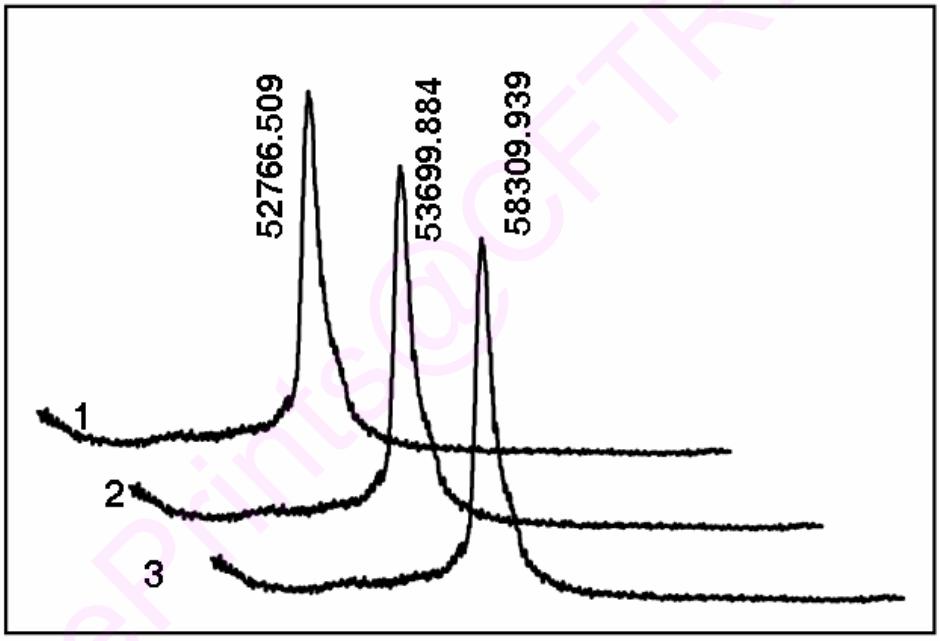

Figure 5. 15. MALDI-MS analysis of mammalian α-1-PIs. Exact M_r determination of the heparin-sepharose purified 1. human, 2. rat and 3. ovine α-1-PI.

pH stability

The effect of pH on the stability of human, rat, porcine and ovine α-1-PI was evaluated using various buffers as described in section 2. 2. 18. Measurement of protease inhibitory activity, post-incubation showed that α-1-PI is most stable at pH of 8.2 with a relatively high stability between 7.0 and 9.0, beyond which its stability decreased. Upon

incubation at pH 4.5, human, rat, porcine and ovine α-1-PI exhibited only 35, 69, 25 and 56 % of the maximal activity. At the extremes of pH α-1-PI lost activity rapidly (Figure 5. 16). The pH stability profile of the four mammalian inhibitors studied correlated well with each other. The purification protocol and protease inhibitory activity assays carried out at pH 8.2 are therefore compatible with the stability of the protein. This pH range also corresponds to the physiological pH of the mammalian systems.

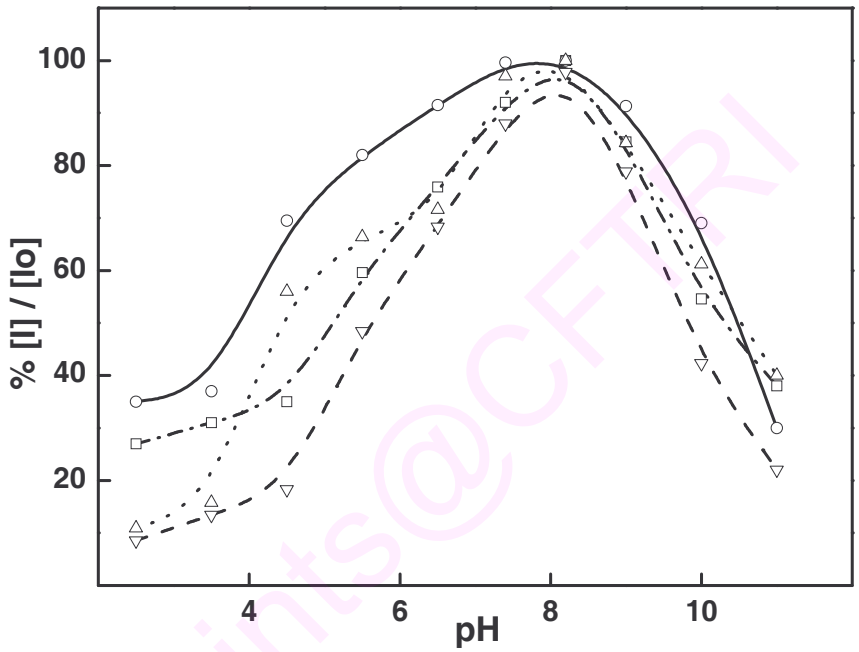

Figure 5. 16. pH stability profile of the purified mammalian α-1-PIs. Human (-□-), rat (-Δ-), ovine (-○-) and porcine (-∇-) α-1-PI. The purified α-1-PIs were incubated in various buffers (pH 2.5-11.0). Protease inhibitory activity assayed in 0.05 M Tris-HCl buffer pH 8.2 using BAPNA as described (Section 2. 2. 3. 2).

Discussion

Heparin is a highly sulfated negatively charged physiological macromolecule that binds diverse proteins including serpins and brings about significant changes with respect to structure and function. Many extracellular matrix proteins, lipases, lipoproteins, microbial proteins, proteases and protease inhibitors are known to bind heparin (Kjellen and Lindahl, 1991). There is a growing interest in the potential role of GAGs as activators in a number of physiological processes (Tersariol et al., 2002, Nader et al., 2004). The distinct accelerating effects of heparin on the inhibitory properties of α-1-PI

are described. The homogeneity and molecular mass of heparin was ascertained by mass spectroscopy (Figure 5. 1). Heparin activated ovine and human α-1-PI almost 45 and 38 fold respectively (Figure 5. 2). The initial screening experiments for α-1-PI binding to heparin showed retardation in the electrophoretic mobility of α-1-PI as a function of heparin concentration (Figure 5. 2B and C). This retarded mobility is attributed to the progressive binding of linearly extended polysaccharide to the inhibitor. Besides, α-1-PI shows a sigmoidal transition upon activation induced by heparin binding, indicative of allosteric modulation (Figure 5. 2A). The association rate constants of α-1-PI with elastase in the presence of heparin were found to be significantly enhanced compared to the native forms (Table 5. 1), although the degree of activation is poorer when weighed against antithrombin-thrombin, antithrombin-factor Xa and HC II-thrombin interactions (Table 5. 1). Fluorimetric titrations with heparin showed that one mole of heparin binds per mole of α-1-PI with a binding constant of $7\pm0.2 \times 10^{-7}$ M at lower concentrations. However, as the heparin concentration is increased a weaker interaction with a binding constant of $2.09\pm2 \times 10^{-6}$ M was observed. Thus heparin binding to α-1-PI follows a two-step binding pattern, an initial high affinity binding followed by a weaker binding. The initial high affinity step probably results in a conformational change which then leads to a ~ 30 fold decrease in the affinity of binding. It is possible that the high affinity binding causes the conformational change required for initial activation and the activation is completed with the binding to a second weaker affinity site on α-1-PI. In AT an initial low affinity binding is followed by a conformational change with a 300 fold increase in binding affinity, accompanied by an increased vulnerability of the RCL to proteolytic processing (Kress and Catanese, 1981; Olson et al., 1992).

Heparin is known to activate AT through an allosteric mechanism and provide a template or bridge on which AT and thrombin interact (Olson and Chuang, 2002). The crystal structure of the AT-thrombin-heparin mimetic ternary complex at a resolution of 2.5 Å confirmed this template mechanism (Li et al., 2004). Heparin is reported to depress the rate constant for the inhibition of neutrophil elastase by α-1-PI (Frommherz et al., 1991). Recently, Spencer et al., (2006) demonstrated that the critical chain length of 12-14 saccharides is required for the onset of neutrophil elastase inhibition after which inhibitory activity increases with chain length. This is in agreement with our observation

that the heparin octasaccharide has no effect on PPE activity. Heparin binding proteins categorically possess a positively charged site at their surface that form regions of high positive charge density and form electrostatic interactions with the acidic groups of heparin (Shirk et al., 1994). Binding is presumed to be mediated by ionic interactions between the sulfate and carboxylate groups of heparin and positively charged side chains of these proteins (Blinder and Tollefsen, 1990). To investigate the importance of other GAGs, we tested the effect of dermatan sulfate and chondroitin sulfate which have only one sulfate group per disaccharide unit as well as that of hyaluronic acid which lacks sulfate groups, and it was observed that none of these had any effect on the rate or inhibition pattern of α-1-PI. An analysis of the heparin binding residues of AT, heparin cofactor II, protease nexin, plasminogen activator inhibitor-1 (PAI-1), protein C-inhibitor, kallistatin and pigment epithelium derived factor (PEDF) indicates that heparin binding residues are those with basic side chains viz. Arg or Lys. Identification of hypothetical ligand binding domains can be achieved through a multiple alignment of amino acid sequences *in silico* to identify conserved residues and by superimposition of 3D structures of family members to identify the conserved signatures of conformations and motifs. The topology search for a positively charged domain on α-1-PI indicates four positive sites on the surface comprising of K^{135}-K^{136} on helix E, K^{233}-K^{234} on the coil immediately succeeding helix F and K^{154}-K^{155}- K^{174} site comprised jointly by helix F and adjoining random coil, and R^{281}-R^{282} on a β-sheet. α -1-PI belongs to a superfamily of serpins and depicts a high degree of sequence and structural homology to AT, antiplasmin and non-inhibitory serpin ovalbumin and a considerable carbohydrate sequence homology (Carrell et al., 1994). It depicts considerable homology towards other heparin binding serpins as well.

K^{125} and K^{133} that are implicated in AT heparin interaction (Carrell, 1999) are conserved in α-1-PIs across the cross-section of mammals. Another basic side-chain residue R^{129} (Yamasaki et al., 2002) that is also implicated in facilitating heparin binding to AT is found replaced by a positively charged Lys in α-1-PI. (Figure 5. 6). Albeit, there are other prominent differences in α-1-PI and antithrombin structures. A comparison of the topology of AT and α-1-PI for the location of the conserved K^{125}, R^{129}, and K^{133} revealed that whereas these three residues constitute a single protruding positive cluster

in AT, same is not the case with α-1-PI, where these three residues are spatially separated (Figure 5. 6B), and hence would constitute a frail site for any electrostatic cooperative interaction. This advocates a potentially different site for heparin binding with α-1-PI compared to AT. However, an additional highly positively charged cluster comprised of K^{154}-K^{155}- K^{174} is observed in α-1-PI (Figure 5. 6B). That Lys residues are responsible for the interaction of α-1-PI and heparin was further ascertained by chemical modification studies. Arg modified α-1-PI showed the same elution pattern as that of unmodified α -1-PI while the Lys modified α-1-PI did not bind to heparin-sepharose (Figure 5. 8). These chemical modification experiments followed by heparin-sepharose binding studies conclusively point towards the role of Lys in heparin α-1-PI interaction. The role of the lysyl rich domain on helix-F was conclusively established by isolating and sequencing the peptide. This was accomplished by digesting heparin- α-1-PI complex with TPCK-trypsin and comparing it with a control α-1-PI digest (Figure 5. 9). Heparin evidently protects K^{154}, K^{155} and K^{156} from accessibility to tryptic cleavage allowing for the identification of the lysyl residues masked by the bound heparin (Figure 5. 9). Amino-terminal sequencing of this discrete peak arising at 27.3 min indicates it to be the heparin binding Lys rich site at helix-F. An *in silico* molecular docking approach was used to identify the heparin binding exosite for α-1-PI. The minimum energy docking site for the heparin octasaccharide was observed to be the protruded Lys rich site at helix-F (Figure 5. 6B). Prediction of the molecular docking at the most positively charged cluster constituted by K^{154}, K^{155} and K^{174} comprised jointly of helix F and the adjoining random coil (Figure 5. 10) is further supported by the peptide sequence. This domain is specific for α-1-PI and is highly conserved across a range of species examined (Figure 5. 7). The spatial considerations which approximate the three positively charged Lys (K^{154}, K^{155} and K^{174} of human α-1-PI), their invariance and the loss of heparin binding property on modification with citraconic anhydride can be used to argue that the lysines are involved in ionic interactions to the heparin (Figure 5. 10). All the α-helices of human α-1-PI except helix-F lie on the backside of the protein. Helix-F lies across the front of β-sheet A and appears to play a prominent role in controlling the opening of the sheet or in stabilizing the five-strand conformation (Yamasaki et al., 2002). Several ligands bound to α-helix F, modulate the serpin reaction through stabilization of transient intermediates

(Komissarov et al., 2007). The root of the RCL is partially inserted into the center of the A sheet (Whisstock et al., 2000). The opening of the sheet and further exposure of RCL renders it a more potent inhibitor with a conformation that is more apposite for interaction with the target protease (Quinsey et al., 2004). The serpins are unique when compared to other serine protease inhibitors in that the reactive site is contained on a mobile peptide loop with the flexibility necessary for complex formation. This mobility is responsible for the modulation of activity necessary for the optimal locked conformation that stabilizes the final serpin-protease complex (Carrell et al., 1994). The data presented here show that the heparin binding site is centered on a conserved row of basic residues in helix-F extending to the adjacent random coil (Figure 5. 6B and 5. 7). As in the case with AT, it is plausible that the flexible RCL of α-1-PI is converted from the initial quiescent form to the more exposed conformation. It is not unreasonable to assume that activation to this optimal conformation is accelerated by heparin binding, which helps stabilize the α-1-PI-protease complex. This premise is supported by the observed loss of ordered structure and shift to increased random structure upon heparin binding (Section 6, Results and Discussion). Coupled with this is the observation that physiologically it is the heparin rich sites, the lungs and the mast cells, which show maximum α-1-PI activity. Therefore, it is not unreasonable to assume that this activation (Figure 5. 2A) is functionally relevant. α-1-PI counters the effect of redundant protease activity, be it endogenous e.g., neutrophil elastase or exogenous from pathogenic microorganisms during inflammatory response. Collectively, these findings imply that α-1-PI has a major role in regulating extra cellular protease activity, and the physiological activator is heparin.

The validity of the heparin α-1-PI interaction model was evaluated experimentally by developing a single step purification protocol in which heparin-sepharose was used to purify α-1-PI from mammalian serum to homogeneity. A 13-26 % recovery of the original protease inhibitory was achieved with a 14-18-fold purification. The specific activity of the purified protein ranged from 630 to 930 TIU/mg, which is convincingly large for any single step purification protocol. Ovine α-1-PI, which possesses a more positively charged domain due to the presence of an additional Lys^{156} residue (Figure 5. 7), binds more avidly to heparin-sepharose compared to human, rat and porcine α-1-PI

(Figure 5. 11), as evident from the elution pattern. Ovine α-1-PI elutes at a more acidic pH compared to rat, human and porcine α-1-PI (Figure 5. 11D). The pH stability studies of human, rat, porcine and ovine α-1-PI were undertaken to analyze the effect of different pH on α-1-PI especially during pH gradient elution (Figure 5. 16). The results reveal that the protein inhibitor is most stable and active at pH 7.4 to 8.2, and therefore, functionally active α-1-PI can be purified and used for augmentation therapy. These results show that the purified α-1-PIs from sheep, rat and pig sera are analogous to human α-1-PI in terms of M_r, inhibition of trypsin and porcine elastase and pH stability (Figure 5. 12, 5. 13 and 5. 16). The exact molecular masses of the four α-1-PIs studied vary between 52,700 to 58,300 as determined by MALDI-TOF (Figure 5. 15). All these results establish that the functional and structural characteristics of mammalian α-1-PIs are similar. The cross-reactivity of the α-1-PIs towards human α-1-PI antibodies raised in rabbit (Figure 5. 14) also shows structural similarities. Thus, α-1-PI is another protein which can be added to the list of already established heparin binding proteins The heparin binding site in α-1-PI is localized not to the D-helix as in AT and HC-II, but to the F-helix region. Although the identified heparin-binding site of ovine α-1-PI may not be surprising considering that it is the most likely anionic binding site consisting of a positively charged cluster, the site is clearly different from that reported for the serpin AT. This region has a sequence of basic lysine residues consistent with the general heparin-binding consensus sequence motif [X-B-B-(B)-X], where B is any residue with basic side chain (Cardin and Weintraub, 1989). Heparin binds to helix D and at the N-terminal of antithrombin and activates it by an order of 10^3. It also binds PAI-1 at the D-helix. The helices D, E and NH_2-terminal stretch play significant roles in case of PEDF. However, the heparin-binding site is located in helix H and NH_2-terminal (A-helix) in case of protein C-inhibitor and kallistatin. A variety of heparin (anion) binding exosites are observed in case of proteases like nexin, thrombin, trypsin, chymotrypsin, elastase and other proteins. Similarly Tjong et al., (2007) also demonstrated that the interaction between heparin sulfate and cobra cardiotoxin depends more on the overall charge cluster organization rather than on their fine structures. Their NMR and molecular docking studies indicate that heparin derived mimetics with different chain length can bind at the same cardiotoxin site surrounding the rigid core region tightened by disulfide bonds. This indicates that the heparin binding

sites are positioned differently in different proteins. Further, the mode of binding and resultant structural and conformational changes, whether similar to AT needs to be established. Further structural studies are required to fully understand the interactions of α-1-PI with heparin and conformational changes which modulate its activity.

This combinatorial approach of multiple sequence alignment, chemical modifications, tryptic peptide mapping and molecular modeling has helped to increase our understanding of the interactions of the model complex of heparin-α-1-PI. The usefulness of modeling in the interpretation of the action of ligands/GAGs for enhancing the activity of clinically useful proteins/serpins is demonstrated. The clear definition of the binding site provides a structural basis for developing heparin analogues that are more specific towards their intended target α-1-PI and therefore less likely to exhibit side effects.

RESULTS AND DISCUSSION

6. Structural Insights into the Heparin Induced Conformational Changes of α-1-Proteinase Inhibitor

Conformational transition is fundamental to the mechanism of functional regulation in proteins and serpins can provide insights into this process. To attribute the physiological activation of α-1-PI by catalytic amounts of heparin octasaccharide requires the information about structural re-orientations of the molecule. Ovine α-1-PI as a model representative molecule was studied for its interactions with heparin to understand and correlate the structure function relationships. The changes in hydrodynamic radius, binding constants and stoichiometry of binding were elucidated using dynamic light scattering, size-exclusion chromatography, equilibrium dialysis studies and fluorescence titrations. Estimation and quantification of ovine α-1-PI secondary structural parameters using CD and FTIR spectroscopy are also presented and discussed in this section.

RESULTS

Stokes' radius determinations

Many of the questions related to biological macromolecules are connected with the shapes of molecules and how they interact with each other. The aim of this study is to expound how interaction can be used to provide information about molecular structure and dimensions and about interactions between molecules. Size exclusion chromatography and dynamic light scattering (DLS) were performed to determine the change in compactness of ovine α-1-PI upon binding to heparin.

i) Size-exclusion chromatography

Size-exclusion chromatography has been used to detect conformational changes in several proteins as a function of shift in Stokes' radii of the proteins (Brems et al., 1985). Size exclusion chromatography and DLS were performed to determine the change in the hydrodynamic radius of ovine α-1-PI molecule upon interaction with heparin. The Stokes' radius of native and heparin complexed α-1-PI were determined by the method of Uversky (1993). A set of proteins of known molecular masses and Stokes' radii (R_S) were used to construct the calibration curve. The effect of different heparin concentrations on the molecular dimensions of ovine α-1-PI evaluated by size-exclusion chromatography is shown in Figure 6. 1. Native α-1-PI eluted as a single symmetrical

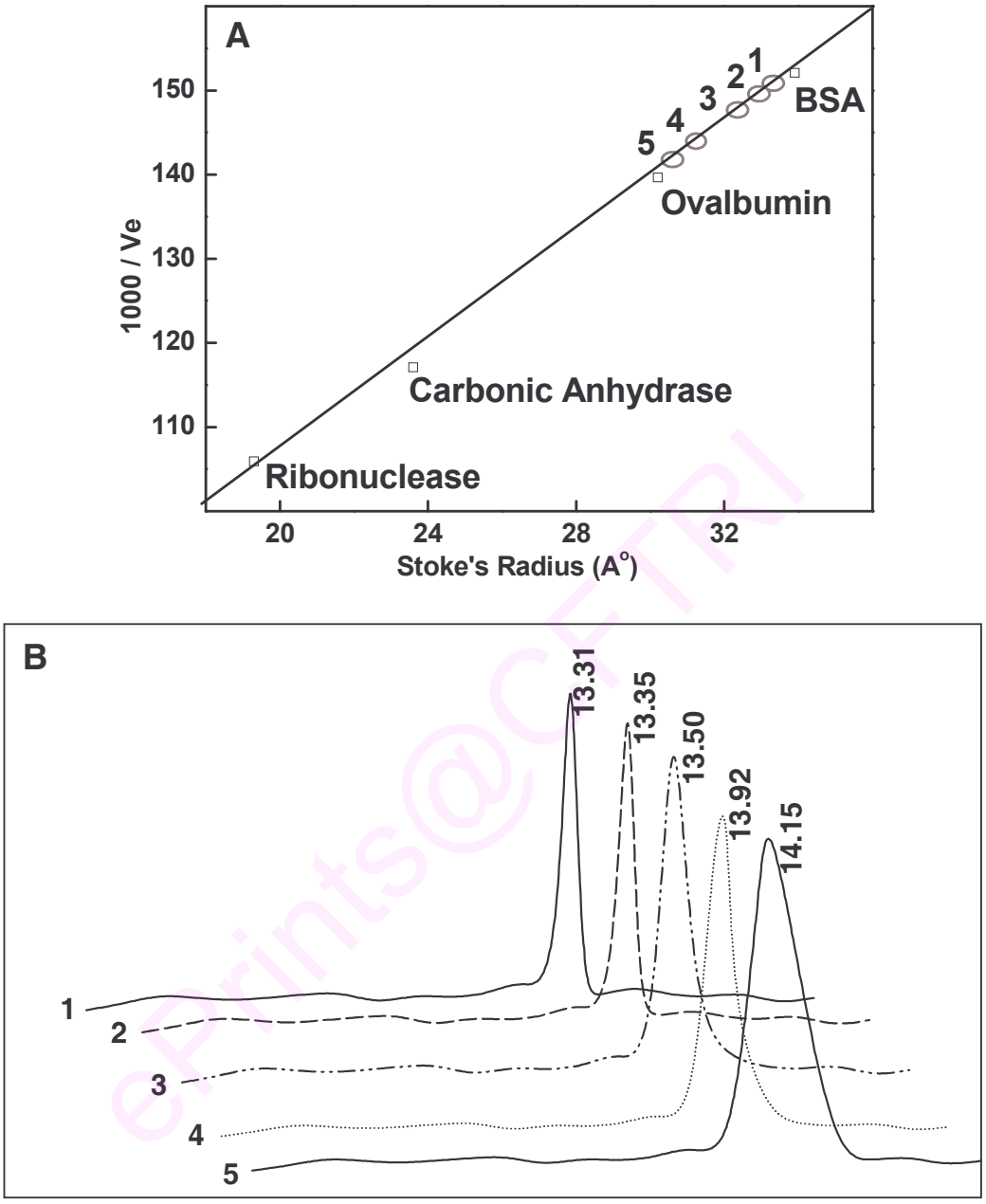

Figure 6. 1. Determination of Stokes' radius of ovine α-1-PI by size-exclusion chromatography. A. Calibration curve for Stokes' radius constructed using ribonuclease (19.3 Å), carbonic anhydrase (23.6 Å), ovalbumin (30.2 Å) and BSA (33.9 Å). 1 (33.5 Å), 2 (33.3 Å), 3 (32.8 Å), 4 (31.4 Å) and 5 (30.7 Å) represent ovine α-1-PI pre-incubated with 0, 1, 2, 5 and 10 μM of heparin respectively in 0.1 M Tris-HCl buffer, pH 7.4. B. Size exclusion chromatography elution profile of α-1-PI activated with heparin showing an increase in R_T with increase in heparin concentration.

peak with a retention time of 13.31 min. In contrast, the heparin activated forms eluted much later (Figure 6. 1B). This increase in the retention time of the heparin complexed α-1-PIs as compared with native α-1-PI could be due to formation of a more compact conformation and a decline in the Stokes' radius. The hydrodynamic radius for native ovine α-1-PI was calculated to be 33.5 ±0.5 Å which decreased to 30.7±0.5 Å in the presence of 10 μM of heparin (Figure 6. 1A).

ii) **Dynamic light scattering (DLS)**

DLS is based on the auto-correlation of the time dependent fluctuations of scattered light intensity, which in turn depends upon the diffusion constant. DLS experiments were performed to further evaluate this compactness of α-1-PI in the presence of heparin.

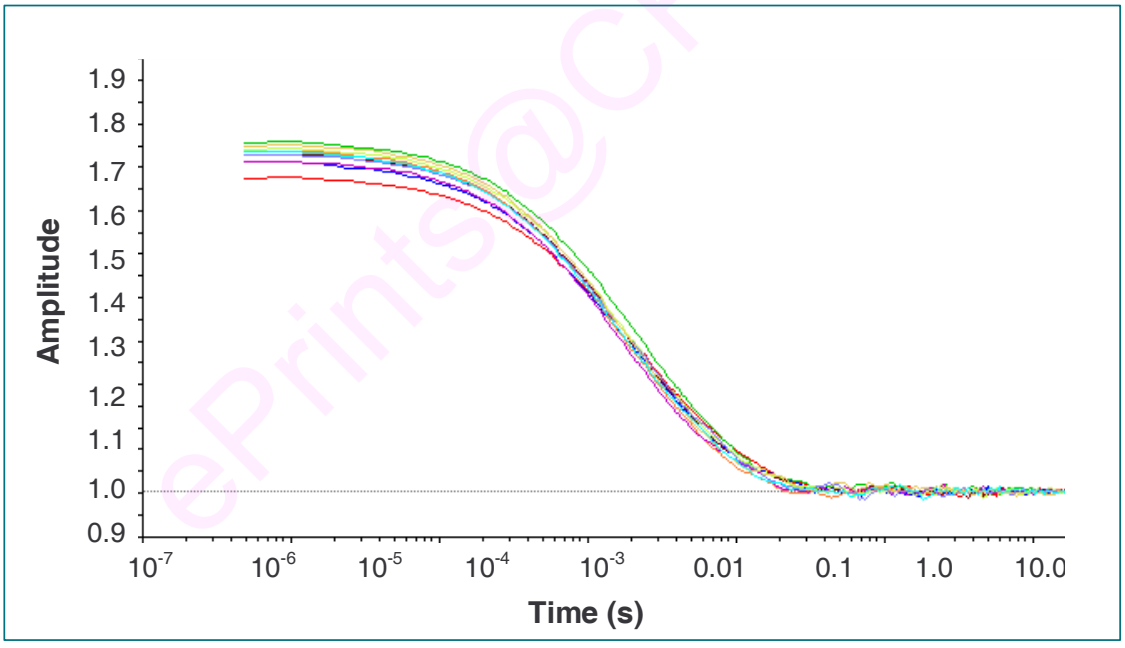

Figure 6. 2. Dependence of the light scattering intensity on time. The curves were obtained upon incubation of ovine α-1-PI (1 mg/mL in 0.1 M sodium phosphate buffer, pH 7.4 containing 0.9 % NaCl) with 0.5 μM heparin.

R_S measured by DLS experiments revealed a similar decreasing trend (Figure 6. 2 and 6. 3) consistent with the information obtained from size exclusion chromatography. A steep decline in R_S of α-1-PI was observed between 0.2 and 4 μM of heparin concentrations beyond which it appeared to remain constant (Figure 6. 3). The observed decrease in R_S establishes a more compact conformation induced when linear charged oligosaccahride chains of heparin bind to α-1-PI.

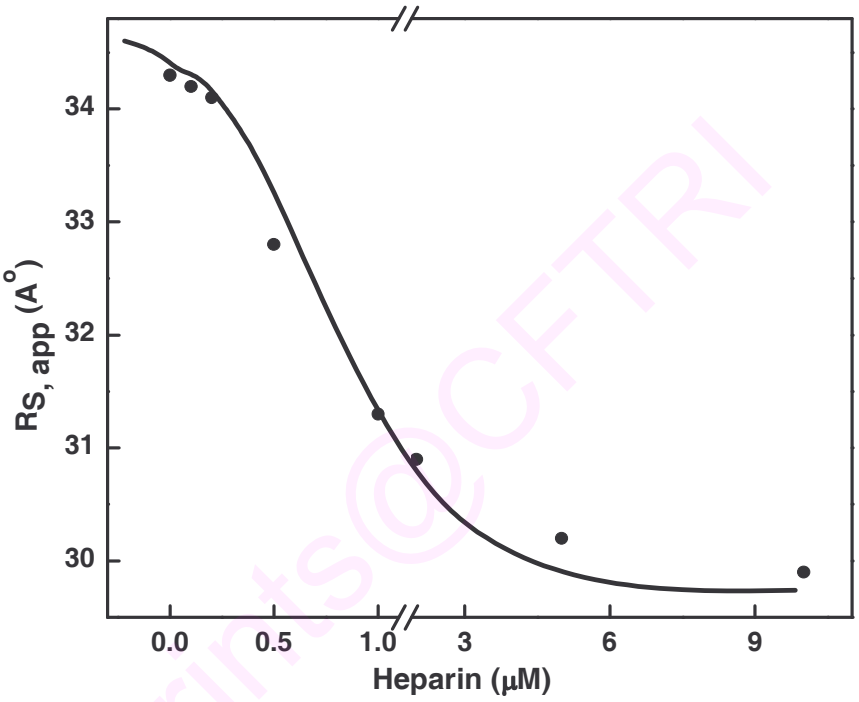

Figure 6. 3. Effect of heparin concentration on the apparent Stokes' radii of ovine α-1-PI. Measurements of ovine α-1-PI (1 μM) Stokes' radii were performed in heparin (0-10 μM) at perpendicular scattering angle.

Light scattering experiments were performed at 325 and 360 nm to ascertain whether the R_S changes by heparin were due to aggregation or not. The light scattering measurements revealed a slight decrease in the absorbance as the heparin concentration increased (Figure 6. 4) suggesting that the activation and observed structural changes were not due to aggregation. Besides, aggregation or precipitation would have resulted in large increase in hydrodynamic radii unlike a decrease in hydrodynamic radii observed upon heparin binding.

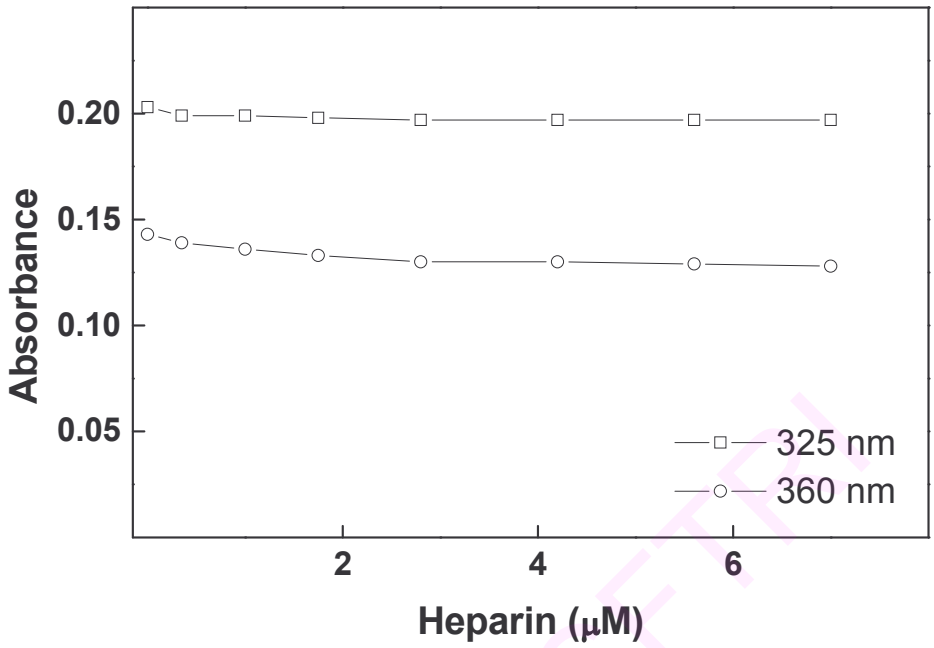

Figure 6. 4. Light scattering measurements of ovine α-1-PI with various heparin concentrations at 325 and 360 nm.

Equilibrium dialysis

The heparin binding constant for α-1-PI was determined by incubating various concentrations of heparin with α-1-PI (10 μM) for 24 h at 4 ºC for equilibrium dialysis. To obtain the number of heparin binding sites, saturation of these sites on α-1-PI is required. The number of heparin molecules bound per mole of protein (ν) is plotted against free heparin concentrations [L]. Saturation of ovine α-1-PI was observed at 15 μM heparin (Figure 6. 5A). Scatchard plot of the above data shows only one high affinity binding site for heparin. The binding constant determined from the slope of the regression line by least square analysis of the Scatchard plot is $2.1 \pm 0.2 \times 10^{-6}$ M (Figure 6. 5B).

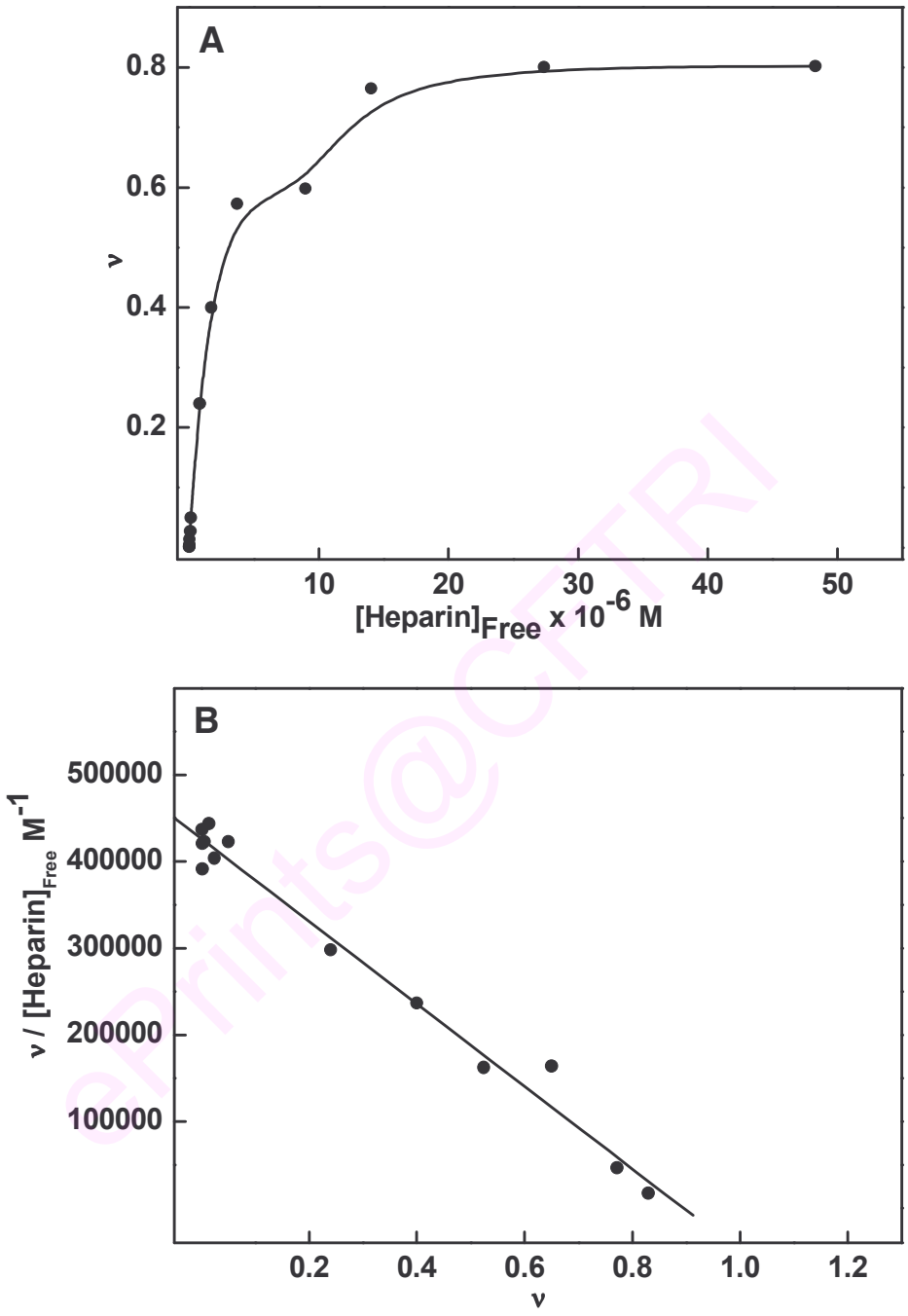

Figure 6. 5. Binding studies of ovine α-1-PI with heparin using equilibrium dialysis. A. Langmuir isotherm for determining binding constant (K_α) of heparin-α-1-PI interaction. A plot of ν (moles of heparin bound to α-1-PI) vs [L] free heparin concentration. B. Scatchard plot showing the relationship between ν/[L] vs ν.

Intrinsic fluorescence studies

In order to characterize the α-1-PI conformational change, further we have utilized fluorescence spectroscopy, which is an extremely sensitive technique that can be used to follow both protein folding and binding events.

The fluorescence spectra of native and activated ovine α-1-PI were measured in a Shimadzu (Model RF-5000) spectrofluorimeter. Intrinsic fluorescence was used to probe the perturbation in protein structure and conformation. Fluorescence emission was measured upon excitation at 282 nm, to follow the emission both from Tyr and Trp residues and at 295 nm to follow the changes in the microenvironment of the Trp residues. α-1-PI was incubated for 15 min in the presence of various concentrations of heparin. The florescence spectrum of ovine α-1-PI shows emission maxima at 336 nm suggesting that the Trp residues are buried in a predominantly hydrophobic milieu shielded from the solvent. The emission spectra of native and heparin activated α-1-PI was measured between 300-500 nm (Figure 6. 6A). The change in the fluorescence intensity was observed without any shift in the wavelength maxima. Figure 6. 6A shows a relative quenching of fluorescence intensity. The decrease in the fluorescence induced by heparin enabled us to titrate α-1-PI with heparin. The fluorescence intensity decreased gradually upto ~ 3 μM beyond which marginal or no further decrease occurred. Heparin induced quenching does not lead to any changes in band shape or the emission wavelength (Figure 6. 6A). The shape of the titration curve was hyperbolic (Figure 6. 6B). A maximum quench of 45±2 % has been observed at 5 μM of heparin, representing 79 % completion of the reaction as deduced from the double reciprocal plot (Figure 6. 6C). . On the assumption that heparin has 'n' independent binding sites on ovine α-1-PI, the binding constant and 'n' were obtained from the non-linear regression curve. The dissociation constant (K_D) for the α-1-PI-heparin complex has been estimated to be 4.7±1 $\times 10^{-6}$ M.

The number of binding sites was calculated from the Scatchard analysis (Figure 6. 7A) to be 1.1±0.2: 1 at lower concentrations of heparin. The binding mode was more complex and non-specific at concentration beyond 1.8±0.2 μM of heparin (Figure 6. 7A).

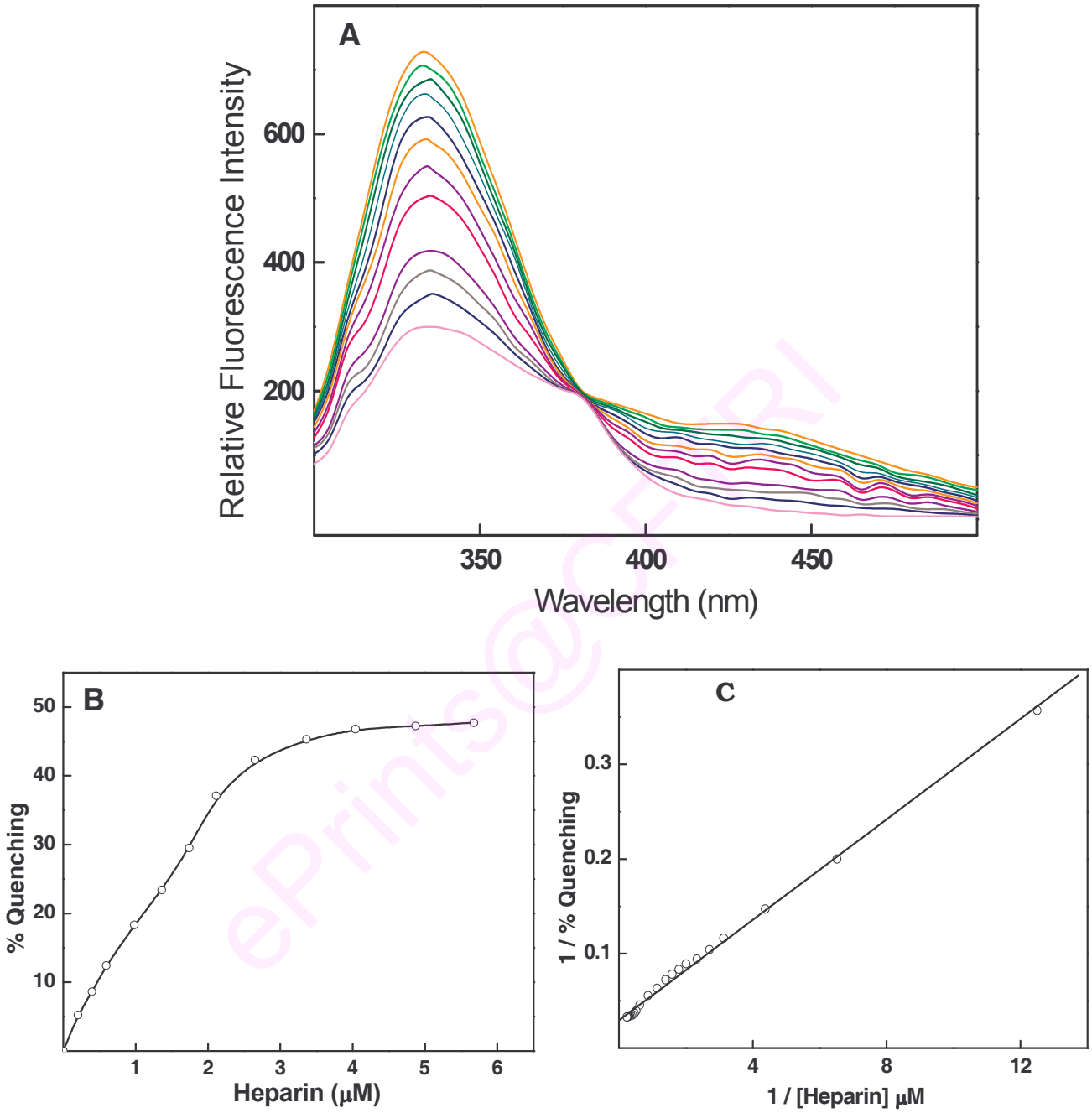

Figure 6. 6. Fluorescence titrations of ovine α-1-PI with heparin. A. Emission spectra of α-1-PI in the presence of 0, 0.2, 0.4, 0.6, 1, 1.5, 2, 2.5, 3, 4 and 5 μM heparin from top to bottom. B. A simplified plot quantifying the extent of heparin induced quenching. C. Double reciprocal plot of this data.

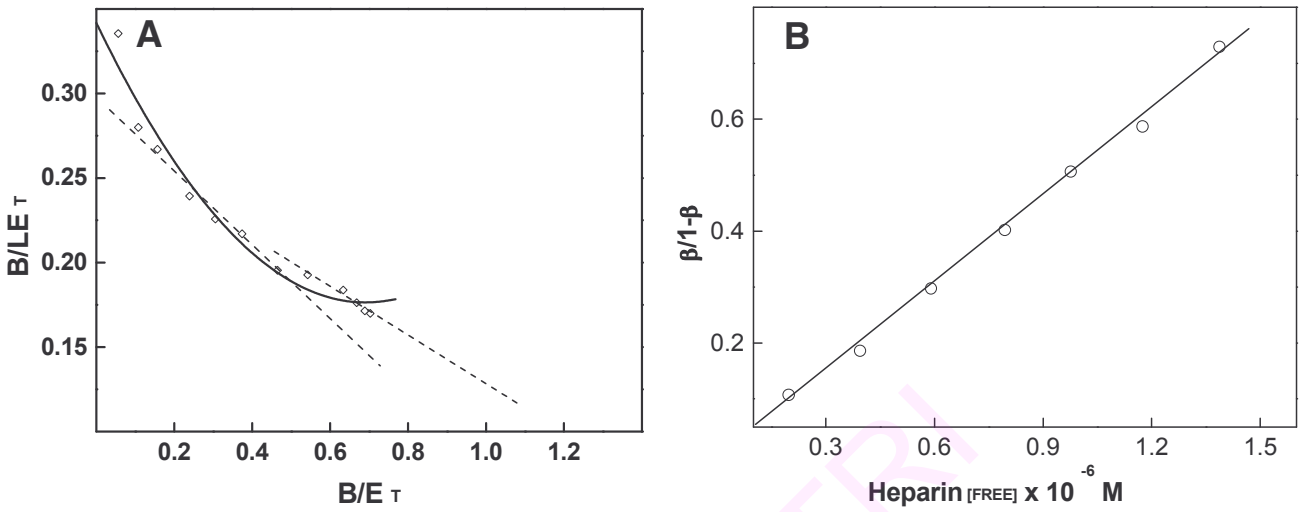

Figure 6. 7. Secondary plots of heparin induced fluorescence quenching data of ovine α-1-PI. A. Scatchard plot of the heparin binding to α-1-PI at pH 7.4, determined by fluorescence titrations. B. Mass action plot of the quenching data to calculate binding constant (K_α) for heparin binding (Lee et al., 1975) (described under section 2.2.30.3.)

At low heparin concentration the binding constant (K_α) for ovine α-1-PI was 1.98±0.2 × 10^{-6} M (Figure 6. 7B), very similar to that of human α-1-PI (Figure 5. 5 of earlier section).

These results provide strong evidence for a conformational change, which probably occurs during the initial binding and activation by heparin. Further binding of heparin beyond that required for maximum activity (6±1 μM) (discussed in earlier section) brings to halt the symmetrical quenching of the fluorescence and reflect gross conformational changes, which could be due to inactivation (Figure 6. 6). The fluorescence data was consistent with a view that the heparin activated forms assume similar conformations but are different from that of the native forms.

Acrylamide quenching of heparin activation

The topographical studies with proteins are carried out by solvent perturbation, chemical modification and quenching of fluorescence by the addition of very low

molecular weight reagents like potassium iodide, oxygen and acrylamide. Tryptophan fluorescence is a good measure of the extent of exposure of these residues to the solvent. The quencher decreases the fluorescence intensity of the excited indole ring. Acrylamide is an excellent uncharged quenching probe that is very sensitive to the exposure of Trp residues in proteins. Collisional quenching experiments with acrylamide were performed to assess the accessibility of tryptophan residues in the heparin activated forms of α-1-PI and corresponding Stern-Volmer constants (K_{sv}) were calculated. Stern-Volmer plots for heparin activated ovine and human α-1-PI showed increasing slopes with increasing heparin concentrations, suggesting that the Trp in the activated forms were more accessible (Figure 6. 8B and 6. 9B).

Table 6. 1. Stern-Volmer constants of ovine and human α-1-PI.

Heparin (μM)	$K_s \times 10^{-3}$ M	
	Human	Ovine
0.00	3.76±0.4	3.25±0.4
0.50	4.17±0.2	3.60±0.2
1.00	4.59±0.3	3.67±0.3
2.00	5.32±0.4	5.10±0.4
5.00	6.67±0.5	5.23±0.5

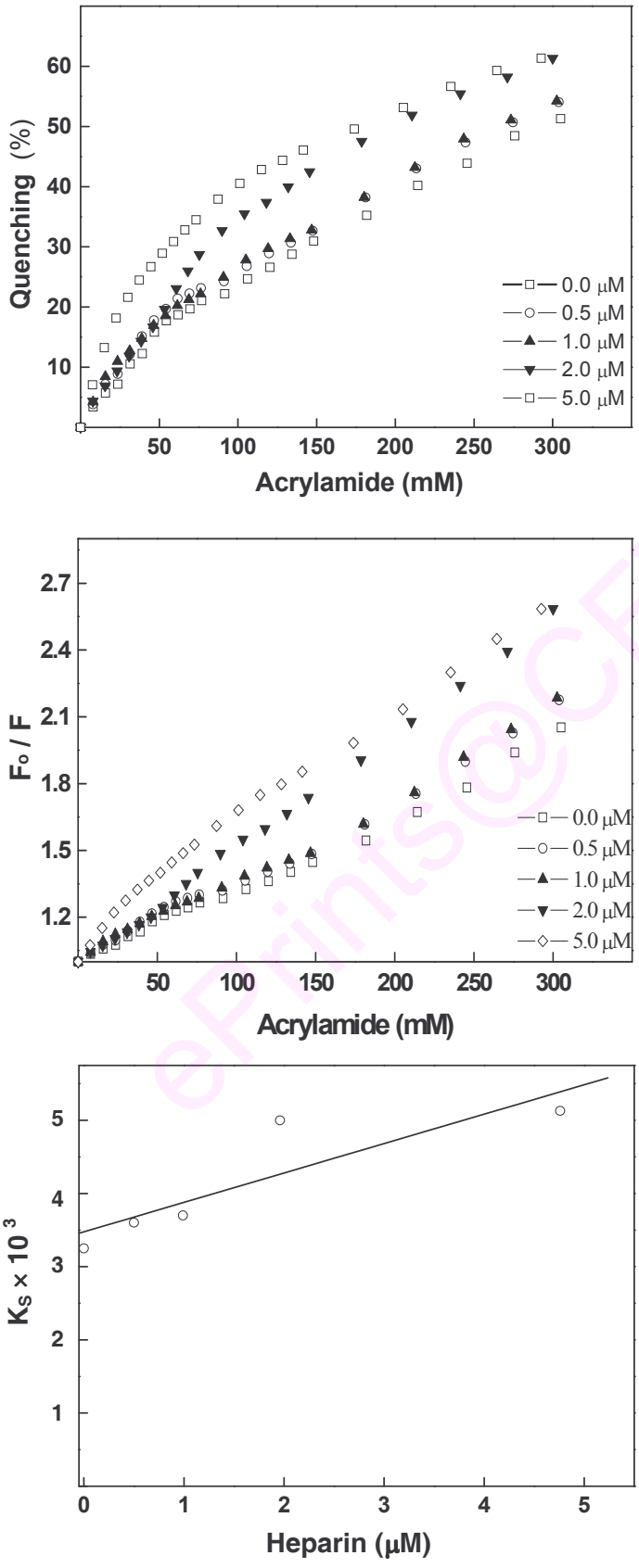

Figure 6. 8. Acrylamide quenching of ovine α-1-PI. A. Percentage quenching of α-1-PI in 50 mM Tris-HCl buffer pH 7.4 containing varying concentration of heparin B. Stern-Volmer plot C. Modified Stern-Volmer plot with varying concentrations of heparin.

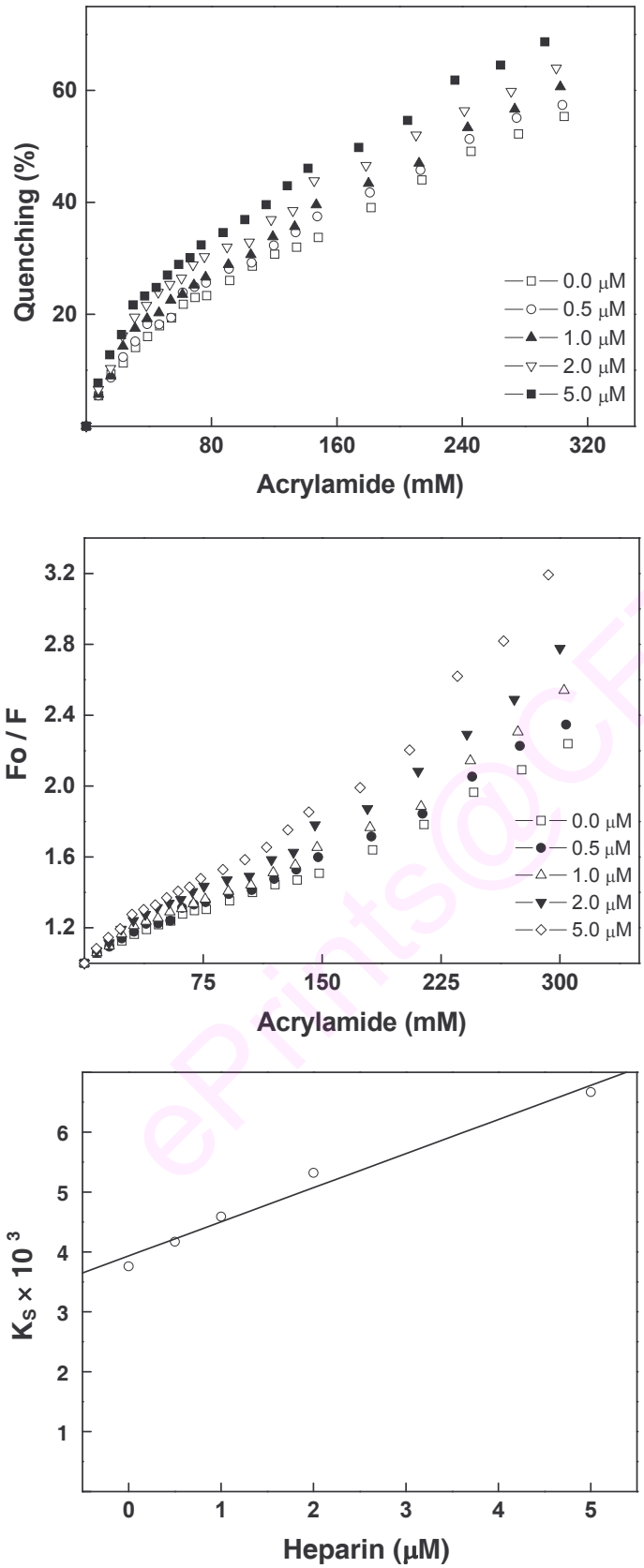

Figure 6. 9. Acrylamide quenching of human α-1-PI. A. Percentage quenching of heparin in 50 mM Tris-HCl buffer pH 7.4 containing varying concentration of heparin. B. Stern-Volmer plot C. Modified Stern-Volmer plot with varying concentrations of heparin.

Native ovine and human α-1-PI had a Stern–Volmer constant of ~ 3.25±0.4 × 10^{-3} and 3.76±0.4 × 10^{-3} M respectively (Table 6. 1). The constant at 0.1 μM heparin are similar to native α-1-PI suggesting that at low concentration little or no change occurs. This data is consistent with the lack of significant activation observed at low heparin concentration (Figure 5. 2A). An increase in Stern-Volmer constant by 1.98 × 10^{-3} and 2.91 × 10^{-3} M for ovine and human α-1-PI following heparin (5.0 μM) activation was indicative of a slightly disrupted tertiary structure with Trps that were more exposed to the solvent. A higher K_{sv} of 5.23±0.5 × 10^{-6} and 6.67±0.5 × 10^{-6} M for heparin activated ovine and human α-1-PI were observed compared to that of 3.25±0.4 × 10^{-6} and 3.76±0.4 × 10^{-6} M for native inhibitors respectively. These results indicate that the milieu around Trp in α-1-PI is altered upon heparin binding. The higher K_{sv} value was also consistent with a more open conformation of heparin-activated α-1-PI. These results taken together with the fluorescence quenching implicate a subtle yet measurable change in the tertiary structure of α-1-PI upon activation with heparin. The percentage exposure of Trp was also marginally increased with increasing heparin concentrations.

FTIR spectroscopic studies

FTIR spectroscopy of the amide III spectral region was used to examine the effect of heparin binding on ovine α-1-PI secondary structure. The spectral bands corresponding to 1330-1295 cm^{-1} are assigned to α-helix, 1295-1270 cm^{-1} to β-turns, 1270-1250 cm^{-1} to random coils and 1250-1220 cm^{-1} to β-sheets respectively (Cai and Singh, 1999). Amide I spectral region (1700-1600 cm^{-1}) although commonly used in secondary structural analysis suffers from several limitations. Cai and Singh (1999) using the relatively weak signals of the amide III spectral region (1350-1200 cm^{-1}) demonstrated that the amide III bands are more suitable for quantitative analysis of protein secondary structure. Therefore, the FTIR spectra of the amide III region were chosen to study changes in the secondary structure of ovine α-1-PI. The amide III spectral analysis of BSA, lysozyme, α-chymotrypsin, Con-A and hemoglobin to estimate secondary structural elements by the above assignments correlated well with the secondary structure reported by CD and X-ray analysis indicating the validity of the method (Schechter and Blout, 1964; Levitt and Greer, 1977).

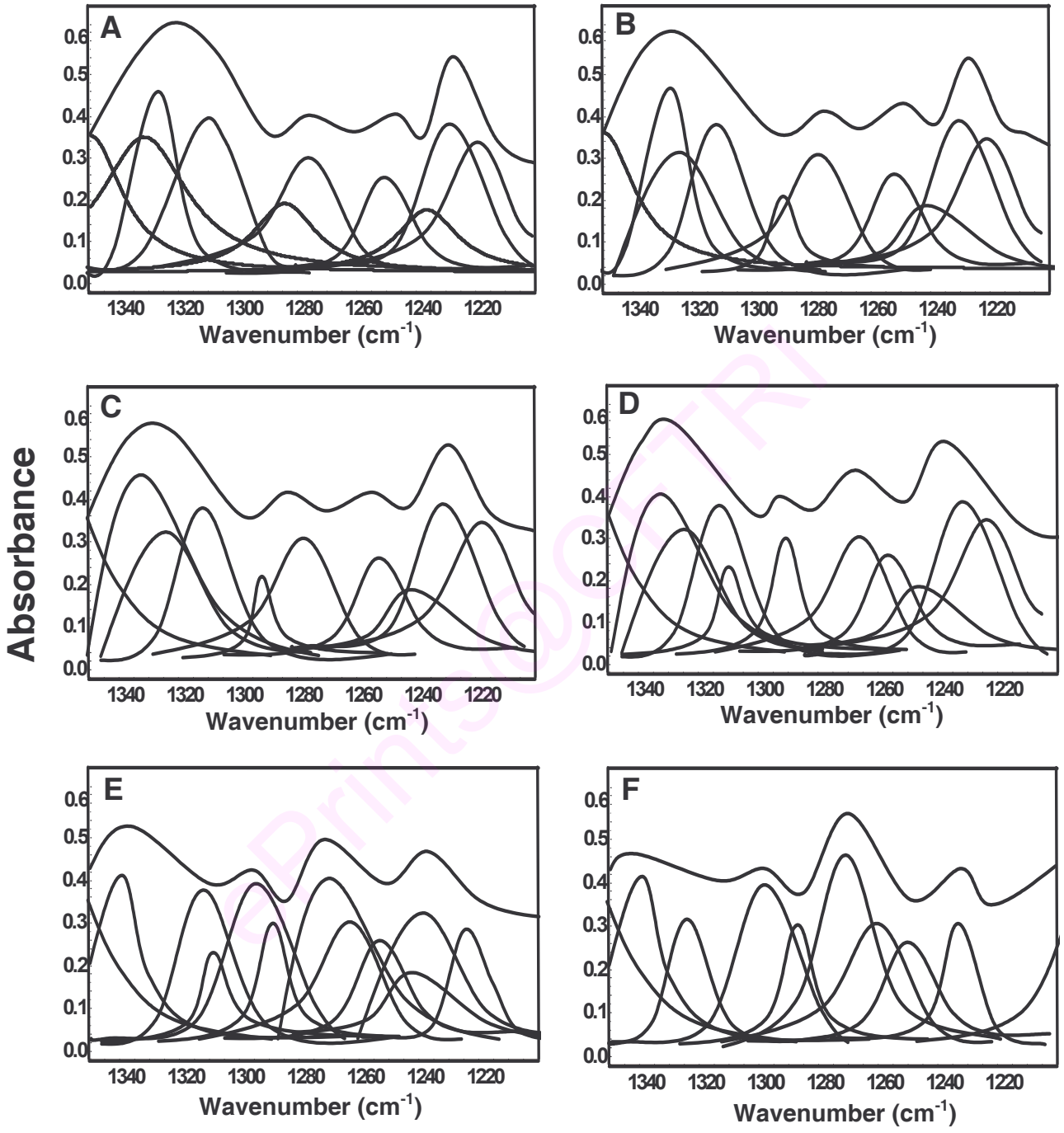

Figure 6. 10. Curve fitting analysis of FTIR spectra of ovine α-1-PI in amide III region. A-F indicate ovine α-1-PI (4 mg/mL) incubated with 0, 0.1, 0.25, 0.5, 1.0 and 2.0 μM of heparin respectively in 0.02 M NaPi buffer, pH 7.4 and lyophilized.

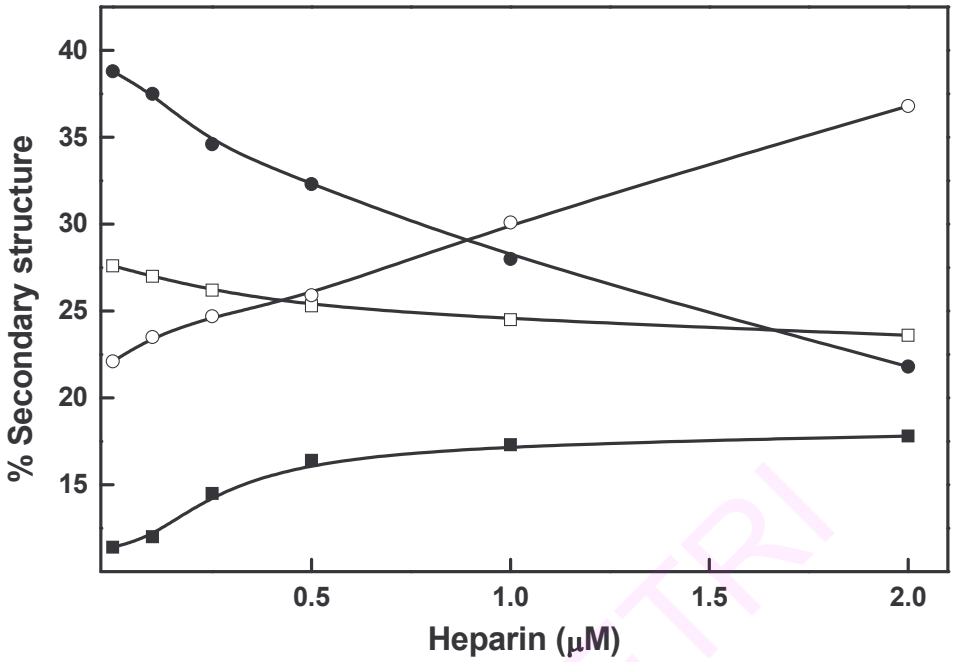

Figure 6. 11. Secondary structural variations of α-1-PI in response to different concentrations of heparin. Plot depicting changes in (-•-) α-helix, (-□-) β-sheet, (-O-) random coil and (-■-) β-turn content of ovine α-1-PI.

Table 6. 2. Ovine α-1-PI secondary structure quantification and comparison in presence of variable concentrations of heparin.

Heparin (μM)	α-Helix	β-Sheet	Random coil	β-Turn
		% Area		
0.0	38.8	27.6	22.1	11.4
0.1	37.5	27.0	23.5	12.0
0.25	34.6	26.2	24.7	14.5
0.5	32.3	25.3	25.9	16.4
1.0	28.0	24.5	30.1	17.3
2.0	21.8	23.6	36.8	17.8

∗Average of three independent experiments. Error, ν±1 cm^{-1}; area±5 %.

Figure 6. 10 shows the FTIR spectra in the amide III region of free α-1-PI and α-1-PI complexed with various heparin concentrations. In the presence of heparin the area under bands (band strength) above 1295 cm^{-1} decreased and moved to the lower wavenumber (Figure 6. 10). Second derivative and Gaussian curve fitting techniques were used to identify the overlapping sub-bands of the various components of protein secondary structures in the amide III region (1350-1200 cm^{-1}). The strength of bands near 1270-1250 cm^{-1} increased with increasing heparin concentration, which is consistent with an increase in the random coil. The decrease in the band strength above 1295 cm^{-1} was dramatic suggesting that the α-helix is very sensitive to heparin binding (Figure 6. 10). The percentages of each secondary structural element calculated from the integrated areas of the component bands in amide III of native ovine α-1-PI revealed that it possesses an α-helical content of 38.8 % and a β sheet content of 27.6 %. The random coil and β turn content were found to be 22.1 % and 11.4 % respectively. The effect of various heparin concentrations on the secondary structural elements of ovine α-1-PI as determined by FTIR spectroscopy is summarized in Figure 6. 11 and Table 6. 2.

FTIR analysis of ovine α-1-PI complexed with increasing heparin concentrations revealed a sharp decline in the α-helical content from 38.8 to 21.8 % while β sheet content decreased marginally from 27.6 to 23.6 % (Figure 6. 11 and Table 6. 2). A corresponding increase in the random coil from 22.1 to 36.8 % and β-turn from 11.4 to 17.8 % was observed when native α-1-PI was complexed with heparin. At saturating concentrations there appears to be a general perturbation of protein structure with no specific co-relation between various secondary structural elements. The values given are average of three independent experiments (error, ν±1 cm^{-1}; area±5 %).

Circular dichroism (CD) studies

CD spectroscopy was also used to analyze and confirm the FTIR changes in secondary structure upon heparin binding. The far-UV CD spectrum of proteins is particularly sensitive to secondary structure and therefore useful in studying conformational changes. The far-UV CD spectra of ovine α-1-PI and complexed with heparin are shown (Figure 6. 12A). The spectra show strong negative ellipticities at 208, 215 and 222 nm suggesting that α-1-PI in the native state is composed of both α-helix

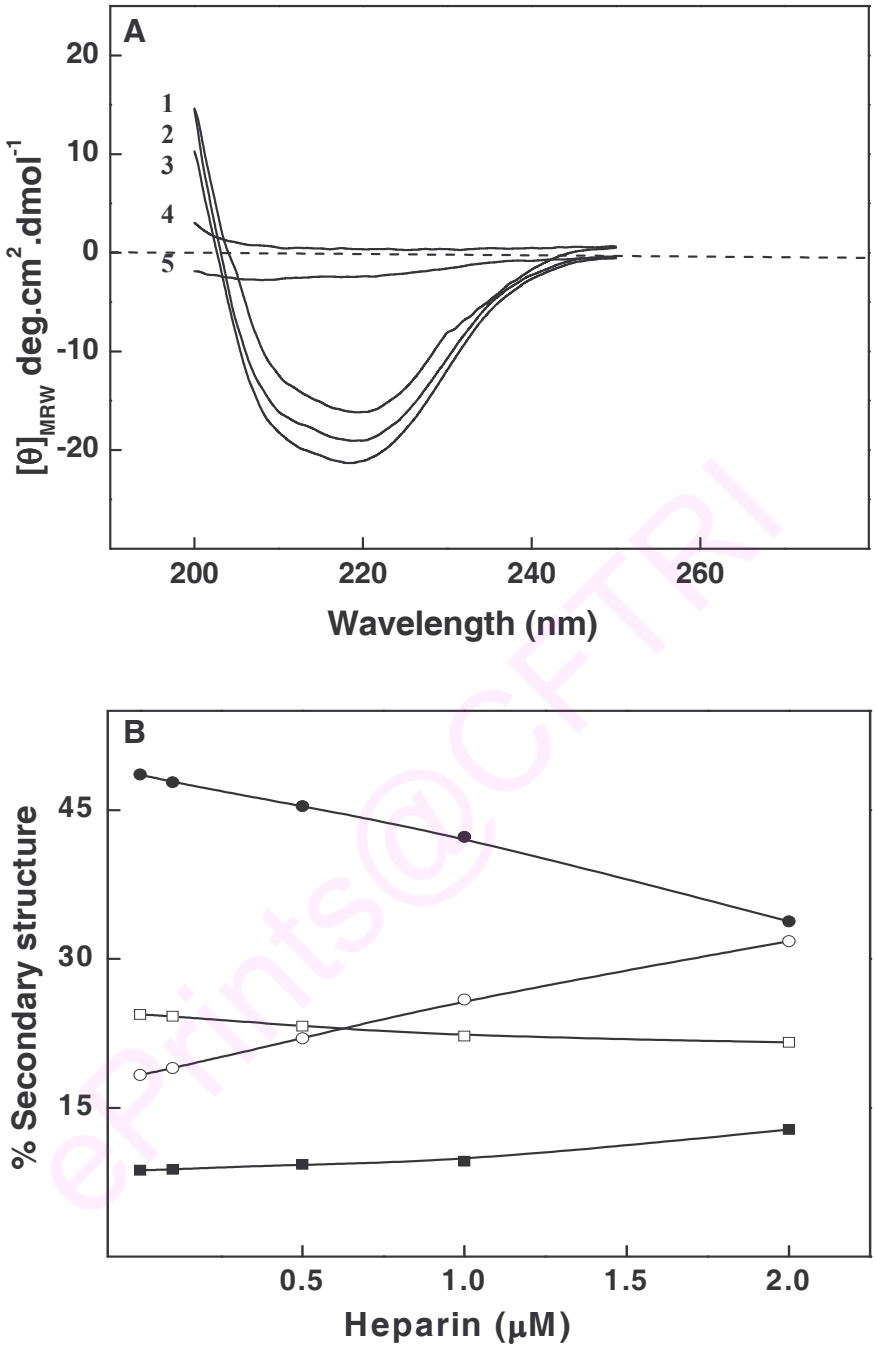

Figure 6. 12. Far UV CD spectra depicting heparin dependent conformational changes of ovine α-1-PI. A. 1, 2, 3, 4 and 5 correspond to spectra for native α-1-PI, α-1-PI + 1 μM heparin, α-1-PI + 2 μM heparin, buffer and heparin blank respectively. B. Plot depicting secondary structural variations of ovine α-1-PI in response to different concentrations of heparin; (-●-) α-helix, (-□-) β-sheet, (-O-) random coil and (-■-) β-turns.

and β-sheet rich regions. An increase in heparin concentration results in a decline in the negative ellipticities of the ordered structures and an increase in random disordered structure (Figure 6. 12B). A quantitative analysis of the protein secondary structure for free α-1-PI showed α-helix (48 %), β-sheet (25 %), β-turn (9%) and aperiodic (18 %). Upon heparin binding the α-helical structures were reduced from 48 to 34%, β-sheet from 25 to 22 %. Concomitantly the β-turn and random structures increased (Figure 6. 12B). These results are consistent with a similar decrease in α-helical content observed by FTIR (Figure 6. 11). The reduction of α-helices and β-sheet in favor of random structure are indicative of partial unfolding of protein in the presence of heparin.

Discussion

What are the conformational changes that take place on heparin binding and how do they activate α-1-PI? The answer to this is far from clear and is going to require an approach that is quite different from that taken on defining the heparin-binding site. The difference is that whereas with the binding site one is looking at a demarcated zone in the molecule, but with the conformational changes it is a sequence of events. So if a structural approach were to be taken, it would require looking at a series of structures on which the sequential changes take place.

Heparin has an astounding ability to bind to an array of proteins, most prominent of them being serpins, especially AT. Heparin binding to AT, heparin co-factor-II and Protein C inhibitor enhances their biological activity enormously. HC-II, PAI-1 and protease nexin-1 interact with heparin through the D-helix, while AT-heparin interaction additionally involves the role of A-helix and certain other basic residues (Jin et al., 1997).

Heparin binds PC-1 at helices A and H (Kuhn et al., 1990) indicating that heparin binding sites differ from serpin to serpin. It binds to a variety of proteases like thrombin, trypsin, acrosin, activated protein C and factor Xa as well (Gettins, 2002). The polyelectrolyte nature of heparin allows it to bind to numerous other plasma proteins like fibrinogen, fibronectin-histidine rich glycoprotein, platelet factor IV, fibroblast growth factor-10, acidic fibroblast growth factor and growth hormone (Joshi et al., 2008; Kamerzell et al., 2006; Burke et al., 1993). The binding is mediated primarily by the expected ionic interactions between carboxylate and sulfate groups of heparin and the basic side chains

of surface Lys and Arg residues (Blinder and Tollefsen, 1990). Heparin binding proteins in general, exhibit a positively charged domain or cluster on the surface irrespective of the overall charge distribution. It is through such domains that the protein interacts with the GAG. Heparin binding to proteins has been correlated with directing proteins to their sites of activity, regulating their inhibitory specificity and the activation (Cooper et al., 1996).

In case of AT, the structural changes that take place upon heparin binding are known, yet how these link with one another remains illusive. Heparin first binds in a rapid reaction to a low-affinity site on AT, which undergoes a conformational change to give a high affinity binding (Olson and Bjork, 1991). As a prototype serpin, the mobility necessary for such linked conformational changes is inherent to α-1-PI (Carrell et al., 1995). The mobile RCL is initially exposed as a substrate to the cognate protease but on cleavage it becomes inserted as a sixth strand in the central β-sheet (A sheet) of the molecule (Loebermann et al., 1984). α-1-PI binding to various ligands, which may act as activators or inhibitors of the protein activity, has not been investigated in detail. To our knowledge the only other study on α-1-PI-ligand interaction is the increased conformational stability of α-1-PI in the presence of citrate (Bottomley and Tew, 2000). Heparin is observed to bind and activate α-1-PI (Gupta and Gowda, 2008). A homogenous heparin octasaccharide binds to human and ovine α-1-PI at helix-F and activates it several fold. The binding site has been identified as the Lys rich cluster of helix-F (Figure 5. 10 of earlier section). The novel observation of heparin activation of α-1-PI may help solve some missing links between α-1-PI production, targeting and co-localization at the sites where maximum activity is desirable viz. lungs and mast cell rich locations, i.e; at the sites of inflammation. Heparin which is present in high concentrations in mast cells and lungs and also lines the arteries and veins activates AT and enhances the rate of reaction of AT and thrombin by an order of ~ 10^3. The GAG heparin used here is an octasaccharide as can be inferred from its molecular mass obtained by MALDI-MS. The present study illustrates that heparin binding induces secondary structural changes in the α-1-PI thereby leading to a compact conformation of α-1-PI. Heparin binding causes a decrease in the R_S of α-1-PI as monitored by DLS and

evidenced from the delayed elution of ovine α-1-PI in the presence of heparin (Figure 6. 1-3). The R_S declined with increasing heparin concentrations indicating that heparin binding leads to a molecular compaction and sturdy configuration of α-1-PI. This decrease in Stokes' radius is concentration dependent and achieves a plateau at ~ 10 μM heparin beyond which little or no alteration in molecular dimensions is observed. This decrease in Stokes' radius of ovine α-1-PI is speculated to arise from a conformational change and hence a systematic study of the conformational changes taking place was initiated. The light scattering measurements at 325 and 360 nm indicate that these changes were not due to aggregation.

Results of the present study indicate that the binding of heparin to ovine α-1-PI by equilibrium dialysis is characterized by the equilibrium constant $2.1\pm0.2 \times 10^{-6}$ M (Figure 6. 5). The binding constant obtained by fluorescence quenching measurements (Figure 6. 6) for heparin to ovine α-1-PI is $1.98\pm0.2 \times 10^{-6}$ M (Figure 6. 7B). Thus there is close agreement in the binding constants obtained for heparin ovine α-1-PI interaction by both direct and indirect methods. The heparin and α-1-PI concentrations are in the micromolar range in the vicinity of mast cells and lung endothelial surfaces. Thus the concentrations used to determine the equilibrium constant can be extrapolated to physiological concentrations locally.

Since the intensity of fluorescence as well as the location of emission maxima is changed when the immediate environment around the fluorescing residues is altered, protein fluorescence has been used as a sensitive monitor of conformational changes in the protein. The fluorescence of the indole of Trp is highly sensitive to its environment, which makes it an ideal residue to report conformational changes and interactions with other molecules (Lakowicz, 1999). It is well known that binding of heparin causes a conformational change that result in activation of AT as an inhibitor. This conformational shift also changes the environment of Trp residues within AT, causing an increase in fluorescence (Van Patten et al., 1999). α-1-PI like AT becomes a more potent inhibitor when the RCL is expelled from the protein and assumes a conformation more suitable for interaction with the target proteinase. Binding of heparin to the serpins induces a series of

conformational changes that results in the movement of the RCL into an extended structure that is poised for action (Whisstock et al., 2000).

The structural changes induced in α-1-PI upon heparin binding were followed both with respect to Trp at 295 nm as well as at 282 nm with respect to general perturbations in protein structure. Fluorescence spectroscopy revealed that there's a quenching of 45 % as heparin binds to α-1-PI. This is in contrast to heparin binding to AT resulting in an enhancement of the fluorescence by 40 % (Olson and Shore, 1981). Therefore, the structural changes differ between the two molecules. These results implicate a subtle yet measurable change in the Trp environment and hence the conformation of α-1-PI upon activation with heparin.

Fluorescence becomes an important tool to examine heparin binding to α-1-PI since the magnitude of relative fluorescence intensity (Figure 6. 6A) provides the sensitivity necessary to determine the dissociation and binding constants for α-1-PI-heparin complexes and to follow relatively rapid conformational changes. Stern-Volmer plots of acrylamide quenching of ovine (Figure 6. 8) and human (Figure 6. 9) α-1-PI indicate an increasing trend as increasing concentrations of heparin (0-5 μM) bind to the inhibitor (Table 6. 1). A close similarity in the Stern-Volmer constants for ovine and human α-1-PI reflects a high level of structural homology between the two. Interpretation of such studies in structural terms has, however, been handicapped by not knowing which of the two Trp are responsible for the fluorescence changes. Besides, the spectral changes could also be due to a perturbation of surface Trp residues by heparin without a conformational change (Villanueva and Danishefsky, 1979; Nordenman et al., 1978; Einarsson and Andersson, 1977).

Trp^{192} (Trp^{194} in human α-1-PI) is one of the most conserved residues within the serpin superfamily being present in 94 % of all known serpins (Irving et al., 2000). Trp^{192} is situated at the top of strand 5A and is oriented towards the hydrophobic core of the serpin, a region known as the "breach". This region consists of a number of highly conserved residues, which play a role in the initial events of RCL insertion. Trp^{192} packs against Phe^{196} (Phe^{198} in human α-1-PI) and Tyr^{242} (Tyr^{244} in human α-1-PI) both of which are highly conserved (> 70 %) and also Leu^{240} (Met^{242} in human α-1-PI), Phe^{250}

(Phe^{252} in human α-1-PI), Leu^{286} (Leu^{288} in human α-1-PI) and Ile^{338} (Ile^{340} in human α-1-PI), which are conserved (> 50 %) among the superfamily (Irving et al., 2000). Trp^{236} (Trp^{238} in human α-1-PI) is situated on the second strand of the B β-sheet and is not highly conserved e.g., in rabbit. Trp^{236} (Trp^{238} in human α-1-PI) lies in a partially surface exposed pocket formed by residues situated on strands 1 and 3 of the B β-sheet (Leu^{227}, Tyr^{229} and Leu^{252} corresponding to Ile^{229}, His^{231} and Leu^{254} in human α-1-PI) and strands 1 and 2 of the C β-sheet Val^{362} and Leu^{284} (Val^{364} and Leu^{286} in human α-1-PI). Therefore, Trp^{192} (Trp^{194} in human α-1-PI) acts as a probe for A β-sheet opening because of its location on strand 3A at the top of the A β-sheet and Trp^{236} (Trp^{238} in human α-1-PI) reports changes around the B β-sheet. This observation should be perceived in liaison with the observed decrease in β-pleat structure (Table 6. 2), although it is not feasible to conclude which of the β-pleats is involved in the conformational change.

Heparin induced ovine α-1-PI quenching depicts fluorescence emission spectra converging at 380 nm with declining intensity. In fluorescence, this point is called as isobestic point and is a specific wavelength at which two or more species have the same emission spectra. The wavelength of this point does not depend on the concentration of α-1-PI or heparin used. The stoichiometry of binding as revealed by both fluorescence spectrometry and equilibrium dialysis were found to be 1.1±0.2 and 1.0±0.2 respectively. Scatchard plot (Figure 6. 7A) indicates a non-linear relationship between heparin binding to ovine α-1-PI indicating an initial high affinity followed by a low affinity interaction. Isoelectrofocussing studies revealed that the pI of ovine α-1-PI drifted from 4.95 in its native form to a more acidic pH upon heparin binding (results not shown).

The conformational studies were further studied by FTIR measurements. FTIR spectroscopy is a useful tool for analysis of the secondary structures of the proteins and is particularly suitable for monitoring subtle conformational changes occurring within proteins (Byler and Susi, 1986). One analytical method which has been steadily evolving and which has resulted in a large number of publications describing global secondary structures has been FTIR. FTIR spectra analysis of the amide III (1350-1200 cm^{-1}) region of native and heparin bound α-1-PI unambiguously indicates that heparin binding causes a global alteration in protein secondary structural parameters. Despite the weaker signals

of amide III region (1230-1320 cm^{-1}) when compared to amide I and II, it has emerged as a promising and routinely used band to estimate protein secondary structure (Singh et al., 1990; Singh et al., 1993; Singh et al., 1994; Griebenow and Klibanov, 1995; Costantino et al., 1995; Bramanti et al., 1997) as it lacks disturbance by the absorbance of H_2O vapour, is relatively free from side-group vibrations and thus, highly sensitive to and diagnostic of secondary structural features. (Anderle and Mendelsohn, 1987; Kaiden et al., 1987). Easily resolved and better-defined amide III bands are also quite suitable for quantitative analysis of protein secondary structure. Amide I spectral region (1750-1600 cm^{-1}) although most commonly used primarily because of its strong signal, suffers from several limitations, including a strong interference from water vibrational band, relatively unstructured spectral contour and overlap of resolved bands correspondingly to various secondary structures. Easily resolved and better defined amide III bands are quite suitable for quantitative analysis of protein secondary structure. Because amide III region generally presents a more feature spectral contour (Jakobsen and Wasacz, 1990), the resolution of bands is easier in this region compared to the amide I region. Side chain effects and the interference from water is not a major problem for the use of amide III region (Fu et al., 1994) and the assignment results from amide III region are acceptable. Although the amide III mode is ~ 5-10 fold weaker in IR band strength than the amide I mode it is detectable with modern instrumentation. The amide III range is relatively free from side-group vibrations and thus highly diagnostic of secondary structure. It is reported that the estimated amounts for major structures agree with the values given by the x-ray crystallography and the CD spectroscopy within 5 % except for when the α-helix content is greater than 60 % (Dong et al, 1990).

Heparin binding results in a decrease of α-helix and β-sheet content by 17 % and 4 % respectively. This decrease in α-helix and β-sheet is concurrent with an increase of β-turn and random coil content of the molecule by 6.4 % and 14.7 % respectively as the heparin concentration is increased from 0 to 2 μM. At higher concentrations of heparin, α-1-PI shows a general perturbation in the secondary structural content and this may be attributed to a weaker binding of heparin as revealed by the second slope of the Scatchard plot (Figure 6. 7A). These results are consistent with the CD data (Figure 6. 12) which

also shows a decrease in the helical content. The differences in the α-helical content between FTIR and CD spectroscopy can be explained by the differences in sample preparation. The decrease in α-helical content can be extrapolated to the presumption that the RCL of α-1-PI which is a protruded coil structure becomes more exposed compared to the native forms and hence the activation. This conformational change may be linked to and implicated in the heparin activation of physiologically important serpins. The observations in the previous section as to the heparin binding site and activation are in general agreement with the structural changes observed here. The series of experiments described in this section, connect the changes with each other.

It is possible that the interaction of heparin with α-1-PI is functionally similar to that of AT, yet different in the structural changes caused. The solvent accessible surface area for a cluster of basic residues is quite high for both AT and α-1-PI (Gupta and Gowda, 2008). In addition to increasing the inhibitory properties of α-1-PI and AT, heparin also interacts with other proteins and regulates their physiological activities and stability. The physical stability of human fibroblast growth factor 1 (FGF1), unstable at physiological temperatures is markedly increased in the presence of sucrose octasulfate (Joshi et al., 2008). The binding of heparin sulfate to both FGF and its receptor (FGFR) facilitates the formation of an FGF/FGFR/heparin complex essential for cell signaling (Plotnikov et al., 2000). Heparan sulfate proteoglycans interact selectively with chemokines and modulate receptor binding and cellular responses (Proudfoot, 2006). Dextran sulfate and heparin markedly inhibit the aggregation of bovine and porcine somatotropin (Joshi et al., 2008), thus increasing protein stability.

The binding of heparin octasaccharide to α-1-PI has been investigated through biochemical and theoretical methods (Section 5, Results and Discussion) as well as biophysical tools. The results correlate well with each other. The various parameters that have a bearing on the binding of the heparin to inhibitor have been derived from the measurements of molecular dimensions, binding constants, protein fluorescence, CD and FTIR spectroscopy.

It is extremely difficult to predict the accurate three dimensional structural re-orientations of the ternary complex of α-1-PI with protease and heparin. However, the

current analysis clearly shows that heparin binding results in general compaction of the main body of the inhibitor and an increasing protrusion of the random coil RCL, which in turn encounters and ensnares the protease with a more rapid and effective approach. The crystal structure of α-1-PI-heparin complex when resolved will help ascertain the above observations.

7. SUMMARY AND CONCLUSIONS

Alpha-1-Proteinase inhibitor, the archetypal member of serpin superfamily is an acute phase protein and primarily protects pulmonary tissues from gratuitous elastase digestion and inhibits neutrophil elastase at sites of inflammation. It inhibits elastase, trypsin and chymotrypsin like enzymes and several other serine proteases.

In the present investigation entitled "**Biochemical and structural characterization of ovine alpha-1-proteinase inhibitor**" attempts have been made to understand the structure function relationships of α-1-PI. A detailed biochemical characterization of ovine α-1-PI has been undertaken and mechanism of multiple protease inhibition elucidated. Further, α-1-PI interaction with negatively charged heparin has been localized in terms of specific residues involved and investigated with respect to both activation and conformational changes. Following are the salient features of the present investigation:

- A homogenous preparation of ovine α-1-PI was obtained by subjecting ovine serum to 40–70 % $(NH_4)_2SO_4$ precipitation followed by blue sepharose, size-exclusion, and Con-A affinity chromatography (Figure 3. 1-3).
- The yield was 11.2 %. The specific activity was 1175 TIU/mg with a 20 fold purification (Table 3. 1). The 11 % recovery of α-1-PI is significantly high when compared to 0.22 % reported earlier.
- The homogeneity of ovine α-1-PI was confirmed by NH_2-terminal sequencing, capillary electrophoresis, RP-HPLC and native PAGE for both protein and activity staining (Figure 3. 4-5).
- The M_r of ovine α-1-PI was 60,000±500 Da by analytical gel filtration chromatography and SDS-PAGE (Figure 3. 7-8). The exact M_r was determined to be 58310 Da by mass spectroscopy.
- Amino-terminal sequence of a closely moving serpin followed by BLAST analysis revealed it to be α-1-antichymotrypsin.
- Ovine α-1-PI is a suicide inhibitor irreversibly inhibiting porcine pancreatic trypsin, elastase and bovine pancreatic chymotrypsin independently (Table 4. 1).

- Ovine α-1-PI binds to porcine pancreatic trypsin at 1: 1 molar ratio. However, porcine pancreatic elastase and bovine pancreatic chymotrypsin are inhibited at a higher molar ratio as revealed by stoichiometry studies; probably because the source is pancreas and not neutrophils (Figure 3. 12).
- The neutral sugar composition of ovine α-1-PI was 14 % slightly higher than human α-1-PI (11 %). The poorer glycosylation of human α-1-PI renders it more thermolabile when compared to ovine α-1-PI (Figure 3. 15).
- The enzymatic deglycosylation of human and ovine α-1-PI results in diminished thermostability of the inhibitors, yet retaining their inhibitory potency (Figure 3. 13 and 3. 16, Table 3. 4).
- Extensive insights into the trypsin, chymotrypsin and elastase interaction with ovine α-1-PI point towards the involvement of Phe^{350} besides the largely conserved Met^{356} in cognate protease recognition and consequent inhibition. The NH_2-terminal sequencing of C-terminal peptides cleaved on interaction with elastase, trypsin, and chymotrypsin prove the presence of diffused sub-sites in the vicinity of Met^{356} (Figure 4. 1).
- Chemical modification of Arg and Met residues indicate that Met has a role to play in elastase inhibition whereas Arg plays a role in trypsin specific inhibition. Lys modification brings about a general decline in inhibition of all the three proteases studied (Figure 4.2 to 4.5, Table 4. 2).
- The model of ovine α-1-PI was constructed using the cDNA deduced amino acid sequence (Brown et al., 1989) using human α-1-PI as the template. The model constructed was used for all further molecular modeling and docking studies (Figure 4. 7).
- The RCL region of the ovine α-1-PI model was docked against elastase, trypsin and chymotrypsin reactive site residues. The docked models indicate that Met^{356} side chain is recognized by elastase and chymotrypsin whereas Phe^{350} is responsible for trypsin specific inhibition. This confirms the earlier results

obtained by NH_2-terminal sequencing of cleaved C-terminal peptides (Figure 4. 8).

- Studies on the inhibition of bovine trypsin and chymotrypsin by the purified α-1-PI indicate that both have essentially the similar K_{ass} values. The K_{ass} value with elastase was an order lower (Table 3. 3) (**Gupta et al., 2008**).
- The protease inhibitory activity of human and ovine α-1-PI is enhanced several fold in the presence of anti-coagulant heparin. The activation is allosteric and is characterized by a two-step binding mechanism. The most effective heparin concentration is 6±0.5 μM with a linear increase observed between 1-6±0.5 μM (Figure 5. 2).
- The heparin octa-saccharide enhances the K_{ass} values for both human and ovine α-1-PI with respect to elastase by 38 and 45 fold respectively (Figure 5. 2). This indicates that heparin binds to and activates α-1-PI like other heparin binding serpins (antithrombin, HC-II and PCI) (Table 5. 1, Figure 5. 5 and 5. 6).
- The pI of ovine α-1-PI was found to be 4.95 similar to 4.5 reported for human α-1-PI (Figure 3. 10). The electrophoretic mobility decreased upon heparin binding (Figure 5. 2).
- A combinatorial approach using multiple sequence alignment, surface topology, chemical modification and tryptic peptide mapping to identify the sequence of the heparin bound peptide indicate that heparin binds to the lysyl rich region of the F-helix of α-1-PI, which differs from that of heparin-antithrombin interactions (Figure 5. 7-10).
- Molecular docking prediction using the MEDock algorithm approximates the three positively charged lysines (K^{154}, K^{155}, K^{174}) of human α-1-PI in this interaction (Figure 5. 10).
- Heparin α-1-PI interaction has been exploited to develop a universal heparin-sepharose affinity purification to obtain homogenous preparations of mammalian

α-1-PIs (human, rat, ovine and porcine) useful for augmentation therapy (Figure 5. 11-14). This single step purification protocol provides 14-18 fold purification.

- The cross-reactivity of purified α-1-PIs with human α-1-PI antibodies raised in rabbit indicated the presence of similar antigenic epitopes in ovine, rat and porcine α-1-PIs (Figure 5. 14).
- SDS-PAGE and mass spectrometric analysis revealed the exact M_r of the heparin sepharose affinity purified human, rat, ovine and porcine α-1-PI to be 52766.5, 53,700, 58310 and 54,865 Da respectively (Figure 5. 13 and 5. 15).
- The purified mammalian α-1-PIs were found to be most stable at pH 8.2 with a relatively high stability between pH 7.0 and 9.0 (Figure 5. 16) (**Gupta and Gowda, 2008)**.
- Ovine α-1-PI adapts a more compact conformation upon heparin binding as revealed by size exclusion chromatography and determination of Stokes' radius using dynamic light scattering (Figure 6. 1-4).
- Fluorescence spectroscopy revealed a quenching of 37 and 45±2 % as heparin binds to human and ovine α-1-PI respectively, without any alteration in the emission maxima. This is in contrast to heparin binding to antithrombin resulting in an enhancement of the fluorescence by 40 %. Therefore, the structural changes differ between the two molecules (Figure 6. 6).
- The binding constant (K_α) of heparin to ovine α-1-PI was $1.98\pm0.2 \times 10^{-6}$ M at lower concentrations of heparin using fluorescence spectroscopy and $2.1\pm0.2 \times 10^{-6}$ M using equilibrium dialysis. The stoichiometry of heparin binding to ovine α-1-PI was 1.1±0.2 both by fluorescence and equilibrium dialysis experiments (Figure 6. 5 and 6. 7).
- Scatchard plot of heparin binding studied by fluorescence spectroscopy indicates a dual binding mode. An initial high affinity interaction is followed by a conformational change in the molecule that facilitates a second low affinity interaction (Figure 5. 5 and 6. 7).

- The Stern-Volmer constants (K_{sv}) for heparin activated ovine and human α-1-PI were found to be 5.13×10^{-6} and 5.67×10^{-6} M respectively, which is significantly higher when compared to native inhibitors (Table 6. 1).
- FTIR spectra analysis of the amide III region of native and heparin bound α-1-PI unambiguously indicates that heparin binding causes a global alteration in protein secondary structural parameters (Figure 6. 10).
- Both the α-helix and β-sheet content undergo a gradual decline with a concomitant increase in random coil and β-turn content when heparin binds to α-1-PI. This decrease in α-helix and β-sheet is concurrent with an increase of β-turn and random coil content of the molecule as the heparin concentration is increased from 0 to 2 μM (Table 6. 2, Figure 6. 11).
- Analysis of the far UV CD spectra also yielded similar results with a significant loss of α-helix and a concomitant gain in the aperiodic structure upon heparin binding (Figure 6. 12).
- In conclusion heparin binding results in general compaction of the main body of the inhibitor and increases the protrusion of the random coil RCL, which in turn encounters and ensnares the protease with a more rapid and effective approach (**Gupta and Gowda, 2008; J. Mol. Struct. in press**).

8. REFERENCES

Abraham, W. M., Sielczak, M. W., Wanner, A., Perruchoud, A. P., Blinder, L., Stevenson, J. S., Ahmed, A., and Yerger, L. D. (1988) Cellular markers of inflammation in the airways of allergic sheep with and without allergen-induced late responses, *Am Rev Respir Dis.* 138, 1565–1571.

Abrams, W. R., Weinbaum, G., Weissbach, L., Weissbach, H., and Brot, N. (1981) Enzymatic reduction of oxidized alpha-1-proteinase inhibitor restores biological activity, *Proc. Natl. Acad. Sci. U.S.A.* 78, 7483- 7486.

*Ahmad, S. T., Natochin, M., Barren, B., Artemyev, N. O., and Tousa, J. E. (2006) Heterologous Expression of Bovine Rhodopsin in *Drosophila* Photoreceptor Cells, *Invest. Ophthal. Vis. Sci.* 47, 3722-3728.

Alino, S. F., Crespo, J., Bobadilla, M., Lejarreta, M., Blaya, C., Crespo, A. (1994) Expression of human alpha 1-antitrypsin in mouse after *in vivo* gene transfer to hepatocytes by small liposomes, *Biochem. Biophys. Res. Commun.* 15, 1023-1030.

Anderle, G., and Mendelsohn, R. (1987) Thermal denaturation of globular proteins. Fourier transform-infrared studies of the amide III spectral region, *Biophys. J.* 52, 69-74.

Anfinsen, C. B. (1973) Principles that govern the folding of protein chains, *Science* 181, 223-30.

Archibald, A. L., Couperwhite, S., Mellink, C. H. M., Mansais, L. Y., Gellin, J. (1996) Porcine alpha-1-antitrypsin (PI): cDNA sequence, polymorphism and assignment to chromosome 7q2.4- > q2.6, *Animal Genetics* 27, 85-89.

ArgusLab 4.0.1 Thompson, M. A., Planaria Software LLC, seattle, WA.

Axelsson, U., and Laurell, C. B. (1965) Hereditary variants of serum alpha-1-antitrypsin, *Am. J. Hum. Genet.* 17, 466–472.

Baglin, T. P., Carrell, R. W., Church, F. C., Esmon, A., and Huntington, J. A. (2002) Crystal structures of native and thrombin-complexed heparin cofactor II reveal a multistep allosteric mechanism, *Proc. Natl. Acad. Sci. U.S.A.* 99, 11079-11084.

Baker, D., Sohl, J. L., and Agard, D. A. (1992) A protein-folding reaction under kinetic control, *Nature* 356, 263-265.

Baksi, K., Rogerson, D. L., and Rushizky, G. W. (1978) Rapid, single-step purification of restriction endonucleases on cibacron blue F3GA-agarose, *Biochemistry* 17**,** 4136–4139.

Balasubramanian, D. and Kumar, C. (1976) Recent studies of the circular dichroism and optical rotatory dispersion of biopolymers, *Appl. Spectrosc. Rev.* 11, 223-286.

Banda, M. J., Clark, E. J., and Werb, Z. (1980) Limited proteolysis by macrophage elastase inactivates human alpha 1-proteinase inhibitor, *J. Exp. Med.* 152, 1563–1570.

Banda, M. J., Clark, E. J., Sinha, S., and Travis, J. (1987) Interaction of mouse macrophage elastase with native and oxidized human alpha 1-proteinase inhibitor, *J. Clin. Invest.* 79, 1314-1317.

Bao, J. J., Fourquet, L., Sifers, R. N., Kidd, V. J., and Woo, S. L. (1988) Molecular structure and sequence homology of a gene related to alpha 1-antitrypsin in the human genome, *Genomics* 2, 165–173.

Barbour, K. W., Wei, F., Brannan, C., Flotte, T. R., Baumann, H., and Berger, F. G. (2002) The murine alpha (1)-proteinase inhibitor gene family: Polymorphism, chromosomal location, and structure, *Genomics* 80, 515-522.

Barrett, A. J., and Rawlings, N. D. (2001) Evolutionary lines of cysteine peptidases. *Biol. Chem.* 382, 727–733.

Baugh, R. J., and Travis, J. (1976) Human leukocyte granule elastase: Rapid isolation and characterization, *Biochemistry* 24, 836–841.

Baumann, U., Huber, R., Bode, W., Grosse, D., Lesjak, M., and Laurell, C. B. (1991) Crystal structure of cleaved human alpha 1-antichymotrypsin at 2.7 Å resolution and its comparison with other serpins. *J. Mol. Biol.* 218, 595-606.

Beatty, K., Bieth, J., and Travis, J. (1980) Kinetics of association of serine proteinases with native and oxidized alpha-1-proteinase inhibitor and alpha-1-antichymotrypsin, *J. Biol. Chem*. 255, 3931-3934.

Beatty, K., Travis, J., and Bieth, J. (1982) The effect of alpha 2-macroglobulin on the interaction of alpha 1-proteinase inhibitor with porcine trypsin, *Biochim. Biophys. Acta* 704, 221–226.

Benning, L. N., Whisstock, J. C., Sun, J., Bird, P. I., and Bottomley, S. P. (2004) The human serpin proteinase inhibitor-9 self-associates at physiological temperatures, *Protein Science* 13, 1859-1864.

Bernhard, O. K., Kapp, E. A., and Simpson, R. J. (2007) Enhanced analysis of the mouse plasma proteome using cysteine-containing tryptic glycopeptides, *J. Proteome Res.* 6, 987-95.

Bidlingmeyer, B. A., Cohen, S. A., and Tarvin, T. L. (1984) Rapid analysis of amino acids using pre-column derivatization, *J. Chromatogr.* 336, 93-104.

Bieth**,** J., Spiess, B., and Wermuth, C. G. (1974) The synthesis and analytical use of a highly sensitive and convenient substrate of elastase, *Biochem. Med.* 11, 350–357.

Bird, C. H., Sutton, V. R., Sun, J., Hirst, C. E., Novak, A., Kumar, S., Trapani, J. A., and Bird, P. I. (1998) Selective regulation of apoptosis: The cytotoxic lymphocyte serpin proteinase inhibitor 9 protects against granzyme B-mediated apoptosis without perturbing the Fas cell death pathway, *Mol. Cell. Biol.* 18, 6387–6398.

Bird, P. I. (1999) Regulation of pro-apoptotic leucocyte granule serine proteinases by intracellular serpins, *Immunol. Cell Biol.* 77, 47-57.

Björk, I., and Nordenman, B. (1976) Acceleration of the reaction between thrombin and antithrombin III by non-stoichiometric amounts of heparin, *Eur. J. Biochem.* 68, 507–511.

Bland, C. E., Ginsburg, H., Silbert, J. E., and Metcalfe, D. D. (1982) Mouse heparin proteoglycan synthesis by mast cell-fibroblast monolayers during lymphocyte-dependent mast cell proliferation, *J. Biol. Chem.* 257, 8661-8666.

Blinder, M. A., and Tollefsen, D. M. (1990) Site-directed mutagenesis of arginine 103 and lysine 185 in the proposed glycosaminoglycan-binding site of heparin cofactor II, *J. Biol. Chem*. 265, 286-291.

Blundell, T. L., Sibanda, B. L., Sternberg, M. J., and Thornton, J. M. (1987) Knowledge-based prediction of protein structures and the design of novel molecules, *Nature* 326, 347-352.

Bock, P. E., Luscombe, M., Marshall, S. E., Pepper, D. S., and Holbrook, J. J. (1980) The multiple complexes formed by the interaction of platelet factor 4 with heparin, *Biochem. J.* 191, 69-76.

Boswell, D. R., Jeppsson, J. O., Brennan, S. O., and Carrell, R. W. (1983) The reactive site of alpha 1-antitrypsin is C-terminal, not N-terminal, *Biochim. Biophys. Acta* 744, 212-218.

Bottomley, S. P., and Tew, D. J. (2000) The citrate ion increases the conformational stability of alpha (1)-antitrypsin, *Biochim. Biophys. Acta* 1481, 11-17.

Boudier, C., Bousquet, J. A., Schauinger, S., Michels, B., and Bieth, J. G. (2007) Reversible inactivation of serpins at acidic pH, *Arch. Biochem. Biophys.* 466, 155-163.

Boutten, A., Venembre, P., Seta, N., Hamelin, J., Aubier, M., Durand, G., and Dehoux, M. S. (1998) Oncostatin M is a potent stimulator of alpha1-antitrypsin secretion in lung epithelial cells: Modulation by transforming growth factor-beta and interferon-gamma, *Am. J. Respir. Cell. Mol. Biol*. 18, 511-520.

Bradford, M. M. (1976) A rapid and sensitive method for the quantitation of microgram quantities of protein utilizing the principle of protein-dye binding, *Anal. Biochem.* 72, 248–254.

Bramanti, E., Benedetti, E., Sagripanti, A., and Papineschi, F. (1997) Determination of secondary structure of normal fibrin from human peripheral blood, *Biopolymers* 41, 545-553.

Brems, D. N., Plaisted, S. M., Havel, H. S., Kauffman, E. W., Stodola, J. D., Eaton, L. C., and White, R. D. (1985) Equilibrium denaturation of pituitary- and recombinant-derived bovine growth hormone, *Biochemistry* 24, 7662-7668.

Brewerton, D. A. (1984) A reappraisal of rheumatic diseases and immunogenetics, *Lancet* 2, 799–802.

*Briscoe, W. A., Kueppers, F., Davis, A. L., Bearn, A. G. (1966) A case of inherited deficiency of serum alpha-antitrypsin associated with pulmonary emphysema, *Am. Rev. Respir. Dis.* 94, 529–539.

Brot, N., and Weissbach, H. (1982) The biochemistry of methionine sulfoxide residues in proteins, *Trends Biochem. Sci*. 7, 137-139.

Brot, N., and Weissbach, H. (1983) Biochemistry and physiological role of methionine sulfoxide residues in proteins, *Arch. Biochem. Biophys.* 223, 271–281.

Brot, N., Fliss, H., Coleman, T., and Weissbach, H. (1984) Enzymatic reduction of methionine sulfoxide residues in proteins and peptides, *Methods Enzymol.* 107, 352–360.

Brown, W. M., Dziegielewska, K. D., Foreman, R. C., Saunders, N. R., and Wu, Y. (1989) Nucleotide and deduced amino acid sequence of sheep alpha-1-antitrypsin, *Nucleic Acids Res.* 17, 6398.

Bruch, M., Weiss, V., and Engel, J. (1988) Plasma serine proteinase inhibitors (serpins) exhibit major conformational changes and a large increase in conformational stability upon cleavage at their reactive sites, *J. Biol. Chem*. 263, 16626-16630.

Bullough, P. A., Hughson, F. M., Skehel, J. J., and Wiley, D. C. (1994) Structure of influenza haemagglutinin at the pH of membrane fusion, *Nature* 371, 37-43.

Burke, C. J., Volkin, D. B., Mach, H., Middaugh, C. R. (1993) Effect of polyanions on the unfolding of acidic fibroblast growth factor, *Biochemistry* 32, 6419-6426.

Burrows, J. A. J., Willis, L. K., and Perlmutter, D. H. (2000) Chemical chaperones mediate increased secretion of mutant α1-antitrypsin (α1-AT) Z: A potential pharmacological strategy for prevention of liver injury and emphysema in α1-AT deficiency, *Proc. Natl. Acad. Sci. U.S.A.* 97**,** 1796–1801.

Byler, D. M., and Susi, H. (1986) Examination of the secondary structure of proteins by deconvolved FTIR spectra, *Biopolymers* 25**,** 469–487.

Cai, S., and Singh, B. R., (1999) Identification of β-turn and random coil amide III infrared bands for secondary structure estimation of proteins, *Biophysical chemistry* 80, 7-20.

Campbell, D. J. (2003) The renin-angiotensin and the kallikrein-kinin systems, *Int. J. Biochem. Cell Biol.* 35, 784-791.

Cardin, A. D., and Weintraub, H. I. R. (1989) Molecular modeling of protein-glycosaminoglycan interactions, *Arteriosclerosis* 9, 21-32.

*Carlson, J. A., Rogers, B. B., Sifers, R. N., Hawkins, H. K., Finegold, M. J., and Woo, S. L. (1988) Accumulation of PiZ alpha 1-antitrypsin causes liver damage in transgenic mice, *J. Clin. Invest*. 82, 26–36.

Carp, H., and Janoff, A. (1979) In vitro suppression of serum elastase-inhibitory capacity by reactive oxygen species generated by phagocytosing polymorphonuclear leukocytes, *J. Clin. Invest.* 63, 793−797.

Carp, H., Miller, F., Hoidal, J. R., and Janoff, A. (1982) Potential mechanism of emphysema: Alpha-1-proteinase inhibitor recovered from lungs of cigarette smokers contains oxidized methionine and has decreased elastase inhibitory capacity, *Proc. Natl. Acad. Sci. U.S.A.* 79, 2041-2045.

Carpenter, M., Strange, C., Jones, Y., Dickson, M., Carter, C., Moseley, M., Gilbert, G. (2007) Does genetic testing result in behavioural health change? Changes in smoking behaviour following testing for alpha-1 antitrypsin deficiency, *Ann. Behav. Med.* 33**,** 22–28.

Carrell, R. W. (1999) How serpins are shaping up, *Science* 285, 1861.

Carrell, R. W., and Stein, P. E. (1996) The biostructural pathology of the serpins: Critical function of sheet opening mechanism, *Biol. Chem. Hoppe-Seyler*, 377, 1-17.

Carrell, R. W., Boswell, D. R., Brennan, S. O., and Owen, M. C. (1980) Active site of alpha 1-antitrypsin: homologous site in antithrombin-III, *Biochem. Biophys. Res. Commun.* 93, 399-402.

Carrell, R. W., Stein, P. E., Fermi, G., and Wardell, M. R. (1994) Biological implications of a 3 Å structure of dimeric antithrombin, *Structure* 2, 257-270.

Carrell, R W., Skinner, R., Warden, M., and Whisstock, J. (1995) Antithrombin and heparin, *Mol. Med. Today* 1, 226-231.

Carrell, R. W., and Travis, J. (1985) α_1-Antitrypsin and the serpins: Variation and countervariation, *Trends Biochem. Sci.* 10, 20-24.

Carrell, R. W., and Lomas, D. A. (1997) Conformational disease, *Lancet* 350, 134-138.

Chandra, T., Kurachi, K., Davie, E. W., and Woo, S. L. (1981) Induction of alpha 1-antitrypsin mRNA and cloning of its cDNA, Biochem. *Biophys. Res. Commun.* 103, 751–758.

Chang, D. T., Oyang, Y., and Lin, J., (2005) MEDock: a web server for efficient prediction of ligand binding sites based on a novel optimization algorithm, *Nucleic Acids Res.* 33, 233-238.

Chao, S., Chai, K. X., Chao, L., and Chao, J. (1990) Molecular cloning and primary structure of rat alpha-1-antitrypsin, *Biochemistry* 29, 323-329.

Choay, J., Petitou, M., Lormeau, J. C., Sinay, P., Casu, B., and Gatti, G. (1983) Structure–activity relationship in heparin : A synthetic pentasaccharide with high affinity for antithrombin III and eliciting high anti-factor Xa activity, *Biochem. Biophys. Res. Commun.* 116, 492-499.

Chow**,** M. K., Lomas, D. A., and Bottomley, S. P. (2004) Promiscuous β-strand interactions and the conformational diseases, *Curr. Med. Chem.* 11, 491–499.

Cichy, J., Potempa, J., and Travis, J. (1997) Biosynthesis of alpha1-proteinase inhibitor by human lung-derived epithelial cells, *J. Biol. Chem.* 272, 8250–8255.

Clark, R. A., Stone, P. J., El Hag, A., Calore, J. D., and Franzblau, C. (1991) Myeloperoxidase-catalyzed inactivation of alpha 1-protease inhibitor by human neutrophils, *J. Biol. Chem.* 256, 3348–3353.

*Cleland, J. L., Powell, M. F., and Shire, S. J. (1993) The development of stable protein formulations: a close look at protein aggregation, deamidation, and oxidation, *Crit. Rev. Ther. Drug Carrier Syst.* 10, 307-77.

Clemmensen, I., and Christensen, F. (1976) Inhibition of urokinase by complex formation with human alpha1-antitrypsin, *Biochim. Biophys. Acta* 429, 591-9.

Coakley, R. J., Taggart, C., Neill, S., and McElvancy, N. G. (2001) Alpha-1 antitrypsin deficiency: Biological answers to clinical questions, *Am. J. Med. Sci.* 321, 33-41.

Cochrane, C. G., Spragg, R., and Revak, S. D. (1983) Pathogenesis of the adult respiratory distress syndrome. Evidence of oxidant activity in bronchoalveolar lavage fluid, *J. Clin. Invest.* 71, 754–761.

Cohen, A. B. (1973) Mechanism of action of alpha-1-antitrypsin, *J. Biol. Chem.* 248, 7055-7059.

Cohen, A.B. (1979) The effects *in vivo* and *in vitro* of oxidative damage to purified alpha-1-antitrypsin and to the enzyme inhibiting activity of plasma, *Am. Rev. Resp. Dis.* 119, 953-960.

Cooper, S. T., Neese, L. L., DiCuccio, M. N., Liles, D. K., Hoffman, M., and Church, F. C. (1996) Vascular Localization of the Heparin-binding Serpins Antithrombin, Heparin Cofactor II, and Protein C Inhibitor, *Clinical and Applied Thrombosis/Hemostasis* 2, 185-191.

Costantino, H. R., Griebenow, K., Mishra, P., and Klibanov, A. M. (1995) Fourier-transform infrared spectroscopic investigation of protein stability in the lyophilized form, *Biochim. Biophys. Acta* 1253, 69–74.

Coughlin, P., Sun, J., Cerruti, L., Salem, H. H., and Bird, P. (1993) Cloning and molecular characterization of a human intracellular serine proteinase inhibitor, *Proc. Natl. Acad. Sci. U. S. A.* 90, 9417–9421.

Courtney, M., Buchwalder, A., Tessier, L., Jaye, M., Benavente, A., Balland, A., Kohli, V., Lathe, R., Tolstoshev, P., and Lecocq, J. (1984) High level production of biologically active human alpha-1-antitrypsin in *E. coli*. *Proc. Natl. Acad. Sci. U.S.A.* 81, 669.

*Cowden, D. I., Fisher, G. E., and Weeks, R. L. (2005) A pilot study comparing the purity, functionality and isoform composition of α-1-proteinase inhibitor (human) products, *Curr. Med. Res. Opin.* 21, 877-883.

Cox, M., and Nelson, D. (2004) *Lehninger, Principles of Biochemistry*, Freeman and Company, New York, ISBN 0-71674339-6.

Curiel, D. T., Chytil, A., Courtney, M., and Crystal, R. G. (1989) Serum alpha 1-antitrypsin deficiency associated with the common S-type (Glu264-Val) mutation results from intracellular degradation of alpha 1-antitrypsin prior to secretion, *J. Biol. Chem.* 264, 10477–10486.

*Delvin, R. H., Yesaki, T.Y., Donaldson, E. M., Du, S. J., and Hew, C. L. (1995) Production of germline transgenic pacific salmonids with dramatically increased growth performance, *Can. J. Fisheries Aqua. Sci.* 52, 1376-1384.

*DeMeo, D. L., and Silverman, E. K. (2004) Alpha1-antitrypsin deficiency: Genetic aspects: Phenotypes and genetic modifiers of emphysema risk, *Thorax* 59, 259-64.

Desai, U., Swanson, R., Bock, S. C., Björk, I., and Olson, S. T. (2000) Role of arginine 129 in heparin binding and activation of antithrombin, *J. Biol. Chem.* 275, 18976-18984.

Devlin, G. L., Chow, M. K., Howlett, G. J., and Bottomley, S. P. (2002) Acid denaturation of α-(1)-antitrypsin: Characterization of a novel mechanism of serpin polymerization, *J. Mol. Biol.* 324, 859–870.

Dewar, M. J. S., Zoebisch, E. G., Healy, E. F., and Stewart, J. J. P. (1985) AM1: A general-purpose quantum mechanical molecular model, *J. Am. Chem. Soc.* 107, 3902-3909.

Dietrich, C. P., Paiva, J. F., Castro, R. A., Chavante, S. F., Jeske, W., Fareed, J., Gorin, P. A., Mendes, A., and Nader, H. B. (1999) Structural features and anticoagulant activities of a novel natural low molecular weight heparin from the shrimp *Penaeus brasiliensis*, *Biochim. Biophys. Acta* 1428, 273-83.

Dixon, H. B. F., and Perham, R. N. (1968) Reversible blocking of amino groups with citraconic anhydride, *Biochem. J.* 109, 312-314.

Djie, M. Z., Le Bonnie, B. F., Hopkins, P. C., Hipler, K., and Stone, S. R. (1996) Role of the P2 residue in determining the specificity of serpins, *Biochemistry* 35, 11461-11469.

Dong, A., Huang, P. and Caughey, W. S. (1990) Protein secondary structures in water from second-derivative amide I infrared spectra, *Biochemistry* 29**,** 3303-3308.

Dowling, W., Thompson, E., Badger, C., Mellquist, J. L., Garrison, A. R., Smith, J. M., Paragas, J., Hogan, R. J., and Schmaljohan, C. (2007) Influences of glycosylation on

antigenicity, immunogenicity, and protective efficacy of ebola virus GP DNA vaccines, *J. Virol.* 81, 1821-1837.

Drechsel, D., Karic, L., and Glaser, C. B. (1984) Affinity chromatography of alpha-1-protease inhibitor using sepharose-4B bound anhydrochymotrypsin, *Anal. Biochem*. 143, 141-145.

*DuBois, M., Gilles, K. A., Hamilton, J. K., Rebers, P. A., and Smith, F. (1956) Colorimetric method for determination of sugars and related substances, *Anal. Chem.* 28, 350-356.

Eden, E., Strange, C., Holladay, B., and Xie, L. (2006) Asthma and allergy in alpha-1 antitrypsin deficiency, *Respir. Med.* 100, 1384–1391.

Einarsson, R., and Andersson, L. O. (1977) Binding of heparin to human antithrombin III as studied by measurements of tryptophan fluorescence, *Biochim. Biophys. Acta.* 490, 104–111.

Elliott, P. R., Abrahams, J. P., and Lomas, D. A. (1998) Wild-type α-1-antitrypsin is in the canonical inhibitory conformation, *J. Mol. Biol.* 275, 419–425.

Elliott, P. R., Lomas, D. A., Carrell, R. W., and Abrahams, J. P. (1996) Inhibitory conformation of the reactive loop of α-1-antitrypsin, *Nat. Struct. Biol.* 3, 676–681.

Ellis, V., Scully, M., MacGregor, I., and Kakkar, V. (1982) Inhibition of human factor Xa by various plasma protease inhibitors, *Biochim. Biophys. Acta* 701, 24-31.

Elzouki, A. N., Segelmark, M., and Wieslander, J. (1994) Strong link between the alpha 1-antitrypsin PiZ allele and Wegener's granulomatosis, *J. Intern. Med.* 236, 543-548.

Erlanger, B. F., Kokowsky, N., and Cohen, W. (1961) The preparation and properties of two new chromogenic substrates of trypsin, *Arch. Biochem. Biophys*. 95, 271-278.

Farndale, A. W., Buttle, D. J., and Barrett, A. J. (1986), Improved quantitation and discrimination of sulfated glycosaminoglycans by use of dimethylene blue, *Biochim. Biophys. Acta* 883, 173-177.

Felicioli, R., Garzelli, B., Vaccari, L., Melfi D., and Balestreri, E. (1997) Activity staining of protein inhibitors of protease on gelatin-containing polyacrylamide gel electrophoresis, *Anal. Biochem.* 244, 176–179.

Felsenstein, J. (1985) Confidence limits on phylogenies: An approach using the bootstrap, *Evolution* 39, 783-791.

*Fermi, C., and Pernossi, L. (1894) Untersuchungen uber die Enzyme, *Vergleichende studie Z. Hyg. Infektionskr* 18, 83-89.

Ferrarotti, I., Scabini, R., Campo, I., Ottaviani, S., Zorzetto, M., Gorrini, M., and Luisetti, M. (2007) Laboratory diagnosis of alpha(1)-antitrypsin deficiency, *Transl. Res.* 150, 267-74.

Fowler, A. A., Walchak, S., Giclas, P. C., Henson, P. H., and Hyres, T. M. (1982) Characterization of anti-proteinase activity in the adult respiratory distress syndrome, *Chest* 81, 50-51.

*Fritz, H., Brey, F. B., Schmal, A., and Werle, E. (1969) Use of water-insoluble derivatives of the trypsin-kallikrein inhibitor for the isolation of kallikrein and plasmin, *Hoppe Seylers Z. Physiol. Chem.* 350, 617-25.

Fritz, H., Brey, F. B., Fink, E., Meier, M., Schiessler, H., and Schirren, C. (1972) Humanakrosin: Gewinnung und Eigenschaften, *Hoppe Seylers Z. Physiol. Chem.* 353, 1943–1949.

Frommherz, K. J., Faller, B., and Bieth, J. G. (1991) Heparin strongly decreases the rate of inhibition of neutrophil elastase by alpha-1-proteinase inhibitor, *J. Biol. Chem.* 266, 15356-15362.

Fu, F. N., DeOliveira, D. B., Trumble, W., Sarkar, H. K., and Singh, B. R. (1994) Secondary structure estimation of proteins using the amide III region of fourier transform infrared spectroscopy: Application to analyze calcium-binding-induced structural changes in calsequestrin, *Appl. Spectrosc.* 48, 1432-1441.

*Fukada, M., and Hinghaul, O. (2000) Cell surface carbohydrates: Cell type-specific expression, *Molecular and Cellular Glycobiology,* Oxford University Press, New York, 12-61.

Gadek, J. E., Fells, G. A., and Crystal, R. G. (1979) Cigarette smoking induces functional antiprotease deficiency in the lower respiratory tract of humans, *Science* 206, 1315-6.

*Gadek, J. E., Klein, H. G., Holland, P. V., and Crystal, R. G. (1981) Replacement therapy of alpha-1-antitrypsin deficiency, *J. Clin. Invest.* 68, 1158-1165.

Galli, S. J. (2000) Mast cells and basophils, *Curr. Opin. Hematol.* 7, 32-9.

Gettins, P. G. W. (2002) Serpin structure, Mechanism and Function, *Chem. Rev.* 102, 4751-4803.

Gettins, P. G. W., Fan, B., Crews, B. C., Turko, I. V., Olson, S. T., and Streus, V. J. (1993) Transmission of conformational change from the heparin-binding site to the reactive center of antithrombin, *Biochemistry* 32, 8385-8389.

Gils, A., and Declerck, P. J. (1998) Structure- function relationships in serpins: current concepts and controversies, *Thromb. Haemost.* 80, 531-541.

Glaser, C. B., Chamorro, M., Crowley, R., Karic, L., Childs, A., and Claderon, M. (1982) The isolation of alpha-1-protease inhibitor by a unique procedure designed for industrial application, *Anal. Biochem.* 124, 364-371.

Gonzales, P. R., Walston, T. D., Camacho, L. O., Kielar, D. M., Church, F. C., Rezaie, A. R., and Cooper, S. T. (2007) Mutation of the H-helix in antithrombin decreases heparin stimulation of protease inhibition, *Biochim. Biophys. Acta* 1774, 1431-1437.

Goodstadt, L., and Ponting, C. P. (2001) CHROMA: consensus-based coloring of multiple alignments for publication, *Bioinformatics* 17, 845-846.

Griebenow, K., and Klibanov, A. M. (1995) Lyophilization induced reversible changes in the secondary structure of proteins, *Proc. Natl. Acad. U.S.A.* 92, 10969-10976.

Griffin, C. A., Calaycay, J., Shively, J. E., and Smith, R. L. (1986) Two plasma fibronectin fragments with different gelatin-binding properties, *Thromb. Res.* 43, 469-77.

Griffiths, S. W., King, J., and Cooney, C. L. (2002) The reactivity and oxidation pathway of cysteine 232 in recombinant human alpha-1-antitrypsin, *J. Biol. Chem.* 277, 25486-25492.

Gupta, V. K., and Gowda, L. R. (2008) Alpha-1-proteinase inhibitor is a heparin binding serpin: Molecular interactions with the Lys rich cluster of helix-F domain, *Biochimie* doi. 10.1016/j.biochi.2008.01.004.

Gupta, V. K., Rao, A. G. A., and Gowda, L. R. (2008) Purification and biochemical chracterization of ovine α-1-proteinase inhibitor: Mechanistic adaptations and role of Phe^{350} and Met^{356}, *Protein Expres. Purif.* 57, 290-302.

Guyton, A. C., and Hall, J. E. (2006) *Textbook of medical physiology*, Elsevier Saunders, U.S.A., 11th Ed. 464.

Guzdek, A., Potempa, J., Dubin, A., and Travis, J. (1990) Comparative properties of human α-1-proteinase inhibitor glycosylation variants, *FEBS LETT.* 272, 125-127.

Habeeb, A. F. S. A. (1966) Determination of tree amino groups in protein by trinitrobenzenesulfonic acid, *Anal. Biochem.* 14, 328–336.

Hadzic, N., Quaglia, A., and Vergani, G. M. (2006) Hepatocellular carcinoma in a 12-year-old child with PiZZ alpha1-antitrypsin deficiency, *Hepatology* 43, 194.

Harhay**,** G. P., Sonstegard, T. S., Keele, J. W., Heaton, M. P., Clawson, M. L., Snelling, W. M., Wiedmann, R. T., Van Tassell, C. P., and Smith**,** T. P. (2005) Characterization of 954 bovine full-CDS cDNA sequences, *BMC Genomics* 6, 166-171.

Harpel, P. C., and Cooper, N. R. (1975) Studies on human plasma C1 inactivator-enzyme interactions: Mechanisms of interaction with C1s, plasmin, and trypsin, *J. Clin. Invest.* 55, 593–604.

*Harris, E. D., DiBona, D. R., and Krane, S. M. (1969) Collagenase in human synovial fluid. *J. Clin. Invest.* 48, 2104–2113.

Haupt, H., Heimburger, N., Kranz, T., and Schwick, H. G. (1970) Isolation and characterization of C1-Inactivator from human plasma, *Eur. J. Biochem.* 17, 254-61.

Hayashi, M., and Yamada, K. M. (1982) Divalent cation modulation of fibronectin binding to heparin and DNA, *J. Biol. Chem.* 257, 5263–5267.

Haynes, R., Osuga, D. T., and Feeney, R. E. (1967) Modification of amino groups in inhibitors of proteolytic enzymes, *Biochemistry* 6, 541-7.

Heath, D. D., Holcman, B., and Shaw, R. J. (1994) *Echinococcus granulosus*: The mechanism of oncosphere lysis by sheep complement and antibody, *Int. J. Parasitol.* 24**,** 929–935.

Heimburger, N. (1975) *In Proteases and biological control* (E. Reich, D.B. Rifkin, E. Shaw, eds.) 367-386, Cold Spring Harbor laboratory, Cold Spring Harbor, N.Y.

*Heimburger, N., and Trobisch, H. (1971) Blood coagulation and fibrinolysis, *Angew. Chem. Int. Ed. Engl.* 10, 85-97.

Hercz, A. (1974) The inhibition of proteinases by human alpha-1-antitrypsin, *Eur. J. Biochem.* 49, 287-292.

Hercz, A. (1985) Proteolytic cleavages in alpha-1-antitrypsin and microheterogeneity, *Biochem. Biophys. Res. Commun.* 128, 195-203.

Hermodson, M., and Mahoney, W. C. (1983) Separation of peptides by reversed-phase high-performance liquid chromatography, *Methods Enzymol.* 91, 352–359.

Heuck, C. C., Schiele, U., Horn, D., Fronda, D., and Ritz, E. (1985) The role of surface charge on the accelerating action of heparin on the antithrombin III-inhibited activity of alpha-thrombin, *J. Biol. Chem.* 260, 4598-4603.

Higgins, D., Thompson, J., Gibson, T., Thompson, J. D., Higgins, D. G., and Gibson, T. J. (1994) CLUSTAL W: Improving the sensitivity of progressive multiple sequence alignment through sequence weighting, position specific gap penalties and weight matrix choice, *Nucleic Acids Res.* 22, 4673-4680.

Higgins, J. D. G., Thompson, D., and Gibson, T. J. (1996) Using CLUSTAL for multiple sequence alignments, *Methods Enzymol.* 266, 383-402.

Hiratsuka, T. (1990) Conformational changes in the 23-kilodalton NH_2 terminal peptide segment of Myosin ATPase associated with ATP hydrolysis, *J. Biol. Chem.* 265, 18786-18790.

Hodges, L. C., Laine, R., and Chan, S. K. (1979) Structure of the oligosaccharide chains in human alpha-1-proteinase inhibitor, *J. Biol. Chem.* 254, 8208-8212.

Holm, L., and Sander, C. (1996) Mapping the Protein Universe, *Science* 273, 595-602.

Hovingh, P., and Linker, A. (1982) An unusual heparan sulfate isolated from lobsters (*Homarus americanus*), *J. Biol. Chem*. 257, 9840-9844.

Hovingh, P., and Linker, A. (1993) Glycosaminoglycans in *Anodonta californiensis*, a Freshwater Mussel, *Biological Bulletin* 185, 263-276.

Huang, C., Lee, M., Huang, F., and Chang, G. (1995) A protease inhibitor of the serpin family is a major protein in carp perimeningeal fluid: cDNA cloning, sequence analysis, and *Escherichia coli* expression, *J. Neurochem.* 64, 1721–1727.

Huber, R., and Carrell, R. W. (1989) Implications of the three-dimensional structure of α-1-antitrypsin for structure and function of serpins, *Biochemistry* 28, 8951−8966.

Humphrey, W., Dalke, A., and Schulten, K. (1996) VMD-Visual Molecular Dynamics, *J. Molec. Graphics* 14, 33-38.

Hunt, L. T., and Dayhoff, M. O. (1980) A surprising new protein superfamily containing ovalbumin, antithrombin-III, and alpha-proteinase inhibitor, *Biochem. Biophys. Res. Commun.* 95, 864-871.

Huntington, J. A. (2006) Shape-shifting serpins-advantages of a mobile mechanism, *Trends Biochem. Sci.* 31, 427–35.

Huntington, J. A., Read, R. J., and Carrell, R. W. (2000) Structure of a serpin-protease complex shows inhibition by deformation, *Nature* 407, 923–926.

*Hussain, M., Vergani, G. M., and Mowat, A. P. (1991) α-1-antitrypsin deficiency and liver disease: Clinical presentation, diagnosis and treatment, *J. Inherit. Metabol. Dis.* 14, 497-511.

Hyvarinen, A., Karhunen, J., and Oja, E. (2001) *Independent component Analysis*, John Wiley and Sons, New York.

Imberty, A., Jacob, L. H., and Pérez, S. (2007) Structural view of glycosaminoglycan-protein interactions, *Carbohydr. Res.* 342, 430-439.

Irving, J. A., Cabrita, L. D., Rossjohn, J., Pike, R. N., Bottomley, S. P., and Whisstock, J. C. (2003) The 1.5 Å crystal structure of a prokaryote serpin: Controlling conformational change in a heated environment, *Structure* 11, 387–397.

Irving, J. A., Pike, R. N., Lesk, A. M., Whisstock, J. C. (2000) Phylogeny of the serpin superfamily: implications of patterns of amino acid conservation for structure and function, *Genome Res.* 10, 1845–1864.

Irving, J. A., Steenbakkers, P. J., Lesk, A. M., Camp, H. J., Pike, R. N., and Whisstock, J. C. (2002) Serpins in prokaryotes, *Mol. Biol. Evol.* 19, 1881–1890.

*James, M. N. G. (1976) Relationship between the structures and activities of some microbial serine proteases: Comparison of the tertiary structures of microbial and pancreatic serine proteases, *Proteolysis and Physiological Regulation*, Editors D.W. Ribbons, D. W. and Brew, K., Academic Press, New York, 125–142.

Janciauskiene, S. (2001) Conformational properties of serine proteinase inhibitors (serpins) confer multiple pathophysiological roles, *Biochim. Biophys. Acta* 1535, 221–235.

Janciauskiene, S., Dominaitiene, R., Stemby, N. H., Piitulainen, E., and Eriksson, S. (2002) Detection of circulating and endothelial cell polymers of Z and wild type α-1-antitrypsin by a monoclonal antibody, *J. Biol. Chem.* 277, 26540–26546.

Janciauskiene, S., Zelvyte, I., Jansson L., and Stevens, T. (2004) Divergent effects of alpha1-antitrypsin on neutrophil activation, in vitro, *Biochem. Biophys. Res. Commun.* 315**,** 288–296.

Jankowski, W. J., Muenchhausen, W., Sulkowski, E., and Carter, W. A. (1976) Binding of human interferons to immobilized Cibacron Blue F3GA: The nature of molecular interaction, *Biochemistry* 15, 5182–5187.

*Janoff, A. (1972) Human granulocyte elastase. Further delineation of its role in connective tissue damage, *Am. J. Pathol.* 68, 579–592.

Janoff, A., Carp, H., Lee, D. K., and Drew, R. T. (1979) Cigarette smoke inhalation decreases alpha-1-antitrypsin activity in rat lung, *Science* 206, 1313−1316.

Jarvis, J. A., Munro, S. L. A., and Craik, D. J. (1992) Homology model of thyroxine binding globulin and elucidation of the thyroid hormone binding site, *Protein Eng*. 5, 61-67.

Jin, L., Abrahams, J. P., Skinner, R., Petitous, M., Pike, R. N., and Carrell, R. W. (1997) The anticoagulant activation of antithrombin by heparin, *Proc. Natl. Acad. Sci. U.S.A.* 94, 14683-14688.

Johansson, J., Gröndal, S., Sjövall. J., Jörnvall, H., and Curstedt, T. (1992) Identification of hydrophobic fragments of alpha 1-antitrypsin and C1 protease inhibitor in human bile, plasma and spleen, *FEBS LETT.* 299, 146-148.

Johnson, D., and Travis, J. (1977) Inactivation of human alpha-1-proteinase inhibitor by thiol proteinases, *Biochem. J.* 163, 639-641.

Johnson, D., and Travis, J. (1978) Structural evidence for methionine at the reactive site of human alpha-1-proteinase inhibitor, *J. Biol. Chem.* 253, 7142-7144.

Johnson, D., and Travis, J. (1979) The oxidative inactivation of human alpha-1-proteinase inhibitor. Further evidence for methionine at the reactive center, *J. Biol. Chem.* 254, 4022-4026.

Joshi, S. B., Kamerzell, T. J., McNown, C., Middaugh, C. R. (2008) The interaction of heparin/polyanions with bovine, porcine and human growth hormone, *J. Pharm. Sci.* 97, 1368-1385.

Kaiden, K., Matsui, T., and Tanaka, S. (1987) Quantitative estimation of α-helix coil content in bovine serum albumin by Fourier transform infra-red spectroscopy, *Appl. Spectrosc.* 41, 861-865.

Kakade, M. M., Simons, N., and Leiner, I. E. (1969) An evaluation of Natural vs. synthetic substrates for measuring the antitryptic activity of Soybean samples, *Cereal Chem.* 46, 518-526.

Kalisz, H. M., Hecht, H. J., Schomburg, D., and Schmid, R. D. (1991) Effects of carbohydrate depletion on the structure, stability and activity of glucose oxidase from *Aspergillus niger*, *Biochim. Biophys. Acta* 1080, 138-142.

Kalsheker, N. (1989) Alpha 1-antitrypsin: Structure, function and molecular biology of the gene, *Biosci. Rep.* 9, 129-138.

Kalsheker, N., Morley, S., and Morgan, K. (2002) Gene regulation of the serine proteinase inhibitors alpha1-antitrypsin and alpha1-antichymotrypsin, *Biochem. Soc. Trans.* 30, 93-98.

Kamerzell, T. J., Unruh, J. R., Johnson, C. K., Middaugh, C. R. (2006) Conformational flexibility, hydration and state parameter fluctuations of fibroblast growth factor-10: Effects of ligand binding, *Biochemistry* 45, 15288-15300.

Kang, U., Baek, J., Ryu, U., Kim, J., Yu, M., and Lee, C. (2004) Kinetic mechanism of protease inhibition by α-1-antitrypsin, *Biochem. Biophys. Res. Commun.* 323, 409-415.

Kapitany, R. A., and Zebrowski, E. J. (1973) A high resolution PAS stain for polyacrylamide gel electrophoresis, *Anal. Biochem.* 56, 361-369.

Kaplan, K. L., Broekman, M. J., Chernoff, A., Lesznik, G. R., and Drillings, M. (1979) Platelet alpha-granule proteins: Studies on release and subcellular localization, *Blood* 53, 604-618.

Karnaukhova, E., Ophir, Y., and Golding, B. (2006) Recombinant human alpha-1-proteinase inhibitor towards therapeutic use, *Amino* Acids 30**,** 317–332.

Katz, D. S., and Christianson, D. W. (1993) Modeling the uncleaved serpin antichymotrypsin and its chymotrypsin complex, *Protein Eng.* 6, 701-709.

Kay, M. A., Baley, P., Rothenberg, S., Leland, F., Fleming, L., Ponder, K. P., Liu, T., Finegold, M., Darlington, G., Pokorny, W., and Woo, S. L. C. (1992) Expression of human alpha-1-antitrypsin in dogs after autologous transplantation of retroviral transduced hepatocytes, *Proc. Natl. Acad. Sci. U.S.A.* 89, 89-93.

Kim, S. J., Woo, J. R., Seo, E. J., Yu M. H., and Ryu, S. E. (2001) A 2.1 Å resolution structure of an uncleaved α-1-antitrypsin shows variability of the reactive centre and other loops, *J. Mol. Biol.* 306, 109-119.

Kjellén, L., and Lindahl, U. (1991) Proteoglycans: Structures and interactions, *Annu. Rev. Biochem.* 60, 443-475.

*Klein, S. L., Strausberg, R. L., Wagner, L., Pontius, J., Clifton S. W., and Richardson, P. (2002) Genetic and genomic tools for *Xenopus* research: The NIH *Xenopus* initiative, *Dev. Dyn.* 225, 384–391.

Klieber, M. A., Underhill, C., Hammond, G. L., and Muller, Y. A. (2007) Corticosteroid-binding globulin, a structural basis for steroid transport and proteinase-triggered release, *J. Biol. Chem.* 282, 29594-29603.

*Knoell, D. L., Ralston, D. R., Coulter, K. R., and Wewers, M. D. (1998) Alpha-1-antitrypsin and protease complexation is induced by lipopolysaccharide, interleukin-1beta, and tumor necrosis factor-alpha in monocytes, *Am. J. Respir. Crit. Care Med.* 157, 246–255.

Köhnlein, T., and Welte, T. (2008) Alpha-1 antitrypsin deficiency: Pathogenesis, clinical presentation, diagnosis, and treatment, *Am. J. Med.* 121, 3-9.

Kojima**,** T., Leone, C. W., Marchildon, G. A., Marcum, J. A., and Rosenberg, R. D. (1992) Isolation and characterization of heparan sulfate proteoglycans produced by cloned rat microvascular endothelial cells, *J. Biol. Chem.* 267, 4859–4569.

Komissarov, A. A., Zhou, A., and Declerck, P. J. (2007) Modulation of serpin reaction through stabilization of transient intermediate by ligands bound to alpha-helix F, *J. Biol. Chem.*282, 26306-26315.

Kress, L. F., and Catanese, J. J. (1981) Identification of the cleavage sites resulting from enzymatic inactivation of human antithrombin III by *Croatalus adamanteus* proteinase II in the presence and absence of heparin, *Biochemistry* 20, 7432-7438.

Kress, L. F., Kurecki, T., Chan, S. K., and Laskowski, M. (1979) Characterization of the inactive fragment resulting from limited proteolysis of human alpha1-proteinase inhibitor by *Crotalus adamanteus* proteinase II, *J. Biol. Chem.* 254, 5317-5320.

Kueppers, F. (1973) Alpha-1-antitrypsin, *Am. J. Hum. Genet.* 25, 677-686.

Kuhn, L. A., Griffin, J. H., Fisher, C. L., Greengard, J. S., Bouma, B. N., España, F., and Tainer, J. A. (1990) Elucidating the structural chemistry of glycosaminoglycan recognition by protein C inhibitor, *Proc. Natl. Acad. Sci. U.S.A.* 87, 8506–8510.

Kumpalume, P., Podmore, A., LePage, C., and Dalton, J. (2007) New process for the manufacture of alpha-1 antitrypsin, *J. Chromatogr. A.* 1148, 31-37.

Laemmli, U. K. (1970) Cleavage of structural proteins during the assembly of the head of bacteriophage T4, *Nature* 227, 680–685.

Lakowicz, J. R. (1999) *Principles of Fluorescence Spectroscopy*, 2nd Ed. Kluwer Academic/Plenum Publishers, New York, 329-330.

Lamkin, G. E., and King, E. E. (1976) Blue Sepharose: A reusable affinity chromatography medium for purification of alcohol dehydrogenase, *Biochem. Biophys. Res. Commun.* 72, 560–565.

Laskowski, Jr., M. and Kato, I. (1980) Protein inhibitors of proteinases, *Annu. Rev. Biochem.* 49, 593−626.

Laskowski, R.A., MacArthur, M. W., Moss, D. S., and Thornton, J. M. (1993) PROCHECK: A program to check the stereochemical quality of protein structures, *J. Appl. Crystallogr.* 26, 283−291.

Laurell, C. B. (1963) Comparison of the agglutinability by rheumatoid arthritic sera of sensitized sheep cells, exposed to human c'1, c'4 and c'2, *Acta Pathol. Microbiol. Scand.* 59, 73-78.

Laurell, C. B. and Eriksson, S. (1963) The electrophoretic alpha-1-globulin pattern in alpha-1-antitrypsin deficiency, *Scand. J. Clin. Lab. Invest.* 15, 132-140.

*Law, R. H., Zhang, Q., McGowan, S., Buckle, A. M., Silverman, G. A., Wong, W., Rosado, C. J., Langendorf, C. G., Pike, R. N., and Bird, P. I. (2006) An overview of the serpin family, *Genome Biol.* 7, 216–220.

Lee, J. C., Harrison, D., and Timasheff, S. N. (1975) Interaction of vinblastin with calf brain microtubule protein, *J. Biol. Chem.* 250, 9276-9282.

Legge, M., Duff, G. B., Potter, H. C., and Hoetjes, M. M. (1984) Maternal serum alpha 1-antitrypsin concentrations in normotensive and hypertensive pregnancies, *J. Clin. Path.* 37, 867-869.

Lehrer, S. S. (1971) Solute perturbation of protein fluorescence. The quenching of the tryptophan fluorescence of model compounds and of lysozyme by iodide ion, *Biochemistry* 10, 3254-3263.

Lehrer, S. S., and Fasman, G. D. (1966) The fluorescence of lysozyme and lysozyme substrate complexes, *Biochem. Biophys. Res. Commun.*23, 133–138.

Lehrer, S. S., and Leavis, P. C. (1978) Solute quenching of protein fluorescence, *Methods Enzymol.* 49, 222-236.

Levitt, M., and Greer, J. (1977) Automatic identification of secondary structure in globular proteins, *J. Mol. Biol.* 114, 181-239.

Li, W., Johnson, D. J. D., Esmon, C. T., and Huntington, J.A. (2004) Structure of the antithrombin-thrombin-heparin ternary complex reveals the antithrombotic mechanism of heparin, *Nat. Struct. Mol. Biol.* 11, 857-862.

Liener, I. E., Garrison, O. R., and Pravda, Z. (1973) The purification of human serum α-1-antitrypsin by affinity chromatography on concanavalin A, *Biochem. Biophys. Res. Commun.* 51, 436–443.

Lijnen, H. R., Hoylaerts, M., and Collen, D. (1983) Heparin binding properties of human histidine-rich glycoprotein. Mechanism and role in the neutralization of heparin in plasma, *J. Biol. Chem.* 258, 3803-3808.

Lindahl, U., Thunberg, L., and Backstrom, G. (1984) Extension and structural variability of the antithrombin-binding sequence in heparin, *J. Biol. Chem.* 259, 12368-12376.

Linhardt, R. J., and Gunay, N. S. (1999) Production and chemical processing of low molecular weight heparins, *Sem. Thromb. Hem.* 3, 5-16.

Linhardt, R. J., Wang, H. M., Loganathan, D., and Bae, J. H. (1992) Search for the heparin antithrombin III-binding site precursor, *J. Biol. Chem.* 267, 2380-2387.

Loebermann, H., Tokuoka, R., Deisenhofer, J., and Huber, R. (1984) Human α-1-proteinase inhibitor. Crystal structure analysis of two crystal modifications, molecular model and preliminary analysis of the implications for function, *J. Mol. Biol.* 177, 531–557.

Lomas, D. A. (1996) New insights into the structural basis of alpha-1-antitrypsin deficiency, *QJM*. 89, 807-12.

Lomas, D. A., and Carrell, R. W. (2002) Serpinopathies and the conformational dementias, *Nat. Rev. Genet.* 3, 759-768.

Lomas, D. A., Evans, D. L., Finch, J. T., and Carrell, R. W. (1992) The mechanism of Z α-1-antitrypsin accumulation in the liver, *Nature* 357, 605–607.

Lomas, D., and Mahadeva, R. (2002) Alpha-1-antitrypsin polymerization and the serpinopathies: Pathobiology and prospects for therapy, *J. Clin. Invest.* 110, 1585-1590.

Long, G. L., Chandra, T., Woo, S. L., Davie, E. W., and Kurachi, K. (1984) Complete sequence of the cDNA for human alpha 1-antitrypsin and the gene for the S variant, *Biochemistry* 23, 4828–4837.

Longas, M. O., Newman, J., and Johnson, A. J. (1980) An improved method for the purification of human fibrinogen, *Int. J. Biochem.* 11, 559-564.

*Luisetti, M., and Travis, J. (1996) Bioengineering: Alpha-1 proteinase inhibitor site specific mutagenesis. The prospect for improving the inhibitor, *Chest* 110, 278-283.

Lundell, N., and Schreitmuller, T. (1999) Sample preparation for peptide mapping. A pharmaceutical quality control perspective, *Anal. Biochem.* 266, 31-47.

Luo, J. L., Tan, W., Ricono, J. M., Korchynskyi, O., Zhang, M., Gonias, S. L., Cheresh, D. A., and Karin, M. (2007) Nuclear cytokine-activated IKK-alpha controls prostate cancer metastasis by repressing Maspin, *Nature* 446, 690-694.

Ma, J., Yee, A., Brewer, H. B. J., Das, S., and Potter, H. (1994) Amyloid-associated proteins α-1-antichymotrypsin and apolipoprotein E promote assembly of Alzheimer β-protein into filaments, *Nature* 372, 92–94.

Machii, R., Sakatume, M., Kubota, R., Kobayashi, S., Gejyo, F., and Shiba, K. (2005) Examination of the molecular diversity of alpha-1-antitrypsin in urine: Deficit of an alpha1 globulin fraction on cellulose acetate membrane electrophoresis, *J. Clin. Lab. Anal.* 19, 16-21.

Mahoney, W. C., and Hermodson, M. A. (1980) Separation of large denatured peptides by reverse phase high performance liquid chromatography: Trifluoroacetic acid as a peptide solvent, *J. Biol. Chem.* 255, 11199-11203.

Maley, F., Trimble, R. B., Tarentino, A. L., and Plummer, T. H. (1989) Characterization of glycoproteins and their associated oligosaccharides through the use of endoglycosidases, *Anal. Biochem.* 180, 195-204.

Marcum, J. A., McKenney, J. B., and Rosenberg, R. D. (1984) Acceleration of thrombin-antithrombin complex formation in rat hindquarters via heparin like molecules bound to the endothelium, *J. Clin. Invest.* 74, 341-350.

Massoud, M., Bischoff, R., Dalemans, W., Pointu, H., Attal, J., Schultz, H., Clesse, D., Stinnakre, M. G., Pavirani, A., and Houdebine, L. M. (1991) Expression of active recombinant human alpha-1-antitrypsin in transgenic rabbits, *J. Biotechnol.* 18, 193-203.

Matheson, N. R., and Travis, J. (1976) Inactivation of human thrombin in the presence of human alpha1-proteinase inhibitor, *Biochem. J.* 159, 495-502.

Matheson, N. R., Wong, P. S., and Travis, J. (1979) Enzymatic inactivation of human alpha-1-proteinase inhibitor by neutrophil myeloperoxidase, *Biochem. Biophys. Res. Commun*. 88, 402-9.

Matheson, N. R., Wong, P.S., Schyler, M., and Travis, J. (1981) Interaction of human alpha-1-proteinase inhibitor with neutrophil myeloperoxidase, *Biochemistry* 20, 331-336.

Matsudaira, P. (1987) Sequence from picomole quantities of proteins electroblotted onto polyvinylidene difluoride membranes, *J. Biol. Chem.* 262, 10035-10038.

*Matsudaira, P. T. (1989) *A Practical Guide to Peptide and Protein Purification for Microsequencing*, Editor, Matsudaira, P.T., Academic Press, Inc., New York, 53–58.

*McCarthy, K., Bhogal, M., Nardi, M., and Hart, D. (1984) Pathogenic factors in bronchopulmonary dysplasia, *Pediatr. Res.* 18, 483-491.

McKerrow, J. M., Keene, W. E., Jeong, K. H. and Werb, Z. (1983) Degradation of extracellular matrix by larvae of *Schistoma mansoni, Lab. Invest.* 49, 185-200.

McRae, B., Nakajima, K., Travis, J., and Powers, J. C. (1980) Studies on reactivity of human leukocyte elastase, cathepsin G. and porcine pancreatic elastase toward peptides including sequences related to the reactive site of alpha-1-proteinase inhibitor, *Biochemistry* 19, 3973-3978.

Meagher, J. L., Beechem, J. M., Olson, S. T., and Gettins, P. G. (1998) Deconvolution of the fluorescence emission spectrum of human antithrombin and identification of the tryptophan residues that are responsive to heparin binding, *J. Biol. Chem.* 273, 23283-23289.

Medcalf, R. L. (2005) Meet the serpins, *FEBS J.* 272, 4841.

Medeiros, G. F., Mendes, A., Castro, R. A., Baú, E. C., Nader, H. B., and Dietrich, C. P. (2000) Distribution of sulfated glycosaminoglycans in the animal kingdom: Widespread occurrence of heparin-like compounds in invertebrates, *Biochim. Biophys. Acta* 1475, 287-294.

Mega, T., Lujan, E., and Yoshida, A. (1980) Studies on the oligosaccharide chains of human alpha-1-proteinase inhibitor, *J. Biol. Chem.* 255, 4057-4061.

Melgarejo, T., Williams, D. A., and Griffith, G. (1996) Isolation and characterization of alpha-1-protease inhibitor from canine plasma, *Am. J. Vet. Res.* 57, 258-263.

Mer, G., Hietter, H., and Lefevre, J.F. (1996) Stabilisation of proteins by glycosylation examined by NMR analysis of a fucosylated proteinase inhibitor, *Nature Struct. Biol.* 3, 45-53.

*Merritt, T. A., Cochrane, C. G., Holcomb, K., Bohl, B., Hallman, M., Strayer, D., Edwards, D. K., and Gluck, L. (1983) Elastase and alpha-1-proteinase inhibitor activity in tracheal aspirates during respiratory distress syndrome, *J. Clin. Invest.* 72, 656-666.

Miesowicz, F. M., Bloch, K. (1979) Purification of hog liver isomerase. Mechanism of isomerization of 3-alkenyl and 3-alkynyl thioesters, *J. Biol. Chem.* 254, 5868-5877.

Mir, R., and Kahn, L. B. (1983) Immunohistochemistry of Hodgkin's disease, *Cancer* 52, 2064-2071.

Mistry, R., Snashall, P. D., Totty, N., Guz, A., and Tetley, T. D. (1991) Isolation and characterization of sheep alpha-1-proteinase inhibitor, *Biochem. J.* 273, 685-690.

Misumi, Y., Ohkubo, K., Sohda, M., Takami, N., Oda, K., and Ikehara, Y. (1990) Intracellular processing of complement pro-C3 and proalbumin is inhibited by rat alpha 1-protease inhibitor variant (Met^{352}-Arg) in transfected cells, *Biochem. Biophys. Res. Commun.* 171, 236-242.

Molmenti, E. P., Perlmutter, D. H., and Rubin, D. C. (1993) Cell-specific expression of alpha-1-antitrypsin in human intestinal epithelium, *J. Clin. Invest.* 92, 2022–2034.

Moraga, F., Lindgren, S., and Janciauskiene, S. (2001) Effects of non-inhibitory alpha-1-antitrypsin on pulmonary human monocyte activation in vitro, *Arch. Biochem. Biophys.* 386, 221-226.

*Morihara, K., Tsuzuki, H., and Oda, K. (1979) Protease and elastase of *Pseudomonas aeruginosa*: Inactivation of human plasma alpha 1-proteinase inhibitor, *Infect. Immun*. 24, 188-193.

Moriya, K., Yoshikawa, M., Saito, K., Ouji, Y., Nishiofuku, M., Hayashi, N., Ishizaka, S., and Fukui, H. (2007) Embryonic stem cells develop into hepatocytes after intrasplenic transplantation in CCl4-treated mice, *World J. Gastroenterol.* 13, 866-873.

Moroi, M., and Aoki, N. (1977) Inhibition of proteases in coagulation, kinin-forming and complement systems by alpha-2-plasmin inhibitor, *J. Biochem.* 82, 969-972.

Moroi, M., and Yamasaki, M. (1974) Mechanism of interaction of bovine trypsin with human alpha-1-antitrypsin, *Biochim. Biophys. Acta* 359, 130-41.

*Morral, N., Parks, R. J., Zhou, H., Langston, C., Schiedner, G., Quinones, J., Graham, F. L., Kochanek, S., and Beaudet, A. L. (1998) High doses of a helper-dependent adenoviral vector yield supraphysiological levels of alpha-1-antitrypsin with negligible toxicity, *Hum. Gene Ther.* 9, 2709-2716.

Mulloy, B., Forster, M. J., Jones, C., and Davies, D. B. (1993) NMR and molecular-modeling studies of the solution conformation of heparin, *Biochem. J.* 293, 849–858.

Nader, H. B., Lopes, C. C., Rocha, H. A., Santos, E. A., and Dietrich, C. P. (2004) Heparins and heparinoids: Occurrence, structure and mechanism of antithrombotic and hemorrhagic activities, *Curr. Pharm. Des.* 10, 951-966.

Nakajima, K., Powers, J. C., Ashe, B. M., and Zimmermann, M. (1979) Mapping the extended substrate binding site of cathepsin G and human leukocyte elastase. Studies with peptide substrates related to the alpha-1-protease inhibitor reactive site, *J. Biol. Chem.* 254, 4027-4031.

Needham, M., and Stockley, R. A. (2004) Alpha 1-antitrypsin deficiency: Clinical manifestations and natural history, *Thorax* 59, 441-445.

Nelson, D. P., and Kiesow, L. A. (1972) Enthalpy of decomposition of hydrogen peroxide by catalase at 25 °C (with molar extinction coefficients of H_2O_2 solutions in the UV), *Anal. Biochem.* 49, 474-478.

Nicholas, K. B., Nicholas, H. B., and Deerfield, D. W. (1997) GeneDoc: Analysis and visualization of genetic variation, *Embnew. News,* 14.

Niemann, M. A., Baggott, J. E., and Miller, E. J. (1997) Binding of SPAAT, the 44-residue C-terminal peptide of alpha-1-antitrypsin, to proteins of the extracellular matrix, *J. Cell Biochem.* 66, 346-357.

Nordenman, B., Danielsson, A., and Björk, I. (1978) The binding of low-affinity and high-affinity heparin to antithrombin: Fluorescence studies, *Eur. J. Biochem.* 90, 1–6.

Ohlsson, K., and Olsson, I. (1973) The neutral proteases of human granulocytes. Isolation and partial characterization of two granulocyte collagenases, *Eur. J. Biochem.* 36, 473-481.

Olsen, G. N., Harris, J. O., Castle, J. R., Waldman, R. H., and Karmgard, H. J. (1975) Alpha-1-antitrypsin content in the serum, alveolar macrophages, and alveolar lavage fluid of smoking and nonsmoking normal subjects, *J. Clin. Invest.* 55, 427–430.

Olson, S. T., and Björk, I. (1991) Predominant contribution of surface approximation to the mechanism of heparin acceleration of the antithrombin-thrombin reaction. Elucidation from salt concentration effects, *J. Biol. Chem.* 266, 6353-6364.

Olson, S. T., and Chuang, Y. J. (2002) Heparin activates antithrombin anticoagulant function by generating new interaction sites (exosites) for blood clotting proteinases, *Trends Cardiovas. Med.* 12, 331-338.

Olson, S. T., Bjork, I., Craig, P. A., Shore, J. D., and Choay, J. (1992) Role of the antithrombin binding penta-saccharide in heparin acceleration of antithrombin-proteinase reactions. Resolution of the antithrombin conformational change contribution to heparin rate enhancement, *J. Biol. Chem.* 267, 12528-12538.

Olson, S. T., and Shore, J. D. (1981) Binding of high affinity heparin to antithrombin III. Characterization of the protein fluorescence enhancement, *J. Biol. Chem.* 256, 11065–11072.

Ordonez, N. G., Manning, J.T., and Hanssen, G. (1983) Alpha-1-antitrypsin in islet cell tumors of the pancreas, *Am. J. Clin. Pathol.* 80, 277–282.

Ortiz, P. G., Skov, B. G., and Benfeldt, E. (2005) Alpha-1-antitrypsin deficiency-associated panniculitis: Case report and review of treatment options, *J. Eur. Acad. Dermatol. Venereol.* 19, 487-490.

Ototani, N., Kikuchi, M., and Yosizawa, Z. (1981) Comparative studies on the structures of highly active and relatively inactive forms of whale heparin, *J. Biochem.* 90, 241–246.

Owen, W. G. (1975) Evidence for the formation of an ester between thrombin and heparin cofactor, *Biochim. Biophys. Acta* 405, 380-387.

Pak, S. C., Kumar, V., Tsu, C., Luke, C. J., Askew, Y. S., Askew, D. J., Mills, D. R., Bromme, D., Silverman, G. A. (2004) SRP-2 is a cross-class inhibitor that participates in postembryonic development of the nematode *Caenorhabditis elegans*: Initial characterization of the clade L serpins *J. Biol. Chem.* 279, 15448-15459.

Parfrey, H., Mahadeva, R.,. and Lomas, D. A. (2003) Alpha-1-antitrypsin deficiency, liver disease and emphysema. Targetting a surface cavity of alpha-1-antitrypsin to prevent conformational disease, *Int. J. Biochem. Cell Biol.* 35, 1002-1014.

Patson, P. A. (2000) Serpins and other serine protease inhibitors, *Immunol. Today* 217, 354.

Patston, P. A., and Schapira, M. (1994) Low-affinity heparin stimulates the inactivation of plasminogen activator inhibitor-1 by thrombin, *Blood* 84, 1164-1172.

Patterson, S. D., Bell, K., and Shaw, D. C. (1991) The equine major plasma serpin multigene family: Partial characterization including sequence of the reactive-site regions, *Biochem. Genet.* 29, 477-499.

Pejler, G., Danielsson, A., Bjork, I., and Lindahl, U. (1987) Structure and antithrombin-binding properties of heparin isolated from the clams *Anomalocardia brasiliana* and *Tivela mactroides*, *J. Biol. Chem.* 262, 11413–11421.

Pemberton, P. A., Stein, P. E., Pepys, M. B., Potter, J. M., and Carrell, R. W. (1988) Hormone binding globulins undergo serpin conformational change in inflammation, *Nature* 336, 257–258.

*Perlmutter, D. H. (2002) Liver injury in alpha-1- antitrypsin deficiency: An aggregated protein induces mitochondrial injury, *J. Clin. Invest.* 110, 1579-83.

Perlmutter, D. H. (2004) Alpha-1-antitrypsin deficiency: diagnosis and treatment, *Clin. Liver Dis.* 8, 839-859.

Peterson, B., Claudia, M. N., Jill, M. P., Frank, C. C., and Michael, N. B. (1987) Identification of a Lysyl residue in antithrombin, which is essential for heparin binding, *J. Biol. Chem.* 262, 8061-8065.

Pike, R. N., Buckle, A. M., Le Bonniec, B. F., and Church, F.C. (2005) Control of the coagulation system by serpins. Getting with a little help from glycosaminoglycans, *FEBS J.* 272, 4842-4851.

Plotnikov, A. N., Hubbard, S. R., Schlessinger, J., Mohammadi, M. (2000) Crystal structures of two FGF-FGFR complexes reveal the determinants of ligand-receptor specificity, *Cell* 101, 413-424.

Plummer, T. H., and Tarentino, A. L. (1991) Purification of the oligosaccharide-cleaving enzymes of *Flavobacterium meningosepticum, Glycobiology* 1, 257-263.

Potempa, J., Watorek, W., and Travis, J. (1986) The inactivation of human plasma α-1-Proteinase inhibitor by proteinases from *Staphylococcus aureus*, *J. Biol. Chem.* 261, 14330-14334.

*Proudfoot, A. E. (2006) The biological relevance of chemokine-proteoglycan interactions, *Biochem. Soc. Trans.* 34, 422-426.

Quinsey, N. S., Greedy, A. L., Bottomley, S. P., Whisstock, J. C., and Pike, R. N. (2004) Antithrombin: in control of coagulation, *Int. J. Biochem. Cell Biol.* 36, 386-389.

Ragg, H. (1986) A new member of the plasma protease inhibitor gene family, *Nucleic Acids Res*. 14, 1073–1088.

Raman, R., Sasisekharan, V., and Sasisekharan, R. (2005) Structural insights into biological roles of protein–glycosaminoglycan interactions, *Chem. Biol.* 12, 267–277.

Rawlings, N. D., Tolle, D. P., and Barrett, A. J. (2004) Evolutionary families of peptidase inhibitors, *Biochem. J.* 378, 705-716.

Reilly, C. F., Tewksbury, D. A., Schechter, N. M., and Travis, J. (1982) Rapid conversion of angiotensin I to angiotensin II by neutrophil and mast cell proteinases, *J. Biol. Chem.* 257, 8619–8622.

Remold, D. E., Chin, J., and Alberts, M. (1992) Sequence and molecular characterization of human monocyte/neutrophil elastase inhibitor, *Proc. Natl. Acad. Sci.U.S.A.*. 89, 5635–5639.

Rimon, A., Shamash, Y., and Shapiro, B. (1966) The plasmin inhibitor of human plasma. IV. Its action on plasmin, trypsin, chymotrypsin, and thrombin, *J. Biol. Chem.* 241, 5102-5107.

*Robert, J., Jakobsen, F., and Wasacz, M. (1990) Infrared Spectra-Structure Correlations and Adsorption Behavior for Helix Proteins, *Appl. Spectroscopy* 44, 1478-1490.

Robert, M. Z., Zell, T. E., Morrison, J. E., and Woodlock, J. J. (1969) Glycoprotein staining following electrophoresis on acrylamide gels, *Anal. Biochem.* 30, 148-152.

Rogers, J., Kalsheker, N., Wallis, S., Speer, A., Coutelle, C. H., Woods, D., and Humphries, S. E. (1983) The isolation of a clone for human alpha-1-antitrypsin and the detection of alpha-1-antitrypsin in mRNA from liver and leukocytes, *Biochem. Biophys. Res. Commun.* 116, 375–382.

Rosenberg, R. D., Oosta, G. M., Jordan, R. E., and Gardner, W. T. (1980) The interaction of heparin with thrombin and antithrombin, *Biochem. Biophys. Res. Commun.* 96, 1200-1208.

Rosenberg, S., Barr, P. J., Najarian, R. C., and Hallewell, R. A. (1984) Recombinant DNA synthesis of a functional, oxidation resistant active center variant of human alpha-1-antitrypsin, *Nature* 312, 77-80.

Saito, A., and Sinohara, H. (1990) Amino acid sequence at the reactive site of rabbit alpha-1-antiproteinases, *J. Biochem.* 108, 80-85.

Saito, A., and Sinohara, H. (1991) Cloning and sequencing of cDNA coding for rabbit alpha-1-antiproteinase F: Amino acid sequence comparison of alpha-1-antiproteinases of six mammals, *J. Biochem.* 109, 158-162.

Sandoval, C., Curtis, H., and Congote, L. F. (2002) Enhanced proliferative effects of a baculovirus-produced fusion protein of insulin-like growth factor and α-1-proteinase inhibitor and improved anti-elastase activity of the inhibitor with glutamate at position 351, *Protein Engineering* 15, 413-418.

Savitzky, A., and Golay, M. J. E. (1964) Smoothing and differentiation of data by simplified least square procedures, *Anal. Chem*. 36, 1627.

Schechter, E., and Blout, E. R. (1964) An analysis of the optical rotatory dispersion of polypeptides and proteins, *Proc. Natl. Acad. Sci. U.S.A.* 51, 695-702.

Schecter, I., and Berger, A. (1967) On the size of the active site in proteases. I. Papain. *Biochem. Biophys. Res. Commun.* 27, 157−162.

Schick, C., Brömme, D., Bartuski, A., Uemura, Y., Schechter, N., Silverman, G. (1998) The reactive site loop of the serpin SCCA1 is essential for cysteine proteinase inhibition, *Proc. Natl. Acad. Sci. U.S A.* 95, 13465-13470.

Schuettelkopf, A. W., and van Aalten, D. M. F. (2004) PRODRG-a tool for high-throughput crystallography of protein-ligand complexes, *Acta Crystallographica*, 60, 1355-1363.

*Schultze, H. E., Heide, K., and Haupt, H. (1962) Alpha-1-antitrypsin aus human serum, *Klin. Wschr*. 8, 428-434.

*Schwick, H. G., Heimburger, N., and Haupt, H. (1966) Antiproteinasen des humanserums, *Z. Gesamte Inn. Med.* 21, 193–198.

Scott, C. F., Schapira, M., James, H. L., Cohen, A. B., and Colman, R. W. (1982) Inactivation of factor XIa by plasma protease inhibitors. Predominant role of alpha-1-protease inhibitor and protective effect of high molecular weight kininogen, *J. Clin. Invest*. 69, 844-852.

Seegers, W. H., Warner, E D., Brinkhous, K. M., and Smith, H. P. (1942) Heparin and the antithrombic activity of plasma, *Science* 96, 300-301.

*Sharp, H. L., Bridges, R. A., Krivit, W., and Freier, E. F. (1969) Cirrhosis associated with alpha-1-antitrypsin deficiency: A previously unrecognized inherited disorder, *J. Lab. Clin. Med.* 73, 934–939.

Shirk, R. A., Elisen, G. L. M., Meijers, J. C. M., and Church, F. C. (1994) Role of the H-helix in heparin binding to Protein C inhibitor, *J. Biol. Chem.* 269, 28690-28695.

Silverman, G. A., Bird, P. I., Carrell, R. W., Church, F. C., Coughlin, P. B., Gettins, P. G., Irving, J. A., Lomas, D. A., Luke, C. J., Moyer, R. W., Pemberton, P. A., Remold-O'Donnell, E., Salvesen, G. S., Travis, J., and Whisstock, J. C. (2001) The serpins are an expanding superfamily of structurally similar but functionally diverse proteins. Evolution, mechanism of inhibition, novel functions, and a revised nomenclature, *J. Biol. Chem.* 276, 33293–33296.

Singh, B. R., Fu, F. N., and Ledoux, D. N. (1994) Crystal and solution structures of superantigenic staphylococcal enterotoxins compared, *Nature Struct. Biol.* 1, 358-360.

Singh, B. R., Linda, A., Caddle, B., Fu, F. N., and Li, B. (1996) Gene probe-based detection of type *E. botulinum* neurotoxin binding protein using polymerase chain reaction , *Toxicon* 34, 737-742.

Singh, B. R., Wasacz, F. M., Strand, S., Jakobsen, R. J., and Gupta, B. R. (1990) Comparative structural analysis of botulinum neurotoxins types A and E using fourier transform infrared and circular dichroic spectroscopies, *J. Protein Chem.* 7, 705-713.

Singhal, R. P., and Atassi,. M. Z. (1971) Immunochemistry of sperm whale of myoglobin. IX. Specific interaction of peptides obtained by cleavage at arginine peptide bonds, *Biochemistry* 10, 1756–1762.

*Sinha, U., Sinha, S., and Janoff, A. (1988) Characterization of sheep alpha-1- proteinase inhibitor. Important differences from the human protein, Am. *Rev. Respir. Dis.* 137, 558-563.

Smith, E. L. (1977) Reversible blocking at arginine by cyclohexanedione, *Methods Enzymol.* 47, 156–161.

Smith, G. F., and Sundboom, J. L. (1981) Heparin and protease inhibition: Heparin complexes with thrombin, plasmin, and trypsin, *Thromb. Res.* 22, 103–114.

Smith, T. F. and Waterman, M. S. (1981) Identification of common molecular subsequences, *J. Mol. Biol.* 147, 195-197.

Speicher, D. W. (1989) Microsequencing with PVDF membranes: Efficient electroblotting, direct protein adsorption and sequencer program modifications, *Techniques in Protein Chemistry* (Ed. T. Hugli) Academic Press, San Diego, 24–35.

Spencer, J. L., Stone, P. J., and Nugent, M. A. (2006) New insights into the inhibition of human neutrophil elastase by heparin, *Biochemistry* 45, 9104-9120.

Spencer, L. T., Humphries, J. E., and Brantly, M. L. (2005) Transgenic Human Alpha 1-Antitrypsin study group, Antibody response to aerosolized transgenic human alpha-1-antitrypsin, *N. Engl. J. Med.* 352, 2030-2031.

Stark, M., Jörnvall, H., and Johansson, J. (1999) Isolation and characterization of hydrophobic polypeptides in human bile, *Eur. J. Biochem.* 266, 209-214.

Stefansson, S., and Lawrence, D. A. (1996) The serpin PAI-1 inhibits cell migration by blocking integrin alpha V beta 3 binding to vitronectin, *Nature* 383, 441-443.

Stein, P. E., Leslie, A. G., Finch, J. T., Turnell, W. G., McLaughlin, P. J., and Carrell, R. W. (1990) Crystal structure of ovalbumin as a model for the reactive centre of serpins, *Nature* 347, 99–102.

Stein, P.E., and Carrell, R. W. (1995) What do dysfunctional serpins tell us about molecular mobility and disease, *Nat. Struct. Biol.* 2, 96–113.

Stratikos, E., and Gettins, P. G. W. (1999) Formation of the covalent serpin-proteinase complex involves translocation of the proteinase by more than 70 Å and full insertion of the reactive centre loop into β-sheet A, *Proc. Natl. Acad. Sci. U.S.A.* 96, 4808-4813.

Subramaniyam, D., Virtala, R., Pawłowski, K., Clausen, I. G., Warkentin, S., Stevens, T., and Janciauskiene, S. (2008) TNF-alpha-induced self expression in human lung endothelial cells is inhibited by native and oxidized alpha1-antitrypsin, Int. *J. Biochem. Cell Biol.* 40, 258-271.

Suzuki, Y., Yoshida, K., Honda, E., and Sinohara, H. (1991) Molecular cloning and sequence analysis of cDNAs coding for guinea pig alpha-1-antiproteinases S and F and contrapsin, *J. Biol. Chem.* 266, 928-932.

*Sveger, T., and Thelin, T. (2000) A future for neonatal alpha-1-antitrypsin screening, *Acta Paediatr.* 89, 628-631.

Sveger, T., Thelin, T., and McNeil, T. F. (1997) Young adults with alpha-1-antitrypsin deficiency identified neonatally: Their health, knowledge about and adaptation to the high-risk condition, *Acta Paediatr*. 86, 37-40.

Szporn, A. H., Dikman, S., and Jagirdar, J. (1984) True histiocytic lymphoma of the thymus. Report of a case and a study of the distribution of histiocytic cells in the fetal and adult thymus, *Am. J. Clin. Pathol.* 82, 734-737.

Taggart, C., Laurean, C. D., Kim, G., McElvaney, N. G., Wehr, N., Moss, J., and Levine, R. L. (2000) Oxidation of either methionine 351 or methionine 358 in alpha-1-antitrypsin causes loss of anti-neutrophil elastase activity, *J. Biol. Chem.* 275, 27258-27265.

Takagi, H., Narumi, H., Nakamura, K., and Sasaki, T. (1990) Amino acid sequence of silkworm (*Bombyx mori*) hemolymph antitrypsin deduced from its cDNA nucleotide sequence: confirmation of its homology with serpins, *J. Biochem.* 108, 372-378.

Takahara, H., and Sinohara, H. (1982) Mouse plasma trypsin inhibitors. Isolation and characterization of alpha-1-antitrypsin and contrapsin, a novel trypsin inhibitor, *J. Biol. Chem.* 257, 2438-2446.

Takamatsu, N., Kojima, M., Taniyama, M., Ohba, K., Uematsu, T., Segawa, C., Tsutou, S., Watanabe, M., Kondo, J., Kondo, N., and Shiba, T. (1997) Expression of multiple α-1-antitrypsin-like genes in hibernating species of the squirrel family, *Gene* 204, 127–132.

Terashima, M., Ejiri, Y., Hashikawa, N., and Yoshida, H. (2000) Effects of sugar concentration on recombinant human alpha (1)-antitrypsin production by genetically engineered rice cell, *Biochem. Eng. J.* 6, 201-205.

*Tersariol, I. L., Pimenta, D. C., Chagas J. R., and Almeida, P. C. (2002) Proteinase activity regulation by glycosaminoglycans, *Braz. J. Med. Biol. Res.* 35, 135-144.

Tetley, T. D., Smith, S. F., Winning, A. J., Foxall, J. M., Cooke, N. T., Burton, G. H., Harris, E., and Guz, A. (1989) The acute effect of cigarette smoking on the neutrophil elastase inhibitory capacity of peripheral lung lavage from asymptomatic volunteers, *Eur. Respir. J.* 2, 802-810.

Thomas, D. P., Curtis, A. D., and Barrowcliffe, T. W. (1984) A collaborative study designed to establish the 4th international standard for heparin, *Thromb. Haemost.* 52, 148-153.

Thompson, S. T., Cass, K. H., and Stellwagen, E. (1975) Blue dextran-sepharose: An affinity column for the dinucleotide fold in proteins, *Proc. Natl. Acad. Sci. U.S.A.* 72, 669-672.

Tjong, S., Chen, T., Huang, W., and Wu, W. (2007) Structure of heparin-derived tetrasaccharide bound to cobra cardiotoxins: Heparin binding at a single protein site with diverse side chain interactions, *Biochemistry* 46, 9941-9952.

Tokoro, Y., Eisen, A. Z., and Jeffrey, J. J. (1972) Characterization of a collagenase from rat skin, *Biochim. Biophys. Acta* 258, 289–302.

Tollefsen, D. M. (1990) Laboratory diagnosis of antithrombin and heparin cofactor II deficiency, *Semin. Thromb. Hemost.* 16, 162-168.

Tonnensen, M. D. (1989) Neutrophil-endothelial cell interactions: Mechanisms of neutrophil adherence to vascular endothelium, *J. Invest. Dermatol.* 93, 53-58.

Towbin, H., Staehelin, T., and Gordon, J. (1979) Electrophoretic transfer of proteins from polyacrylamide gels to nitrocellulose sheets: Procedure and some applications, *Proc. Natl. Acad. Sci. U.S.A.* 76, 4350–4354.

Travis, J., and Salvesen, G. S. (1983) Human plasma proteinase inhibitors, *Annu. Rev. Biochem.* 52**,** 655–709.

Travis, J., Bowen, J., Tewksbury, D., Johnson, D., and Pannell, R. (1976) Isolation of albumin from whole human plasma and fractionation of albumin depleted plasma, *Biochem. J.* 157, 301-306.

Travis, J., Garner, D., and Bowen, J. (1978) Human alpha-1-antichymotrypsin: Purification and properties, *Biochemistry* 17, 5647-5651.

Travis, J., Owen, M., George, P., Carrell, R., Rosenberg, S., Hallewell, R. A., and Barr, P. J. (1985) Isolation and properties of human alpha-1-proteinase inhibitor variants produced in yeast, *J. Biol. Chem.* 260, 4384-4389.

*Tsan, M. F. C., and Jasmine, W. (1980) Oxidation of methionine by human polymorphonuclear leukocytes, *J. Clin. Invest.* 65, 1041-1050.

Tumova, S., Woods, A., and Couchman, J. R. (2000) Heparan sulfate chains from Glypican and Syndecans bind the Hep II domain of fibronectin similarly despite minor structural differences, *J. Biol. Chem.* 275, 9410 - 9417.

Tuttle, W. C., and Jones, R. K. (1975) Fluorescent antibody studies of alpha-1-antitrypsin in adult human lung, *Am. J. Clin. Pathol.* 64, 477–482.

Uversky, V. N. (1993) Use of fast protein size-exclusion liquid chromatography to study the unfolding of proteins which denature through the molten globule, *Biochemistry* 32, 13288-13298.

Van Boeckel, C. A., Grootenhuis, P. D., and Visser, A. (1994) A mechanism for heparin-induced potentiation of antithrombin III, *Nat. Struct. Biol.* 1, 423-425.

Van Gent, D., Sharp, P., Morgan, K., and Kalsheker, N. (2003) Serpins: Structure, function and molecular evolution, *Int. J. Biochem. Cell Biol.* 35, 1536–1547.

Van Patten, S. M., Hanson, E., Bernasconi, R., Zhang, K., Manavalan, P., Cole, E. S., McPherson, J. M., and Edmunds, T. (1999) Oxidation of methionine residues in antithrombin. Effects on biological activity and heparin binding, *J. Biol. Chem.* 274, 10268-10276.

Vasishta, A., Baker, P.R., Preece, P.E., Wood, R. A. B. and Cuschieri, A. (1984) Serum proteinase like peptidase activities and proteinase inhibitors in women with breast disease, *Biochim. Biophys. Acta* 704, 267-271.

Vaughan, L., Lorier, M. A., and Carrell, R. W. (1982) Alpha-1-antitrypsin microheterogeneity. Isolation and physiological significance of isoforms, *Biochim. Biophys. Acta* 701, 339-345.

Villanueva, G., and Danishefsky, I. (1979) Conformational changes accompanying the binding of antithrombin III to thrombin, *Biochemistry* 18, 810-817.

Virca, G. D., Lyerly, D., Kreger, A., and Travis, J. (1982) Inactivation of alpha-1-proteinase inhibitor by *Serratia marcescens* metalloproteinase, *Biochim. Biophys. Acta* 704, 267-273.

Vriend, G. (1990) WHATIF: A molecular modeling and drug design program, *J. Mol. Graph.* 8, 52-56.

Wall, M., Moe, E., Eisenberg, J., Powers, M., Buist, N., and Buist, A. S. (1990) Long-term follow-up of a cohort of children with alpha-1-antitrypsin deficiency, *J. Pediatr.* 116, 248–251.

*Warda, M., Mao, W., Toida, T., and Linhardt, R. J. (2003) Turkey intestine as a commercial source of heparin? Comparative structural studies of intestinal avian and mammalian glycosaminoglycans, *Comp. Biochem. Physiol. B. Biochem. Mol. Biol.* 134, 189-197.

Whinna, H. C., Blinder, M. A., Szewczyk, M., Tollefsen, D. M., and Church, F. C. (1991) Role of lysine 173 in heparin binding to heparin cofactor II, *J. Biol. Chem.* 266, 8129-8135.

Whisstock, J. C., and Bottomley, S. P. (2006) Molecular gymnastics: Serpin structure, folding and misfolding, *Curr. Opin. Struct. Biol.* 16, 761-768.

Whisstock, J. C., Pike, R. N., Jin, L., Skinner, R., Pei, X. Y., Carrell, R. W., and Lesk, A. M. (2000) Conformational changes in serpins: II. The mechanism of activation of antithrombin by heparin*, J. Mol. Biol.* 301, 1287-1305.

Wiley, D. C., and Skehel, J. J. (1987) The structure and function of the hemagglutinin membrane glycoprotein of influenza virus, *Annu. Rev. Biochem.* 56, 365-394.

Wintroub, B. U., Klickstein, L. B., Watt, K. W. K. (1981) A human neutrophil-dependent pathway for generation of angiotensin II. Purification of the product and identification as angiotensin II, *J. Clin. Invest.* 68, 484–490.

Wong, P. S., and Travis, J. (1980) Isolation and properties in oxidized alpha-1-proteinase inhibitors from human rheumatoid synovial fluid, *Biochem. Biophys. Res. Commun.* 96, 1449-1454.

Wood, A. M., and Stockley, R. A. (2007) Alpha one antitrypsin deficiency: From gene to treatment, *Respiration* 74, 481-492.

Yamasaki, M., Arii, Y., Mikami, B., and Hirose, M. (2002) Loop inserted and thermostabilized structure of P1-P1` cleaved ovalbumin mutant R339T, *J. Mol. Biol.* 315, 113-120.

Yang, J. T., Wu, C. S. C., Martinez, H. M. (1986) Calculation of protein conformation from circular dichroism, *Methods Enzymol.* 130, 208-269.

*Yang, P., Tremaine, W. J., Meyer, R. L., and Prakash, U. B. (2000) Alpha-1-antitrypsin deficiency and inflammatory bowel disease, *Mayo Clin. Proc.* 75, 450-455.

Zbikowska, H. M., Soukhareva, N., Behnam, R., Lubon, H., Hammond, D., and Soukharev, S. (2002) Uromodulin promoter directs high-level expression of biologically active human alpha-1-antitrypsin into mouse urine, *Biochem. J.* 365, 7-11.

Zelvyte, I., Stevens, T., Westin, U., and Janciauskiene, S. (2004) Alpha-1-antitrypsin and its C-terminal fragment attenuate effects of degranulated neutrophil-conditioned medium on lung cancer HCC cells, in vitro, *Cancer Cell Int.* 4, 7.

Zhou, A., and Carrell, R. W. (2008) Dimers initiate and propagate serine protease inhibitor polymerization, *J. Mol. Biol.* 375, 36-42.

Zhou, A., Wei, Z., Read, R. J., and Carrell, R. W. (2006) Structural mechanism for the carriage and release of thyroxine in the blood, *Proc. Natl. Acad. Sci. U.S.A.*. 13321-13326.

*Ziomek, C. A. (1998) Commercialization of proteins produced in the mammary gland, *Theriogenology* 49, 139-144.

Zor, T., and Selinger, Z. (1996) Linearization of the Bradford protein assay increases its sensitivity: theoretical and experimental studies, *Anal. Biochem.* 236, 302-308.

Zou, Z., Anisowicz, A., Hendrix, M. J., Thor, A., Neveu, M., Sheng, S., Rafidi, K., Seftor, E., and Sager, R. (1994) Maspin, a serpin with tumor-suppressing activity in human mammary epithelial cells, *Science* 263, 526-529.

*Taken from cross-reference, original paper not seen or only abstract read via Pubmed.